Weathered multi-walled carbon nanotubes in the aquatic environment: fate, bioaccumulation, effects, and mixture toxicity

Von der Fakultät für Mathematik, Informatik und Naturwissenschaften der RWTH Aachen University zur Erlangung des akademischen Grades einer Doktorin der Naturwissenschaften genehmigte Dissertation

vorgelegt von

Irina Politowski
M. Sc. Ökotoxikologie
aus Olpe, Deutschland

Berichter: Univ.-Prof. Dr. rer. nat. Andreas Schäffer

apl. Prof. Dr. Erwin Klumpp

Tag der mündlichen Prüfung: 26.08.2021

"Jeder dumme Junge
kann einen Käfer zertreten.
Aber alle Professoren der Welt
können keinen herstellen."

Arthur Schopenhauer († 1860)

Eidesstattliche Erklärung

Ich, Irina Politowski

erkläre hiermit, dass diese Dissertation und die darin dargelegten Inhalte die eigenen sind und selbstständig, als Ergebnis der eigenen originären Forschung, generiert wurden.

Hiermit erkläre ich an Eides statt

1. Diese Arbeit wurde vollständig oder größtenteils in der Phase als Doktorand dieser Fakultät und Universität angefertigt;

2. Sofern irgendein Bestandteil dieser Dissertation zuvor für einen akademischen Abschluss oder eine andere Qualifikation an dieser oder einer anderen Institution verwendet wurde, wurde dies klar angezeigt;

3. Wenn immer andere eigene- oder Veröffentlichungen Dritter herangezogen wurden, wurden diese klar benannt;

4. Wenn aus anderen eigenen- oder Veröffentlichungen Dritter zitiert wurde, wurde stets die Quelle hierfür angegeben. Diese Dissertation ist vollständig meine eigene Arbeit, mit der Ausnahme solcher Zitate;

5. Alle wesentlichen Quellen von Unterstützung wurden benannt;

6. Wenn immer ein Teil dieser Dissertation auf der Zusammenarbeit mit anderen basiert, wurde von mir klar gekennzeichnet, was von anderen und was von mir selbst erarbeitet wurde;

7. Ein Teil oder Teile dieser Arbeit wurden zuvor veröffentlicht und zwar in:

<u>Publikationen</u>

- Politowski, I., Wittmers, F., Hennig, M. P., Siebers, N., Goffart, B., Roß-Nickoll, M., Ottermanns, R. and Schäffer, A. (2021). A trophic transfer study: accumulation of multi-walled carbon nanotubes associated to green algae in water flea *Daphnia magna*. NanoImpact 22: 100303.

- Politowski, I., Regnery, P., Hennig, M. P., Siebers, N., Ottermanns, R. and Schäffer, A. (2021). Fate of weathered multi-walled carbon nanotubes in an aquatic sediment system. Chemosphere 277: 130319.

<u>Vorträge</u>

- Politowski, I., Hennig, M. P., Wittmers, F., Hollert, H., Schäffer, A. (2017): Influence of weathered multiwalled carbon nanotubes in the environment: chronic and mixture effects with the biocide triclocarban as co-contaminant on freshwater algae. Young Water Researchers Symposium at RWTH Aachen University on November 24, 2017 in Aachen, Germany.

- Hennig, M. P., Politowski, I., Schäffer, A. (2017): Influence of weathered multiwalled carbon nanotubes in the environment: chronic and mixture effects with the biocide triclocarban as co-contaminant on freshwater algae. NANO-Transfer International Conference & Winter School on October 19 and 20, 2017 in Aachen, Germany.

Poster Präsentationen

- Politowski, I., Hennig, M. P., Wittmers, F., Hollert, H., Schäffer, A. (2019): Bioaccumulation of radiolabelled weathered multiwalled carbon nanotubes in various aquatic organisms: water and dietary exposure. SETAC Europe 29th Annual Meeting (May 2019, Helsinki, Finland).

- Politowski, I., Hennig, M. P., Hollert, H., Schäffer, A. (2018): Influence of weathered multiwalled carbon nanotubes in the environment: chronic and mixture effects with the biocide triclocarban as co-contaminant on freshwater algae. SETAC Europe 28th Annual Meeting (May 2018, Rome, Italy)

- Politowski, I., Hennig, M. P., Regnery, P., Voigt, K., Schäffer, A. (2018): CNT exposure to freshwater green algae *Pseudokirchneriella subcapitata* and *Chlamydomonas reinhardtii*: uptake and chronic effects. NanoTox 2018 - 9th International Conference on Nanotoxicology (September 2018, Neuss, Germany).

- Politowski, I., Hennig, M. P., Schäffer, A. (2017): NANO-Transfer: Das Verhalten gealterter Kohlenstoffnanoröhren in der aquatischen Umwelt. NanoCare-Clustertreffen im Mai 2017, Karlsruhe, Deutschland.

Aachen, den 07.01.2022

(Irina Politowski)

Acknowledgements

I would like to take this opportunity to thank all those who have supported me in the preparation of this thesis. In particular:

First and foremost, I would like to thank Prof. Dr. Andreas Schäffer for granting me a doctoral position at his institute. Thank you for the great time and the many new experiences I have had over the years. And above all, thanks for your tireless help in correcting my work and for your countless big and small support.

For being the second assessor of my thesis, I would also like to thank Prof. Dr. Erwin Klumpp. Thanks for your interest in my topic.

Furthermore, I would like to thank Prof. Dr. Martina Roß-Nickoll for accepting the position of third reviewer in my examination board.

I would like to cordially thank my supervisor Dr. Michael Patrick Hennig very much: for his friendship, his scientific support and his ability to motivate me again and again. For the interesting journeys we have undertaken together and for the way of understanding me. Without you it would not have been the same. Micha, what can I say: It was hell on earth, but it is done!

I would like to thank Dr. Hanna Maes for entrusting me with such a large and comprehensive project. Thank you for letting me get to know you and for the open-minded way you accepted me into the NANO working group.

I would like to thank Dr. Nina Siebers from the Department Agrosphere (IBG-3) at the Institute of Bio- and Geosciences (Forschungszentrum Jülich GmbH) for her help in characterizing the nanomaterials and identifying CNT-algal interactions. Thank you for your very open and friendly nature of our meetings and e-mail correspondence.

Also, I want to thank Dr. Monika Hammers-Wirtz, Silke Classen and Dr. Tido Strauss as well as their team from the Research Institute for Ecosystem Analysis and Assessment gaiac for the constant help and assistance during the work on the project Nano-Transfer.

Furthermore, I would like to thank Prof. Dr. Henner Hollert and Dr. Sabrina Schiwy for their reliable and energetic support in coordinating, planning, and conducting the animal experiments with *Danio rerio*. Without you, these experiments would simply have been impossible.

I would like to thank Dr. Richard Ottermanns for his sympathic concise way of bringing the world of statistics a little closer to me. Thank you for letting me ask all the questions.

Further, I would like to thank Prof. Dr. Heinz Sturm and Dr. Ulrike Braun from the Bundesanstalt für Materialforschung und -prüfung (BAM, Division 6.6, Berlin, Germany) for their extensive efforts to characterize our weathered nanomaterials.

Thanks also extended to Prof. Dr. Kilian Smith (Head of Environmental Chemistry, University of Applied Sciences Magdeburg-Stendal, Germany) and David Kämpfer (Deputy group leader, Institute for Environmental Research, RWTH Aachen University, Germany) for valuable discussions both during the investigation and in preparation of the chapter about 'Trojan-horse' effects.

Special thanks go to my Bachelor and Master students that worked in the frame of my PhD thesis: Philipp Regnery, Fabian Wittmers, Lena Benner, Martin Siedt, Katrin Voigt and Joe Reiser. It was a pleasure to have worked with you guys.

I would like to thank Dr. Hannah Holzmann for the many wonderful hours we spent together. Be it out on the meadow for lunch or hiking with bag and baggage. Thank you for your friendship.

I want to thank my dear colleagues at the Institute for Environmental Research at RWTH Aachen University. Thank you for a great working atmosphere and for the many helping hands. Especially, I want to thank Birgitta Goffart, Brigitte Thiede and Hildegard Patti, our technical assistants, for always contributing good ideas and making my daily lab routine easier with their support.

Einen herzlichen Dank an meine Eltern, meine Schwester und meine Großmutter, die mich zu Hause immer mit offenen Armen empfangen haben und eine erholsame Ablenkung gegenüber dem Uni-Alltag waren. Danke für die vielen amüsanten Gespräche und dass ihr mich, während Studium und Promotion immer unterstützt habt.

Finally, but most of all, I would like to thank my long-time favorite person and partner Duc Trung Luu for his unlimited understanding and support.

This research was supported by the European Project NANO-Transfer that received funding from the Bundesministerium für Bildung und Forschung (BMBF) under agreement with the FP7 ERA-NET SIINN (grant no. 03XP0061A).

Table of contents

List of abbreviations ..... **XV**

List of figures ..... **XVII**

List of tables ..... **XXI**

Summary ..... **XXV**

Zusammenfassung ..... **XXIX**

1 Overall introduction **1**

1.1 Nanomaterials **2**

1.1.1 Overview 2

1.1.2 Carbon nanotubes 3

1.1.3 Environmental fate 4

1.1.4 Interaction of CNT with aquatic biota 5

1.1.5 Adsorption of chemicals on CNT and the "Trojan-horse" phenomenon 6

1.2 The biocide triclocarban **8**

1.2.1 General informations 8

1.2.2 Environmental concentrations 9

1.2.3 Impacts of triclocarban in the environment 10

1.3 Objectives of this study **12**

1.4 References **13**

2 Distribution of weathered multi-walled carbon nanotubes in an aquatic sediment system **21**

2.1 Summary **22**

2.2 Introduction **23**

2.3 Materials and methods **25**

2.3.1 Manufacturing of ^{14}C-labeled MWCNT (^{14}C-MWCNT) 25

2.3.2 MWCNT weathering 25

2.3.3 Origin and preparation of sediment and water 26

2.3.4 Sedimentation of ^{14}C-wMWCNT 27

2.3.5 Distribution of ^{14}C-wMWCNT in an aquatic sediment system 27

2.3.6 Detection and quantification of ^{14}C-wMWCNT 28

2.3.7 Data evaluation and statistical analysis 29

2.4 Results **30**

2.4.1 Sedimentation of ^{14}C-wMWCNT 30

2.4.2 Distribution of ^{14}C-wMWCNT 31

2.5 Discussion **32**

2.6 Conclusion and outlook **35**

2.7 Suplementary information (SI) **36**

2.7.1 Method and results from transmission electron microscopy (TEM) 36

2.7.2 Method and results from thermogravimetric analysis (TGA) and Fourier-transform infrared spectroscopy (FTIR) 37

2.7.3 Detection and quantification of ^{14}C-wMWCNT in a natural sediment sample using liquid scintillation counting (LSC) 38

2.7.4 Data interpretation using CAKE (Computer Assisted Kinetic Evaluation, version 3.3, Tessella) 44
2.7.4.1 Sedimentation experiment 44
2.7.4.1.1 In presence of sediment (+sediment) 44
2.7.4.1.2 In absence of sediment (-sediment) 46
2.7.4.2 Distribution experiment 47
2.8 References 49
***3* Uptake of multi-walled carbon nanotubes associated to green algae in water flea *Daphnia magna – a trophic transfer investigation* 53**
3.1 Summary 54
3.2 Introduction 55
3.3 Materials and methods 57
3.3.1 Manufacturing of ^{14}C-labeled MWCNT (^{14}C-MWCNT) 57
3.3.2 Weathering and dispersion of nanomaterials 57
3.3.3 Settling of ^{14}C-wMWCNT in a static test system 57
3.3.4 Test organisms 58
3.3.5 Micro batch experiments for wMWCNT characterization 58
3.3.6 Quantification of ^{14}C-wMWCNT interaction with green algae 59
3.3.7 Uptake of ^{14}C-wMWCNT by *D. magna* 59
3.3.8 Elimination of ^{14}C-wMWCNT by *D. magna* 61
3.3.9 Uptake of ^{14}C-wMWCNT in a *D. magna* population 61
3.3.10 Data evaluation and statistical analysis 63
3.4 Results 64
3.4.1 Sedimentation of ^{14}C-wMWCNT 64
3.4.2 Nanomaterial characterization 64
3.4.3 ^{14}C-wMWCNT interaction with green algae 66
3.4.4 ^{14}C-wMWCNT uptake and elimination by *D. magna* 67
3.4.5 ^{14}C-wMWCNT uptake by D. magna population 69
3.5 Discussion 71
3.5.1 Dispersion and settling of wMWCNT 71
3.5.2 Nanomaterial interaction with green algae 72
3.5.3 Nanomaterial uptake by *D. magna* 73
3.5.4 Nanomaterial excretion by *D. magna* 75
3.5.5 Accumulation of wMWCNT by *D. magna* population 76
3.6 Conclusion and outlook 77
3.7 Supplementary information (SI) 79
3.7.1 Settling of ^{14}C-wMWCNT 79
3.7.2 Transmission electron microscopy (TEM) 80
3.7.3 Method for density gradient centrifugation 81
3.7.4 Interaction of nanomaterials with green algae 83
3.7.5 Weight of *Daphnia magna* in uptake and excretion experiment 84
3.7.6 Composition of test media 86
3.7.6.1 M4 medium 86
3.7.6.2 Culture medium BG 11 87
3.7.6.3 Culture medium according to Kuhl and Lorenzen (1964) 87
3.8 References 88

4 First quantitative study on accumulation of weathered multi-walled carbon nanotubes in zebrafish *Danio rerio* under simulated environmental conditions 93

4.1 Summary 94

4.2 Introduction 95

4.3 Materials and methods 96

4.3.1 Synthesis and purification of ^{14}C-labeled MWCNT (^{14}C-MWCNT) 96

4.3.2 Weathering of nanomaterials 96

4.3.3 Test organisms 96

4.3.4 Experimental Setup 97

4.3.4.1 Microcosm study I: uptake and elimination of wMWCNT by zebrafish *D. rerio* 97

4.3.4.2 Microcosm study II: bioaccumulation of wMWCNT by *D. rerio* (trophic transfer) 98

4.3.5 Quantification of radioactivity 99

4.3.6 Data evaluation 101

4.4 Results 101

4.4.1 Microcosm study I: uptake of wMWCNT by zebrafish *D. rerio* 101

4.4.2 Microcosm study I: elimination of wMWCNT by zebrafish *D. rerio* 102

4.4.3 Microcosm study II: bioaccumulation of wMWCNT by *D. rerio* (trophic transfer) 103

4.5 Discussion 107

4.6 Conclusion and outlook 109

4.7 Supplementary information (SI) 110

4.7.1 Test organism 110

4.7.2 Sampling, anesthesia and dissection of fish 110

4.7.3 Quantification of ^{14}C-wMWCNT in the water phase in microcosm tanks 111

4.8 References 115

5 A study to investigate the 'Trojan-horse' effect of the biocide triclocarban and weathered multi-walled carbon nanotubes to green algae and freshwater crustacean ... 119

5.1 Summary 120

5.2 Introduction 121

5.3 Materials and methods 123

5.3.1 Synthesis and purification of ^{14}C-labeled MWCNT (^{14}C-MWCNT) 123

5.3.2 Weathering of nanomaterials 123

5.3.3 Adsorption of ^{14}C-triclocarban on weathered MWCNT in freshwater medium 123

5.3.4 Test organisms 125

5.3.5 Algal growth inhibition test 125

5.3.6 *Daphnia magna* acute immobilisation test 127

5.3.7 High performance liquid chromatography (HPLC) 127

5.3.8 Data evaluation 128

5.4 Results 130

5.4.1 Adsorption of TCC on wMWCNT 130

5.4.2 Effects of wMWCNT 132

5.4.3 'Trojan-horse' effects 135

5.4.3.1 Green algae 135

5.4.3.2 Daphnids 138

5.5 Discussion 139

5.5.1 Adsorption of TCC on wMWCNT 139

5.5.2 Effects of wMWCNT 141
5.5.3 'Trojan-horse' effects 144
5.5.3.1 Green algae 144
5.5.3.2 Daphnids 148
5.6 Conclusion and outlook 150
5.7 Supplementary information (SI) 151
5.7.1 Test media composition 151
5.7.2 Calibration curves to determine algal density 152
5.8 References 153
6 Final discussion and statement 159
7 Appendix i
(A) Contributions in publications and chapters ii
(B) Peer-reviewed publications iv
(C) Conference contributions v
(D) Supervision vii

List of abbreviations

-	in absence of
+	in presence of
×	multiplication
µ	growth rate
^{14}C	radiolabeled carbon
^{14}C-MWCNT	radiolabeled MWCNT
^{14}C-TCC	chlorophenyl ring-radiolabeled triclocarban
^{14}C-wMWCNT	radiolabeled and weathered MWCNT
AR	applied radioactivity
BAF	bioaccumulation factor
BCF	bioconcentration factor
Bq	becquerel
C-MNM	carbon-based manufactured nanomaterials
CNT	carbon nanotubes
CO_2	carbon dioxide
C_{POM}	concentration in POM
C_w	freely dissolved concentration (real concentration)
DAM	Dubinin-Ashtakhov model
DMS	dimethyl sulfide
DMSO	dimethyl sulfoxide
DOM	dissolved organic matter
dpm	disintegrations per minute
DRC	dose-response curve
dw	dry weight
$EC_{10/20/50}$	10%/20%/50% effective concentration
ECHA	European Chemicals Agency
ε_{SW}	effective adsorption potential
H_2O_2	hydrogen peroxide
HOC	hydrophobic organic contaminants
HPLC	high performance liquid chromatography
J	joule
k_1	uptake rate constant
k_2	elimination rate constant
K_{MWCNT}	distribution coefficient of TCC between water phase and MWCNT
K_{OW}	octanol-water distribution coefficient
K_{POM}	distribution coefficient of TCC between water phase and POM
LSC	liquid scintillation counting
Lx	lux
M4	M4 Elendt medium (artificial fresh water)
MWCNT	multi-walled carbon nanotubes
NM	nanomaterials
NOEC/LOEC	no/lowest observed effect concentration
NOM	natural organic matter

OECD	Organization for Economic Cooperation and Development, also algal test medium
PAH	polycyclic aromatic hydrocarbons
POM	polyoxymethylene
PPCP	pharmaceutical and personal care products
Q^0	maximum adsorption capacity
R^2	coefficient of determination
RA	radioactivity
REACH	Registration, Evaluation, Authorization and Restriction of Chemicals
rpm	rotations per minute
sw	water solubility
SWCNT	single-walled carbon nanotubes
t	tons
T	temperature (K)
TCC	triclocarban
TEM	transmission electron microscopy
t_{eq}	equilibration time point
UV	ultraviolet
wMWCNT	weathered MWCNT

List of figures

Figure 1.1: Transmission electron microscopy images of carbon nanotubes (pictures were taken by Dr. Nina Siebers from Forschungszentrum Jülich GmbH, Germany). 3

Figure 1.2: Simplified version of the 'Trojan-horse' phenomenon (own illustration). The precondition for a 'Trojan-horse' effect is the adsorption of a chemical substance (e.g., organic contaminant) onto a transporter material (e.g., CNT) and the subsequent uptake of this complex by an organism. After incorporation of the complex, either (1.) desorption of the chemical substance occurs and there is an effect enhancement compared to exposure of the organism to the chemical substance alone, or (2.) adsorption of the contaminant to the carrier material is stable and there is a reduced effect compared to exposure of the organism to the contaminant alone. 7

Figure 1.3: Chemical structure of triclocarban (self-made image based on TCC Consortium 2010). 8

Figure 2.1: Graphical summary of chapter 2. 22

Figure 2.2: Deposition of radioactively labeled and weathered multi-walled carbon nanotubes (^{14}C-wMWCNT) in a water sediment system (+sediment) and in a system containing natural water only (-sediment). A ^{14}C-wMWCNT concentration of 110.7 ± 3.4 µg L^{-1} and 109.2 ± 1.0 µg L^{-1} was applied for +sediment (A) and -sediment (B) scenario, respectively. The proportion of decrease (%) of the applied radioactivity over the test period is shown. Error bars indicate standard deviation on the mean of four replicates. The amount of radioactivity measured at the beginning (0 h) of the test was set to 100%. A SFO (Single First-Order) model using CAKE was fitted to the experimental data. 30

Figure 2.3: Distribution of radioactivity (in % of applied radioactivity) among sediment, water phase, water sediment contact layer, mineralized portion and radioactivity adsorbed to the used glassware over time (2 h, 1, 2, 7, 21 days, 3 and 6 months) after applying ^{14}C-wMWCNT (134.7 ± 12.3 µg L^{-1}) to an aquatic sediment system. Σ: sum of recovered radioactivity. Error bars indicate standard deviation on the mean of four replicates. 31

Figure 2.4: Transmission electron microscopy (TEM) images of pristine (A) and weathered (B) MWCNT (unlabeled) (taken by Dr. Nina Siebers from Forschungszentrum Jülich GmbH). 36

Figure 2.5: TGA and FTIR analyses of pristine (continuous line) and weathered (dashed line) multi-walled carbon nanotubes (MWCNT). Mass loss refers to an initial weight of 2.91 mg and 3.19 mg of pristine and weathered MWCNT, respectively. 37

Figure 3.1: Graphical summary of chapter 3. 54

Figure 3.2: Deposition of ^{14}C-wMWCNT in a static water phase (M4 medium) over 21 days (d). The measured amount of radioactivity at t = 0 d was set to 100%. The proportion of decrease (%) of the initially applied radioactivity over the test period is shown. An exponential decay equation model was fitted to the experimental data. Data points represent single replicates (n = 4). (R^2 = coefficient of determination) 64

Figure 3.3 (A - E): Transmission electron microscopy (TEM) images of wMWCNT in association with green alga *R. subcapitata* (A), wMWCNT dispersion (0.1 mg L-1) (B) and excreted wMWCNT by *D. magna* after uptake period of 24 h (C). D and E show the light microscopy image of an adult *D. magna* exposed to 100 µg wMWCNT L^{-1} and without exposure over a period of 72 h, respectively. 65

Figure 3.4: Weathered multi-walled carbon nanotube (wMWCNT) concentration linked to green algae over time. A ^{14}C-wMWCNT concentration of 100 µg L^{-1} was applied to suspensions of *R. subcapitata* (circles) and *C. reinhardtii* (squares) (A). The mean values and standard deviations are given (n = 4). For all timepoints, mean values for uptake of wMWCNT in *R. subcapitata* and *C. reinhardtii* proved to be significantly different (visualized using the letters a and b, t-test, α = 0.05). An exponential fit was plotted for the corresponding growth curves, algal density (cells mL^{-1}) was measured over time in uptake experiment (B). Growth rates for *C. reinhardtii* and *R. subcapitata* are µ = 0.014 h^{-1} and µ = 0.010 h^{-1}, respectively. A significant difference over time was identified (two-sample t-test). Data points represent single replicates (n = 4). 67

Figure 3.5: Uptake of ^{14}C-wMWCNT in *D. magna* after waterborne exposure (circles) and trophic transfer (asterisks). For trophic transfer green algae *R. subcapitata* was pre-loaded by radioactively labeled wMWCNT over 72 hours (h). A one compartment model (R^2 = 0.96) was fitted to experimental data of uptake via water exposure (solid line, 0 h – 18 h). Additionally, the further course of the modelling is shown (dotted line). An exponential fit was adapted to areas with uptake decline for water exposure (dashed line, 18 h – 72 h) and trophic transfer (dashed line) scenario. Error bars indicate standard deviation (n = 4). For all timepoints, mean values of uptake *via* water exposure and trophic transfer proved to be significantly different (visualized using the letters a and b, t-test, α = 0.05). 68

Figure 3.6: Internal ^{14}C-wMWCNT concentration in *D. magna* after depuration over a period of 48 hours (h). Start wMWCNT-concentration in -algae (circles) and +algae (asterisks) scenario was calculated from five and seven replicates, respectively. *Daphnia* were fed with green algae (0.1 mg carbon) after transfer to clean medium. Elimination rates (k_2) were determined (exponential fit) to 0.032 h^{-1} and 1.079 h^{-1} in scenario -algae and +algae, respectively. Elimination in presence and absence of algae was significantly different over time (two-sample t-test). Error bars indicate standard deviation (n = 4). 69

Figure 3.7: *D. magna* population dynamics. In 800 mL M4 medium, a population of *D. magna* developed from initially 5 neonate and 3 adult animals over 28 days. *D. magna* were fed daily 0.5 mg carbon (green algae). Two wMWCNT concentrations were tested: 0 mg L^{-1} (Control, circles) and 0.1 mg L^{-1} (asterisks). The total number of individuals over time is given. Error bars indicate the standard deviation on the mean of four replicates (n = 4). The combination of the letters a and b visualizes the identified significant difference (t-test, α = 0.05). 70

Figure 3.8: Uptake of ^{14}C-wMWCNT in a developing *D. magna* population over 28 days. Renewal of medium and simultaneous reapplication of ^{14}C-wMWCNT was performed once a week. Error bars indicate standard deviations for arithmetic average of four replicates (n = 4). 70

Figure 3.9: Graphical Summary (Hockey Stick model, CAKE). 79

Figure 3.10: Transmission electron microscope (TEM) images from green alga *Raphidocelis subcapitata* associated with wMWCNT. Associated wMWCNT were highlighted by a black arrow or a white circle (contact site was enlarged). (Pictures were taken by Dr. Nina Siebers from Forschungszentrum Jülich GmbH). 80

Figure 3.11: Three layers bottom up: Ludox, algae and water (distilled water and medium) after density gradient centrifugation. 81

Figure 3.12: Presumptive agglomerates of wMWCNT in uptake experiment with *Raphidocelis subcapitata*, observed after 72 h of exposure. 83

Figure 3.13: Dry weight of *Daphnia magna* neonates (10 individuals) after water exposure and trophic transfer (dietary exposure) to ^{14}C-wMWCNT over a period of 72 hours. 84

Figure 3.14: Dry weight of *Daphnia magna* neonates (10 individuals) after uptake of ^{14}C-wMWCNT for 24 h and an elimination period of 48 h in presence (+algae) and absence (-algae) of food. ... 85

Figure 4.1: Graphical summary of chapter 4. 94

Figure 4.2: Experimental setup for uptake and elimination of wMWCNT by zebrafish *Danio rerio* (microcosm study I). 98
Figure 4.3: Experimental setup for bioaccumulation of wMWCNT by *Danio rerio* (trophic transfer, microcosm study II). 100
Figure 4.4: Concentration of weathered multi-walled carbon nanotubes (wMWCNT) in zebrafish *Danio rerio* for uptake and elimination scenarios in function of time. (A) Uptake of wMWCNT in digestive tract of zebrafish (asterisks, left Y-axis, Y1) and complete fish (unfilled circles, right Y-axis, Y2) after exposure to 100 µg wMWCNT L^{-1} via water phase. A one compartment model (blue dotted line) is fitted to the data. (B) Uptake of wMWCNT in digestive tract of zebrafish (asterisks, left Y-axis, Y1) and complete fish (unfilled circles, right Y-axis, Y2) after exposure to 100 µg wMWCNT L^{-1} via water phase and to a wMWCNT pre-contaminated population of *Daphnia magna*. (C) Elimination of wMWCNT from digestive tract of zebrafish and (D) from complete fish in clean fish water, after uptake of 100 µg wMWCNT L^{-1} via water phase over two weeks. An exponential model is fitted to data sets from elimination experiment (R^2: coefficient of determination). 103
Figure 4.5: Distribution of ^{14}C-wMWCNT in fish water (45 L) after application (0 h) and during test period in the uptake (tank 1 (A)) and elimination experiment (uptake phase, tank 2 (B)). Water renewals and the simultaneous application of 0.1 mg wMWCNT L^{-1} (black dashed line) were performed after 72, 168 and 240 h. On days of the water change the radioactivity in the water phase was measured twice, once before (black triangles) and once after the water change (red triangles). Four replicates were drawn out of one tank. 111
Figure 5.1: Graphical summary of chapter 5. 120
Figure 5.2: Experimental design in adsorption study to determine the distribution of ^{14}C-triclocarban (^{14}C-TCC) between water phase and weathered multiwalled carbon nanotubes (wMWCNT). (1.) Two-phase and (2.) three-phase test system with polyoxymethylene (POM) for the determination of distribution coefficients K_{POM} and K_{wMWCNT}, respectively. In both approaches, six different ^{14}C-TCC concentrations were tested. The distribution of ^{14}C-TCC between water phase and nanomaterial was investigated for three different wMWCNT concentrations: 100, 400 and 1000 µg L^{-1}. Incubation for all samples was at 18 ± 1 °C for 21 days horizontal on a laboratory shaker (120 rpm, dark). 124
Figure 5.3: Example chromatogram of a control sample generated in the sorption study. The signal strength (mAU/cps (counts per second)) is plotted against time. The retention time for the ^{14}C-TCC standard was 9.52 min for radioactive channel and 9.22 min for DAD detector. Peak area was integrated using software Elysia Raytest GINA X™ (Version 10.1, Servicepack 2). 128
Figure 5.4: Logarithmic isotherm for the sorption of ^{14}C-TCC on POM (A) and sorption isotherms for the adsorption of ^{14}C-TCC on wMWCNT in three different nanomaterial concentrations (100, 400 and 1000 µg L^{-1}) (B). C_W is the TCC concentration in aqueous phase (µg L^{-1}), C_{POM} represents the absorbed TCC concentration to POM (µg kg^{-1}) and C_{CNT} demonstrates the TCC concentration adsorbed to wMWCNT (µg kg^{-1}). In A, data points represent the mean on four replicates ± standard deviation, the dashed trend line was fitted using Microsoft Excel®. In B, single replicates are shown (n = 4), the coloured lines were fitted using the parameters received from the Dubinin-Astakhov model (DAM) (Microsoft Excel®, GraphPad Prism 5). (R^2 = coefficient of determination). 131
Figure 5.5: Toxicity of wMWCNT to green algae *Raphidocelis subcapitata* (A, B) and *Chlamydomonas reinhardtii* (C, D) at low (left panels A and C) and high (B and D) wMWCNT concentrations. A wMWCNT concentration range from 0.1 to 16 mg L^{-1} was tested. Algal cell count (yield per time point, mean of n = 3 and standard deviations) is plotted against nanomaterial concentration. Investigated time units were 0, 24, 48 and 72 hours. Data sets were evaluated using ToxRat® and asterisk show significant differences to control samples for yield end point. 133

Figure 5.6: Dose response curves (DRC) after a test on acute immobilization (%) of *D. magna* at different wMWCNT concentrations in the presence (green squares) and absence of food (blue circles) over 48 hours. Data points show the mean of four replicates. Solid lines demonstrate the Probit fit of DRC. Dotted lines show the lower and upper 95% confidence intervals for the – food scenario. For the + food scenario no 95% confidence intervals could be determined by using ToxRat®. 134

Figure 5.7: Dose response curves (DRC) after investigating growth inhibition (%) of different triclocarban (TCC) concentrations in the presence (yellow circles) and absence of 100 µg wMWCNT L^{-1} (green squares) to the green algae *Chlamydomonas reinhardtii* (A, B) and *Raphidocelis subcapitata* (C, D) over 72 hours. Growth inhibition was plotted against nominal TCC concentration (A, C) and against the freely dissolved TCC concentration (B, D). Data points show single values of three replicates. Solid and dashed lines illustrate the Probit fit of DRC. Dotted lines show the lower and upper 95% confidence intervals calculated by ToxRat®. .. 136

Figure 5.8: Algal growth inhibition test - investigating the effect of various wMWCNT concentrations (mg L^{-1}) on the toxicity of triclocarban (TCC) to green algae *Chlamydomonas reinhardtii* (A) and *Raphidocelis subcapitata* (B). Nominal TCC concentration was 51 µg L^{-1} for *C. reinhardtii* and 60 µg L^{-1} for *R. subcapitata*. The obtained yield of algal cells after 0, 24, 48 and 72 hours is given. PC TCC: positive control of TCC without the application of wMWCNT. Whiskers indicate standard deviation on the mean of three replicates..... 137

Figure 5.9: Dose response curves (DRC) after investigating acute immobilization (%) of *D. magna* at different triclocarban (TCC) concentrations (nominal, µg L^{-1}) in the presence (red circles) and absence (blue squares) of 100 µg wMWCNT L^{-1} over 48 hours. Immobilization (%) was plotted against nominal TCC concentration (A) and against the freely dissolved TCC concentration (B). Data points show the mean of four replicates. Solid and dashed line reveal the Probit fit of DRC. Dotted lines represent the 95% confidence intervals calculated using ToxRat®. 138

Figure 5.10: Considerations about possible mechanisms after the mixed exposure of weathered multi-walled carbon nanotubes (wMWCNT) and the biocide triclocarban towards green algae. The extent of sorption depends on the ratio of wMWCNT to TCC in aqueous phase: low concentrations of nanomaterial lead to incomplete sorption of TCC, i.e., freely dissolved TCC is still bioavailable. Arrows represent: ↑ enhanced toxicity expected, ↓ decreased toxicity expected and → unaltered toxicity expected. Self-made illustration based on Naasz et al. (2018)..... 146

Figure 5.11: Calibration curves for the conversion of measured extinction (excitation wavelength: 485 nm, emission wavelength: 685 nm) to algal density (cells mL^{-1}) for the green algae *Chlamydomonas reinhardtii* (A) and *Raphidocelis subcapitata* (B). Enumeration of algal cells was performed in the test medium described in Tab. 5.5. (R^2 = coefficient of determination). 152

List of tables

Table 1.1: Characteristics on the antibacterial agent triclocarban. 8
Table 2.1: Data modelling using Tessella CAKE (version 3.3) for the sedimentation of ^{14}C-wMWCNT in an aquatic sediment system over 28 days and over six months in a deposition and a partitioning study, respectively. The chosen compartment model was Single First-Order (SFO). Half-life (DT_{50}) and disappearance times after 90 days (DT_{90}) are given. Additional statistical characteristics are Chi^2 (error in %) and r^2 (observed vs. predicted data). 32
Table 2.2: Results from preliminary experiment – quantification of radioactivity amount of ^{14}C-wMWCNT in natural sediment samples using liquid scintillation counting (LSC). Five ^{14}C-wMWCNT concentrations (I – V) were applied to dried sediment samples (two replicates (repl.) per concentration) and an amount of ≤ 0.05 g sediment was subsequently measured by means of LSC to quantify the enclosed amount of radioactivity (RA). The shown RA amounts in samples (Becquerel = Bq) were derived from the 10 min LSC measurements. Arithmetic mean (Mean) and standard deviation (SD) are given for every specification. 39
Table 2.3: Results from preliminary experiment – quantification of radioactivity amount of ^{14}C-wMWCNT in natural sediment samples using liquid scintillation counting (LSC). The applied radioactivity (RA) amount per sediment sample (20.1 ± 0.1 g) in Becquerel (Bq) is given. Additionally, the target RA in 0.01 g sediment was calculated to compare the amount to the recovered RA in 0.01 g sediment. Also, the total recovery is presented and arithmetic mean (mean) and standard deviation (SD) was calculated (in %). 43
Table 3.1: Statistical characteristics for all data (Hockey Stick model, CAKE). 79
Table 3.2: Total associated amount of wMWCNT (µg) to *C. reinhardtii* and *R. subcapitata* and the total dry weight of green algae in one sample (100 mL) from the experiment on interaction of wMWCNT with green algae. A total amount of 12 – 13 µg ^{14}C-wMWCNT was applied at test start. Values listed in the table were estimated by extrapolation of the subsamples taken during the experiment. The means and standard deviations on four replicates are given. 83
Table 3.3: Dry weight (mg) of *Daphnia magna* neonates (10 individuals) in uptake experiment (water exposure and trophic transfer (dietary exposure)). SD = standard deviation. 84
Table 3.4: Dry weight (mg) of *Daphnia magna* neonates (10 individuals) in excretion experiment (food conditions: -algae and + algae). SD = standard deviation. 85
Table 3.5: Composition and preparation of M4 medium for tests with *D. magna*. Stock and test solutions were prepared using deionized water. The vitamin stock was stored frozen in small aliquots. Vitamins were added to the prepared media shortly before use. For more information see OECD No. 202. 86
Table 3.6: Composition and preparation of culture medium BG 11 for tests with *C. reinhardtii*. Stock and test solutions were prepared using deionized water. The medium was prepared according to BG 11 medium for Cyanobacteria provided by the Culture Collection of Algae (SAG, Göttingen University). 87
Table 3.7: Composition and preparation of culture medium according to Kuhl and Lorenzen (1964) for tests with *R. subcapitata*. Stock and test solutions were prepared using deionized water. ... 87
Table 4.1: Partitioning of wMWCNT in different compartments of zebrafish (microcosm study I, uptake experiment). *D. rerio* was exposed to 100 µg ^{14}C-wMWCNT L^{-1} in fish water (water phase exposure) over 14 days (336 h). The percentage of the total amount of recovered radioactivity (%) in different compartments of zebrafish is presented. The sum depicts the total amount of wMWCNT associated (ingested or attached) to one single fish and is expressed as wMWCNT in µg. The mean value (Mean) and standard deviation (SD) on six replicates (five replicates after 168 h) is shown. 104

Table 4.2: Partitioning of wMWCNT in different compartments of zebrafish (microcosm study I, elimination experiment). *D. rerio* was exposed to 100 µg ^{14}C-wMWCNT L^{-1} in fish water (water phase exposure) over 14 days, followed by a 96 h depuration period. The percentage of the total amount of recovered radioactivity (%) in different compartments of zebrafish is presented. The sum depicts the total amount of wMWCNT associated to one single fish and is expressed as wMWCNT in µg. The mean value (Mean) and standard deviation (SD) on six replicates is shown. 105

Table 4.3: Partitioning of wMWCNT in different compartments of zebrafish (microcosm study II). *D. rerio* was exposed to 100 µg ^{14}C-wMWCNT L^{-1} in fish water (water phase exposure) over 96 h, whereby the test system additionally contained ^{14}C-wMWCNT pre-exposed *D. magna* of all sizes. The percentage of the total amount of recovered radioactivity (%) in different compartments of zebrafish is presented. The sum depicts the total amount of wMWCNT associated to one single fish and is expressed as wMWCNT in µg. The mean value (Mean) and standard deviation (SD) on six replicates is shown. 106

Table 4.4: Partitioning of wMWCNT in different compartments of zebrafish (microcosm study I, uptake experiment). *D. rerio* (wet weight: 306 ± 79 mg) was exposed to 100 µg ^{14}C-wMWCNT L^{-1} in fish water (waterborne exposure) over 14 days (336 h). The uptake of wMWCNT in different compartments of zebrafish and per complete fish is presented (µg g^{-1} dw^{-1}). The respective dry weight of every single fish is represented (mg). The mean value (Mean) and standard deviation (SD) on six replicates (five replicates after 168 h) is shown. 112

Table 4.5: Partitioning of wMWCNT in different compartments of zebrafish (microcosm study I, elimination experiment). *D. rerio* (wet weight: 331 ± 60 mg) was exposed to 100 µg ^{14}C-wMWCNT L^{-1} in fish water (waterborne exposure) over 14 days, followed by a 96 h depuration period. The uptake of wMWCNT in different compartments of zebrafish and in complete fish is presented (µg g^{-1} dw^{-1}). The respective dry weight of every single fish is represented (mg). The mean value (Mean) and standard deviation (SD) on six replicates is shown. 113

Table 4.6: Partitioning of wMWCNT in different compartments of zebrafish (microcosm study II). *D. rerio* (wet weight: 310 ± 89 mg) was exposed to 100 µg ^{14}C-wMWCNT L^{-1} in fish water (water phase exposure) over 96 h, whereby the test system additionally contained ^{14}C-wMWCNT loaded *D. magna* of all sizes. The uptake of wMWCNT in different compartments of zebrafish and in complete fish is presented (µg g^{-1} dw^{-1}). The respective dry weight of every single fish is represented (mg). The mean value (Mean) and standard deviation (SD) on six replicates is shown. 114

Table 5.1: Gradient program of the used HPLC method. 128

Table 5.2: Distribution coefficients (log K_{wMWCNT}) ± standard deviation and fitting parameters ± standard error of the sorption isotherms (Dubinin-Astakhov model, DAM) describing the distribution of ^{14}C-triclocarban between aqueous solution and dispersed wMWCNT in three different concentrations (100, 400 and 1000 µg L^{-1}). DAM was applied using GraphPad Prism 5 (USA). (R^2: coefficient of determination) 132

Table 5.3: Effect concentrations (72 h) for the exposure of green algae *Chlamydomonas reinhardtii* and *Raphidocelis subcapitata* to various wMWCNT concentrations (mg L^{-1}). Yield and growth rate were investigated for endpoints. $EC_{10/20/50}$: effective concentration for 10/20/50% reduction; NOEC: no observed effect concentration; LOEC: lowest observed effect concentration. (LCL-UCL): lower 95% confidence limit to upper 95% confidence limit. 134

Table 5.4: Summary of toxicological endpoints for green algae *C. reinhardtii* and *R. subcapitata* and crustacean *D. magna* in triclocarban (TCC, µg L^{-1}) effect studies in presence (+ wMWCNT) and absence of wMWCNT. TCC_{nom} represents the nominal applied TCC concentration to the tests, whereas $TCC_{fDissolved}$ stands for the calculated fraction of freely dissolved TCC in the test system with wMWCNT. The listed $EC_{10/20/50}$ (EC = effect concentration) gives the TCC concentration at which 10, 20 and 50% effect occurs. NOEC: no observed effect concentration; LOEC: lowest observed effect concentration. For green algae, the inhibition of growth rate after 72 h was investigated as endpoint. In case of *D. magna*, immobility after 48 h was recorded. L/UCL: lower and upper confidence limit. 139

Table 5.5: Composition of the aqueous phase in the test for the adsorption of triclocarban on weathered MWCNT. The medium is a deviation of the OECD algal growth medium from OECD Guideline No. 201 (OECD, 2006). For sterilisation, the stock solutions were either filtered using a membrane filtration (pore diameter: 0.2 µm) or by autoclaving (120 °C, 15 min) and stored at 4 °C in the dark. 151

Table 6.1: Summary of maximum body burdens and accumulation factors for uptake of wMWCNT (0.1 mg L^{-1}) by different freshwater organisms at various test conditions. 161

Summary

In recent years, the production of carbon nanotubes (CNT) has been optimized to an industrial scale extent. Therefore, and due to the widespread application of CNT in various consumer products, an increased release of the nanomaterials into the aquatic environment can be expected. Since only little is known about their distribution among different aquatic compartments, the partitioning of radiolabeled and weathered multi-walled CNT (^{14}C-wMWCNT) in an aquatic sediment system over a period of 180 days (d) was investigated. The application of a nanomaterial concentration of 100 µg L^{-1} was performed via the water phase. Over time, the applied wMWCNT deposited exponentially from the water phase and accumulated in the sediment phase. After two hours of incubation just 77%, after seven days 30% and after 180 d only 0.03% of the applied radioactivity (AR) remained in the water phase. The respective values for the disappearance times DT_{50} and DT_{90} were 3.2 d and 10.7 d. In addition, minor mineralization of ^{14}C-wMWCNT to $^{14}CO_2$ was observed with values below 0.06% of AR.

Moreover, a study was performed to estimate the settling of wMWCNT in a water phase in the presence and absence of a sediment phase for 28 d in an agitated test system. We found no influence of a sediment phase on the sedimentation behavior of wMWCNT in the water phase: after 6.5 d and 7.3 d 50% of the applied wMWCNT subsided with and without sediment, respectively. At static test conditions we found a DT_{50} of 3.9 d and a DT_{90} of 12.8 d. The slow removal of wMWCNT from the water body by deposition into sediment implies that in addition to sediment-dwelling organisms, pelagic organisms are also at risk of exposure to CNT and vulnerable to nanomaterial accumulation.

The impact of CNT on pelagic organisms was investigated in further studies. At first, experiments to examine the uptake of ^{14}C-wMWCNT (100 µg L^{-1}) in green algae, daphnids and fish were performed. We showed that wMWCNT interact and associate with the green algae *Chlamydomonas reinhardtii* and *Raphidocelis subcapitata*. A maximum for nanomaterial accumulation of 1.6 ± 0.4 µg ^{14}C-wMWCNT mg^{-1} dry weight^{-1} (dw^{-1}) and 0.7 ± 0.3 µg ^{14}C-wMWCNT mg^{-1} dw^{-1} after 24 h and 48 h was observed, respectively. To study trophic transfer, *R. subcapitata* was subsequently loaded with ^{14}C-wMWCNT and fed to primary consumer *Daphnia magna*. Trophic transfer of wMWCNT in daphnids was compared to ^{14}C-wMWCNT uptake by the water fleas from the water phase without algae. A maximum body burden of 0.07 ± 0.01 µg mg^{-1} dw^{-1} and 7.1 ± 1.5 µg mg^{-1} dw^{-1} for *D. magna* was measured after trophic transfer and waterborne exposure, respectively. This result indicated no CNT accumulation after short-term exposure by trophic transfer. Additionally, an elimination of the accumulated nanomaterials from the organisms' guts was demonstrated and feeding algae facilitated their excretion.

A study on accumulation of ^{14}C-wMWCNT in a growing population of *D. magna* revealed further a maximum uptake of 0.7 ± 0.2 µg mg^{-1} dw^{-1}. And therefore, the calculated bioaccumulation factor (BAF)

after 28 d of 6700 ± 2900 L kg^{-1} is above the limit that indicates a chemical is bioaccumulative in the European Union Regulation REACH and this is why food chain transport can be assumed.

In an aquatic ecosystem, organisms from the first-line to the top trophic level can be affected due to nanomaterial exposure. To address this concern, moreover, we investigated the accumulation of ^{14}C-wMWCNT in the zebrafish *Danio rerio* in microcosm experiments. The distribution of nanomaterials in different body compartments, e. g. gill and gastrointestinal tract, was quantified. Uptake of 100 µg ^{14}C-wMWCNT L^{-1} in *D. rerio* was determined over a period of two weeks via water phase exposure. The mean uptake over time was 91 µg wMWCNT g^{-1} dw^{-1} and the main part (> 50%) of CNT uptake thereby was localized in the gastrointestinal tract. The calculated BAF was 851 L kg^{-1}. Elimination of accumulated wMWCNT over time was observed in all investigated body compartments. The animals were fed twice daily and a body burden at the end of the elimination phase of 1.9 ± 1.3 µg wMWCNT g^{-1} dw^{-1} was obtained.

A second experiment was performed by exposing *D. rerio* to a ^{14}C-wMWCNT loaded *Daphnia* population. At the time of exposure of the zebrafish, a body burden of 1.5 ± 0.3 µg wMWCNT mg^{-1} dw^{-1} was calculated for *D. magna*. During the test period of 96 h a mean wMWCNT body burden for the zebrafish of 96 µg wMWCNT g^{-1} dw^{-1} was quantified. The wMWCNT accumulated mostly in the gastrointestinal tract (> 80%) as well, which indicates that the uptake of the nanomaterials by consumers occurs mainly via the alimentary system.

Moreover, CNT are known to adsorb organic compounds and thus the fate of environmental pollutants might be changed. Hence, the interaction of unlabeled weathered multi-walled CNT (wMWCNT) and the biocide triclocarban (TCC) was examined. Effect studies with both, nanomaterial and antibacterial agent (in single and combined approaches), on growth of *Chlamydomonas reinhardtii* and *Raphidocelis subcapitata* and immobilization of *Daphnia magna* were performed. For combined approaches so called 'Trojan-horse' effects (a chemical adsorbs onto a carrier material like CNT and the complex is subsequently taken up by an organism) were investigated. At first, the adsorption of TCC onto different wMWCNT concentrations was determined using radiolabeled TCC (^{14}C-TCC) and with a log K_{wMWCNT} value of 7.36 ± 0.44 L kg^{-1} a strong adsorption capacity of wMWCNT towards TCC was identified. Ecotoxicity tests showed that the exposure to wMWCNT alone reveal first effects in the mg L^{-1} range for green algae and crustacean. TCC alone caused 50% effect (EC_{50}) at 20.6 µg L^{-1}, 22.1 µg L^{-1} and 36.5 µg L^{-1} in *D. magna*, *C. reinhardtii* and *R. subcapitata*, respectively. After the addition of 100 µg wMWCNT L^{-1} to the test series with TCC in the algal growth inhibition test, a reduction in toxicity for *C. reinhardtii* and an increase in toxicity for *R. subcapitata* was observed. The inhibitory effect of TCC on green algae was reduced when wMWCNT concentrations above 100 µg L^{-1} were added to the test medium. Above 1 mg wMWCNT L^{-1} no difference to the control was detected

for both algal species. For *D. magna*, the addition of 100 µg wMWCNT L^{-1} had no impact on TCC toxicity regarding immobilization. Because of our results and the fact that algae do not absorb CNT to a large extent, we conclude no 'Trojan-horse' effect for the tested green algae. However, the strong adsorption of TCC to CNT and the well-accumulated nanomaterials in *Daphnia magna* suggest a true 'Trojan-horse' effect for water fleas.

In summary, the results show that the long residence time of CNT in the water column, ranging from several days to weeks, and their accumulation in sediment lead to the exposure of benthic as well as pelagic organisms. Aquatic sediment systems with different properties and various types of CNT should be designed and investigated to confirm our findings of long-term stability of CNT and their distribution in such systems. Water dispersed CNT bind to algal cells to a large extent and therefore green algae associated CNT might promote food web transfer. In case of *D. magna*, trophic transfer resulted in orders of magnitude lower body burdens compared to waterborne exposure indicating no bioaccumulation. On the other hand, the investigation of CNT uptake in a growing *D. magna* population revealed a steady state body burden in daphnids after 14 days (BAF >2000) but no toxic effects compared to the control groups. Thus, the results indicate that an accumulation of CNT by *D. magna* is possible, but dependent on the given environmental conditions (e.g., water volume, dispersion of nanomaterials).

Bioaccumulation of CNT does not occur in the classical sense, since the nanomaterials, regardless of the test organism (primary or secondary consumer), are mainly absorbed via the gastrointestinal tract from which the absorbed CNT are subsequently excreted. It remains to be investigated whether and to what extent the ingested CNT cause long-term damage to the exposed animals. Finally, long residence times of CNT at low concentrations in the water phase increase the interaction of nanomaterials and pelagic organisms and therefore might lead to food-chain transport of CNT.

Moreover, acute effects of MWCNT on green algae and crustacean are expected in the mg L^{-1} range, concluding no risk with the current magnitudes lower predicted environmental concentration. For the same reason, no influence of CNT on the fate of the aquatic contaminant TCC is expected in the environment. Only at very high nanomaterial concentrations (mg L^{-1}), adsorption of TCC was quantitatively large enough to change the test outcome. But with the current increase of CNT production, besides the monitoring of this single nanomaterial, mixture and 'Trojan-horse' effects need to be considered as well.

Zusammenfassung

Die Produktion von Kohlenstoffnanoröhren (englisch: carbon nanotubes, CNT) ist in den letzten Jahren deutlich angestiegen und hat ein industrielles Ausmaß erreicht. Nicht nur an Produktionsorten, sondern auch durch den vermehrten Einsatz von CNT in verschiedenen Anwendungsbereichen, kann von einer erhöhten Freisetzung der Nanomaterialien in Ökosysteme unserer Erde ausgegangen werden. Über deren Verteilung in verschiedenen aquatischen Kompartimenten ist nur wenig bekannt, deshalb wurde zunächst die Verteilung von radioaktiv markierten (^{14}C) und verwitterten (englisch: weathered) mehrwandigen CNT (^{14}C-wMWCNT) in einem Wasser/Sedimentsystem über einen Zeitraum von 180 Tagen (d) untersucht. Die Applikation der Nanomaterialkonzentration von 100 µg L^{-1} erfolgte über die Wasserphase. Mit der Zeit sind die applizierten wMWCNT exponentiell aus der Wasserphase absedimentiert und haben sich gleichzeitig in der Sedimentphase angereichert. Nach einer zweistündigen Inkubation verblieben noch 77 %, nach sieben Tagen 30 % und nach 180 d nur noch 0,03 % der applizierten Radioaktivität (AR) in der Wasserphase. Die entsprechenden Werte für die Zeiten mit der die ^{14}C-wMWCNT zu 50 % (DT_{50}) und 90 % (DT_{90}) aus der Wasserphase verschwunden sind (dissipation time, DT) betrugen 3,2 d und 10,7 d. Darüber hinaus wurde eine sehr geringe Mineralisierungsrate von ^{14}C-wMWCNT zu $^{14}CO_2$ mit Werten unter 0,06 % der AR beobachtet.

Des Weiteren wurde eine Studie durchgeführt, um die Absedimentation von wMWCNT in einer Wasserphase in An- und Abwesenheit einer Sedimentphase über einen Zeitraum von 28 d in einem unsteten Testsystem abzuschätzen. Es konnte kein Einfluss einer Sedimentphase auf das Sedimentationsverhalten von wMWCNT in einer Wasserphase festgestellt werden. Nach 6,5 d und 7,3 d sedimentierten jeweils 50 % der applizierten wMWCNT mit bzw. ohne Sediment ab. Unter statischen Testbedingungen konnte eine DT_{50} von 3,9 d und eine DT_{90} von 12,8 d beobachtet werden. Die verzögerte Sedimentation von wMWCNT in einem Wasserkörper und deren Ablagerung im Sediment impliziert, dass, zusätzlich zu den im Sediment lebenden Organismen, auch pelagische Organismen einem Expositionsrisiko durch CNT ausgesetzt sind und folglich für eine Akkumulation des Nanomaterials empfänglich sind.

Die Auswirkungen von wMWCNT auf pelagische Organismen wurden in weiteren Studien untersucht. Zunächst wurden Experimente zur Untersuchung der Aufnahme von ^{14}C-wMWCNT (100 µg L^{-1}) in Grünalgen, Daphnien und Fischen durchgeführt. Es konnte gezeigt werden, dass wMWCNT mit den Grünalgen *Chlamydomonas reinhardtii* und *Raphidocelis subcapitata* interagieren und assoziieren. Die entsprechende maximale ^{14}C-wMWCNT Aufnahme lag bei 1,6 ± 0,4 µg mg^{-1} Trockengewicht^{-1} (dw^{-1}) nach 24 h und bei 0,7 ± 0,3 µg mg^{-1} dw^{-1} nach 48 h. Zur Untersuchung des Nahrungsnetztransfers wurde *R. subcapitata* anschließend mit ^{14}C-wMWCNT beladen und folglich an den Primärkonsumenten *Daphnia magna* verfüttert. Die Anreicherung von ^{14}C-wMWCNT in Daphnien über den

Nahrungstransfer wurde mit der ^{14}C-wMWCNT Aufnahme durch die Wasserflöhe aus der Wasserphase ohne Algen verglichen. Es wurde jeweils eine maximale Körperbelastung von 0,07 ± 0,01 µg mg^{-1} dw^{-1} nach Nahrungstransfer und von 7,1 ± 1,5 µg mg^{-1} dw^{-1} nach Wasserexposition ohne Futterzugabe für *D. magna* gemessen. Dieses Ergebnis deutet daraufhin, dass eine kurzfristige CNT Exposition mittels Nahrungstransfer zu keiner Anreicherung der Nanomaterialien führt. Darüber hinaus wurde eine Elimination der akkumulierten Nanomaterialien aus dem Magen-Darm-Trakt der Organismen nachgewiesen, wobei die Fütterung von Algen deren Ausscheidung erleichterte.

Eine weitere Studie zur Akkumulation von ^{14}C-wMWCNT in einer heranwachsenden Population von *D. magna* ergab weiterhin eine maximale Aufnahme von 0,7 ± 0,2 µg mg^{-1} dw^{-1}. Damit liegt der berechnete Bioakkumulationsfaktor (BAF) nach 28 d mit 6700 ± 2900 L kg^{-1} über dem Grenzwert, der eine Chemikalie nach der EU-Verordnung REACH als bioakkumulierend ausweist, weshalb von einem Transport entlang der Nahrungskette ausgegangen werden kann.

In einem aquatischen Ökosystem können Organismen von der untersten bis zur obersten trophischen Ebene durch die Exposition gegenüber Nanomaterialien beeinträchtigt werden. Um diesen Aspekt zu betrachten, wurde die Akkumulation von ^{14}C-wMWCNT im Zebrabärbling *Danio rerio* in Mikrokosmos-Experimenten untersucht. Die Verteilung der Nanomaterialien in verschiedenen Körperteilen des Fisches (z. B. Kiemen und Magen-Darm-Trakt) wurde quantifiziert. Die Aufnahme von 100 µg ^{14}C-wMWCNT L^{-1} in *D. rerio* wurde über einen Zeitraum von zwei Wochen mittels Wasserphasenexposition bestimmt. Die mittlere Aufnahme über die Zeit betrug 91 µg wMWCNT g^{-1} dw^{-1} und der Hauptteil (> 50 %) der CNT-Aufnahme war dabei im Gastrointestinaltrakt lokalisiert. Der berechnete BAF betrug 851 L kg^{-1}. Die Ausscheidung von akkumulierten wMWCNT über die Zeit wurde in allen untersuchten Körperkompartimenten beobachtet. Die Tiere wurden zweimal täglich gefüttert und es wurde eine Körperbelastung am Ende der Eliminationsphase von 1,9 ± 1,3 µg wMWCNT g^{-1} dw^{-1} ermittelt.

In einem zweiten Experiment wurde *D. rerio* an einer mit ^{14}C-wMWCNT beladenen Daphnien-population exponiert. Zum Zeitpunkt der Exposition der Zebrafische wurde für *D. magna* eine Körperbelastung von 1,5 ± 0,3 µg mg^{-1} dw^{-1} berechnet. Über die Testdauer von 96 h wurde eine mittlere wMWCNT-Körperbelastung für die Zebrafische von 96 µg wMWCNT g^{-1} dw^{-1} gemessen. Ebenfalls in diesem Testdesign reicherten sich die ^{14}C-wMWCNT überwiegend im Magen-Darm-Trakt an (> 80 %), was darauf hindeutet, dass die Aufnahme der Nanomaterialien durch Konsumenten hauptsächlich über das alimentäre System erfolgt.

Darüber hinaus ist bekannt, dass CNT organische Verbindungen adsorbieren und somit das Schicksal von Umweltschadstoffen verändert werden kann. Aufgrund dessen wurde die Wechselwirkung von

unmarkierten wMWCNT und dem Biozid Triclocarban (TCC) untersucht. Es wurden Effektstudien mit beiden Substanzen, Nanomaterial und antibakteriellem Mittel (in einzelnen und kombinierten Ansätzen), hinsichtlich des Wachstums von *C. reinhardtii* und *R. subcapitata* und der Immobilisierung von *D. magna*, durchgeführt. In den kombinierten Ansätzen wurden so genannte "Trojan-horse" Effekte (eine Chemikalie adsorbiert an ein Trägermaterial wie CNT und der Komplex wird anschließend von einem Organismus aufgenommen) untersucht.

Zunächst wurde die Adsorption von radioaktiv markiertem TCC (^{14}C-TCC) an verschiedene wMWCNT-Konzentrationen bestimmt und mit einem Wert für log K_{wMWCNT} von 7,36 ± 0,44 L kg^{-1} eine starke Adsorptionskapazität von CNT gegenüber TCC festgestellt. Ökotoxizitätstests haben gezeigt, dass die Exposition mit wMWCNT allein jeweils erste Effekte im mg L^{-1} Bereich für Grünalgen und Daphnien aufzeigt. TCC allein verursachte 50 % Effekt (EC_{50}) bei 20,6 µg TCC L^{-1}, 22,1 µg TCC L^{-1} und 36,5 µg TCC L^{-1} jeweils in *D. magna*, *C. reinhardtii* und *R. subcapitata*. Nach der Zugabe von 100 µg wMWCNT L^{-1} zur TCC-Testreihe im Algenwachstumshemmtest wurde eine Abnahme der Toxizität für *C. reinhardtii* und eine Zunahme der Toxizität für *R. subcapitata* beobachtet. Die hemmende Wirkung von TCC auf Grünalgen wurde generell reduziert, wenn dem Testmedium wMWCNT-Konzentrationen über 100 µg L^{-1} zugesetzt wurden und oberhalb von 1 mg wMWCNT L^{-1} konnte für beide Algenarten kein Wachstumsunterschied zur Kontrolle festgestellt werden. Für *D. magna* hatte die Zugabe von 100 µg wMWCNT L^{-1} keinen Einfluss auf die TCC-Toxizität hinsichtlich der Immobilisierung. Aufgrund unserer Ergebnisse und der Tatsache, dass CNT von Algen nicht in großem Umfang absorbiert werden, kann von keinem "Trojan-horse" Effekt für die getesteten Grünalgen ausgegangen werden. Die starke Adsorption von TCC an CNT und die starke Akkumulation von Nanomaterialien in *D. magna* lassen jedoch auf einen wahren "Trojan-horse" Effekt für die Krebstiere schließen.

Zusammenfassend zeigen die Ergebnisse, dass die lange Verweildauer von CNT in der Wassersäule, die von mehreren Tagen bis zu Wochen reicht, und ihre Akkumulation im Sediment zu einer Exposition von pelagischen und benthischen Organismen führt. Aquatische Sedimentsysteme mit unterschiedlichen Eigenschaften sowie verschiedenen CNT-Typen sollten weiterhin untersucht werden, um die gewonnenen Erkenntnisse über die Langzeitstabilität von CNT und deren Verteilung in derartigen Systemen zu bestätigen und auszuweiten.

In Wasser dispergierte CNT binden zu einem großen Teil an Algenzellen, sodass es zu einer Übertragung der CNT im Nahrungsnetz kommen kann. Im Fall von *D. magna* führte der Nahrungstransfer zu Körperbelastungen, die um Größenordnungen kleiner waren im Vergleich zur Wasserexposition, was auf eine sehr geringe, bis nicht vorhandene Bioakkumulation unter Umweltbedingungen hinweist. Andererseits ergab die Untersuchung der CNT-Aufnahme in einer heranwachsenden *D. magna*

Population eine Steady-State Körperbelastung nach 14 Tagen (BAF >2000), aber keine toxischen Effekte im Vergleich zu den Kontrollgruppen. Somit deuten die Ergebnisse darauf hin, dass eine Akkumulation von CNT durch *D. magna* möglich ist, jedoch abhängig von den Bedingungen im Testsystem ist (z.B. Wasservolumen und Verteilung der Nanomaterialien).

Eine Bioakkumulation von CNT im klassischen Sinne findet nicht statt, da die Nanomaterialien, unabhängig vom Testorganismus (Primär- oder Sekundärkonsument), hauptsächlich über den Magen-Darm-Trakt aufgenommen werden, aus dem die aufgenommenen CNT anschließend wieder ausgeschieden werden. Ob und inwieweit die aufgenommenen CNT die exponierten Tiere langfristig schädigen, muss noch untersucht werden. Schließlich erhöhen lange Verweilzeiten von CNT bei niedrigen Konzentrationen in der Wasserphase die Wechselwirkung von Nanomaterialien und pelagischen Organismen und können daher zu einem Nahrungskettentransport von CNT führen.

Des Weiteren werden akute Effekte von MWCNT auf Grünalgen und Daphnien im mg L^{-1} Bereich erwartet, was auf kein Risiko bei der derzeit um Größenordnungen niedrigeren abgeschätzten Umweltkonzentration (PEC) schließen lässt. Aus dem gleichen Grund wird auch kein Einfluss von CNT auf das Schicksal des aquatischen Schadstoffs TCC in der Umwelt erwartet. Erst ab Nanomaterialkonzentrationen fünf Größenordnungen über der PEC war die Adsorption von TCC ausreichend groß genug, um das Testergebnis zu beeinflussen. Mit der derzeitigen Zunahme der CNT-Produktion müssen jedoch, neben der Überwachung der Einzelsubstanz, Mischungs- und "Trojan-horse" Effekte weiter berücksichtigt und untersucht werden.

1 Overall introduction

At the beginning of this thesis, a general introduction covering all relevant topics including the objectives of this work is provided. Furthermore, four different experimental sections are presented (chapters 2 - 5), each of which has the following topic-specific structure: introduction, materials and methods, results and discussion. Finally, an overall conclusion and outlook is given.

1.1 Nanomaterials

1.1.1 Overview

Natural nanoscale particles have existed on this earth for millions of years. Since humans have developed techniques to synthesize and manipulate nanomaterials (NM), they are applied in manifold areas: electronics, pharmaceuticals, cosmetics, energy, catalysts, and material applications (Nowack and Bucheli, 2007). The European Commission (2011/696/EU) made the following proposal for the definition of a nanomaterial: nanomaterial means an elemental material, generated or produced in processes, containing particles in an unbound state, as an aggregate or agglomerate, and in which at least 50% of the particles have one or more external dimensions in the size range of 1 to 100 nm. Among the group of nanomaterials, nanoparticles are defined as materials with at least two dimensions between 1 and 100 nm (Klaine et al., 2008; Europäische Kommission, 2011). In the framework of the concretization of the registration requirements for nanomaterials, in 2018, this definition was included in the annexes of the REACH-Regulation (UBA, Germany, 2021a). REACH is short for: registration, evaluation, authorization and restriction of chemicals within the EU. The REACH-Regulation is based on the precept that manufacturers, importers and downstream users must ensure that they manufacture, marketing and use chemicals that do not harm human health or the environment. In accordance with the precautionary principle, REACH thus shifts regulatory responsibility to industry regarding the generation of safety data and, in part, also to their evaluation in order to ensure the safe use of their substances, mixtures and articles (BMU, Germany, 2021).

The nanoscale nature of a substance is not necessarily synonymous with risk and for a long time there was no consensus on whether a separate form was needed for the assessment of nanomaterials compared to classical chemicals. However, nanomaterials have specific properties (e.g., in size, geometry, crystal forms and surface structures) that distinguish them from other chemicals. Surface properties can differ significantly between nanoscale and nonnanoscale forms, but also within the different nanoforms of a chemical substance. Consequently, the behavior and effects of the nanoscale forms of a chemical may differ significantly from the behavior of that chemical already known and studied. Similarly, the effects of a nanoform may not be describable with existing tools (UBA, Germany, 2021b). Because of this, direct portability of behavior and effect data is not possible and a separate assessment of nanomaterials and nanoforms has come into force in January 2020. In the future, detailed data on nanomaterials and their nanoforms will be required from manufacturers, importers

and downstream users in the course of registration with the European Chemicals Agency (ECHA) (BMU, Germany, 2021).

1.1.2 Carbon nanotubes

Within carbonaceous nanomaterials (CNM), carbon nanotubes (CNT, Fig. 1.1) are probably among the best known. CNT consist of only elemental carbon, which is arranged to hexagons, due to sp^2 hybridization (Iijima, 1991). Consequently, the tubes look like rolled up graphene sheets in the nanoscale range (Tsuji et al., 2006). Based on the number of graphene sheet tubes, one differentiates between single-walled CNT (SWCNT), double-walled CNT (DWCNT) and multi-walled CNT (MWCNT). The multi-walled version of CNT was first discovered by Iijima (1991) using electron microscopy. SWCNT are cylindrical with typical diameters of 0.7 – 1 nm (Odom et al., 1998). In contrast, MWCNT have coaxial cylinders with a spacing between the layers of about 0.34 nm and their diameter usually varies between 2 to 25 nm (Ajayan, 1999). Due to their outstanding thermal, electrical and mechanical properties, CNT found applications in the following areas: nanocomposites (Barra et al., 2019), energy storage (Wang et al., 2018), as adsorption material for water remediation (Ma et al., 2012), as drug carriers (Saleemi et al., 2020) and others. To change the surface structure or charge of CNT, these were further functionalized (e.g., with carboxyl groups or polyethyleneimine) and coated (e.g., with lysophophatidylcholine) (Roberts et al., 2007; Petersen et al., 2011; Jang and Hwang, 2018).

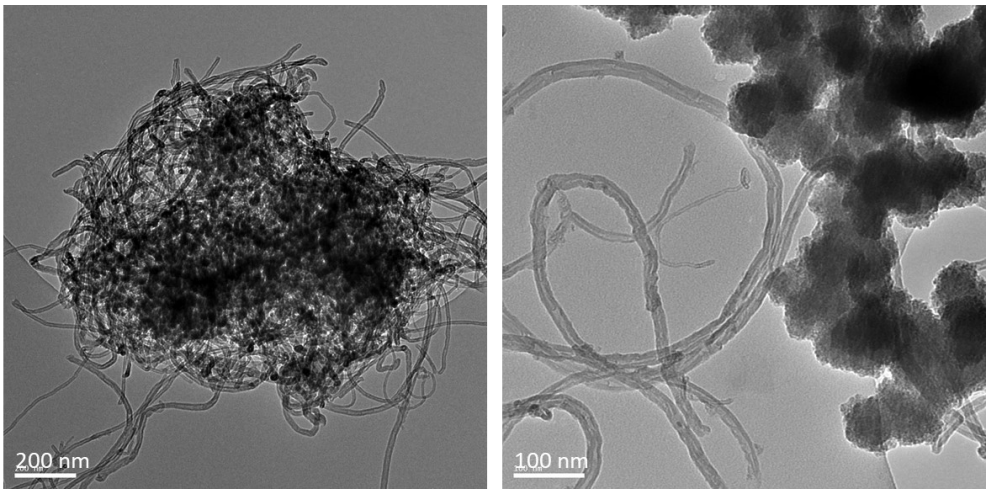

Figure 1.1: Transmission electron microscopy images of carbon nanotubes (pictures were taken by Dr. Nina Siebers from Forschungszentrum Jülich GmbH, Germany).

Since there is a wide range of applications for CNT, their production has increased recently. In 2014, the company OCSiAL commissioned the first industrial-scale device to produce graphene nanotubes. As of today, OCSiAL produces 80 tons of CNT annually which accounts for over 95% of the CNT world market (OCSiAL, 2020a). The product, which is marketed under the name TUBALL™, is a single-walled CNT with an outer diameter of 1.6 nm and a length of 5 µm. In contrast to MWCNT, SWCNT offer the

advantage of producing conductive materials in any color or without color (transparent). When using MWCNT, so far only black materials can be produced. Another major advantage of SWCNT is that improved mechanical properties are already achieved at a proportion of 0.01 wt%. In comparison, 0.5% - 5% of MWCNT is required to achieve the same characteristics (OCSiAL, 2020b). TUBALL™ SWCNT (TUBALL™, 2020a) are marketed in Europe and North America and other global markets. They are the first to be registered in accordance with the EU's REACH-Regulations with a recently confirmed tonnage of 100 tons of nanotubes annually. Additionally, US EPA (United States Environmental Protection Agency) is regulating the nanotube product as a new chemical substance and in 2019 authorized the sale of OCSiAL products in the USA (TUBALL™, 2020b). Therefore, an increase in environmental CNT concentration is to be expected in the next decades.

1.1.3 Environmental fate

During lifetime cycle of CNT, most of the material is released during synthesis and handling (Yeganeh et al., 2008; Tsai et al., 2009). CNT are mainly used in polymer composites (e.g., nanotubes embedded in plastics) and therefore, the disposal of these might, if CNT separate from the composite matrix, further contribute to CNT release into the environment. The assumed final repositories for CNT-containing products are recycling, waste incineration and landfilling processes (Gottschalk et al., 2015). During use and after disposal the products are exposed to mechanical stress and weathering, e.g., solar irradiation, temperature, moisture or salinity which leads to the detachment of low CNT amounts (Harper et al., 2015). Recent studies showed that the decomposition of CNT-containing nanocomposites induced the release of nanomaterials (Hirth et al., 2013; Schlagenhauf et al., 2015; Rhiem et al., 2016; Hennig et al., 2019). Due to the abovementioned reasons, the exposure of environmental compartments with nanotubes has so far been classified as marginal (Gottschalk et al., 2015). The predicted environmental concentration (PEC) of CNT in surface waters and sediment is in the ng L^{-1} and µg kg^{-1} y^{-1} range, respectively (Sun et al., 2014).

Not only nanocomposites, but also original or released CNT material experience changes after entering the environment, e.g., by photooxidation, physico-chemical processes or degradation (Zhang et al., 2013; Flores-Cervantes et al., 2014). Aquatic ecosystems offer particularly good conditions for such transformation processes (Klaine et al., 2008). Additionally, the interaction of CNT with pelagic and sediment-dwelling organisms has been observed several times (Templeton et al., 2006; Petersen et al., 2008a; Petersen et al., 2011a; Maes et al., 2014; Cano et al., 2017). Moreover, zooplankton ingest CNT and the passage of nanomaterials through the gastrointestinal tract leads to changes in the parent material (Petersen et al., 2009; Guo et al., 2013). For example, Roberts et al. (2007) observed that after ingestion of lipid coated CNT, clumped lipid free CNT were excreted. Therefore, these processes modify physicochemical characteristics of CNT which further effects their partitioning and impacts.

In addition, dispersed CNT in aqueous phase tend to form agglomerates and consequently to settle down in the water column, which leads to the deposition of agglomerates into the sediment phase (Zhang et al., 2011; Schierz et al., 2014). The dispersion stability of CNT in a water body is strongly dependent on the physical and chemical properties of the nanomaterials themselves and the surrounding medium (Hyung et al., 2007; Peijnenburg et al., 2015). Particularly pristine CNT are characterized by a strong hydrophobicity, which clearly promotes the formation of agglomerates and subsequent sedimentation behavior. Due to the deposition of nanomaterials into the sediment phase, it is assumed that benthic organisms are exposed to a higher risk compared to pelagic organisms (Petersen et al., 2011b; Schierz et al., 2014).

Furthermore, natural organic matter (NOM) and ionic strength have an indirect influence on the dispersion stability of CNT. It has been observed that the presence of NOM, due to the promoted electrostatic/steric repulsion between nanomaterials, has a stabilizing effect on a CNT dispersion. On the other hand, an increased ionic strength (especially divalent cations, e.g., Ca^{2+}, Mg^{2+}) leads to a suppression of electrostatic/steric repulsion and therefore to an increased agglomeration of the nanomaterials, which consequently shortens their residence time in aqueous phase (Hyung et al., 2007; Li and Huang, 2010; Saleh et al., 2010; Lin et al., 2012). Eventually, the distribution of CNT in aqueous systems is dependent on various factors and thus dynamic processes, resulting in unstable dispersions. As a result, CNT concentrations in aquatic test systems change over time (Glomstad et al., 2018).

1.1.4 Interaction of CNT with aquatic biota

Over the last two decades, bioaccumulation and interaction of CNT considering different aquatic and terrestrial organisms were examined (Petersen et al., 2008a, b; Petersen et al., 2009; Maes et al., 2014; Rhiem et al., 2015). Quantifying bioaccumulation of CNT in organic compartments like organisms, sediments and soils is very challenging due to the carbonaceous nature of these nanomaterials (Bjorkland et al., 2017). Therefore, methods using radioactively labeled nanomaterials were mostly adopted (Parks et al., 2013; Mortimer et al., 2016). Several studies reported that CNT were taken up by aquatic organisms but assumed that this accumulation is mainly located in the intestine (Petersen et al., 2008b, a; Petersen et al., 2009; Hou et al., 2013; Jackson et al., 2013; Parks et al., 2013). The passage of membranes (e.g., the gut tract wall) and the accumulation in lipid tissues as requirement for bioaccumulation of traditional chemicals has not yet been confirmed for CNT (Mackay and Fraser, 2000; Zhang et al., 2015; Bjorkland et al., 2017). Additionally, it was observed that the presence of a suitable food source facilitates the excretion of accumulated nanomaterials (Gillis et al., 2005; Kennedy et al., 2008; Guo et al., 2013). Therefore, a low bioaccumulation potential for CNT is expected (Bjorkland et al., 2017).

Furthermore, imaging techniques (e.g., electron microscopy) were used to visualize the accumulation of CNT in aquatic organisms. After their exposure to water dispersed CNT, it was observed that the nanomaterials clogged to filtration organs and stuck to carapaces of *Daphnia magna* (Roberts et al., 2007), coated the gills of rainbow trout (Smith et al., 2007), as well as being found in the gastrointestinal tract of various aquatic organisms (Templeton et al., 2006; Roberts et al., 2007; Petersen et al., 2009).

Besides CNT bioaccumulation in organisms of aquatic ecosystems, toxic effects of CNT have been investigated as well (Baun et al., 2008; Blaise et al., 2008; Mwangi et al., 2012; Bacchetta et al., 2018; Zhu et al., 2018). Since these studies indicated adverse effects onto the test organisms at nanomaterial concentrations several orders of magnitude above the PEC, there is a great need for ecotoxicological research considering long-term exposure using low nanomaterial concentrations with chronic endpoints in aquatic invertebrates.

1.1.5 Adsorption of chemicals on CNT and the "Trojan-horse" phenomenon

The input of anthropogenic substances and materials into our ecosystems is a well-known issue. Especially in the aquatic environment, many different pollutants encounter each other through the various input pathways leading to direct and indirect interactions between the contaminants. One form of direct interaction is the adsorption of chemical substances (e.g., pharmaceuticals or polycyclic aromatic hydrocarbons) onto nanomaterials, e.g., CNT (Yang and Xing, 2007; Oleszczuk et al., 2009). Compared to the free substance, the fate, bioavailability and toxicity of the adsorbed contaminant probably will be altered (Velzeboer et al., 2014).

The adsorption of chemicals on CNT is based on different mechanisms (Yang and Xing, 2010; Apul and Karanfil, 2015). For molecules without charge, nonspecific Van der Waals interactions play a key role for the adsorption of chemicals to hydrophobic adsorbents (Crittenden et al., 1999; Yang et al., 2008). In the past years, the adsorption of hydrophobic organic chemicals (HOC's) to CNT was reported (Yang and Xing, 2007; Oleszczuk et al., 2009; Schwab et al., 2014; Zindler et al., 2016). However, to understand adsorption by CNM, besides hydrophobic interactions, further bonding forces must be considered (Yang et al., 2008). Therefore, π-π interactions between aromatic substances and the delocalized valence electrons of the graphitic structure of the CNT surface represent another adsorption force (Wang et al., 2009; Apul and Karanfil, 2015). In addition, the formation of hydrogen bonds (i.e., electrostatic attraction depending on polarity) between surfaces of functionalized CNT and pollutants with functional groups (e.g., hydroxyl, carboxyl or amino groups) can further lead to adsorption (Lin and Xing, 2008; Apul and Karanfil, 2015). Moreover, electrostatic interactions of charged substances (i.e., ionizable chemicals or charged surfaces of CNT) (Apul and Karanfil, 2015) and covalent bonds are possible (Yang and Xing, 2010). Since covalent binding of HOC's to CNT is a strong

form of adsorption and mostly irreversible, covalent alterations have been used to functionalize CNM (Hussain et al., 2009; Yang and Xing, 2010). Due to their excellent adsorption properties, CNT were considered in remediation approaches and for the application in local drug delivery systems (Hua et al., 2017; Newland et al., 2018; Saleemi et al., 2020).

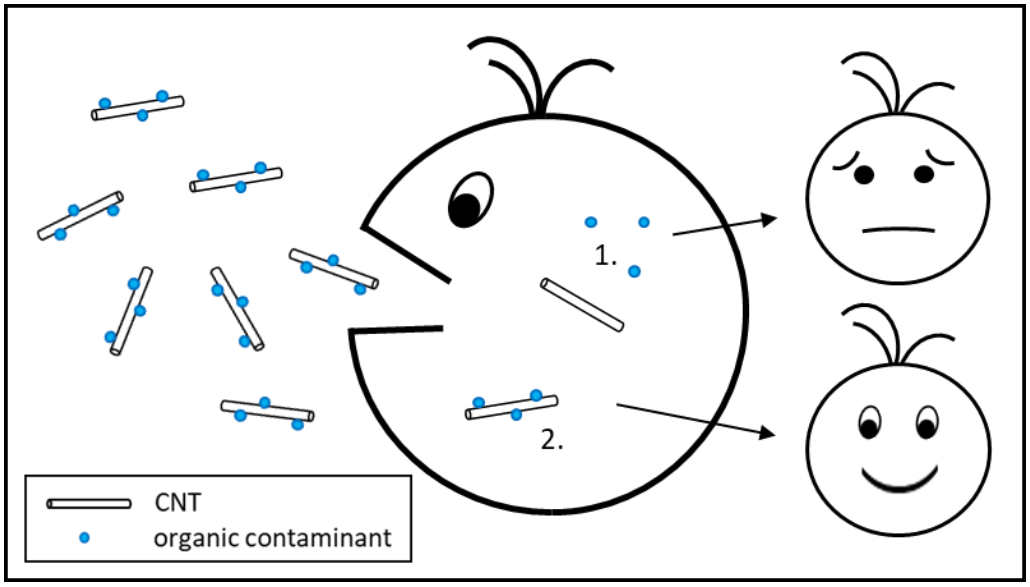

Figure 1.2: Simplified version of the 'Trojan-horse' phenomenon (own illustration). The precondition for a 'Trojan-horse' effect is the adsorption of a chemical substance (e.g., organic contaminant) onto a transporter material (e.g., CNT) and the subsequent uptake of this complex by an organism. After incorporation of the complex, either (1.) desorption of the chemical substance occurs and there is an effect enhancement compared to exposure of the organism to the chemical substance alone, or (2.) adsorption of the contaminant to the carrier material is stable and there is a reduced effect compared to exposure of the organism to the contaminant alone.

In natural ecosystems adsorption of an organic substance onto a nanomaterial can lead to the so called 'Trojan-horse' effect. The 'Trojan-horse' effect is described by the uptake of a complex consisting of an adsorbed substance and sorbent by an organism (Fig. 1.2), whereas the nanomaterial acts as a vector for the pollutant. Limbach et al. (2007) coined the term 'Trojan-horse type mechanism' first to describe the facilitated transport of cobalt in lung epithelial cells when the cells are exposed to cobalt oxide nanoparticles as opposed to cobalt ions alone and therefore increased the adverse effects. Later, Hartmann and Baun (2010) extended the term to clarify the carrier function of nanoparticles for chemicals, which may lead to an easier uptake and consequently to an altered toxicity. Naasz et al. (2018) additionally considered the aspect of adsorption and desorption interactions of nanoparticles and chemicals in detail and classified the different mechanisms of action. As shown in Fig. 1.2, the desorption or irreversible adsorption of the chemical to the carrier material influences the outcome of the mixed exposure. To investigate such mixture toxicities, the biocide triclocarban was selected in this work and its effects in the presence and absence of CNT were evaluated using aquatic test systems.

1.2 The biocide triclocarban

1.2.1 General informations

Triclocarban (TCC, 3,4,4´-trichlorocarbanilide, CAS 101-20-2, see Fig. 1.3) is a common antibacterial agent used in household and personal care products (Sapkota et al., 2007; Schebb et al., 2011a). Due to its sanitizing properties, TCC is used in soaps, shower gels, cosmetics, and detergents as well as in cleaning products and agents (TCC Consortium, 2002; Heidler et al., 2006; Sapkota et al., 2007). TCC is a bacteriostatic agent, active only against Gram-positive bacteria (Heinze and Yackovich, 1988). With an estimated consumption of 2.6 ± 0.7 mg per capita per day, TCC is considered a high production volume chemical in the United States ($2.3 – 4.7 \times 10^5$ kg y^{-1}) (TCC Consortium, 2002; Heidler et al., 2006; Miller et al., 2008).

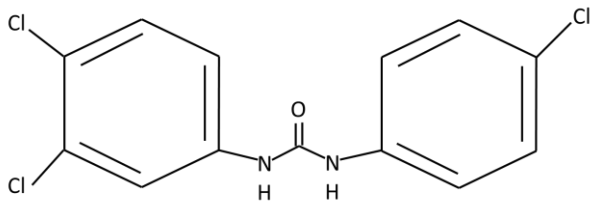

Figure 1.3: Chemical structure of triclocarban (self-made image based on TCC Consortium 2010).

Table 1.1: Characteristics on the antibacterial agent triclocarban.

Information on Triclocarban (TCC)		
CAS number	101-20-2	TCC Consortium (2002)
Chemical formula	$C_{13}H_9Cl_3N_2O$	
Molar mass	315.58 g mol^{-1}	calculated
Water solubility	Experimental:	
	0.045 mg L^{-1} (25 °C)	Snyder et al. (2010)
	0.11 mg L^{-1} (20 °C)	TCC Consortium (2002)
	Predicted:	
	0.65 – 1.55 mg L^{-1} (25 °C)	Halden and Paull (2005)
Log K_{OW}	Experimental:	
	3.5	Snyder et al. (2010)
	4.2	TCC Consortium (2002)
	Predicted:	Halden and Paull (2005)
	4.9 (25 °C, pH 7)	

The content of TCC in 84% of personal care products in the United States ranges from 0.1 to 5 wt% (TCC Consortium, 2002). Due to its enormous consumption, it is found in samples taken from the human body (e.g., blood plasma and urine samples) (Schebb et al., 2011b; Asimakopoulos et al., 2014) as well as human TCC metabolites are found in sewage sludge samples (Pycke et al., 2014). Concerns regarding the use of TCC primarily target its environmental concentrations (Halden and Paull, 2004),

persistence (Heidler et al., 2006; Ying et al., 2007; Miller et al., 2008), toxicity (Gao et al., 2015; Barros et al., 2017), bioaccumulation potential (Coogan et al., 2007; Higgins et al., 2009), endocrine effects (Chen et al., 2008), and its potential to promote antibacterial resistance (Walsh et al., 2003). TCC shows a low water solubility (0.045 mg L^{-1} at 25 °C), but a moderate high log K_{OW} (Tab. 1.1) indicating a possible high bioaccumulation potential (Halden and Paull, 2005). Due to the aromatic and chlorinated structures of the urea biocide, a low biodegradation potential and a tendency for environmental persistence is assumed (Halden and Paull, 2005; Heidler et al., 2006). Besides TCC, the diaryl urea compound triclosan (TCS) is integrated in sanitizing agents as well and was the object of recent research (Wang et al., 2014; Geiss et al., 2016; Mulla et al., 2016).

Due to the lack of suitable methods for the detection of TCC and TCS in environmental media, the two chlorocarbanilide substances were only marginally considered from a scientific point of view and were applied in a large volume unevaluated for more than 50 years (Halden and Paull, 2005; Sapkota et al., 2007). In 2014, Rolf U. Halden (Halden, 2014) drew attention to the fact that substances similar to TCC and TCS structures (e.g., hexachlorophene) had already been withdrawn from the market for certain applications due to undesirable side effects such as persistence and ecotoxicity. In his publication, Halden asserts that the use of these bacteriostatic agents in medical use has its benefits, but that there is a need to ban TCC and TCS from products for the common consumer. Following, the U.S. Food and Drug Administration banned TCC and TCS in over-the-counter products in September 2016, with a couple of exceptions (Halden et al., 2017). Additionally, Kim and Rhee (2016) reported that an antibacterial soap amended with 0.3% TCC has no more effective efficacy against Gram-positive and Gram-negative bacteria, except for *Enterococcus faecalis*, than plain soaps. In the EU, TCC is currently (year 2020) under evaluation in the framework of the Community rolling action plan (European Chemical Agency) for concerns about reprotoxicity and its role as an endocrine disruptor (French Agency for food; environmental and occupational health and safety (anses), 2018).

1.2.2 Environmental concentrations

Because TCC containing products such as soaps, toothpastes and medical disinfectants are washed down the drain after their usage, domestic effluents loaded with the pollutant run into wastewater treatment plants (WWTP) (Gautam et al., 2014). Since an incomplete TCC removal from wastewater was observed and a removal of only 97% was gained under perfect conditions, the main pathway of TCC into the environment after its usage is through effluents from WWTPs and sewage sludge applications onto fields (Gledhill, 1975; Heidler et al., 2006; Higgins et al., 2009). TCC concentrations of 2.17 – 5.97 µg g^{-1} dry weight were detected in activated sludge and biosolids of WWTPs in Ontario (Canada) (Chu and Metcalfe, 2007). Further, Halden and Paull (2005) identified the spill (i.e., by leakage) of wastewater as an additional input path of antibiotic agents into surface waters.

Consequently, TCC has been detected in surface water, suspended sediments and bed sediments (Halden and Paull, 2005; Gautam et al., 2014). For environmental degradation it is assumed that TCC primarily decompose to its chloroaniline units which are further degraded, e.g., by photolysis or microbes (Gledhill, 1975; Zeyer and Kearney, 1982; Hwang et al., 1987). Mulla et al. (2016) first reported the degradation of TCC (4 mg L^{-1}) by the TCS-degrading *Sphingomonas sp.* strain YL-JM2C with the following main metabolites: 3,4-dichloroaniline, 4-chloroaniline and 4-chlorocatechol. On the other hand, TCC might be accumulated in soils and sediments (Higgins et al., 2009; Higgins et al., 2011). Respective half-lives of 60, 120 and 540 days for TCC in surface water, soil and sediment were calculated (Halden and Paull, 2005). Environmental concentration of TCC in surface water of urban streams in the Greater Baltimore area (Maryland, USA) was 6.8 µg L^{-1} (Halden and Paull, 2005). In Fountain Creek and Arkansas River (Colorado, USA) a lower TCC concentration of 4.5 to 47.3 ng L^{-1} was found in surface water. At the same sampling site, concentrations of 4.1 to 57.3 ng TCC g^{-1} were detected in suspended sediment and bed sediments (Gautam et al., 2014). Venkatesan et al. (2012) found TCC concentrations of up to 822 ng g^{-1} in samples from bed sediments collected close to WWTPs effluents in Minnesota (USA). In comparison, TCC concentrations of 0.17 to 0.19 ng g^{-1}, 8.4 to 12.9 ng g^{-1} and 158 to 492 ng g^{-1} at an increasing organic matter content of 4.6%, 6.5% and 7.4% were detected in sediments 100 m downstream from WWTPs in France, respectively (Souchier et al., 2015). Although, in Europe, the use of TCC is more limited compared to the USA and Canada (Sapkota et al., 2007) amounts detected in sediments are of the same magnitude. Therefore, TCC is attracting attention in scientific circles on both continents regarding its hazard potential.

1.2.3 Impacts of triclocarban in the environment

The lipophilic properties of TCC, like a limited water solubility (0.11 mg L^{-1} at 20 °C, Tab. 1.1) and a moderate log K_{OW} of 3.5 to 4.9 (see Tab. 1.1) suggest that TCC will preferentially accumulate in biota. Schebb et al. (2011b) reported that small amounts of TCC are adsorbed by the human epidermis during showering when using antibacterial soaps. Further, bioaccumulation of TCC in different aquatic organisms was observed. A research team of the University of North Texas (USA) revealed TCC accumulation in algae (bioaccumulation factor (BAF) = 2,700) after sampling algae and water on-site from the Pecan Creek (Texas, USA) (Coogan et al., 2007). Subsequently, they inserted caged snails (*Helisoma trivolvis*), grazing on algae, at a WWTP outflow in the same river for two weeks and observed a BAF of 1,600 and therefore indicated a rapid bioaccumulation of TCC by snails receiving the contaminant *via* WWTP effluents (Coogan and La Point, 2008). Moreover, a log bioconcentration factor (BCF) of 2.9 for larval medaka (*Oryzias latipes*) was revealed after an exposure to 20 µg TCC L^{-1} for 24 h (Schebb et al., 2011a). The sediment-dwelling oligochaete *Lumbriculus variegatus* showed also a fast TCC uptake. After the exposure of *L. variegatus* to TCC spiked sediment for 5 days, a maximum body burden of 1,310 µg g^{-1}_{lipid} was observed (Higgins et al., 2009). Additionally, it was found that TCC

accumulates in plants (roots and shoots) grown on constructed wetlands near the City of Denton's Pecan Creek WWTP (Texas, USA) in the ng g^{-1} range (Zarate et al., 2012).

In comparison to bioaccumulation of TCC, more research was performed considering effects of TCC to aquatic biota. Tamura et al. (2013) conducted tests on acute toxicity using green algae *Pseudokirchneriella subcapitata* (72 h EC_{50}: 29 µg L^{-1}), *Daphnia magna* (48 h EC_{50}: 10 µg L^{-1}) and *Oryzias latipes* (96 h LC_{50}: 85 µg L^{-1}). Another study observed a lower sensibility of *D. magna* to the antimicrobial agent TCC. Simon et al. (2015) tested neonate, juvenile and adult individuals and calculated 96 h EC_{50} values of 12.7, 33.2 and 25.7 µg TCC L^{-1}, respectively. In addition, a 24 h LC_{50} of 17.8 µg TCC L^{-1} for *Artemia salina* was reported (Xu et al., 2015).

Moreover, the amphipod *Gammarus locusta* was exposed (60 days, chronic exposure) to environmentally relevant TCC concentrations (100, 500 and 2500 ng L^{-1}) whereas no significant impacts on growth and reproduction, but adverse effects on oxidative stress indicating biochemical markers and behavioral aspects (i.e., path, total distance travelled and average speed) were observed (Barros et al., 2017). Oxidative stress triggered by TCC was further observed in zebrafish and in catfish embryos *(Rhamdia quelen*) (Wei et al., 2018; Gomes et al., 2021).

Interestingly, it was found that growth of *Tetrahymena thermophila* is only inhibited from a TCC concentration of 295 µg L^{-1} (24 h EC_{50}) but at TCC concentrations of 1.0 µg L^{-1} statistically significant DNA damage was detected indicating genotoxic properties for the biocide (Gao et al., 2015). Evidence for the genotoxicity of TCC was also found during tests with *A. salina* (Xu et al., 2015).

Furthermore, researchers suggest that TCC represents a new type of endocrine disruptor (Ahn et al., 2008; Chen et al., 2008). Chen et al. (2008) observed that despite the little or no endocrine activity of TCC and other urea compounds, the presence of TCC enhanced the testosterone induced androgen receptor-mediated transcriptional activity in *in vitro* tests. Subsequently, when TCC and testosterone were added to the diet of castrated male rats a significant amplification of male sex organs, compared to the testosterone and TCC alone scenarios, was observed (Chen et al., 2008). Additionally, more recent studies observed endocrine effects of TCC on reproduction in freshwater mudsnail *Potamopyrgus antipodarum* with lowest observed effect concentrations below 1 µg L^{-1} (Giudice and Young, 2010; Geiss et al., 2016) and on the offspring of female Wistar rats when dams were orally exposed to TCC during pregnancy (Costa et al., 2020).

1.3 Objectives of this study

Since the current PEC for CNT is very low and nanomaterial containing products are mostly used for several years, the risk posed by CNT is also expected to be very low. However, due to the steadily growing production volumes over the last six years, an increased release cannot be excluded and ecotoxicological research in this area is further needed. The main objective of this work was to investigate the transfer of CNT in the food chain of freshwater ecosystems.

In **chapter 2**, the behavior and fate of weathered MWCNT (wMWCNT) in a water sediment system is examined. Nanomaterial distribution among compartments and decay times are determined.

Chapter 3 deals with the bioaccumulation of wMWCNT in green algae (*Raphidocelis subcapitata* and *Chlamydomonas reinhardtii*) and *Daphnia magna* as an example for primary producers and primary consumer, respectively. It is examined whether loading of CNT to green algae prior to uptake experiments with *D. magna* (dietary exposure) has an impact on accumulation of nanomaterials compared to waterborne exposure. In order to investigate population dynamics, this study further investigates bioaccumulation of wMWCNT in a growing *D. magna* population.

In **chapter 4**, the accumulation of wMWCNT in fish (*Danio rerio*) to complete the aquatic food chain (secondary consumer) is examined. Using large scale microcosm batch systems, thirty individuals of *D. rerio* were exposed at once to wMWCNT concentrations of 100 µg L^{-1} in order to assess bioconcentration and biomagnification.

Chapter 5 discusses the so-called 'Trojan-horse' effect. Within this section, the impact of the presence of wMWCNT on the toxicity of the selected organic contaminant TCC is investigated using the abovementioned green algae and planktonic crustacean *D. magna*. In case of green algae, it is examined if the addition of wMWCNT will alter the growth inhibition induced by TCC and what role the applied nanomaterial concentration plays in changing the outcome of growth inhibition test. Further, the presence of food on wMWCNT toxicity to *D. magna* is assessed. To better understand interaction of nanomaterials and contaminant, the adsorption of TCC onto wMWCNT is also investigated.

The weathering of the nanomaterials prior to their use in the various test systems is intended to simulate the exposure of the nanomaterials to sunlight and thus such experiments represent a higher environmental relevance. Furthermore, to ensure a reliable detection of the substances used (nanomaterial or chemical), radioactively labeled (^{14}C) substances were used in most of the experiments.

1.4 References

Ahn, K.C., Zhao, B., Chen, J., Cherednichenko, G., Sanmarti, E., Denison, M.S., Lasley, B., Pessah, I.N., Kultz, D., Chang, D.P., Gee, S.J., Hammock, B.D., 2008. In vitro biologic activities of the antimicrobials triclocarban, its analogs, and triclosan in bioassay screens: receptor-based bioassay screens. Environ Health Perspect 116, 1203-1210.

Ajayan, P.M., 1999. Nanotubes from Carbon. Chem Rev 99, 1787-1800.

Apul, O.G., Karanfil, T., 2015. Adsorption of synthetic organic contaminants by carbon nanotubes: a critical review. Water Res 68, 34-55.

Asimakopoulos, A.G., Thomaidis, N.S., Kannan, K., 2014. Widespread occurrence of bisphenol A diglycidyl ethers, p-hydroxybenzoic acid esters (parabens), benzophenone type-UV filters, triclosan, and triclocarban in human urine from Athens, Greece. Sci Total Environ 470-471, 1243-1249.

Bacchetta, R., Santo, N., Valenti, I., Maggioni, D., Longhi, M., Tremolada, P., 2018. Comparative toxicity of three differently shaped carbon nanomaterials on Daphnia magna: does a shape effect exist? Nanotoxicology 12, 201-223.

Barra, G., Guadagno, L., Vertuccio, L., Simonet, B., Santos, B., Zarrelli, M., Arena, M., Viscardi, M., 2019. Different Methods of Dispersing Carbon Nanotubes in Epoxy Resin and Initial Evaluation of the Obtained Nanocomposite as a Matrix of Carbon Fiber Reinforced Laminate in Terms of Vibroacoustic Performance and Flammability. Materials 12.

Barros, S., Montes, R., Quintana, J.B., Rodil, R., Oliveira, J.M., Santos, M.M., Neuparth, T., 2017. Chronic effects of triclocarban in the amphipod Gammarus locusta: Behavioural and biochemical impairment. Ecotoxicol Environ Saf 135, 276-283.

Baun, A., Hartmann, N.B., Grieger, K., Kusk, K.O., 2008. Ecotoxicity of engineered nanoparticles to aquatic invertebrates: a brief review and recommendations for future toxicity testing. Ecotoxicology 17, 387-395.

Bjorkland, R., Tobias, D., Petersen, E.J., 2017. Increasing evidence indicates low bioaccumulation of carbon nanotubes. Environ Sci Nano 4, 747-766.

Blaise, C., Gagne, F., Ferard, J.F., Eullaffroy, P., 2008. Ecotoxicity of selected nano-materials to aquatic organisms. Environmental Toxicology 23, 591-598.

Bundesministerium für Umwelt, Naturschutz und nukleare Sicherheit (BMU, Germany), 2021. Künftig einheitliche EU-Regeln für Nanomaterialien. URL: https://www.bmu.de/pressemitteilung/kuenftig-einheitliche-eu-regeln-fuer-nanomaterialien/. Retrieved 02/07/2021; 11:23 am.

Cano, A.M., Maul, J.D., Saed, M., Shah, S.A., Green, M.J., Canas-Carrell, J.E., 2017. Bioaccumulation, stress, and swimming impairment in Daphnia magna exposed to multiwalled carbon nanotubes, graphene, and graphene oxide. Environ Toxicol Chem.

Chen, J., Ahn, K.C., Gee, N.A., Ahmed, M.I., Duleba, A.J., Zhao, L., Gee, S.J., Hammock, B.D., Lasley, B.L., 2008. Triclocarban enhances testosterone action: a new type of endocrine disruptor? Endocrinology 149, 1173-1179.

Chu, S., Metcalfe, C.D., 2007. Simultaneous determination of triclocarban and triclosan in municipal biosolids by liquid chromatography tandem mass spectrometry. J Chromatogr A 1164, 212-218.

Consortium, T., 2002. High Production Volume (HPV) Chemical Challenge Program Data Availability and Screening Level Assessment for Triclocarban.

Coogan, M.A., Edziyie, R.E., La Point, T.W., Venables, B.J., 2007. Algal bioaccumulation of triclocarban, triclosan, and methyl-triclosan in a North Texas wastewater treatment plant receiving stream. Chemosphere 67, 1911-1918.

Coogan, M.A., La Point, T.W., 2008. Snail bioaccumulation of triclocarban, triclosan, and methyltriclosan in a North Texas, USA, stream affected by wastewater treatment plant runoff. Environ Toxicol Chem 27, 1788-1793.

Costa, N.O., Borges, L.I., Cavalcanti, L.F., Montagnini, B.G., Anselmo Franci, J.A., Kiss, A.C.I., Gerardin, D.C.C., 2020. In utero and lactational exposure to triclocarban: reproductive effects on female rat offspring. J Appl Toxicol 40, 504-514.

Crittenden, J.C., Sanongraj, S., Bulloch, J.L., Hand, D.W., Rogers, T.N., Speth, T.F., Ulmer, M., 1999. Correlation of Aqueous-Phase Adsorption Isotherms. Environmental Science & Technology 33, 2926-2933.

Europäische Kommission. L 275/38 Amtsblatt der Europäischen Union 20.10.2011. EMPFEHLUNG DER KOMMISSION vom 18. Oktober 2011 zur Definition von Nanomaterialien. (2011/696/EU). URL: https://eur-lex.europa.eu/LexUriServ/LexUriServ.do?uri=OJ:L:2011:275:0038:0040:DE:PDF. Retrieved 03/15/2021; 13:57 pm.

Flores-Cervantes, D.X., Maes, H.M., Schaffer, A., Hollender, J., Kohler, H.P., 2014. Slow biotransformation of carbon nanotubes by horseradish peroxidase. Environ Sci Technol 48, 4826-4834.

French Agency for food; environmental and occupational health and safety (anses) (2018). "Justification Document for the Selection of a CoRAP Substance- Triclocarban." Justification Document for the Selection of a CoRAP Substance. URL:https://echa.europa.eu/documents/10162/9801478/corap_update_2018-2020_en.pdf/85e5f709-da61-8b06-855c-79302dc17c70. Retrieved 03/08/2021; 3:16 pm.

Gao, L., Yuan, T., Cheng, P., Bai, Q., Zhou, C., Ao, J., Wang, W., Zhang, H., 2015. Effects of triclosan and triclocarban on the growth inhibition, cell viability, genotoxicity and multixenobiotic resistance responses of Tetrahymena thermophila. Chemosphere 139, 434-440.

Gautam, P., Carsella, J.S., Kinney, C.A., 2014. Presence and transport of the antimicrobials triclocarban and triclosan in a wastewater-dominated stream and freshwater environment. Water Res 48, 247-256.

Geiss, C., Ruppert, K., Heidelbach, T., Oehlmann, J., 2016. The antimicrobial agents triclocarban and triclosan as potent modulators of reproduction in Potamopyrgus antipodarum (Mollusca: Hydrobiidae). J Environ Sci Health A Tox Hazard Subst Environ Eng 51, 1173-1179.

Gillis, P.L., Chow-Fraser, P., Ranville, J.F., Ross, P.E., Wood, C.M., 2005. Daphnia need to be gut-cleared too: the effect of exposure to and ingestion of metal-contaminated sediment on the gut-clearance patterns of D. magna. Aquat Toxicol 71, 143-154.

Giudice, B.D., Young, T.M., 2010. The antimicrobial triclocarban stimulates embryo production in the freshwater mudsnail Potamopyrgus antipodarum. Environ Toxicol Chem 29, 966-970.

Gledhill, W.E., 1975. Biodegradation of 3,4,4'-Trichlorocarbanilide, Tcc, in Sewage and Activated-Sludge. Water Research 9, 649-654.

Glomstad, B., Zindler, F., Jenssen, B.M., Booth, A.M., 2018. Dispersibility and dispersion stability of carbon nanotubes in synthetic aquatic growth media and natural freshwater. Chemosphere 201, 269-277.

Gomes, M.F., de Paula, V.D.S., Martins, L.R.R., Garcia, J.R.E., Yamamoto, F.Y., de Freitas, A.M., 2021. Sublethal effects of triclosan and triclocarban at environmental concentrations in silver catfish (Rhamdia quelen) embryos. Chemosphere 263.

Gottschalk, F., Lassen, C., Kjoelholt, J., Christensen, F., Nowack, B., 2015. Modeling Flows and Concentrations of Nine Engineered Nanomaterials in the Danish Environment. Int J Env Res Pub He 12, 5581-5602.

Guo, X., Dong, S., Petersen, E.J., Gao, S., Huang, Q., Mao, L., 2013. Biological uptake and depuration of radio-labeled graphene by Daphnia magna. Environ Sci Technol 47, 12524-12531.

Halden, R.U., 2014. On the need and speed of regulating triclosan and triclocarban in the United States. Environ Sci Technol 48, 3603-3611.

Halden, R.U., Lindeman, A.E., Aiello, A.E., Andrews, D., Arnold, W.A., Fair, P., Fuoco, R.E., Geer, L.A., Johnson, P.I., Lohmann, R., McNeill, K., Sacks, V.P., Schettler, T., Weber, R., Zoeller, R.T., Blum, A., 2017. The Florence Statement on Triclosan and Triclocarban. Environ Health Perspect 125, 064501.

Halden, R.U., Paull, D.H., 2004. Analysis of triclocarban in aquatic samples by liquid chromatography electrospray ionization mass spectrometry. Environ Sci Technol 38, 4849-4855.

Halden, R.U., Paull, D.H., 2005. Co-occurrence of triclocarban and triclosan in U.S. water resources. Environ Sci Technol 39, 1420-1426.

Harper, S., Wohlleben, W., Doa, M., Nowack, B., Clancy, S., Canady, R., Maynard, A., 2015. Measuring nanomaterial release from carbon nanotube composites: review of the state of the science. 4th International Conference on Safe Production and Use of Nanomaterials (Nanosafe2014) 617.

Hartmann, N.B., Baun, A., 2010. The nano cocktail: ecotoxicological effects of engineered nanoparticles in chemical mixtures. Integr Environ Assess Manag 6, 311-313.

Heidler, J., Sapkota, A., Halden, R.U., 2006. Partitioning, persistence, and accumulation in digested sludge of the topical antiseptic triclocarban during wastewater treatment. Environ Sci Technol 40, 3634-3639.

Heinze, J.E., Yackovich, F., 1988. Washing with Contaminated Bar Soap Is Unlikely to Transfer Bacteria. Epidemiol Infect 101, 135-142.

Hennig, M.P., Maes, H.M., Ottermanns, R., Schaffer, A., Siebers, N., 2019. Release of radiolabeled multi-walled carbon nanotubes (C-14-MWCNT) from epoxy nanocomposites into quartz sand-water systems and their uptake by Lumbriculus variegatus. Nanoimpact 14.

Higgins, C.P., Paesani, Z.J., Chalew, T.E., Halden, R.U., 2009. Bioaccumulation of triclocarban in Lumbriculus variegatus. Environ Toxicol Chem 28, 2580-2586.

Higgins, C.P., Paesani, Z.J., Chalew, T.E., Halden, R.U., Hundal, L.S., 2011. Persistence of triclocarban and triclosan in soils after land application of biosolids and bioaccumulation in Eisenia foetida. Environ Toxicol Chem 30, 556-563.

Hirth, S., Cena, L., Cox, G., Tomovic, Z., Peters, T., Wohlleben, W., 2013. Scenarios and methods that induce protruding or released CNTs after degradation of nanocomposite materials. J Nanopart Res 15, 1504.

Hou, W.C., Westerhoff, P., Posner, J.D., 2013. Biological accumulation of engineered nanomaterials: a review of current knowledge. Environ Sci Process Impacts 15, 103-122.

Hua, S., Gong, J.L., Zeng, G.M., Yao, F.B., Guo, M., Ou, X.M., 2017. Remediation of organochlorine pesticides contaminated lake sediment using activated carbon and carbon nanotubes. Chemosphere 177, 65-76.

Hussain, C.M., Saridara, C., Mitra, S., 2009. Modifying the sorption properties of multi-walled carbon nanotubes via covalent functionalization. Analyst 134, 1928-1933.

Hwang, H.M., Hodson, R.E., Lee, R.F., 1987. Degradation of Aniline and Chloroanilines by Sunlight and Microbes in Estuarine Water. Water Research 21, 309-316.

Hyung, H., Fortner, J.D., Hughes, J.B., Kim, J.H., 2007. Natural organic matter stabilizes carbon nanotubes in the aqueous phase. Environmental Science & Technology 41, 179-184.

Iijima, S., 1991. Helical Microtubules of Graphitic Carbon. Nature 354, 56-58.

Jackson, P., Jacobsen, N.R., Baun, A., Birkedal, R., Kuhnel, D., Jensen, K.A., Vogel, U., Wallin, H., 2013. Bioaccumulation and ecotoxicity of carbon nanotubes. Chem Cent J 7, 154.

Jang, M.H., Hwang, Y.S., 2018. Effects of functionalized multi-walled carbon nanotubes on toxicity and bioaccumulation of lead in Daphnia magna. PLoS One 13 (3), e0194935. https://doi. org/10.1371/journal.pone.0194935.

Kennedy, A.J., Hull, M.S., Steevens, J.A., Dontsova, K.M., Chappell, M.A., Gunter, J.C., Weiss, C.A., Jr., 2008. Factors influencing the partitioning and toxicity of nanotubes in the aquatic environment. Environ Toxicol Chem 27, 1932-1941.

Kim, S.A., Rhee, M.S., 2016. Microbicidal effects of plain soap vs triclocarban-based antibacterial soap. J Hosp Infect 94, 276-280.

Klaine, S.J., Alvarez, P.J., Batley, G.E., Fernandes, T.F., Handy, R.D., Lyon, D.Y., Mahendra, S., McLaughlin, M.J., Lead, J.R., 2008. Nanomaterials in the environment: behavior, fate, bioavailability, and effects. Environ Toxicol Chem 27, 1825-1851.

Li, M.H., Huang, C.P., 2010. Stability of oxidized single-walled carbon nanotubes in the presence of simple electrolytes and humic acid. Carbon 48, 4527-4534.

Limbach, L.K., Wick, P., Manser, P., Grass, R.N., Bruinink, A., Stark, W.J., 2007. Exposure of engineered nanoparticles to human lung epithelial cells: influence of chemical composition and catalytic activity on oxidative stress. Environ Sci Technol 41, 4158-4163.

Lin, D., Li, T., Yang, K., Wu, F., 2012. The relationship between humic acid (HA) adsorption on and stabilizing multiwalled carbon nanotubes (MWNTs) in water: effects of HA, MWNT and solution properties. J Hazard Mater 241-242, 404-410.

Lin, D., Xing, B., 2008. Tannic acid adsorption and its role for stabilizing carbon nanotube suspensions. Environ Sci Technol 42, 5917-5923.

Ma, J., Yu, F., Zhou, L., Jin, L., Yang, M., Luan, J., Tang, Y., Fan, H., Yuan, Z., Chen, J., 2012. Enhanced adsorptive removal of methyl orange and methylene blue from aqueous solution by alkali-activated multiwalled carbon nanotubes. ACS Appl Mater Interfaces 4, 5749-5760.

Mackay, D., Fraser, A., 2000. Kenneth Mellanby Review Award. Bioaccumulation of persistent organic chemicals: mechanisms and models. Environ Pollut 110, 375-391.

Maes, H.M., Stibany, F., Giefers, S., Daniels, B., Deutschmann, B., Baumgartner, W., Schaffer, A., 2014. Accumulation and distribution of multiwalled carbon nanotubes in zebrafish (Danio rerio). Environ Sci Technol 48, 12256-12264.

Miller, T.R., Heidler, J., Chillrud, S.N., DeLaquil, A., Ritchie, J.C., Mihalic, J.N., Bopp, R., Halden, R.U., 2008. Fate of triclosan and evidence for reductive dechlorination of triclocarban in estuarine sediments. Environ Sci Technol 42, 4570-4576.

Mortimer, M., Petersen, E.J., Buchholz, B.A., Orias, E., Holden, P.A., 2016. Bioaccumulation of Multiwall Carbon Nanotubes in Tetrahymena thermophila by Direct Feeding or Trophic Transfer. Environ Sci Technol 50, 8876-8885.

Mulla, S.I., Hu, A., Wang, Y., Sun, Q., Huang, S.L., Wang, H., Yu, C.P., 2016. Degradation of triclocarban by a triclosan-degrading Sphingomonas sp. strain YL-JM2C. Chemosphere 144, 292-296.

Mwangi, J.N., Wang, N., Ingersoll, C.G., Hardesty, D.K., Brunson, E.L., Li, H., Deng, B., 2012. Toxicity of carbon nanotubes to freshwater aquatic invertebrates. Environ Toxicol Chem 31, 1823-1830.

Naasz, S., Altenburger, R., Kuhnel, D., 2018. Environmental mixtures of nanomaterials and chemicals: The Trojan-horse phenomenon and its relevance for ecotoxicity. Sci Total Environ 635, 1170-1181.

Newland, B., Taplan, C., Pette, D., Friedrichs, J., Steinhart, M., Wang, W., Voit, B., Seib, F.P., Werner, C., 2018. Soft and flexible poly(ethylene glycol) nanotubes for local drug delivery. Nanoscale 10, 8413-8421.

Nowack, B., Bucheli, T.D., 2007. Occurrence, behavior and effects of nanoparticles in the environment. Environ Pollut 150, 5-22.

OCSiAL, 2020a. About. URL: https://ocsial.com/about/. Retrieved 12/15/2020; 10:17 am.

OCSiAL, 2020b. Graphen-Nanoröhren. URL: https://ocsial.com/de/nanotubes/. Retrieved 12/15/2020; 10:20 am.

Odom, T.W., Huang, J.L., Kim, P., Lieber, C.M., 1998. Atomic structure and electronic properties of single-walled carbon nanotubes. Abstr Pap Am Chem S 216, U77-U78.

Oleszczuk, P., Pan, B., Xing, B.S., 2009. Adsorption and Desorption of Oxytetracycline and Carbamazepine by Multiwalled Carbon Nanotubes. Environmental Science & Technology 43, 9167-9173.

Parks, A.N., Portis, L.M., Schierz, P.A., Washburn, K.M., Perron, M.M., Burgess, R.M., Ho, K.T., Chandler, G.T., Ferguson, P.L., 2013. Bioaccumulation and toxicity of single-walled carbon nanotubes to benthic organisms at the base of the marine food chain. Environ Toxicol Chem 32, 1270-1277.

Peijnenburg, W.J.G.M., Baalousha, M., Chen, J.W., Chaudry, Q., Von der kammer, F., Kuhlbusch, T.A.J., Lead, J., Nickel, C., Quik, J.T.K., Renker, M., Wang, Z., Koelmans, A.A., 2015. A Review of the Properties and Processes Determining the Fate of Engineered Nanomaterials in the Aquatic Environment. Crit Rev Env Sci Tec 45, 2084-2134.

Petersen, E.J., Akkanen, J., Kukkonen, J.V., Weber, W.J., Jr., 2009. Biological uptake and depuration of carbon nanotubes by Daphnia magna. Environ Sci Technol 43, 2969-2975.

Petersen, E.J., Huang, Q., Weber, W.J., 2008a. Ecological uptake and depuration of carbon nanotubes by Lumbriculus variegatus. Environ Health Perspect 116, 496-500.

Petersen, E.J., Huang, Q., Weber, W.J., Jr., 2008b. Bioaccumulation of radio-labeled carbon nanotubes by Eisenia foetida. Environ Sci Technol 42, 3090-3095.

Petersen, E.J., Pinto, R.A., Mai, D.J., Landrum, P.F., Weber, W.J., Jr., 2011a. Influence of polyethyleneimine graftings of multi-walled carbon nanotubes on their accumulation and elimination by and toxicity to Daphnia magna. Environ Sci Technol 45, 1133-1138.

Petersen, E.J., Zhang, L., Mattison, N.T., O'Carroll, D.M., Whelton, A.J., Uddin, N., Nguyen, T., Huang, Q., Henry, T.B., Holbrook, R.D., Chen, K.L., 2011b. Potential release pathways, environmental fate, and ecological risks of carbon nanotubes. Environ Sci Technol 45, 9837-9856.

Pycke, B.F., Roll, I.B., Brownawell, B.J., Kinney, C.A., Furlong, E.T., Kolpin, D.W., Halden, R.U., 2014. Transformation products and human metabolites of triclocarban and triclosan in sewage sludge across the United States. Environ Sci Technol 48, 7881-7890.

Rhiem, S., Barthel, A.K., Meyer-Plath, A., Hennig, M.P., Wachtendorf, V., Sturm, H., Schaffer, A., Maes, H.M., 2016. Release of (14)C-labelled carbon nanotubes from polycarbonate composites. Environ Pollut 215, 356-365.

Rhiem, S., Riding, M.J., Baumgartner, W., Martin, F.L., Semple, K.T., Jones, K.C., Schaffer, A., Maes, H.M., 2015. Interactions of multiwalled carbon nanotubes with algal cells: quantification of association, visualization of uptake, and measurement of alterations in the composition of cells. Environ Pollut 196, 431-439.

Roberts, A.P., Mount, A.S., Seda, B., Souther, J., Qiao, R., Lin, S., Ke, P.C., Rao, A.M., Klaine, S.J., 2007. In vivo biomodification of lipid-coated carbon nanotubes by Daphnia magna. Environ Sci Technol 41, 3025-3029.

Saleemi, M.A., Kong, Y.L., Yong, P.V.C., Wong, E.H., 2020. An overview of recent development in therapeutic drug carrier system using carbon nanotubes. J Drug Deliv Sci Tec 59.

Saleh, N.B., Pfefferle, L.D., Elimelech, M., 2010. Influence of biomacromolecules and humic acid on the aggregation kinetics of single-walled carbon nanotubes. Environ Sci Technol 44, 2412-2418.

Sapkota, A., Heidler, J., Halden, R.U., 2007. Detection of triclocarban and two co-contaminating chlorocarbanilides in US aquatic environments using isotope dilution liquid chromatography tandem mass spectrometry. Environ Res 103, 21-29.

Schebb, N.H., Flores, I., Kurobe, T., Franze, B., Ranganathan, A., Hammock, B.D., Teh, S.J., 2011a. Bioconcentration, metabolism and excretion of triclocarban in larval Qurt medaka (Oryzias latipes). Aquat Toxicol 105, 448-454.

Schebb, N.H., Inceoglu, B., Ahn, K.C., Morisseau, C., Gee, S.J., Hammock, B.D., 2011b. Investigation of human exposure to triclocarban after showering and preliminary evaluation of its biological effects. Environ Sci Technol 45, 3109-3115.

Schierz, A., Espinasse, B., Wiesner, M.R., Bisesi, J.H., Sabo-Attwood, T., Ferguson, P.L., 2014. Fate of single walled carbon nanotubes in wetland ecosystems. Environ-Sci Nano 1, 574-583.

Schlagenhauf, L., Buerki-Thurnherr, T., Kuo, Y.Y., Wichser, A., Nuesch, F., Wick, P., Wang, J., 2015. Carbon Nanotubes Released from an Epoxy-Based Nanocomposite: Quantification and Particle Toxicity. Environ Sci Technol 49, 10616-10623.

Schwab, F., Camenzuli, L., Knauer, K., Nowack, B., Magrez, A., Sigg, L., Bucheli, T.D., 2014. Sorption kinetics and equilibrium of the herbicide diuron to carbon nanotubes or soot in absence and presence of algae. Environ Pollut 192, 147-153.

Simon, A., Preuss, T.G., Schaffer, A., Hollert, H., Maes, H.M., 2015. Population level effects of multiwalled carbon nanotubes in Daphnia magna exposed to pulses of triclocarban. Ecotoxicology 24, 1199-1212.

Smith, C.J., Shaw, B.J., Handy, R.D., 2007. Toxicity of single walled carbon nanotubes to rainbow trout, (Oncorhynchus mykiss): respiratory toxicity, organ pathologies, and other physiological effects. Aquat Toxicol 82, 94-109.

Snyder, E.H., O'Connor, G.A., McAvoy, D.C., 2010. Measured physicochemical characteristics and biosolids-borne concentrations of the antimicrobial Triclocarban (TCC). Sci Total Environ 408, 2667-2673.

Souchier, M., Benali-Raclot, D., Benanou, D., Boireau, V., Gomez, E., Casellas, C., Chiron, S., 2015. Screening triclocarban and its transformation products in river sediment using liquid chromatography and high resolution mass spectrometry. Sci Total Environ 502, 199-205.

Sun, T.Y., Gottschalk, F., Hungerbuhler, K., Nowack, B., 2014. Comprehensive probabilistic modelling of environmental emissions of engineered nanomaterials. Environ Pollut 185, 69-76.

Tamura, I., Kagota, K., Yasuda, Y., Yoneda, S., Morita, J., Nakada, N., Kameda, Y., Kimura, K., Tatarazako, N., Yamamoto, H., 2013. Ecotoxicity and screening level ecotoxicological risk assessment of five antimicrobial agents: triclosan, triclocarban, resorcinol, phenoxyethanol and p-thymol. J Appl Toxicol 33, 1222-1229.

TCC Consortium. High Production Volume (HPV) Chemical Challenge Program Data Availability and Screening Level Assessment for Triclocarban, CAS#: 101-20-2, 2002. In Exposure and Risk Screening Methods for Consumer Product Ingredients. The Soap and Detergent Association. Washington DC, USA (April, 2005). URL: https://www.aciscience.org/docs/Exposure_and_Risk_Screening_Methods.pdf. Retrieved 03/08/2021; 3:16 pm.

Templeton, R.C., Ferguson, P.L., Washburn, K.M., Scrivens, W.A., Chandler, G.T., 2006. Life-cycle effects of single-walled carbon nanotubes (SWNTs) on an estuarine meiobenthic copepod. Environ Sci Technol 40, 7387-7393.

Tsai, S.J., Hofmann, M., Hallock, M., Ada, E., Kong, J., Ellenbecker, M., 2009. Characterization and Evaluation of Nanoparticle Release during the Synthesis of Single-Walled and Multiwalled Carbon Nanotubes by Chemical Vapor Deposition. Environmental Science & Technology 43, 6017-6023.

Tsuji, J.S., Maynard, A.D., Howard, P.C., James, J.T., Lam, C.W., Warheit, D.B., Santamaria, A.B., 2006. Research strategies for safety evaluation of nanomaterials, part IV: risk assessment of nanoparticles. Toxicol Sci 89, 42-50.

TUBALL™, 2020a. Graphen-Nanoröhren. URL: https://tuball.com/about-tuball. Retrieved 12/15/2020; 10:27 am.

TUBALL™, 2020b. Gesundheit und Sicherheit. URL: https://tuball.com/de/pages/health-safety. Retrieved 12/15/2020; 10:58 am.

Umweltbundesamt (UBA, Germany), 2021a. Nanomaterialien-Anpassung der REACH Verordnung. URL: https://www.umweltbundesamt.de/nanomaterialien-anpassung-der-reach-verordnung. Retrieved 02/07/2021; 11:23 am.

Umweltbundesamt (UBA, Germany), 2021b. Warum sind Nanomaterialien anders? URL: https://www.umweltbundesamt.de/sites/default/files/medien/362/dokumente/factsheet_warum_sind_nanomaterialen_anders_bf.pdf. Retrieved 02/07/2021; 11:23 am.

Velzeboer, I., Kwadijk, C.J., Koelmans, A.A., 2014. Strong sorption of PCBs to nanoplastics, microplastics, carbon nanotubes, and fullerenes. Environ Sci Technol 48, 4869-4876.

Venkatesan, A.K., Pycke, B.F., Barber, L.B., Lee, K.E., Halden, R.U., 2012. Occurrence of triclosan, triclocarban, and its lesser chlorinated congeners in Minnesota freshwater sediments collected near wastewater treatment plants. J Hazard Mater 229-230, 29-35.

Walsh, S.E., Maillard, J.Y., Russell, A.D., Catrenich, C.E., Charbonneau, D.L., Bartolo, R.G., 2003. Development of bacterial resistance to several biocides and effects on antibiotic susceptibility. Journal of Hospital Infection 55, 98-107.

Wang, J.G., Liu, H.Z., Zhang, X.Y., Li, X., Liu, X.R., Kang, F.Y., 2018. Green Synthesis of Hierarchically Porous Carbon Nanotubes as Advanced Materials for High-Efficient Energy Storage. Small 14.

Wang, X.K., Jiang, X.J., Wang, Y.N., Sun, J., Wang, C., Shen, T.T., 2014. Occurrence, distribution, and multi-phase partitioning of triclocarban and triclosan in an urban river receiving wastewater treatment plants effluent in China. Environ Sci Pollut Res Int 21, 7065-7074.

Wang, X.L., Tao, S., Xing, B.S., 2009. Sorption and Competition of Aromatic Compounds and Humic Acid on Multiwalled Carbon Nanotubes. Environmental Science & Technology 43, 6214-6219.

Wei, J., Zhou, T., Hu, Z., Li, Y., Yuan, H., Zhao, K., Zhang, H., Liu, C., 2018. Effects of triclocarban on oxidative stress and innate immune response in zebrafish embryos. Chemosphere 210, 93-101.

Xu, X., Lu, Y., Zhang, D., Wang, Y., Zhou, X., Xu, H., Mei, Y., 2015. Toxic Assessment of Triclosan and Triclocarban on Artemia salina. Bull Environ Contam Toxicol 95, 728-733.

Yang, K., Wu, W., Jing, Q., Zhu, L., 2008. Aqueous Adsorption of Aniline, Phenol, and their Substitutes by Multi-Walled Carbon Nanotubes. Environmental Science & Technology 42, 7931-7936.

Yang, K., Xing, B., 2007. Desorption of polycyclic aromatic hydrocarbons from carbon nanomaterials in water. Environ Pollut 145, 529-537.

Yang, K., Xing, B., 2010. Adsorption of organic compounds by carbon nanomaterials in aqueous phase: Polanyi theory and its application. Chem Rev 110, 5989-6008.

Yeganeh, B., Kull, C.M., Hull, M.S., Marr, L.C., 2008. Characterization of airborne particles during production of carbonaceous nanomaterials. Environ Sci Technol 42, 4600-4606.

Ying, G.G., Yu, X.Y., Kookana, R.S., 2007. Biological degradation of triclocarban and triclosan in a soil under aerobic and anaerobic conditions and comparison with environmental fate modelling. Environ Pollut 150, 300-305.

Zarate, F.M., Jr., Schulwitz, S.E., Stevens, K.J., Venables, B.J., 2012. Bioconcentration of triclosan, methyl-triclosan, and triclocarban in the plants and sediments of a constructed wetland. Chemosphere 88, 323-329.

Zeyer, J., Kearney, P.C., 1982. Microbial-Degradation of Para-Chloroaniline as Sole Carbon and Nitrogen-Source. Pestic Biochem Phys 17, 215-223.

Zhang, L., Petersen, E.J., Habteselassie, M.Y., Mao, L., Huang, Q., 2013. Degradation of multiwall carbon nanotubes by bacteria. Environ Pollut 181, 335-339.

Zhang, L.W., Petersen, E.J., Huang, Q.G., 2011. Phase Distribution of C-14-Labeled Multiwalled Carbon Nanotubes in Aqueous Systems Containing Model Solids: Peat. Environmental Science & Technology 45, 1356-1362.

Zhang, Y., Zhu, L., Zhou, Y., Chen, J.M., 2015. Accumulation and elimination of iron oxide nanomaterials in zebrafish (Danio rerio) upon chronic aqueous exposure. J Environ Sci-China 30, 223-230.

Zhu, B., Zhu, S., Li, J., Hui, X., Wang, G.X., 2018. The developmental toxicity, bioaccumulation and distribution of oxidized single walled carbon nanotubes in Artemia salina. Toxicol Res (Camb) 7, 897-906.

Zindler, F., Glomstad, B., Altin, D., Liu, J., Jenssen, B.M., Booth, A.M., 2016. Phenanthrene Bioavailability and Toxicity to Daphnia magna in the Presence of Carbon Nanotubes with Different Physicochemical Properties. Environ Sci Technol 50, 12446-12454.

2 Distribution of weathered multi-walled carbon nanotubes in an aquatic sediment system[1]

[1] This chapter has been published in a modified version in Chemosphere.

2.1 Summary

The widespread application of carbon nanotubes (CNT) in various consumer products leads to their inevitable release into aquatic systems. But only little is known about their distribution among aquatic compartments. In this study, we investigated the partitioning of radiolabeled, weathered multi-walled CNT (^{14}C-wMWCNT) in an aquatic sediment system over a period of 180 days (d). The applied nanomaterial concentration in water phase was 100 µg L^{-1}. Over time, the wMWCNT disappeared exponentially from the water phase and simultaneously accumulated in the sediment phase. After two hours incubation just 77%, after seven days 30% and after 180 d only 0.03% of applied radioactivity (AR) remained in the water phase. The respective values for the disappearance times DT_{50} and DT_{90} were 3.2 d and 10.7 d. Further, minor mineralization of ^{14}C-wMWCNT to $^{14}CO_2$ was observed with values below 0.06% of AR. In addition, a study was carried out to estimate the deposition of wMWCNT in the water phase with and without sediment in the test system for 28 d. We found no influence of a sediment phase on the sedimentation behavior of wMWCNT in the water phase: After 6.5 d and 7.3 d 50% of the applied wMWCNT subsided in the presence and absence of sediment, respectively. The slow removal of wMWCNT from the water body by deposition into sediment implies that in addition to sediment-dwelling organisms, pelagic organisms are also at risk of exposure to nanomaterials and prone for their uptake.

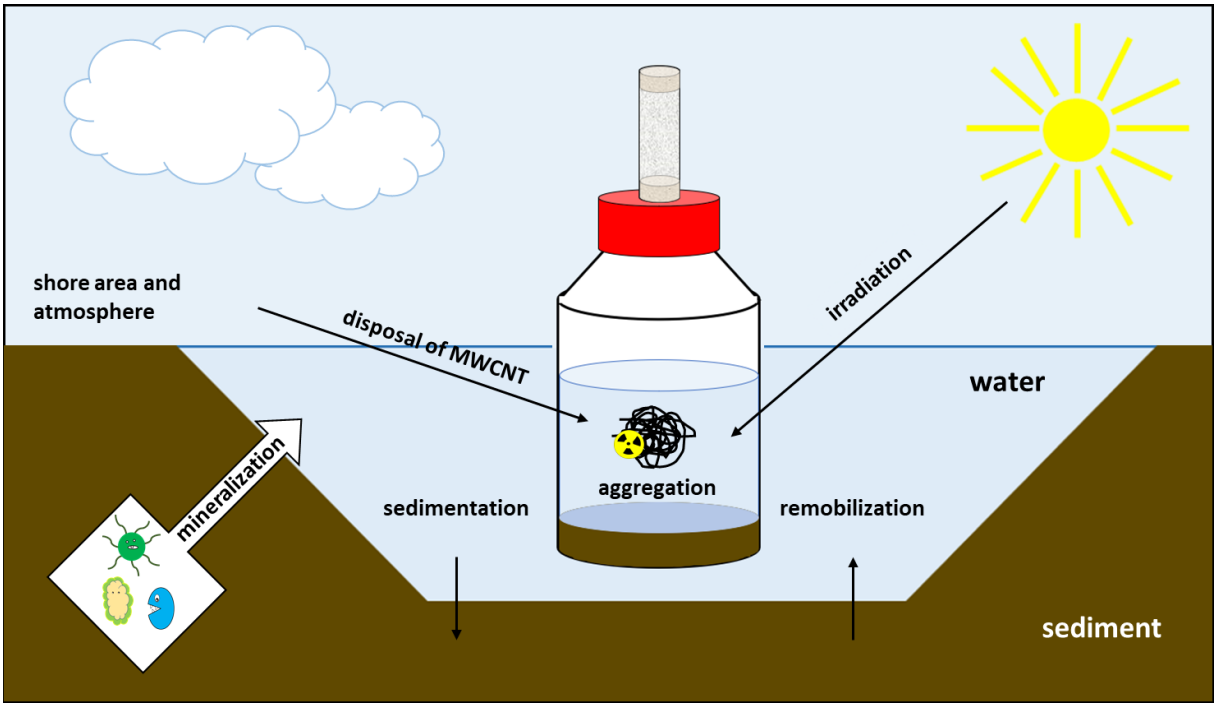

Figure 2.1: Graphical summary of chapter 2.

2.2 Introduction

Carbon nanotubes (CNT) are nanoscale tubes containing only sp^2 hybridized carbon, arranged to hexagons. A distinction is made between single-walled (SWCNT) and multi-walled CNT (MWCNT), whereby the MWCNT are characterized by several tubes wound into one another. The aromatic carbon based nature of CNT gives them specific properties, such as good electrical conductivity, high tensile strength at a low density and their hydrophobic and hollow structure provides binding sites for chemical substances and pollutants (Iijima, 1991, 2002; Kennedy et al., 2008; Mauter and Elimelech, 2008). Hence, CNT are applied in the following areas: nanocomposites (Barra et al., 2019), energy storage (Wang et al., 2018), water treatment (Zaib et al., 2014; Huang et al., 2020), nanostructured fibrous scaffolds (Xia et al., 2019) and others. Comprehensive modelling of the release of CNT into the environment in Europe showed that at the end of their life cycle, nanomaterials are disposed either in landfills or in waste incineration plants (Sun et al., 2014). Since no major environmental input is expected from this handling and the entry of CNT from industrial sites is classified as very low, the predicted environmental concentration (PEC) for CNT in surface waters is estimated in the lower ng L^{-1} range (Gottschalk et al., 2009; Gottschalk and Nowack, 2011), and in sediments at least one order of magnitude higher (Gottschalk et al., 2015). Due to their advantages, an extension of CNT production is expected, which will lead to an increased release of nanomaterials to environmental compartments, both on land and in waters.

In the past, the behavior of CNT in aqueous phase has been investigated several times. It was shown that physicochemical properties of the nanomaterials, the dispersion methods and the composition of the exposure media used (ionic strength, acids, etc.) have an influence on the dispersion stability of the CNT in aqueous medium and therefore on their fate and bioavailability (Glomstad et al., 2018). In literature, accumulation of CNT in the pelagic zooplankton *Daphnia magna* and the sediment-dwelling organism *Lumbriculus variegatus* was quantified, whereas body burdens of *D. magna* decreased after 24 h of uptake, caused by the settling of CNT over time (Petersen et al., 2008; Petersen et al., 2009; Petersen et al., 2011). To better understand and estimate the behavior of CNT as well as interactions between nanomaterials and biota in aquatic systems, there is a need to investigate the deposition of CNT in laboratory scale. Consequently, we performed a study on partitioning of CNT in an aqueous sediment system in accordance with OECD Guideline 308.

Further, the presence of additives such as surfactants or dissolved organic matter (DOM) in the aqueous phase can generate an electrostatic repulsion between the individual nanoparticles, which results in a reduction of agglomeration kinetics. On the other hand, a greater ionic strength leads to the suppression of the electrostatic repulsion and collision of nanoparticles results in increased agglomeration (Park et al., 2006; Hyung et al., 2007; Hyung and Kim, 2008; Saleh et al., 2008; Zhou et

al., 2015). A study by Zhang et al. (2011) has also shown that DOM-MWCNT composites in aqueous solution are less susceptible to the effects of high ionic strength.

In addition, Zhang et al. (2012) showed that clay and shale minerals exhibit a binding affinity for MWCNT, which causes nanomaterials to move more rapidly from the aqueous phase to the solid phase. The abovementioned process either leads to an increase or a decrease of the residence time of the nanomaterials in the water phase. Especially in case of pristine nanomaterials, hydrophobic properties cause strong agglomeration processes by Van der Waals forces, finally accelerating deposition to the sediment (Zhou et al., 2015; Glomstad et al., 2018). A half-live of 9 min for MWCNT (100 mg L^{-1}) and of 7.4 h for SWCNT (2.5 mg L^{-1}) was found for the deposition of CNT in water column (Kennedy et al., 2008; Schierz et al., 2014). Consequently, little is known about the deposition and partitioning considering low MWCNT concentrations. Therefore, we investigated the distribution of weathered MWCNT at lower concentrations than used in previous studies in a naturally simulated water sediment system. To track the partitioning among the different compartments we used radioactively labeled (^{14}C) CNT and developed a method to reliably quantify ^{14}C-MWCNT in sediment phase without sample combustion.

As a result of deposition and during their life cycle, CNT will end up in the sediment phase of aquatic systems. However, the distribution of CNT between water and sediment and their biodegradability is not yet well understood (Petersen et al., 2011b). The very slow mineralization and degradation of CNT by bacteria, fungi or enzymes, in part co-metabolically with an additional carbon source, has already been investigated in laboratory experiments. CNT, like black carbon (half-life of about 1400 years), are therefore among the most recalcitrant materials (Kuzyakov et al., 2009; Zhang et al., 2013; Flores-Cervantes et al., 2014; Parks et al., 2015).

Here, we aimed to study the behavior of weathered MWCNT in an aquatic sediment batch system and the distribution of the nanomaterials between aqueous and solid phase and to quantify the mineralization rate over a period of 180 days. In order to gain a better understanding of the sedimentation of MWCNT in the selected test system, the deposition of MWCNT in natural water with and without sediment phase was also examined. Sedimentation kinetics of CNT in aqueous phase are already available, but they result from studies in which high concentrations of nanomaterials were used (Kennedy et al., 2008; Schierz et al., 2014). In our study, the chosen MWCNT test concentration for both experiments was considerably lower, i.e., 100 µg L^{-1}. In surface waters, the PEC for CNT is in the ng L^{-1} range, so experiments approaching lower concentrations are necessary. Besides, the use of high CNT concentrations may lead to the erroneous results regarding the sedimentation of nanomaterials in the water column.

2.3 Materials and methods

2.3.1 Manufacturing of ^{14}C-labeled MWCNT (^{14}C-MWCNT)

Synthesis of ^{14}C-MWCNT has already been described elsewhere (Maes et al., 2014; Rhiem et al., 2015). Briefly, ^{14}C-MWCNT were synthesized by catalytic chemical vapour deposition. The ^{14}C label of produced ^{14}C MWCNT was located at the carbon framework. Obtained ^{14}C-MWCNT were washed using 12.5% hydrochloric acid solution to remove residues of metal catalyst, resulting in a C-purity for the product of 95%. Produced ^{14}C-MWCNT consist of 3 - 15 walls (4 nm for inner and 5 - 20 nm for outer diameter) and a length of ≥ 1 µm (Rhiem et al., 2015). Unlabeled MWCNT (Baytubes® C150P) were provided by Bayer Technology Services GmbH (BTS, Leverkusen, Germany) and produced under the same conditions as ^{14}C-MWCNT. The structural similarity of the nanomaterials was shown by means of transmission electron microscopy (TEM) (Rhiem et al., 2016).

2.3.2 MWCNT weathering

Weathering of labeled and unlabeled MWCNT was performed by simulated sunlight radiation for three months (2160 h) using a weathering testing apparatus (Suntest™ CPS+, Altas Material Testing Technology, Germany, standard black temperature 65 °C, dry conditions). The device provided light with a wavelength range of 300 to 400 nm due to an air-cooled xenon lamp (1500 W) with a daylight UV filter. Irradiation intensity was set to 65 W m^{-2} and the total applied energy was 505441 kJ m^{-2}. During the exposure, samples (^{14}C) MWCNT) were placed into petri dishes with glued-on lids made of quartz glass (transmissibility for UV light). Meanwhile, the internal sample table was cooled with a constant flow of cold water. Samples were shaken once a day and the position of sample bins was changed weekly in order to achieve a uniform irradiation.

After the weathering process, the specific radioactivity of ^{14}C-labeled weathered MWCNT (^{14}C-wMWCNT) was determined. Therefore, three ^{14}C-wMWCNT suspensions with 102, 186 and 488 µg of ^{14}C-wMWCNT in 102, 186 and 488 mL of deionized water, respectively, were prepared. After addition of nanomaterials, they were washed under the water surface using a pipette. Subsequently, the flask was put into an ice bath and ^{14}C-wMWCNT were dispersed by means of ultrasonication with a micro tip for 2 × 10 min (Sonopuls HD 2070, 70 W, pulse: 0.2 s, pause: 0.8 s, Bandelin, Germany) or until no more agglomerated nanomaterial was visible. Subsequently, six aliquots of 1 mL were withdrawn from each dispersion, mixed with 2 mL of Ultima Gold™ XR scintillation cocktail (Perkin Elmer, Germany) and the amount of radioactivity was determined by means of LSC (liquid scintillation counter, Hidex 600/300 SL, Finland). Since, after homogenization, 1 µg of ^{14}C-wMWCNT was contained in 1 mL dispersion, the specific radioactivity (MBq mg^{-1}) could be calculated using the mean value of subsamples to 1.66 MBq mg^{-1}.

In order to characterize wMWCNT, thermogravimetric analysis (TGA) coupled to a Fourier-transform infrared spectrometer (FTIR) (see SI, Fig. 2.5) and TEM (SI, Fig. 2.4) methods were used. Neither differences nor heterogeneous functionalities on surface structures compared to the pristine material were detected. The observation from TGA/FTIR analysis could be based on autoxidation of the pristine MWCNT, which occurs due to prolonged storage. This is a surface functionalization depending on the surface occupancy. Other explanations could be that, e.g., COOH functionalities have decarboxylated over time and the oxidative functionalities could not be detected for this reason, or that the measurement method was not sufficiently sensitive to detect the surface modifications that have occurred. In addition, no macrostructural changes in the construction of the CNT strands could be visualized by means of TEM. Like pristine MWCNT, the weathered material showed small agglomerates and single strand exfoliated CNT after dispersion.

2.3.3 Origin and preparation of sediment and water

Sediment and water used for the test system were previously collected from a local rainwater retention basin in Aachen (Germany). Sampled sediment was sieved to remove raw material (2 mm) and gently mixed to guarantee a homogeneous test mass (storage conditions: 4 °C in darkness). Natural structures and living organisms (≤ 2 mm) were sustained. Sediment characterization revealed a heavy silty sand (sand: 50%; silt: 47%; clay: 3%), with a total carbon content of 3.3 ± 0.1% and total organic carbon (TOC) of 2.7 ± 0.04% (Element Analyzer (CHN), elementar Analysensysteme GmbH, vario EL III, Germany), a loss on ignition of the dried sediment of 7.0 ± 0.3% and a dry weight of 45.4 ± 3.4%. To determine microbial activity in sediment, a dimethyl sulfoxide (DMSO) reduction test was performed (Alef and Kleiner, 1989). For this, sediment (1 g, air-dried for four hours) was placed in glass vials (20 mL volume) and a DMSO solution of 5% (v/v; in water) was added. The vials were closed immediately by a gas tight screw cap with septum inlet. The test was carried out in five replicates. Samples were incubated for 24 h at 27 °C. After incubation, the produced DMS was determined by taking a sample from the vial headspace with a gas tight syringe (Hamilton, 100 µL) and subjected to GC-MS analysis (Agilent Technologies 6890N, Software: MSD ChemStation (Agilent), Injection: 250 °C, injection in split mode (one sample in 60 s), MS: 5973 MSD, 150 °C (Agilent)). Helium was used as carrier gas (1.0 mL min^{-1}). An Optima-35MS column (Macherey und Nagel) with a length of 30.0 m and an inner diameter of 0.25 mm was used. Test was performed according to Griebler and Slezak (2001). The DMSO reduction rate is expressed as ng DMS g^{-1} dw^{-1} h^{-1}. Microbial activity of the sampled sediment was 269.4 ± 25.2 ng DMS g^{-1} dw^{-1} h^{-1}. Natural water was stored at 4 °C in closed containers and filtered using gauze (mesh size: 63 µm) before use.

2.3.4 Sedimentation of ^{14}C-wMWCNT

Deposition of CNT in water phase was tested for a ^{14}C-wMWCNT concentration of 100 µg L^{-1} in the presence (+sediment) and absence (-sediment) of sediment over 28 d. Per scenario four replicates were prepared. The study was performed in 250 mL glass flasks. Prior to test start, sediment (80 mL natural sediment, see 2.5.3) was incubated with overlaying tap water of 5 mL for seven days to adapt the sediment to the test conditions (18 ± 1 °C, 60 rpm, darkness). In the scenario without sediment, four flasks were filled with 5 mL tap water for pre-incubation. For test start, ^{14}C-wMWCNT agglomerates were weighed on a microbalance (MYA 5.3Y, Radwag) and transferred to a flask containing 105.7 mL natural water and dispersed for 10 min as described above. Afterwards 2×2.5 mL of this stock dispersion was transferred to 787.5 mL natural water. The aqueous phases were again treated by means of ultrasonication tip for 10 min (see above) to obtain the test dispersions. The two-stage dispersion process as described is a deviation from the method of Rhiem et al. (2015). An investigation using TEM revealed that wMWCNT test dispersion contains small agglomerates as well as single tubes (length: 0.2 to ≥ 1 µm, see SI) and is therefore appropriate for the dispersion of wMWCNT in aqueous solution.

Directly after sonication, three aliquots of 1 mL were withdrawn out of test dispersions, 2 mL of scintillation cocktail were added, and samples submitted to LSC to verify ^{14}C-wMWCNT concentration and homogeneity. Immediately after sonication, a respective volume of 175 mL out of test dispersions was applied to the prepared test systems. A concentration of 110.7 ± 3.4 µg L^{-1} and 109.2 ± 1.0 µg L^{-1} was obtained for +sediment and -sediment scenario, respectively. During application, swirling of the sediment surface was avoided as good as possible. Aliquots of 1 mL were withdrawn regularly from the top layer of water surfaces (layer depth: 0.5 cm) of all treatments and radioactivity measurement was performed as described above. Shaking was paused during sampling time (28 d), but flasks were not taken from the shaker, in order to reduce disturbance of the test systems. Decrease of radioactivity was extrapolated for the whole water body based on the taken aliquot.

2.3.5 Distribution of ^{14}C-wMWCNT in an aquatic sediment system

The partitioning of ^{14}C-wMWCNT in a natural water sediment system was determined after 2 h, 1, 2, 7, 21 days, and further after 3 and 6 months in four replicates each. Tested ^{14}C-wMWCNT concentration was 100 µg L^{-1}. The study was performed following the OECD Guideline 308 with some deviations as described hereinafter. Prior to CNT application, 250 mL flasks were filled with 80 g naturally moist sediment and covered with 5 mL tap water. Every flask was closed by a screw cap with integrated CO_2-trap containing soda lime and was incubated for 7 d (conditions: 18 ± 1 °C, 60 rpm, darkness). Additionally, two control groups (control: without nanomaterial; negative control:

unlabeled wMWCNT (100 µg L^{-1})) were prepared. After acclimatization, the application of nanomaterials via the water phase was performed.

Labeled and unlabeled wMWCNT were weighed on a microbalance and added to a glass flask containing 50 mL natural water, respectively. Stock dispersions were treated by sonication for 10 min as described above. Afterwards the stock dispersions were transferred to different flasks containing natural water to gain the ^{14}C-wMWCNT test concentration and dispersed another time (10 min). Nanomaterial concentration and homogeneity of test dispersion was monitored directly after sonication (see above). The achieved ^{14}C-wMWCNT test concentration was 134.7 ± 12.3 µg L^{-1} (which corresponds to a radioactivity amount of 38.8 ± 3.7 kBq per sample). Detection limit for measurement using LSC was at 1 Bq, which corresponds to about 0.6 ng ^{14}C-wMWCNT. Therefore, and in respect to work with natural sediment, the chosen nanomaterial concentration was needed, to detect reliably nanomaterial concentration in the used matrix. Using a glass pipette, application of 175 mL stock dispersion was carried out carefully, in order to avoid disturbance of sediment surface. Each flask was capped with a screw cap with integrated CO_2-trap and incubated under the same conditions as described for pre-incubation.

2.3.6 Detection and quantification of ^{14}C-wMWCNT

To quantify the formation of $^{14}CO_2$ as inorganic end product of microbial activity, soda lime pellets from CO_2 trap were dissolved in 25% hydrochloric acid solution (60 – 70 mL) and released $^{14}CO_2$ was absorbed by a provided scintillation cocktail (Oxysolve C-400 scintillation cocktail, Zinsser Analytic, Frankfurt a.M., Germany) in four LSC vials per replicate. After complete solution of soda lime pellets, the used equipment was flushed by nitrogen gas to collect all the developed $^{14}CO_2$. Radioactivity was measured by means of LSC. For calculation of total $^{14}CO_2$ amount per sample values from all four vials were summarized. Subsequently, removing of water phase was performed carefully using a glass pipette in order to prevent the collection of sediment particles. The water phase was filled completely into a prepared glass flask and weight was recorded. Afterwards, the water phase containing flask was placed in an ice bath and the present nanomaterials were dispersed for 10 min as described above. After homogenization, the water phase was subsampled (three aliquots of 10 g per replicate) and radioactivity was determined by means of LSC. To investigate the amount of settled CNT on the sediments surface, the water-sediment contact layer was sampled separately from the sediment. After water phase removal, the flasks were placed at a 45 degree angle for 15 min and the water-sediment contact layer was sampled afterwards with a Pasteur pipette and measured using LSC. To quantify the amount of ^{14}C-wMWCNT absorbed by the forming biofilm on the inner test vessel wall over time, the test vessel wall was then cleaned using a moist tissue. The tissue was mixed with 20 mL scintillation

cocktail and subjected to LSC. The remaining sediment phase was dried for 24 h at 105 °C and dry weight was determined.

Subsequently, the dried sediment was transferred to a ceramic mortar and grinded by hand to fine sand. To quantify the amount of ^{14}C-wMWCNT included in the sediment phase ten aliquots of ≤ 0.05 g per replicate were weighed in LSC vials and 0.5 mL of 35% hydrogen peroxide was added. The vials were swayed manually and incubated for 24 h at 60 °C. To suspend the sediment after drying, 0.5 mL ultrapure water was added, and the samples were gently shaken by hand. Afterwards 19.5 mL scintillation cocktail was added, and the vials were kept for 24 h in the dark at 4 °C. After cooling down, samples were acclimatized to room temperature and prior to LSC measurement, vials were placed in an ultrasonication bath and homogenized for 1 min. In a pre-test, the influence of sediment particles on quenching of flashes during LSC measurement (using an appropriate blank) was investigated (data is shown in the SI at 2.10.3). In brief, a known amount of radioactivity (^{14}C-wMWCNT) was applied onto 20.1 ± 0.1 g sediment (dry weight), homogenized and samples were incubated at 60 °C overnight. Subsequently, the sediment was pestled and twelve aliquots of ≤ 0.05 g per sample were weighed into LSC vials, treated with H_2O_2 and submitted to LSC measurement. It was shown that there is no impact on efficiency of LSC measurement when particles of sediment (provided that the sample size is ≤ 0.05 g per replicate) are present in the sample. Since the recovery of ^{14}C-wMWCNT in sediment was consistent of up to 105 ± 3%, no application of a correction factor to CNT recuperation was needed.

2.3.7 Data evaluation and statistical analysis

Collected data were processed using Microsoft Excel® (Microsoft Office 365 ProPlus), GraphPad Prism (GraphPad Prism 5, USA), SigmaPlot (version 12.0, USA) and R (version 4.0.3, Austria). Outliers were identified by Dixon's Q test (α = 0.05). To identify differences to zero for decreasing wMWCNT concentrations in water phase and the results for mineralization, a one-sample t-test (one-tailed, α = 0.05) was performed. Raw data were tested for normality distribution with Kolmogorov-Smirnov test (p value = 0.05).

Kinetics for the sedimentation of wMWCNT (disappearance times = DT) were calculated and evaluated using Tessella Computer Assisted Kinetic Evaluation (CAKE, version 3.3). Usually, this program is intended to fit degradation kinetics of chemicals and their metabolites in line with FOCUS (FOrum for the Coordination of pesticide fate models and their USe) or NAFTA (North American Free Trade Agreement) guidelines. Regarding to the loss of ^{14}C-wMWCNT amount in a water phase as a decay like behavior, CAKE was found to be suitable. Due to the best resulting fit parameters, we chose the SFO model (Single First-Order kinetics, see SI at 2.10.4). Differences between treatments (+/- sediment) in deposition study were identified by comparing t-distributed 95% confidence intervals of slopes (k-value) from decay models.

2.4 Results

2.4.1 Sedimentation of ^{14}C-wMWCNT

Weathered MWCNT deposited from top layer of water surface over time. Since t-distributed 95% confidence intervals of exponent k from the applied decay model overlapped, no significant difference between +sediment (0.095 – 0.118) and -sediment (0.087 – 0.102) scenario was found (see SI, Tab. 2.5 and 2.12). A more homogenous distribution of data in absence of sediment and a fluctuating course of data in presence of sediment, indicated by bigger standard deviations (e.g., on day 1, 15 and 17), was observed (Fig. 2.2). However, after a few days 50% of the dispersed wMWCNT have sedimented in both test systems. Sedimentation half-lives (DT_{50}) modelled by CAKE (Tab. 2.1) amounted to 6.5 d and 7.3 d in the +sediment and -sediment scenario, respectively. The applied model showed a good fit to the observed deposition data set with a coefficient of determination above 0.97 (Tab. 2.1). Nevertheless, no significant difference between the scenarios was depicted, somewhat faster sedimentation in presence of sediment is indicated by a DT_{90} of 21.7 d compared to the DT_{90} of 24.3 d in the scenario without sediment.

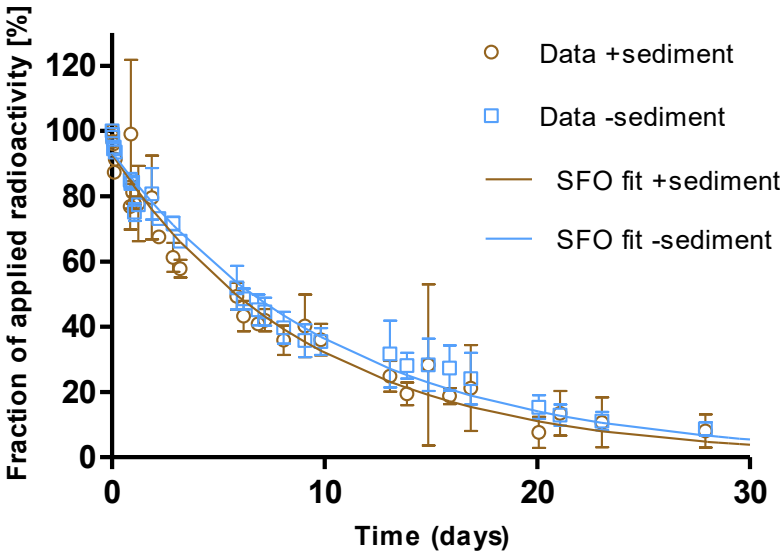

Figure 2.2: Deposition of radioactively labeled and weathered multi-walled carbon nanotubes (^{14}C-wMWCNT) in a water sediment system (+sediment) and in a system containing natural water only (-sediment). A ^{14}C-wMWCNT concentration of 110.7 ± 3.4 µg L^{-1} and 109.2 ± 1.0 µg L^{-1} was applied for +sediment (A) and -sediment (B) scenario, respectively. The proportion of decrease (%) of the applied radioactivity over the test period is shown. Error bars indicate standard deviation on the mean of four replicates. The amount of radioactivity measured at the beginning (0 h) of the test was set to 100%. A SFO (Single First-Order) model using CAKE was fitted to the experimental data.

However, in neither of the two scenarios complete sedimentation of the nanomaterials was observed within the test period. A respective residual amount of 8 ± 5% and 9 ± 2% was still detectable in the top layer of the water phase in the +sediment and -sediment approaches, respectively, even after 28 d.

2.4.2 Distribution of ^{14}C-wMWCNT

The distribution of radioactivity – applied as weathered radiolabeled MWCNT (^{14}C-wMWCNT) – among different compartments (sediment, water phase, water-sediment contact layer, mineralized amount and glass adsorbed radioactivity) in an aquatic sediment system is shown in Figure 2.3. The total recovery of ^{14}C ranged between 83% and 98%. It was observed that the amount of radioactivity in the water phase decreased over time. After two hours incubation just 77 ± 3%, after seven days 30 ± 15% and after 180 d 0.03 ± 0.01% of applied radioactivity (AR) was detected in the water phase. Therefore, a wMWCNT concentration of 0.04 µg L^{-1} remained in aqueous phase after 180 d. The suspended wMWCNT amounts in water phase after three and six months were rather low but statistically significantly different from zero (one-sample t-test, $\alpha = 0.05$). The respective sedimentation kinetics for DT_{50} and DT_{90} calculated by CAKE were 3.2 d and 10.7 d. The amount of radioactivity in the sediment increased over time. After two hours of incubation, already 19 ± 4% was detected in the sediment and with termination of the study (six months), a total of 85 ± 4% of AR was found in the sediment. The more radioactivity was detected in the sediment, the lower were the recoveries (for instance: 86% after six months).

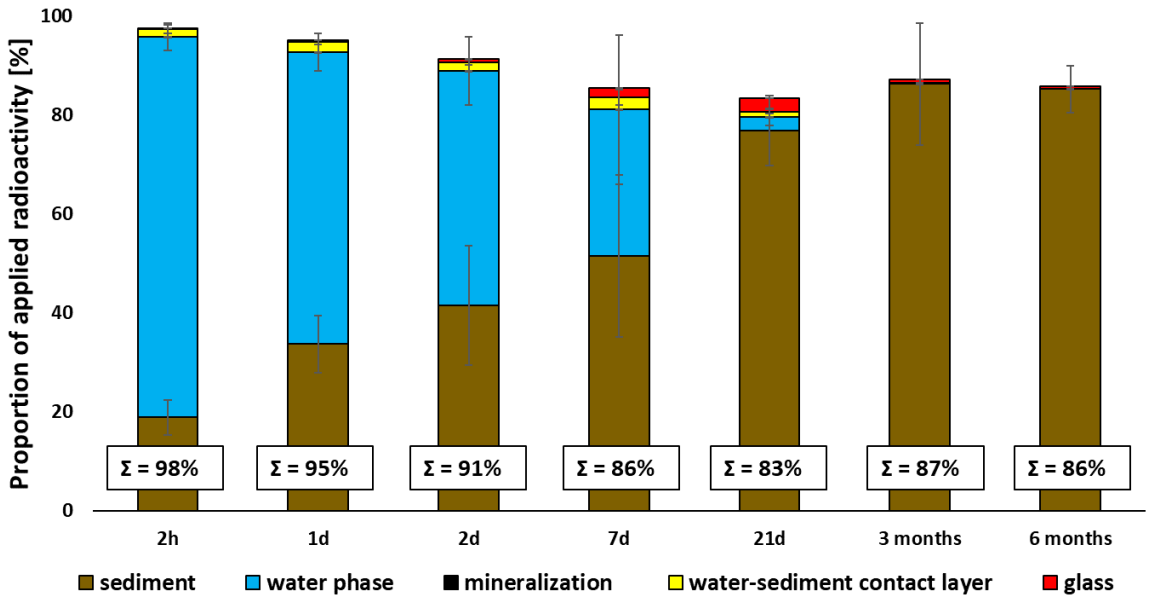

Figure 2.3: Distribution of radioactivity (in % of applied radioactivity) among sediment, water phase, water sediment contact layer, mineralized portion and radioactivity adsorbed to the used glassware over time (2 h, 1, 2, 7, 21 days, 3 and 6 months) after applying ^{14}C-wMWCNT (134.7 ± 12.3 µg L^{-1}) to an aquatic sediment system. Σ: sum of recovered radioactivity. Error bars indicate standard deviation on the mean of four replicates.

The portion of radioactivity in the water-sediment contact layer never exceeded 3% of AR and after three and six months of incubation amounted to only 0.08 ± 0.04% and 0.02 ± 0.01% of AR, respectively. Results showed that mineralization was very low, as a total of 0.02 ± 0.008%, 0.01 ±

0.003% and 0.06 ± 0.04% of AR was found after 21 d, three and six months, respectively. But statistical analysis showed that the abovementioned amounts found for complete degradation were statistically significantly different from zero (one-sample t-test, α = 0.05). Adsorption of the nanotubes to glass and the formed biofilm on the inner vessel wall was negligible, values ranged from 0.2 to 2.7% of AR. Dissolved oxygen, determined in the controls, ranged between 6.8 mg L^{-1} and 8.9 mg L^{-1} over time (75% - 97% of saturation at 20 °C) indicating water phase of the test system was oxic. The pH value in the water phases of the samples was almost constant over time and varied between 7.6 and 8.2.

Table 2.1: Data modelling using Tessella CAKE (version 3.3) for the sedimentation of ^{14}C-wMWCNT in an aquatic sediment system over 28 days and over six months in a deposition and a partitioning study, respectively. The chosen compartment model was Single First-Order (SFO). Half-life (DT_{50}) and disappearance times after 90 days (DT_{90}) are given. Additional statistical characteristics are Chi^2 (error in %) and r^2 (observed vs. predicted data).

	Deposition study		Partitioning study
sediment	+	-	+
sampling	aliquots from top layer of water surface (depth: 0.5 cm)		total water compartment
DT_{50} (d)	6.5	7.3	3.2
DT_{90} (d)	21.7	24.3	10.7
Chi^2	8.4*	5.8*	16.8*
r^2	0.97*	0.98*	0.95*

*denotes a nonsignificant lack of fit (Chi^2, 5% two-sided) and a significant slope (r, 5% one-sided).

2.5 Discussion

In the present study the deposition of 100 µg wMWCNT L^{-1} was observed in a natural water sediment system under controlled laboratory conditions. Since the 95% confidence intervals for k-values overlapped, there was no statistically significant difference in the deposition kinetics in the presence and absence of sediment (Fig. 2.2). We had expected that DOM introduced via the sediment would delay CNT agglomeration and discharge from the water phase, but this was not confirmed. Natural organic matter (NOM) is known to prevent agglomeration of CNT particles when present in aqueous solution, thereby increasing the dispersion stability of nanomaterials (Hyung et al., 2007). However, the sediment used consisted of 50% sand with an organic carbon content of 2.7%, which may have resulted in an insufficient amount of NOM being flushed out of the sediment and into the water phase. Contrary to our expectations the +sediment scenario showed a somewhat faster sedimentation behavior. Since the presence of sediment in the system can influence the ionic strength of the overlaying water phase, it is probable that it led to an increased sedimentation of the nanomaterials as described in the literature (Zhou et al., 2015; Glomstad et al., 2018).

The study on the partitioning of ^{14}C-wMWCNT in a water sediment system has shown that the nanomaterials are deposited into the sediment over time and thus disappeared, except for some

residuals, from the water phase. Even though we were able to show in a preliminary experiment, that the amount of radioactivity in the sediment phase can be reliably detected, the recovery decreased to below 90% after an incubation period of 7 days (Fig. 2.3). The fact that an increasing concentration of ^{14}C-wMWCNT in the sediment phase leads to a decreasing recovery rate leads to the assumption that the nanomaterials interacted with components of the sediment (Zhang et al., 2012), which consequently reduced detectability.

However, it was shown that after a test duration of 90 days more than 99.9% of AR disappeared from the water phase (significant amounts of 0.06% after 90 d; 0.03% after 180 d remained suspended). Although it has been shown that CNT can be stabilized in the water column to a certain extent depending on the water chemistry (Zhang et al., 2011; Glomstad et al., 2018), the nanomaterials are very likely to merge with the sediment at a certain time point.

In the environment, particles in the water phase are under constant influence of water turbulence and aquatic fauna. It is conceivable that nanomaterials in raw form as well as in complexes with, e.g., DOM are ingested by organisms and excreted with the faeces (Gillis et al., 2005; Kennedy et al., 2008; Petersen et al., 2011a; Maes et al., 2014), which consequently precipitate out of the water column and become embedded in the sediment. In the past, it was observed that the presence of organisms in a nanomaterial suspension promotes agglomeration of the particles and thus an increased sedimentation was observed, e.g., by passage through the gastrointestinal tract of animals, which can lead to agglutinated and insoluble agglomerates (Patra et al., 2011; Guo et al., 2013). The same was observed for coated SWCNT after intestinal passage by *Daphnia*, where the lipid layer could be reabsorbed by the organism and uncoated and clumped SWCNT were excreted (Roberts et al., 2007). On the other hand, Mao et al. (2016) showed that, during digestion excreted proteins of *Limnodrilus hoffmeisteri* coated few layer graphene (FLG) present in the water phase, which increased their solubility, leading to reduced sedimentation of FLG in the presence of *L. hoffmeisteri*.

The sediment surface represents an active interface between the aqueous and the solid phase. We showed that sedimented wMWCNT do not accumulate in the water-sediment contact layer but enter the sediment immediately after deposition, presumably due to a high binding affinity to the sediments clay mineral content of about 3% and a TOC content of 2.7%. Organic matter has aromatic ring structures as well as aliphatic molecule chains, due to π - π or CH - π interactions they tend to adsorb MWCNT (Lin and Xing, 2008; Piao et al., 2009; Zhang et al., 2012). Furthermore, it was assumed that cations and extracellular polymeric substances support bridging between CNT and NOM or within CNT particles (Zhou et al., 2015; Glomstad et al., 2018). Bouchard et al. (2017) investigated MWCNT deposition in Brier Creek (Georgia, USA) using the Water Quality Analysis Simulation Program. These studies indicated that in natural systems the disappearance of MWCNT from the upper sediment layers

is triggered by burial by settling particles, resuspension and the subsequent transport of sediment particles. Therefore, it is assumed that the nanomaterials follow the same transport path as the particles to which they are attached (Bouchard et al., 2017). Subsequently, MWCNT can affect benthic organisms and microorganisms, depending on their bioavailability. Furthermore, remobilization of the sedimented CNT, e.g., by bioturbation of sediment-dwelling organisms or during flooding events, is conceivable (Bouchard et al., 2017). However, some studies found that MWCNT deposition is mostly not reversible (Chang and Bouchard, 2013; Bouchard et al., 2015; Zhao et al., 2016).

Final degradation of ^{14}C-wMWCNT to $^{14}CO_2$ was observed in the partitioning study but to a very small extent. Assuming that the mineralization kinetics is based on a linear model, the data set from six months sampling of the present study would result in a half-life of > 400 years. Flores-Cervantes et al. (2014) quantified $^{14}CO_2$ evolved from a test system where ^{14}C-CNT were exposed to horseradish peroxidase and H_2O_2 and calculated half-lives of about 80 years. In addition, two further studies prove that CNT are recalcitrant substances. The co-metabolic degradation of ^{14}C-MWCNT by a bacterial community over seven days showed mineralization rates of 2 to 6.8% (Zhang et al., 2013). A significantly lower mineralization rate of less than 0.1% was observed for the degradation of ^{14}C-SWCNT by the fungus *Trametes versicolor* in pure form or introduced into sediment or sludge over a period of six months (Parks et al., 2015). The values for mineralization determined in our study are thus in the lower range of the values already documented. No external microorganisms were added to our test system and the measured microbial activity in the used sediment with 269 ng DMS g^{-1} dw^{-1} h^{-1} is in the lower range compared to literature values (Lopez and Duarte, 2004).

Additionally, a weak antibacterial effect of MWCNT has been confirmed in the past so that an adverse effect on the bacterial community in the sediment cannot be excluded. (Kang et al., 2008; Baek et al., 2019). The MWCNT investigated in this study were weathered before use, but no differences in surface structure compared to pristine MWCNT were detected using TGA and FTIR (see SI). The chemical structure of carbon nanotubes suggests a high persistence of these materials. However, it is known that defects in the graphite structure, that may occur during weathering, provide vulnerabilities for degradation by microorganisms. These include vacancies in the nanotube network, open ends, sp^3 hybridizations and stone-wales defects (Yao et al., 1998; Hirsch, 2002; Niyogi et al., 2002; Tasis et al., 2006). Correspondingly, we showed that MWCNT become degraded but at a very slow rate.

The partitioning study revealed sedimentation kinetics of 3.2 d and 10.7 d (DT_{50} and DT_{90}, respectively). Although the partitioning study was conducted under the same conditions as the deposition study, the half-lives obtained differed slightly (Tab. 2.1). This difference may have been caused by the different sampling technique of the water phases. While in the deposition study only the top of the water surface was sampled, in the partitioning study the entire water phase was examined. During the

sampling of the deposition study, it was also noticed that a biological film was present on top of the water surface, which probably contained an increased amount of ^{14}C-wMWCNT and thus led to an overestimation of the wMWCNT concentration in the water phase.

In our studies, slower sedimentation kinetics compared to other studies were observed. Kennedy et al. (2008) obtained a DT_{50} of 9 min for the sedimentation of MWCNT (100 mg L^{-1}) in water containing NOM and Schierz et al. (2014) showed a DT_{50} of 7.5 h for the sedimentation of SWCNT (2.5 mg L^{-1}) in a mesocosm study. Since in both studies the water phase contained NOM, it can be assumed that the short half-lives observed in the literature are due to the initially much higher CNT concentrations used compared to the lower nanomaterial concentration applied in our study. The influence of the spiked concentration on agglomeration and stability in aqueous phase was also observed for few-layer graphene (FLG) and identified as a key factor. Within the study, Su et al. (2017) observed that the agglomeration rate of nanomaterial decreased with increasing dilution of FLG suspension. At low CNT concentrations in the water phase, as in our study, the probability of encounter and thus the frequency of agglomeration is considerably reduced, compared with concentrations in the mg L^{-1} range. The predicted environmental concentration of CNT in surface waters is in the lower ng L^{-1} range, so in general more experimental work should be performed in even lower concentration ranges. The slow sedimentation kinetics of wMWCNT clearly implies that not only sediment dwelling organisms but also those living in the water phase are exposed to engineered carbon nanomaterials.

2.6 Conclusion and outlook

The long residence time of CNT in the water column, ranging from several days to weeks, and their accumulation in sediment lead to the exposure of pelagic and benthic organisms. Aquatic sediment systems with different sediment and water properties as well as different types of CNT should be studied and designed to confirm our findings of long-term stability of CNT and their distribution in water sediment systems. Thus, our study and future work can contribute to a better assessment of the transport of nanomaterials in water as input parameters for modeling approaches.

2.7 Suplementary information (SI)

2.7.1 Method and results from transmission electron microscopy (TEM)

Pristine and weathered MWCNT were visualized by means of transmission electron microscopy (TEM). For this, MWCNT were dispersed as described in materials and methods section and loaded onto copper grids (Plano GmbH) for TEM analysis. The copper grids were submerged in the nanomaterial suspension directly after the dispersion procedure and subsequently placed on a filter heated up to 50 °C. After drying, the copper grids were subjected to TEM analysis using a Philips CM 20 FEG operating at 200 keV.

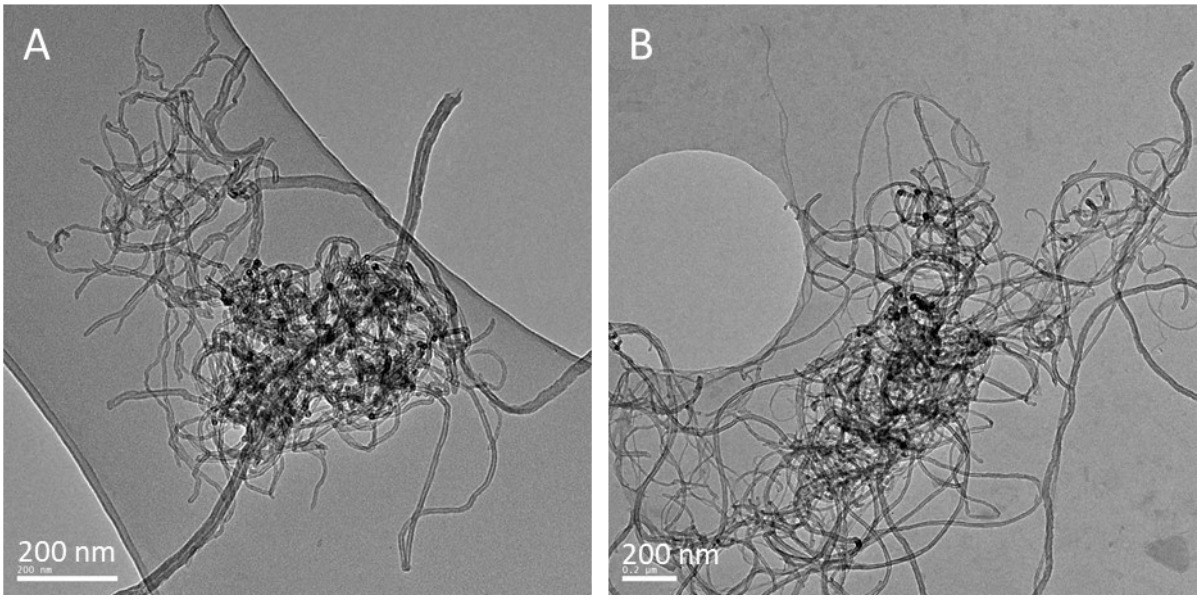

Figure 2.4: Transmission electron microscopy (TEM) images of pristine (A) and weathered (B) MWCNT (unlabeled) (taken by Dr. Nina Siebers from Forschungszentrum Jülich GmbH).

2.7.2 Method and results from thermogravimetric analysis (TGA) and Fourier-transform infrared spectroscopy (FTIR)

TGA-FTIR measurements were performed using a TGA/DSC3+ thermo balance (Mettler Toledo, Columbus, USA) coupled with an FTIR spectrometer (Nicolet iS50 Advanced FT-IR, Thermo Fisher Scientific, Waltham, USA) equipped with a gas measuring cell (260 °C). The transfer line used (inner diameter: 1 mm) was maintained at 250 °C. The FTIR measurements were performed over a range of 4000 – 400 cm^{-1} with a resolution of 4 cm^{-1} and a scan rate of 16 scans per spectrum. 3 mg of the test material were measured six times each using 150 µL aluminum oxide crucibles. Heating rates of 10 K min^{-1} were applied from 25 °C up to 900 °C. A nitrogen flow of 30 ml min^{-1} passes through the TGA and FTIR system. At 600 °C the gas is switched to synthetic air.

The TGA analyses showed that the mass loss vs. temperature profiles of pristine and weathered CNT are congruent, no differences have been detected when normalizing to the slightly different initial weights of pristine (2.91 mg) and weathered (3.19 mg) CNT. Typically, a mass loss would have been expected in the range of 300-600 °C for the weathered CNT, in case of oxidized surface functionalities that would be released during heating. Additionally, the release of CO and CO_2 from such functional groups would have been expected in the FTIR analyses which, however, was not the case.

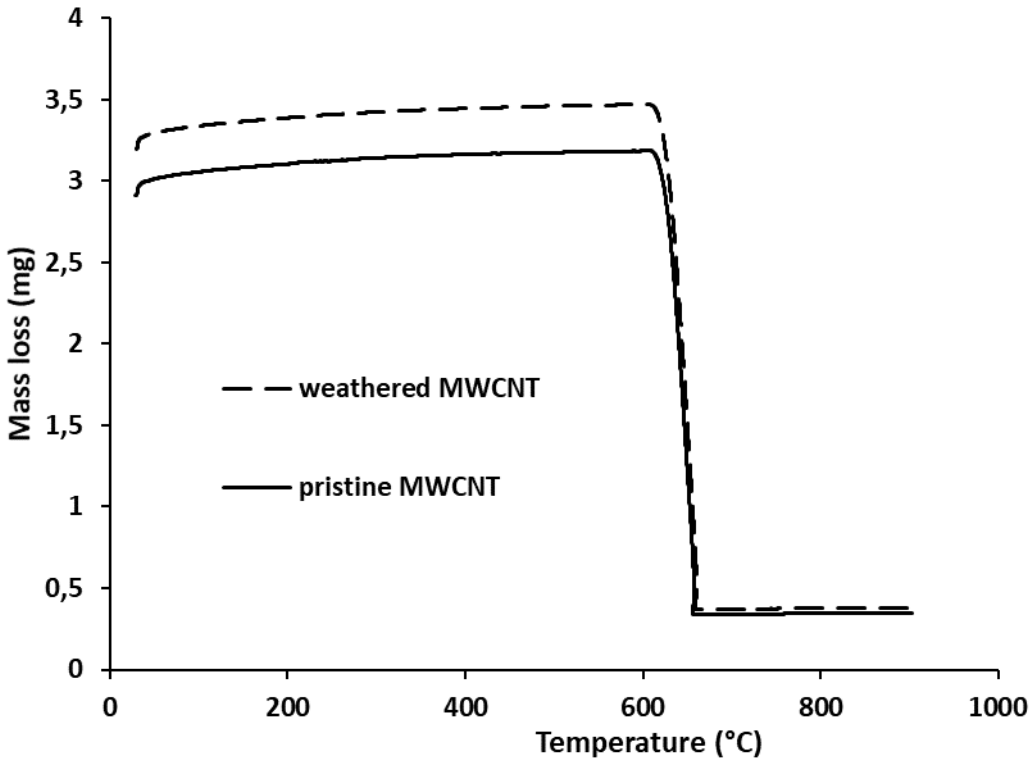

Figure 2.5: TGA and FTIR analyses of pristine (continuous line) and weathered (dashed line) multi-walled carbon nanotubes (MWCNT). Mass loss refers to an initial weight of 2.91 mg and 3.19 mg of pristine and weathered MWCNT, respectively.

2.7.3 Detection and quantification of ^{14}C-wMWCNT in a natural sediment sample using liquid scintillation counting (LSC)

Usually, the amount of radioactivity in sediment or soil samples is quantified by using an oxidizer. Here, the radioactive biological samples are burned at a temperature of 900 °C and the resulting $^{14}CO_2$ is trapped and measured using LSC. Since MWCNT have a thermal stability of up to 1300 °C, depending on the atmosphere (Mahajan et al., 2013), it has been found that unburned ^{14}C-CNT material remained in the combustion tube after sample burns (emerged contaminations). Therefore, we developed an alternative method to reliably quantify the amount of radioactivity in sediment samples using LSC only. For this purpose, we applied a known amount of ^{14}C-wMWCNT to sediment in a preliminary experiment and determined the recovery after only a short incubation period.

Five different ^{14}C-wMWCNT suspensions (I -V) were prepared for the experiment, which were selected to approximate the experimental conditions (dry weight of sediment: ca. 30 g; ^{14}C-wMWCNT per sample: 24 µg). To prepare the stock dispersion, 500 µg of ^{14}C-wMWCNT were dispersed in 50 mL of natural water. To check the dispersion success, three aliquots of 1 mL were measured by means of LSC. Subsequently, 0.1, 0.3, 0.8, 3.0, and 8.0 mL (1, 3, 8, 30, and 80 µg ^{14}C-wMWCNT) of the stock dispersion were applied to 20 g (20.1 ± 0.1 g) of dried (105 °C) and homogenized sediment (in 200 mL beakers) (two replicates per ^{14}C-wMWCNT concentration). Along the application process, aliquots (100, 300 and 800 µL for ^{14}C-wMWCNT concentrations I to III, respectively; 1 mL for ^{14}C-wMWCNT concentrations IV and V, respectively) were taken from the stock dispersion and filled into LSC vials containing 2 mL of Ultima Gold™ XR scintillation cocktail (Perkin Elmer, Germany) to check the stability of the stock dispersion during application time and to establish the 100% value. Each sample was made up with natural water to the extent that 15.4 mL of water was added. This served to maintain the maximum water holding capacity and at the same time to be able to mix the sediment well after application. Homogenization of the applied samples was performed using a metal spatula. Samples were placed in a drying oven overnight at 60 °C and then finely pestled using a porcelain mortar before transferring ≤ 0.05 g of sediment from each sample into pre-weighed LSC vials (twelve replicates) (Tab. 2.2). The exact weight was determined for each aliquot and 0.5 mL of 35% H_2O_2 was added and subsequently, the samples were placed overnight in a drying oven at 60 °C. The dried sediment was dissolved the following day with 0.5 mL of distilled water and overlaid with 19.5 mL of LSC Cocktail. Consequently, to ensure the reaction of the substance mixture, the samples were incubated overnight at 4 °C in the dark. Thereafter, the samples were brought to room temperature and placed in an ultrasonic bath for one minute. Immediately afterwards, the prepared samples were measured by LSC for one minute and then for 10 min to exclude any influence of the ultrasonic treatment. Finally, the recovered amount of radioactivity was compared with the applied radioactivity amount. A recovery of 105 ± 3% (Tab. 2.3)

showed that the method used is suitable to determine the amount of radioactivity (^{14}C-wMWCNT) in natural sediment samples.

Table 2.2: Results from preliminary experiment – quantification of radioactivity amount of ^{14}C-wMWCNT in natural sediment samples using liquid scintillation counting (LSC). Five ^{14}C-wMWCNT concentrations (I – V) were applied to dried sediment samples (two replicates (repl.) per concentration) and an amount of ≤ 0.05 g sediment was subsequently measured by means of LSC to quantify the enclosed amount of radioactivity (RA). The shown RA amounts in samples (Becquerel = Bq) were derived from the 10 min LSC measurements. Arithmetic mean (Mean) and standard deviation (SD) are given for every specification.

^{14}C-wMWCNT conc. I	weight of sediment sample (g)	RA amount in sample (Bq)	RA amount in 0.01 g sediment (Bq)
1 (repl. #1)	0.043	2.933	0.676
2 (repl. #1)	0.041	3.300	0.809
3 (repl. #1)	0.030	2.633	0.871
4 (repl. #1)	0.033	2.717	0.815
5 (repl. #1)	0.038	3.050	0.799
6 (repl. #1)	0.033	12.600*	3.833*
7 (repl. #1)	0.032	3.900	1.207
8 (repl. #1)	0.035	3.467	0.977
9 (repl. #1)	0.032	3.133	0.971
10 (repl. #1)	0.025	3.333	1.310
11 (repl. #1)	0.027	2.283	0.835
12 (repl. #1)	0.026	3.667	1.387
Mean	0.033	3.129	0.969
SD	0.006	0.474	0.232
^{14}C-wMWCNT conc. I	weight of sediment sample (g)	RA amount in sample (Bq)	RA amount in 0.01 g sediment (Bq)
1 (repl. #2)	0.029	2.733	0.958
2 (repl. #2)	0.045	3.367	0.741
3 (repl. #2)	0.030	2.400	0.812
4 (repl. #2)	0.032	2.583	0.806
5 (repl. #2)	0.027	5.733*	2.126*
6 (repl. #2)	0.041	3.217	0.793
7 (repl. #2)	0.031	3.667	1.170
8 (repl. #2)	0.027	3.200	1.191
9 (repl. #2)	0.038	3.050	0.796
10 (repl. #2)	0.028	2.617	0.936
11 (repl. #2)	0.028	2.200	0.791
12 (repl. #2)	0.031	3.200	1.040
Mean	0.032	2.930	0.912
SD	0.006	0.452	0.160
^{14}C-wMWCNT conc. II	weight of sediment sample (g)	RA amount in sample (Bq)	RA amount in 0.01 g sediment (Bq)
1 (repl. #1)	0.033	7.000	2.146
2 (repl. #1)	0.027	5.583	2.086
3 (repl. #1)	0.032	6.217	1.930

4 (repl. #1)	0.037	10.200	2.734
5 (repl. #1)	0.028	9.100	3.234
6 (repl. #1)	0.027	7.250	2.689
7 (repl. #1)	0.027	5.567	2.040
8 (repl. #1)	0.029	6.267	2.129
9 (repl. #1)	0.028	5.483	1.961
10 (repl. #1)	0.027	5.233	1.920
11 (repl. #1)	0.036	5.967	1.677
12 (repl. #1)	0.028	6.017	2.178
Mean	0.030	6.657	2.227
SD	0.004	1.536	0.438
^{14}C-wMWCNT conc. II	weight of sediment sample (g)	RA amount in sample (Bq)	RA amount in 0.01 g sediment (Bq)
1 (repl. #2)	0.028	6.350	2.260
2 (repl. #2)	0.030	6.233	2.104
3 (repl. #2)	0.034	6.400	1.877
4 (repl. #2)	0.024	4.767	1.966
5 (repl. #2)	0.031	6.250	1.996
6 (repl. #2)	0.037	7.333	1.979
7 (repl. #2)	0.032	6.750	2.133
8 (repl. #2)	0.029	5.367	1.824
9 (repl. #2)	0.027	6.183	2.273
10 (repl. #2)	0.028	5.317	1.886
11 (repl. #2)	0.026	4.967	1.936
12 (repl. #2)	0.028	5.717	2.068
Mean	0.030	5.969	2.025
SD	0.004	0.757	0.146
^{14}C-wMWCNT conc. III	weight of sediment sample (g)	RA amount in sample (Bq)	RA amount in 0.01 g sediment (Bq)
1 (repl. #1)	0.024	14.033	5.891
2 (repl. #1)	0.036	18.067	4.984
3 (repl. #1)	0.033	16.900	5.189
4 (repl. #1)	0.030	14.017	4.688
5 (repl. #1)	0.037	16.967	4.592
6 (repl. #1)	0.035	16.333	4.718
7 (repl. #1)	0.037	20.567	5.577
8 (repl. #1)	0.034	17.800	5.237
9 (repl. #1)	0.034	20.333	6.007
10 (repl. #1)	0.034	23.383	6.869
11 (repl. #1)	0.033	18.483	5.603
12 (repl. #1)	0.030	15.883	5.247
Mean	0.033	17.731	5.383
SD	0.004	2.723	0.656
^{14}C-wMWCNT conc. III	weight of sediment sample (g)	RA amount in sample (Bq)	RA amount in 0.01 g sediment (Bq)
1 (repl. #2)	0.035	31.300*	8.864*
2 (repl. #2)	0.029	17.817	6.046

3 (repl. #2)	0.023	11.600	4.989
4 (repl. #2)	0.030	18.200	6.114
5 (repl. #2)	0.037	21.767	5.858
6 (repl. #2)	0.031	18.000	5.738
7 (repl. #2)	0.028	15.317	5.496
8 (repl. #2)	0.024	16.383	6.701
9 (repl. #2)	0.027	12.950	4.713
10 (repl. #2)	0.029	lost sample	lost sample
11 (repl. #2)	0.029	15.383	5.281
12 (repl. #2)	0.030	14.367	4.823
Mean	0.032	16.178	5.576
SD	0.006	2.933	0.635
^{14}C-wMWCNT conc. IV	weight of sediment sample (g)	RA amount in sample (Bq)	RA amount in 0.01 g sediment (Bq)
1 (repl. #1)	0.026	54.433	21.066
2 (repl. #1)	0.028	57.667	20.442
3 (repl. #1)	0.030	64.067	21.278
4 (repl. #1)	0.034	73.750	21.820
5 (repl. #1)	0.034	65.333	19.375
6 (repl. #1)	0.029	54.350	18.619
7 (repl. #1)	0.026	52.950	20.280
8 (repl. #1)	0.030	70.150	23.580
9 (repl. #1)	0.029	65.183	22.625
10 (repl. #1)	0.024	48.450	20.095
11 (repl. #1)	0.026	48.500	18.894
12 (repl. #1)	0.036	75.033	20.930
Mean	0.029	60.822	20.750
SD	0.004	9.369	1.468
^{14}C-wMWCNT conc. IV	weight of sediment sample (g)	RA amount in sample (Bq)	RA amount in 0.01 g sediment (Bq)
1 (repl. #2)	0.027	55.667	20.679
2 (repl. #2)	0.033	63.433	19.440
3 (repl. #2)	0.027	63.900	23.424
4 (repl. #2)	0.024	45.650	18.926
5 (repl. #2)	0.023	57.550	25.341
6 (repl. #2)	0.029	59.683	20.294
7 (repl. #2)	0.033	62.133	19.065
8 (repl. #2)	0.021	45.767	21.982
9 (repl. #2)	0.034	61.983	18.409
10 (repl. #2)	0.026	52.900	20.237
11 (repl. #2)	0.023	44.867	19.264
12 (repl. #2)	0.022	43.267	19.542
Mean	0.027	54.733	20.550
SD	0.004	7.951	2.062
^{14}C-wMWCNT conc. V	weight of sediment sample (g)	RA amount in sample (Bq)	RA amount in 0.01 g sediment (Bq)
1 (repl. #1)	0.029	152.917	52.531

2 (repl. #1)	0.024	128.617	53.324
3 (repl. #1)	0.036	186.000	51.883
4 (repl. #1)	0.033	161.833	48.892
5 (repl. #1)	0.027	138.433	51.712
6 (repl. #1)	0.033	168.667	51.266
7 (repl. #1)	0.030	179.050	59.624
8 (repl. #1)	0.025	151.967	61.750
9 (repl. #1)	0.027	155.467	57.073
10 (repl. #1)	0.018	100.067	56.439
11 (repl. #1)	0.027	164.317	61.198
12 (repl. #1)	0.033	181.383	54.437
Mean	0.028	155.726	55.011
SD	0.005	24.405	4.186
^{14}C-wMWCNT conc. V	weight of sediment sample (g)	RA amount in sample (Bq)	RA amount in 0.01 g sediment (Bq)
1 (repl. #2)	0.030	163.883	54.902
2 (repl. #2)	0.027	159.283	58.069
3 (repl. #2)	0.035	208.650	58.907
4 (repl. #2)	0.032	178.633	55.270
5 (repl. #2)	0.031	194.983	62.215
6 (repl. #2)	0.029	174.917	59.944
7 (repl. #2)	0.025	154.467	60.694
8 (repl. #2)	0.034	197.967	58.225
9 (repl. #2)	0.035	198.267	56.166
10 (repl. #2)	0.033	174.833	53.663
11 (repl. #2)	0.034	181.400	52.610
12 (repl. #2)	0.036	197.483	54.765
Mean	0.032	182.064	57.119
SD	0.003	17.461	3.002

*Outlier according to Dixon's Q test ($\alpha = 0.05$); Outliers were excluded from calculations for arithmetic mean and standard deviation.

Table 2.3: Results from preliminary experiment – quantification of radioactivity amount of ^{14}C-wMWCNT in natural sediment samples using liquid scintillation counting (LSC). The applied radioactivity (RA) amount per sediment sample (20.1 ± 0.1 g) in Becquerel (Bq) is given. Additionally, the target RA in 0.01 g sediment was calculated to compare the amount to the recovered RA in 0.01 g sediment. Also, the total recovery is presented and arithmetic mean (mean) and standard deviation (SD) was calculated (in %).

^{14}C-wMWCNT conc.	applied RA amount per 20 g sediment (Bq)	target RA in 0.01 g sediment (Bq)	recovered RA in 0.01 g sediment (Bq)	recovery (%)	Mean recovery (%)	SD recovery (%)
I	1312.34	0.65	0.94	143.61*	105.01	3.18
II	3885.28	1.94	2.13	109.70		
III	10667.51	5.32	5.47	102.83		
IV	40052.98	19.82	20.65	104.18		
V	108965.42	54.26	56.07	103.32		

*Outlier according to Dixon's Q test (α = 0.05); Outliers were excluded from calculations for arithmetic mean and standard deviation.

2.7.4 Data interpretation using CAKE (Computer Assisted Kinetic Evaluation, version 3.3, Tessella)

An SFO (Single First-Order) model was applied to the data from sedimentation and distribution experiment. For details see the following guidance document:

Guidance document on estimating persistence and degradation kinetics from environmental fate studies on pesticides in EU registration. Report of the FOCUS Work Group on Degradation Kinetics, EC Document Reference Sanco/10058/2005, version 2.0, 434 pp. (52 p.)

Equation (integrated form):

$$M = M_0\, e^{-kt}$$

M = total amount of chemical present at time t

M_0 = total amount of chemical present at time t=0

k = rate constant

Endpoints:

$$DT_x = \frac{ln\frac{100}{100-x}}{k}; \qquad DT_{50} = \frac{ln2}{k}; \qquad DT_{90} = \frac{ln10}{k}$$

2.7.4.1 Sedimentation experiment

2.7.4.1.1 In presence of sediment (+sediment)

Table 2.4: Initial values for this step.

Parameter	Initial Value	Bounds	Fixed
Parent_0	100	0 to (unbounded)	No
k_Parent	0.1	0 to (unbounded)	No

Table 2.5: Estimated values.

Parameter	Value	s	Prob. > t	Lower (90%) CI	Upper (90%) CI	Lower (95%) CI	Upper (95%) CI
Parent_0	92.85	1.729	N/A	89.92	95.79	89.32	96.39
k_Parent	0.1064	0.005508	2.11E-018	0.09701	0.1157	0.09511	0.118

Table 2.6: Chi^2

Parameter	Error %	Degrees of Freedom
All data	8.38	29
Parent	8.38	29

Table 2.7: Decay times.

Compartment	DT_{50} (days)	DT_{90} (days)
Parent	6.52	21.7

Table 2.8: Additional statistics.

Parameter	r^2 (Obs. v Pred.)	Efficiency
All data	0.9707	0.9701
Parent	0.9707	0.9701

Table 2.9: Parameter correlation.

	Parent_0	k_Parent
Parent_0	1	0.52
k_Parent	0.52	1

Table 2.10: Observed vs. Predicted

Compartment parent

Time (days)	Value (%)	Predicted Value	Residual
0	100	92.85	7.146
0.03	98.43	92.56	5.872
0.04	96.85	92.46	4.39
0.07	95.99	92.17	3.825
0.11	87.34	91.77	-4.434
0.15	91.42	91.38	0.03564
0.85	76.84	84.83	-7.987
0.89	99.06	84.47	14.59
0.97	81.18	83.75	-2.571
1.06	77.77	82.95	-5.183
1.24	77.78	81.38	-3.6
1.88	79.6	76.02	3.576
2.2	67.55	73.48	-5.93
2.87	61.24	68.43	-7.186
3.2	57.78	66.07	-8.285
5.88	49.39	49.68	-0.2885
6.2	43.27	48.02	-4.746
6.88	40.94	44.67	-3.725
7.2	42.03	43.17	-1.141
8.08	35.88	39.31	-3.433
9.08	40.27	35.35	4.924
9.83	36.07	32.64	3.434
13.08	24.81	23.1	1.713
13.87	19.43	21.24	-1.805
14.87	28.35	19.09	9.257
15.87	18.75	17.17	1.584
16.87	21.22	15.43	5.786
20.07	7.65	10.98	-3.331
21.07	13.49	9.873	3.617
23.05	10.71	7.998	2.712
27.91	8.06	4.769	3.291

2.7.4.1.2 In absence of sediment (-sediment)

Table 2.11: Initial values for this step.

Parameter	Initial Value	Bounds	Fixed
Parent_0	100	0 to (unbounded)	No
k_Parent	0.1	0 to (unbounded)	No

Table 2.12: Estimated values.

Parameter	Value	s	Prob. > t	Lower (90%) CI	Upper (90%) CI	Lower (95%) CI	Upper (95%) CI
Parent_0	93.44	1.225	N/A	91.36	95.53	90.94	95.95
k_Parent	0.09458	0.003477	1.72E-022	0.08868	0.1005	0.08747	0.102

Table 2.13: Chi^2

Parameter	Error %	Degrees of Freedom
All data	5.77	29
Parent	5.77	29

Table 2.14: Decay times.

Compartment	DT_{50} (days)	DT_{90} (days)
Parent	7.33	24.3

Table 2.15: Additional statistics.

Parameter	r^2 (Obs. v Pred.)	Efficiency
All data	0.9838	0.9833
Parent	0.9838	0.9833

Table 2.16: Parameter correlation.

	Parent_0	k_Parent
Parent_0	1	0.5253
k_Parent	0.5253	1

Table 2.17: Observed vs. Predicted

Compartment parent

Time (days)	Value (%)	Predicted Value	Residual
0	100	93.44	6.556
0.03	98.92	93.18	5.741
0.04	98.09	93.09	4.999
0.07	94.55	92.83	1.723
0.11	95.04	92.48	2.563
0.15	93.54	92.13	1.412
0.85	84.95	86.23	-1.276
0.89	83.95	85.9	-1.95
0.97	84.22	85.25	-1.033
1.06	75.16	84.53	-9.37
1.24	77.41	83.1	-5.693
1.88	80.81	78.22	2.588
2.2	73.15	75.89	-2.74
2.87	71.65	71.23	0.4203
3.2	66.23	69.04	-2.811
5.88	51.98	53.58	-1.602
6.2	48.55	51.99	-3.435
6.88	45.18	48.75	-3.566
7.2	44.6	47.29	-2.693
8.08	39.74	43.52	-3.776
9.08	35.76	39.59	-3.829
9.83	35.47	36.88	-1.408
13.08	31.65	27.12	4.532
13.87	28.07	25.17	2.904
14.87	28.32	22.9	5.425
15.87	27.36	20.83	6.532
16.87	24.09	18.95	5.141
20.07	15.38	14	1.38
21.07	12.93	12.74	0.1933
23.05	11.09	10.56	0.5285
27.91	8.68	6.669	2.011

2.7.4.2 Distribution experiment

Table 2.18: Initial values for this step.

Parameter	Initial Value	Bounds	Fixed
Parent_0	100	0 to (unbounded)	No
k_Parent	0.1	0 to (unbounded)	No

Table 2.19: Estimated values.

Parameter	Value	s	Prob. > t	Lower (90%) CI	Upper (90%) CI	Lower (95%) CI	Upper (95%) CI
Parent_0	84.36	6.311	N/A	72.1	96.62	68.92	99.8
k_Parent	0.2151	0.05991	0.005752	0.09866	0.3315	0.06848	0.362

Table 2.20: Chi^2

Parameter	Error %	Degrees of Freedom
All data	16.8	6
Parent	16.8	6

Table 2.21: Decay times.

Compartment	DT_{50} (days)	DT_{90} (days)
Parent	3.22	10.7

Table 2.22: Additional statistics.

Parameter	r^2 (Obs. v Pred.)	Efficiency
All data	0.9459	0.9448
Parent	0.9459	0.9448

Table 2.23: Parameter correlation.

	Parent_0	k_Parent
Parent_0	1	0.4989
k_Parent	0.4989	1

Table 2.24: Observed vs. Predicted

Compartment parent

Time (days)	Value (%)	Predicted Value	Residual
0	100	84.36	15.64
0.083	77	82.87	-5.867
1	59	68.03	-9.034
2	47	54.87	-7.868
7	30	18.72	11.28
21	3	0.9217	2.078
90	0.1	0	0.1
180	0.03	0	0.03

2.8 References

Alef, K., Kleiner, D., 1989. Rapid and Sensitive Determination of Microbial Activity in Soils and in Soil Aggregates by Dimethylsulfoxide Reduction. Biol Fert Soils 8, 349-355.

Baek, S., Joo, S.H., Su, C., Toborek, M., 2019. Antibacterial effects of graphene- and carbon-nanotube-based nanohybrids on Escherichia coli: Implications for treating multidrug-resistant bacteria. Journal of Environmental Management 247, 214 - 223.

Barra, G., Guadagno, L., Vertuccio, L., Simonet, B., Santos, B., Zarrelli, M., Arena, M., Viscardi, M., 2019. Different Methods of Dispersing Carbon Nanotubes in Epoxy Resin and Initial Evaluation of the Obtained Nanocomposite as a Matrix of Carbon Fiber Reinforced Laminate in Terms of Vibroacoustic Performance and Flammability. Materials 12.

Bouchard, D., Knightes, C., Chang, X., Avant, B., 2017. Simulating Multiwalled Carbon Nanotube Transport in Surface Water Systems Using the Water Quality Analysis Simulation Program (WASP). Environ Sci Technol 51, 11174-11184.

Bouchard, D., Chang, X., Chowdhury, I., 2015. Heteroaggregation of multiwalled carbon nanotubes with sediments. Environmental Nanotechnology, Monitoring & Management 4, 42 - 50.

Chang, X., Bouchard, D.C., 2013. Multiwalled carbon nanotube deposition on model environmental surfaces. Environ Sci Technol 47, 10372-10380.

Flores-Cervantes, D.X., Maes, H.M., Schaffer, A., Hollender, J., Kohler, H.P., 2014. Slow biotransformation of carbon nanotubes by horseradish peroxidase. Environ Sci Technol 48, 4826-4834.

Gillis, P.L., Chow-Fraser, P., Ranville, J.F., Ross, P.E., Wood, C.M., 2005. Daphnia need to be gut-cleared too: the effect of exposure to and ingestion of metal-contaminated sediment on the gut-clearance patterns of D. magna. Aquat Toxicol 71, 143-154.

Glomstad, B., Zindler, F., Jenssen, B.M., Booth, A.M., 2018. Dispersibility and dispersion stability of carbon nanotubes in synthetic aquatic growth media and natural freshwater. Chemosphere 201, 269-277.

Gottschalk, F., Lassen, C., Kjoelholt, J., Christensen, F., Nowack, B., 2015. Modeling Flows and Concentrations of Nine Engineered Nanomaterials in the Danish Environment. Int J Env Res Pub He 12, 5581-5602.

Gottschalk, F., Nowack, B., 2011. The release of engineered nanomaterials to the environment. J Environ Monitor 13, 1145-1155.

Gottschalk, F., Sonderer, T., Scholz, R.W., Nowack, B., 2009. Modeled environmental concentrations of engineered nanomaterials (TiO(2), ZnO, Ag, CNT, Fullerenes) for different regions. Environ Sci Technol 43, 9216-9222.

Griebler, C., Slezak, D., 2001. Microbial activity in aquatic environments measured by dimethyl sulfoxide reduction and intercomparison with commonly used methods. Appl Environ Microbiol 67, 100-109.

Guo, X., Dong, S., Petersen, E.J., Gao, S., Huang, Q., Mao, L., 2013. Biological uptake and depuration of radio-labeled graphene by Daphnia magna. Environ Sci Technol 47, 12524-12531.

Hirsch, A., 2002. Functionalization of single-walled carbon nanotubes. Angewandte Chemie - International Edition 41, 1853-1859.

Huang, L., Li, Z., Luo, Y., Zhang, N., Qi, W., Jiang, E., Bao, J., Zhang, X., Zheng, W., An, B., He, G., 2020. Low-pressure Loose GO Composite Membrane Intercalated by CNT for Effective Dye/salt Separation. Separation and Purification Technology, doi: https://doi.org/10.1016/j.seppur.2020.117839

Hyung, H., Fortner, J.D., Hughes, J.B., Kim, J.H., 2007. Natural organic matter stabilizes carbon nanotubes in the aqueous phase. Environmental Science & Technology 41, 179-184.

Hyung, H., Kim, J.H., 2008. Natural organic matter (NOM) adsorption to multi-walled carbon nanotubes: Effect of NOM characteristics and water quality parameters. Environmental Science & Technology 42, 4416-4421.

Iijima, S., 1991. Helical Microtubules of Graphitic Carbon. Nature 354, 56-58.

Iijima, S., 2002. Carbon nanotubes: past, present, and future. Physica B 323, 1-5.

Kang, S., Herzberg, M., Rodrigues, D.F., Elimelech, M., 2008. Antibacterial Effects of Carbon Nanotubes: Size Does Matter! Langmuir 24, 6409-6413.

Kennedy, A.J., Hull, M.S., Steevens, J.A., Dontsova, K.M., Chappell, M.A., Gunter, J.C., Weiss, C.A., Jr., 2008. Factors influencing the partitioning and toxicity of nanotubes in the aquatic environment. Environ Toxicol Chem 27, 1932-1941.

Kuzyakov, Y., Subbotina, I., Chen, H., Bogomolova, I., Xu, X., 2009. Black carbon decomposition and incorporation into soil microbial biomass estimated by 14C labeling. Soil Biology and Biochemistry 41, 210-219.

Lin, D., Xing, B., 2008. Tannic acid adsorption and its role for stabilizing carbon nanotube suspensions. Environ Sci Technol 42, 5917-5923.

Lopez, N.I., Duarte, C.M., 2004. Dimethyl sulfoxide (DMSO) reduction potential in mediterranean seagrass (Posidonia oceanica) sediments. J Sea Res 51, 11-20.

Maes, H.M., Stibany, F., Giefers, S., Daniels, B., Deutschmann, B., Baumgartner, W., Schaffer, A., 2014. Accumulation and distribution of multiwalled carbon nanotubes in zebrafish (Danio rerio). Environ Sci Technol 48, 12256-12264.

Mao, L., Liu, C., Lu, K., Su, Y., Gu, C., Huang, Q., Petersen, E.J., 2016. Exposure of few layer graphene to Limnodrilus hoffmeisteri modifies the graphene and changes its bioaccumulation by other organisms. Carbon N Y 109, 566-574.

Mauter, M.S., Elimelech, M., 2008. Environmental applications of carbon-based nanomaterials. Environ Sci Technol 42, 5843-5859.

Niyogi, S., Hamon, M.A., Hu, H., Zhao, B., Bhowmik, P., Sen, R., Itkis, M.E., Haddon, R.C., 2002. Chemistry of single-walled carbon nanotubes. Accounts of Chemical Research 35, 1105-1113.

Park, T.J., Banerjee, S., Hemraj-Benny, T., Wong, S.S., 2006. Purification strategies and purity visualization techniques for single-walled carbon nanotubes. J Mater Chem 16, 141-154.

Parks, A.N., Chandler, G.T., Ho, K.T., Burgess, R.M., Ferguson, P.L., 2015. Environmental biodegradability of [(1)(4)C] single-walled carbon nanotubes by Trametes versicolor and natural microbial cultures found in New Bedford Harbor sediment and aerated wastewater treatment plant sludge. Environ Toxicol Chem 34, 247-251.

Patra, M., Ma, X., Isaacson, C., Bouchard, D., Poynton, H., Lazorchak, J.M., Rogers, K.R., 2011. Changes in agglomeration of fullerenes during ingestion and excretion in Thamnocephalus platyurus. Environ Toxicol Chem 30, 828-835.

Petersen, E.J., Pinto, R.A., Mai, D.J., Landrum, P.F., Weber, W.J., Jr., 2011a. Influence of polyethyleneimine graftings of multi-walled carbon nanotubes on their accumulation and elimination by and toxicity to Daphnia magna. Environ Sci Technol 45, 1133-1138.

Petersen, E.J., Zhang, L., Mattison, N.T., O'Carroll, D.M., Whelton, A.J., Uddin, N., Nguyen, T., Huang, Q., Henry, T.B., Holbrook, R.D., Chen, K.L., 2011b. Potential release pathways, environmental fate, and ecological risks of carbon nanotubes. Environ Sci Technol 45, 9837-9856.

Petersen, E.J., Akkanen, J., Kukkonen, J.V., Weber, W.J., Jr., 2009. Biological uptake and depuration of carbon nanotubes by Daphnia magna. Environ Sci Technol 43, 2969-2975.

Petersen, E.J., Huang, Q., Weber, W.J., 2008. Ecological uptake and depuration of carbon nanotubes by Lumbriculus variegatus. Environ Health Perspect 116, 496-500.

Piao, L., Liu, Q., Li, Y., Wang, C., 2009. The adsorption of L-phenylalanine on oxidized single-walled carbon nanotubes. J Nanosci Nanotechnol 9, 1394-1399.

Rhiem, S., Barthel, A.K., Meyer-Plath, A., Hennig, M.P., Wachtendorf, V., Sturm, H., Schaffer, A., Maes, H.M., 2016. Release of (14)C-labelled carbon nanotubes from polycarbonate composites. Environ Pollut 215, 356-365.

Rhiem, S., Riding, M.J., Baumgartner, W., Martin, F.L., Semple, K.T., Jones, K.C., Schaffer, A., Maes, H.M., 2015. Interactions of multiwalled carbon nanotubes with algal cells: quantification of association, visualization of uptake, and measurement of alterations in the composition of cells. Environ Pollut 196, 431-439.

Roberts, A.P., Mount, A.S., Seda, B., Souther, J., Qiao, R., Lin, S., Ke, P.C., Rao, A.M., Klaine, S.J., 2007. In vivo biomodification of lipid-coated carbon nanotubes by Daphnia magna. Environ Sci Technol 41, 3025-3029.

Saleh, N.B., Pfefferle, L.D., Elimelech, M., 2008. Aggregation kinetics of multiwalled carbon nanotubes in aquatic systems: measurements and environmental implications. Environ Sci Technol 42, 7963-7969.

Schierz, A., Espinasse, B., Wiesner, M.R., Bisesi, J.H., Sabo-Attwood, T., Ferguson, P.L., 2014. Fate of single walled carbon nanotubes in wetland ecosystems. Environ-Sci Nano 1, 574-583.

Su, Y., Yang, G.Q., Lu, K., Petersen, E.J., Mao, L., 2017. Colloidal properties and stability of aqueous suspensions of few-layer graphene: Importance of graphene concentration. Environmental Pollution 220, 469-477.

Sun, T.Y., Gottschalk, F., Hungerbuhler, K., Nowack, B., 2014. Comprehensive probabilistic modelling of environmental emissions of engineered nanomaterials. Environ Pollut 185, 69-76.

Tasis, D., Tagmatarchis, N., Bianco, A., Prato, M., 2006. Chemistry of Carbon Nanotubes. Chemical Reviews 106, 1105-1136.

Wang, J.G., Liu, H.Z., Zhang, X.Y., Li, X., Liu, X.R., Kang, F.Y., 2018. Green Synthesis of Hierarchically Porous Carbon Nanotubes as Advanced Materials for High-Efficient Energy Storage. Small 14.

Xia, Y., Li, S., Nie, C.X., Zhang, J.G., Zhou, S.Q., Yang, H., Li, M.J., Li, W.Z., Cheng, C., Haag, R., 2019. A multivalent polyanion-dispersed carbon nanotube toward highly bioactive nanostructured fibrous stem cell scaffolds. Appl Mater Today 16, 518-528.

Yao, N., Lordi, V., Ma, S.X.C., Dujardin, E., Krishnan, A., Treacy, M.M.J., Ebbesen, T.W., 1998. Structure and oxidation patterns of carbon nanotubes. Journal of Materials Research 13, 2432-2437.

Zaib, Q., Aina, O.D., Ahmad, F., 2014. Using multi-walled carbon nanotubes (MWNTs) for oilfield produced water treatment with environmentally acceptable endpoints. Environ Sci Process Impacts 16, 2039-2047.

Zhang, L., Petersen, E.J., Habteselassie, M.Y., Mao, L., Huang, Q., 2013. Degradation of multiwall carbon nanotubes by bacteria. Environ Pollut 181, 335-339.

Zhang, L., Petersen, E.J., Zhang, W., Chen, Y., Cabrera, M., Huang, Q., 2012. Interactions of 14C-labeled multi-walled carbon nanotubes with soil minerals in water. Environ Pollut 166, 75-81.

Zhang, L.W., Petersen, E.J., Huang, Q.G., 2011. Phase Distribution of C-14-Labeled Multiwalled Carbon Nanotubes in Aqueous Systems Containing Model Solids: Peat. Environmental Science & Technology 45, 1356-1362.

Zhao, Q., Petersen, E.J., Cornelis, G., Wang, X., Guo, X., Tao, S., Xing, B., 2016. Retention of 14C-labeled multiwall carbon nanotubes by humic acid and polymers: Roles of macromolecule properties. Carbon N Y 99, 229-237.

Zhou, L., Zhu, D., Zhang, S., Pan, B., 2015. A settling curve modeling method for quantitative description of the dispersion stability of carbon nanotubes in aquatic environments. J Environ Sci (China) 29, 1-10.

3 Uptake of multi-walled carbon nanotubes associated to green algae in water flea *Daphnia magna* – *a trophic transfer investigation*[2]

[2] This chapter has been published in a modified version in NanoImpact.

3.1 Summary

Carbon nanotubes (CNT) are promising nanomaterials in modern nanotechnology and their use in many different applications leads to an inevitable release into the aquatic environment. In this study, we quantified trophic transfer of ^{14}C-labeled weathered multi-walled carbon nanotubes (^{14}C-wMWCNT) from green algae to primary consumer *Daphnia magna* in a concentration of 100 µg L^{-1}. Trophic transfer of wMWCNT was compared to the uptake by daphnids exposed to nanomaterials in the water phase without algae. We found that the nanomaterials associated to the green algae *Chlamydomonas reinhardtii* and *Raphidocelis subcapitata*. After the exposition of algae, the nanotubes accumulated to a maximum of 1.6 ± 0.4 µg ^{14}C-wMWCNT mg^{-1} dry $weight^{-1}$ (dw^{-1}) and 0.7 ± 0.3 µg ^{14}C-wMWCNT mg^{-1} dw^{-1} after 24 h and 48 h, respectively. To study trophic transfer, *R. subcapitata* was loaded with ^{14}C-wMWCNT and subsequently fed to *D. magna*. A maximum body burden of 0.07 ± 0.01 µg ^{14}C-wMWCNT mg^{-1} dw^{-1} and 7.1 ± 1.5 µg ^{14}C-wMWCNT mg^{-1} dw^{-1} for *D. magna* after trophic transfer and waterborne exposure was measured, respectively, indicating no CNT accumulation after short-term exposure *via* trophic transfer. Additionally, the animals eliminated nanomaterials from their guts, while feeding algae facilitated their excretion. Further, accumulation of ^{14}C-wMWCNT in a growing population of *D. magna* revealed a maximum uptake of 0.7 ± 0.2 µg mg^{-1} dw^{-1}. Therefore, the calculated bioaccumulation factor (BAF) after 28 d of 6700 ± 2900 L kg^{-1} is above the limit that indicates a chemical is bioaccumulative in the European Union Regulation REACH. Although wMWCNT did not bioaccumulate in neonate *D. magna* after trophic transfer, wMWCNT enriched in a 28 d growing *D. magna* population regardless of daily feeding, which increases the risk of CNT accumulation along the aquatic food chain.

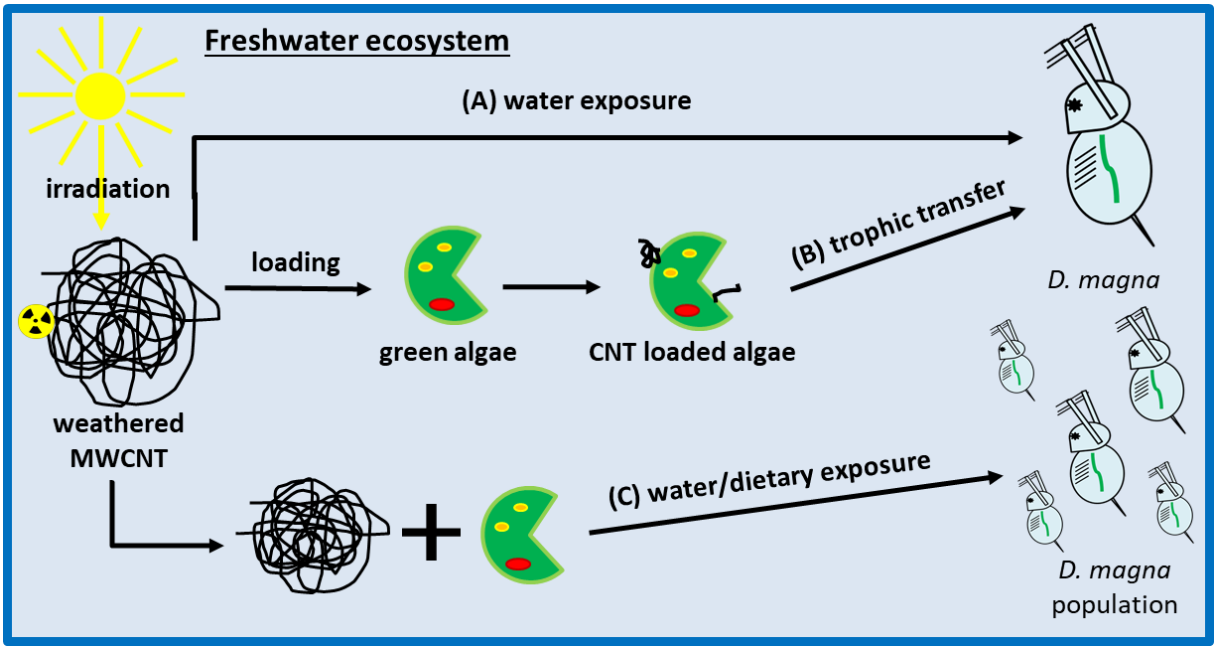

Figure 3.1: Graphical summary of chapter 3.

3.2 Introduction

Nanotechnology and nanoscience have gained more and more attention over the past 20 years (Roco, 2011). Since their discovery in 1991 (Iijima, 1991), the production of carbon nanotubes (CNT) rose continuously and in 2020, the industrial company OCSIAL announced the commissioning of the largest plant for the production of CNT to date, which will produce 100 tons of CNT annually (KunststoffWeb, 2020; OCSIAL, 2020). Due to their novel and alterable properties CNT are used in manifold applications like nanocomposites (Barra et al., 2019), energy storage (Mauter and Elimelech, 2008; Thauer et al., 2020), drug delivery (Newland et al., 2018) and water treatment (Zaib et al., 2014).

Within the life cycle of CNT, most of the material is released during synthesis and handling (Yeganeh et al., 2008; Tsai et al., 2009). CNT are most widely used in nanocomposites, i.e., plastic materials with embedded CNT, which is why their disposal can result in additional CNT release. For nanocomposites it was reported that the plastic polymer degrades by UV irradiation leaving the nanotube network exposed on the nanocomposites surface. Further, physical transformation processes, e.g., by abrasion, or sunlight can impair the CNT network leading to the release of nanomaterial (Wohlleben et al., 2013; Petersen et al., 2014; Hou et al., 2014; Schlagenhauf et al., 2015). Eventually, either through direct disposal of CNT-containing products in aqueous compartments, or through their weathering on landfills and subsequent leaching into water bodies, CNT enter the aquatic environment (Sarma et al., 2015). Thereby CNT will interact with co-contaminants and natural particles (Holden et al., 2016; Naasz et al. 2018; Glomstad et al., 2018). While lingering in the environment, weathering impacts (e.g., irradiation) might alter physico-chemical properties of CNT and as a result influence their environmental behavior like bioaccumulation and toxicity to organisms (Mitrano et al., 2015).

Bioaccumulation is generally defined as the increase in internal concentration of chemicals in an organism exceeding the concentration in the surrounding medium, food or both (Gobas et al., 2009). To date, accumulation of CNT in aquatic organisms was investigated but due to the lack of suitable quantification methods (Mortimer et al., 2016), nanomaterial concentrations, several orders of magnitude higher than found in natural environments, were used (Parks et al. 2013; Maes et al. 2014; Rhiem et al. 2015; Zhu et al. 2018), except for a few studies (Petersen et al., 2009; Petersen et al. 2011; Cano et al., 2017; Cano et al., 2018). Since the estimated environmental concentration of CNT is in the ng L^{-1} range (Gottschalk et al., 2009; Gottschalk and Nowack 2011), there is a need for studies that approach such low concentrations. Consequently, we quantified the association of CNT to algae in the µg L^{-1} range which is below the tested concentration in other studies.

Despite of the CNT concentrations used, CNT generally show a low bioaccumulation potential (Bjorkland et al., 2017), since these nanomaterials do not pass membranes like classical compounds and are therefore mainly accumulated in the gastrointestinal tract, as well as adhering to external

structures (e.g., gill, skin). In addition, it was increasingly observed that orally ingested CNT are eliminated again, especially after food intake, which leads to a low body burden in the organism (Petersen et al., 2009; Guo et al., 2013; Maes et al., 2014). As under environmental conditions mostly food is available, trophic transfer thus needs to be the focus of further research.

Since green algae represent primary producers in the aquatic food chain the interaction with and the uptake of radioactively labeled MWCNT (1 mg L^{-1}) in *Desmodesmus subspicatus* was reported by Rhiem et al. (2015). Using radioactive labeling, the uptake of multi-walled CNT (MWCNT) was also quantified in five to seven days old *Daphnia magna* where a maximum body burden of 63 µg mg^{-1} after exposure to 400 µg L^{-1} over 24 h was obtained (Petersen et al., 2009). The exposure of the same stock of *D. magna* with 250 µg L^{-1} of polyethyleneimine grafted MWCNT resulted in a maximum internal concentration of 12 µg mg^{-1} (Petersen et al., 2011). In both studies, elimination into clean medium was low, however, in the presence of algae, nearly complete excretion of nanomaterial was observed, leading to low bioaccumulation. Guo et al. (2013) worked with *D. magna* neonates to investigate the uptake of ^{14}C-labeled graphene. At 250 µg graphene L^{-1} the maximum body burden was 7.8 µg mg^{-1}, whereas depuration in clean water led to nearly no change in body burden after 24 h, but as in case of CNT, excretion was facilitated in the presence of algae. Since neonate daphnids show a higher sensitivity toward chemical exposure than adult animals (Gerritsen et al., 1998; Preuss et al., 2010), the data obtained from the studies performed with adult *Daphnia* are of limited value. Therefore, the accumulation of CNT in neonate *D. magna* is still unknown but necessary and consequently in this study, we focussed on the uptake of CNT in neonate animals.

In more recent studies the accumulation of pristine MWCNT (0.1 mg L^{-1}), applied together with algae, in *D. magna* (five to 15 days old) was quantified using a microwave induced heating technique. An enrichment of above 0.2 µg MWCNT g^{-1} after 24 h in a *D. magna* population of 60 individuals and of 0.02 to 0.05 µg MWCNT g^{-1} (BCF < 1) after three days (ten animals in 50 mL) indicated a low bioaccumulation of CNT in *D. magna* under environmentally relevant feeding conditions (Cano et al., 2017; Cano et al., 2018). Further, trophic transfer of MWCNT from bacteria *Pseudomonas aeruginosa* to protozoan *Tetrahymena thermophila* (Mortimer et al., 2016) and from water flea *D. magna* to fathead minnow (Cano et al., 2018) was recently observed. These more complex studies demonstrated the food web transfer of CNT over a short period of time, using animals that were several days to weeks old but did neither look at population dynamics, nor long-term exposures. Consequently, the influence of complexity of test systems and prolonged investigations on enrichment of CNT in *D. magna* remains to be unclear. To close this knowledge gap, we investigated the accumulation of weathered CNT in a growing population of *D. magna* in long-term exposure, using radiolabeled nanomaterials.

So far, only few studies on carbonaceous nanomaterials have been performed at concentrations that are expected in the environment caused by the absence of quantification methods for CNT in complex environmental matrices. We aimed to investigate trophic transfer of ^{14}C-MWCNT from green algae to *D. magna* under low nanomaterial concentrations. Herein, the presence of nutrition on uptake and depuration was assessed. Additionally, we performed a long-term microcosm experiment to gather information on uptake of ^{14}C-MWCNT in a growing population of *D. magna*, which, to our knowledge, has not been investigated until now.

3.3 Materials and methods

3.3.1 Manufacturing of ^{14}C-labeled MWCNT (^{14}C-MWCNT)

For a detailed description of synthesis of ^{14}C-MWCNT see section 2.3.1 in chapter 2.

3.3.2 Weathering and dispersion of nanomaterials

For weathering and characterization of MWCNT see section 2.3.2 in chapter 2.

For the dispersion of CNT, the needed amount of either labeled or unlabeled wMWCNT was weighted on a microbalance (MYA 5.3Y, Radwag) and filled in a flask containing 50 mL (volume was adjusted according to CNT quantity) of the required test medium. Subsequently, the flask was put into an ice bath and nanomaterials were dispersed by means of ultrasonication with a micro tip for 10 min (Sonopuls HD 2070, 70 W, pulse: 0.2 s, pause: 0.8 s). Subsequently, the stock dispersion was diluted by test medium and dispersed a second time as described above to obtain the target test dispersion. The used dispersion method has already been described (Rhiem et al., 2015; Hennig et al., 2019). Herein, the two-stage dispersion process as described is a deviation from this method. An investigation using TEM revealed that wMWCNT test dispersion contained small agglomerates as well as single tubes (length: 0.2 - 1 µm) and was therefore appropriate for dispersion of wMWCNT in aqueous solution.

3.3.3 Settling of ^{14}C-wMWCNT in a static test system

The deposition behavior of ^{14}C-wMWCNT (100 µg L^{-1}) in a static test system was assessed. A total amount of 219 µg ^{14}C-wMWCNT was weighted and filled in a flask containing M4 test medium (main constituents: 294 mg $CaCl_2 \times 2\ H_2O\ L^{-1}$, 123.3 mg $MgSO_4 \times 7\ H_2O\ L^{-1}$, 5.8 mg KCl L^{-1}, 64.8 mg $NaHCO_3\ L^{-1}$, see SI) with a pH value between 7 and 8 (OECD, 2004) and dispersed as described above. Subsequently, the stock dispersion was diluted by test medium and dispersed a second time to obtain 2 × 550 mL (100 µg ^{14}C-wMWCNT L^{-1}) test dispersions. Two subsamples of 1 mL were drawn, 2 mL of Ultima Gold™ XR scintillation cocktail (Perkin Elmer, Germany) were added and samples were submitted to LSC (liquid scintillation counter, Hidex SL 600, Hidex, Germany) to verify the achieved ^{14}C-wMWCNT concentration, respectively. Out of test dispersions four replicates with each 250 mL were prepared in glass flasks. Samples were incubated at a temperature of 20 ± 2 °C and a photoperiod of

16 h light/8 h dark. At test start (0 h), radioactivity of each replicate was determined by means of LSC (100% value: 107 ± 2 µg L^{-1}). For sampling, an aliquot of 1 mL was drawn from the water surface (layer depth of 0.5 cm) of one replicate. Initially, a sample was taken every 15 minutes. During the experiment, the interval between the individual measurements was increased continuously. The last sample was taken on day 21.

3.3.4 Test organisms

Green algae *Chlamydomonas reinhardtii* (strain no. 23.90) and *Raphidocelis subcapitata* (strain no. 61.81) were obtained from SAG Göttingen and cultured in BG 11 culture medium (SAG, 2013) and culture medium according to Kuhl and Lorenzen (1964), respectively. Cultures of algae were kept at 20 ± 2 °C, permanent aeration and constant illumination. Renewal of medium was performed every two weeks. *Daphnia magna* (Straus) were cultured in M4 medium (OECD, 2004) (20 ± 2 °C, 16 h dark/8 h light photoperiod). Daphnids were fed daily, except on weekends from a culture of the green alga *Desmodesmus subspicatus*. In addition, *Daphnia* was fed with yeast (*Saccharomyces cerevisiae*) once a week during medium renewal.

3.3.5 Micro batch experiments for wMWCNT characterization

The following approaches were prepared in small-scale:

a) wMWCNT dispersion (0.1 mg L^{-1}, 20 mL)

b) wMWCNT (1 mg L^{-1}) and green algae *R. subcapitata* (2 × 20 mL, 24 h)

c) wMWCNT (1 mg L^{-1}) and five adult *D. magna* (100 mL) – uptake for 24 h (water exposure) and excretion for 24 h in presence of algae

d) wMWCNT (0.1 mg L^{-1}) and three adult daphnids (100 mL) for 72 h.

M4 medium was used for all test approaches. A wMWCNT concentration of 1 mg L^{-1} was chosen in b) and c) as former tests using a wMWCNT concentration of 0.1 mg L^{-1} have not led to qualitative results (data not shown). Dispersion of nanomaterial was performed as described above. Scenario a) – c) have been characterized by means of TEM. To characterize wMWCNT in dispersion, copper grids (Plano GmbH) for TEM analysis were submerged in nanomaterial dispersion directly after assembly and placed on a filter heated up to 50 °C. In presence of organisms, subsamples of maximum 40 µL (2 × 20 µL) were taken from the bottom of test vessels using a pipette and placed onto copper grids. During the process, copper grids were placed on a paper filter. Samples were dried as described above. After desiccation, copper grids were subjected to TEM analysis using a Philips CM 20 FEG operating at 200 keV. Test organisms of scenario d) were analyzed using a light microscope to visualize internalized nanomaterials.

3.3.6 Quantification of ^{14}C-wMWCNT interaction with green algae

A suspension of green alga *Chlamydomonas reinhardtii* was separated from culture medium by centrifugation (10 min, 943 × *g*) and resuspended in BG 11 medium (main constituents: 150 mg $NaNO_3$ L^{-1}, 4 mg $K_2HPO_4 \times H_2O$ L^{-1}, 7.5 mg $MgSO_4 \times 7\ H_2O$ L^{-1}, 3.6 mg $CaCl_2 \times 2\ H_2O$ L^{-1}, pH value between 7 and 8, see SI). Cell density was determined using a fluorescence reader (Tecan M200, Männedorf, Schweiz, Software: Magellan). A quantity of 703 µg ^{14}C-wMWCNT was weighted out on a microbalance (MYA 5.3Y, Radwag) and dispersed in 100 mL BG 11 medium for 10 min as described above. Three times, 12.7 mL of this dispersion were then diluted each with 737.3 mL BG 11 medium in a flask and dispersed for further 10 min in order to obtain an application volume of 2250 mL (3 × 750 mL suspension). Four aliquots of 1 mL were drawn from each bottle and analyzed using LSC. Furthermore, 84 mL of each ^{14}C-wMWCNT dispersion were mixed with 16 mL algal suspension in a 250 mL Erlenmeyer flask. In this way, a ^{14}C-wMWCNT concentration of 122 ± 2 µg L^{-1} and an algal cell density of 1×10^6 cells mL^{-1} was achieved. The prepared samples were weighted and incubated at 22 ± 2 °C at a diurnal rhythm of 16 h light to 8 h dark on a laboratory shaker (80 rpm). Immediately after completion (t = 0 h) and after 24, 48, 72 and 96 h four replicates were sampled. Three aliquots of 0.5 g were taken and measured by means of LSC to determine the 100% value. Algal density was determined as well. In case of t = 0 h this corresponded to an initial concentration of 1×10^6 cells mL^{-1}. Subsequently, free CNT were separated from CNT associated to algae by means of density gradient centrifugation (see SI). The suitability of this method was already described before (Rhiem et al., 2015). After the last step of separation and washing algal cells with BG 11 medium, one to three drops of remaining algal pellet (five times per sample) were placed in a single well on a 24-well plate and filled up with BG 11 medium to a weight of 2 g (corresponding to 2 mL) and cell count was determined. The contents of each well were subsequently transferred completely (rinsed using methanol) to an LSC vial. The following measurement of the sample using LSC revealed the amount of ^{14}C-wMWCNT associated with the algal cells. A complete recovery was performed by quantifying radioactivity in all compartments accruing during reprocessing (see SI under 3.7.3). The same was performed using the green algae *Raphidocelis subcapitata*. An initial ^{14}C-wMWCNT concentration of 123 ± 3 µg L^{-1} and an algal density of 2×10^6 cells mL^{-1} was applied in culture medium (main constituents: 1011 mg KNO_3 L^{-1}, 621 mg $NaH_2PO_4 \times H_2O$ L^{-1}, 71 mg Na_2HPO_4 L^{-1}, 246.5 mg $MgSO_4 \times 7\ H_2O$ L^{-1}, 14.7 mg $CaCl_2 \times 2\ H_2O$ L^{-1}, pH between 7 and 8, see SI). A higher starting cell count in the case of *R. subcapitata* was necessary to ensure the success of density gradient centrifugation at the time of the first sampling (t = 0 h).

3.3.7 Uptake of ^{14}C-wMWCNT by *D. magna*

Uptake of ^{14}C-wMWCNT in *D. magna* was investigated via water exposure and trophic transfer. Body burden (application: 100 µg ^{14}C-wMWCNT L^{-1}) was determined after 2, 18, 24, 48 and 72 h in four replicates each (water exposure: 72 h, n = 5; trophic transfer: 2 and 24 h, n = 5). As test medium,

oxygen saturated M4 medium was used. For water exposure a total mass of 107 µg ^{14}C-wMWCNT was weighted on a microbalance (MYA 5.3Y, Radwag), transferred to a flask containing 100 mL of test medium and dispersed as described above. Afterwards, a certain volume (32.71 mL) was taken from this stock dispersion and diluted by test medium (317.29 mL) to obtain the test dispersion with 100 µg ^{14}C-wMWCNT L^{-1} (2 × 350 mL). The test solution was dispersed for another 10 min (see above). Homogeneity and ^{14}C-wMWCNT concentration in test dispersion were monitored directly after sonication. Therefore, three aliquots of 1 mL were mixed with 2 mL of Ultima Gold™ XR scintillation cocktail (Perkin Elmer, Germany) and measured by means of LSC.

Immediately after LSC measurements, 30 mL of test dispersion were filled in small glass beakers. Radioactivity in every test beaker (2 × 0.5 mL) was determined using LSC. Achieved ^{14}C-wMWCNT concentration was 116 ± 5 µg L^{-1} instead of 100 µg L^{-1}. 10 daphnids ≤ 24 h were placed into each beaker. Test organisms were kept at a temperature of 20 ± 2 °C and a photoperiod of 16 h light/8 h dark. The animals were not fed during this experiment and were last fed 24 h before test start.

For sampling, daphnids were taken out of test beakers, placed into a plain glass dish and washed two times extensively with test medium and distilled water. Washed animals were then transferred to aluminium boats and dried at 65 °C for 24 h. The amount of radioactivity in test beakers and in water phases from cleaning steps was determined by LSC (obviously immobile or dead organisms were captured in this fraction). Glass ware and used pipettes were cleaned using methanol moistened tissues. To quantify the radioactivity of ^{14}C-wMWCNT attached to the working utensils, tissues were submitted to LSC as well. After determination of dry weight, test animals were transferred to a micro glass mortar and homogenized using methanol. In this way, radioactivity trapped in the animals was released and detected by LSC to avoid a defective quantification due to quenching processes by animal's carapace or compact agglomerated CNT. Afterwards, the crushed animal/methanol mass was transferred to an LSC Vial. The micro mortar was cleaned carefully, and water used for rinsing was placed in the same scintillation vial. Quantification of accumulated radioactivity in *D. magna* was performed by means of LSC.

For the trophic transfer experiment, the green alga *Raphidocelis subcapitata* was pre-loaded by ^{14}C-wMWCNT and subsequently fed to *D. magna*. A two weeks old culture of *R. subcapitata* was centrifuged (10 min, 943 × *g*) and the pellet was resuspended in 100 mL Kuhl medium. A total of 790 µg ^{14}C-wMWCNT was weighted on a micro balance and dispersed in 100 mL culture medium as described above. This dispersion was further diluted by 550 mL culture medium and dispersed again for 10 min. Algal suspension was added to ^{14}C-wMWCNT dispersion and incubated for three days (aerated in a round-bottomed flask) as described for *D. magna* previously. Determined ^{14}C wMWCNT

concentration was 1.3 mg L^{-1}. After incubation algae were centrifuged (10 min, 943 × *g*), supernatant discarded and the pellet washed (centrifugation, 10 min, 943 × *g*) two times using 50 mL of M4 medium.

The remaining algal pellet was resuspended in culture medium. ^{14}C-wMWCNT concentration was determined using LSC up to 1.5 mg L^{-1}. For the volume of test medium required (750 mL) and a ^{14}C wMWCNT concentration of 120 µg L^{-1} (see water exposure) a volume of 58.8 mL of suspension with ^{14}C-wMWCNT-loaded algae was diluted with M4 medium to 750 mL test medium. Concentration of algae was 1.6×10^6 cells mL^{-1}. A test concentration of 120.3 µg ^{14}C-wMWCNT L^{-1} was verified by means of LSC (three aliquots each 1 mL). Setup of test, incubation and determination of body burden was performed as described in case of water exposure.

3.3.8 Elimination of ^{14}C-wMWCNT by *D. magna*

Uptake of 120 µg ^{14}C-wMWCNT L^{-1} in *D. magna* was conducted for 24 h. 120 µg ^{14}C-wMWCNT were weighted on a microbalance and transferred to a flask containing 100 mL M4 medium. After dispersion, twice 45 mL of stock dispersion were diluted by 405 mL M4 medium and dispersed for another 10 min (for dispersion details see above) to obtain a test dispersion of 120 µg ^{14}C-wMWCNT L^{-1}. Aliquots were taken and measured by means of LSC. Aberration from one test dispersion to another was only about 3% and the effect on uptake and elimination of CNT in *D. magna* is considered as admissible. The test setup was the same as described for uptake experiments, 27 samples were prepared. After uptake phase, seven replicates were sampled to calculate 100% value (0 h) for excretion experiment. The test organisms from the remaining 20 samples were transferred to clean M4 medium. For every replicate, daphnids were taken out and washed vigorously using pipettes to subduct nanomaterial attached to the animal's surface. With a small amount of fresh M4 medium the daphnids were then transferred into the elimination beakers. Time was noted for every beaker to verify the start of excretion process. The described test approach was prepared twice. One test was set up for excretion in water phase (without food, -algae) and one for excretion in presence of food (+algae). Due to poor recovery, only five replicates were included in the calculation of the 100% value at 0 h for the scenario without algae. After animal transfer to clean medium, 0.1 mg carbon through green alga *D. subspicatus* was added to the samples. For incubation conditions see the uptake experiment. Four replicates (three replicates after 48 h in the scenario without algae) were sampled after 2.5, 5, 19, 24 and 48 h, respectively. Sampling of test animals and quantification of accumulated nanomaterial was performed as described above.

3.3.9 Uptake of ^{14}C-wMWCNT in a *D. magna* population

Uptake of 100 µg ^{14}C-wMWCNT L^{-1} was assessed over 4 weeks in an evolving population of *D. magna*. A total of 1.8 mg ^{14}C-wMWCNT was weighted out on a microbalance and dispersed for 10 min

(Sonopuls HD 2070, 70 W, pulse: 0.2 s, pause: 0.8 s) in 200 mL ice bath cooled M4 medium. Volume for stock dispersion was doubled in this case due to the high amount of ^{14}C-wMWCNT required. Afterwards a volume of 22.75 mL was diluted by 1977.25 mL M4 medium and dispersed for another 10 min (see above). Two aliquots of 1 mL were taken from each test dispersion and radioactivity was measured using LSC. 800 mL of ^{14}C-wMWCNT test dispersion were filled in 1 L glass beakers. Subsequently 3 adult (3 to 4 weeks old) and 5 neonate (≤ 24 h) daphnids were placed into each sample and gentle aeration was fixed to the beakers. Additionally, four controls without ^{14}C-wMWCNT were prepared for supervision of *D. magna* population growth at every sampling time. Samples were kept at 20 ± 2 °C and a photoperiod of 16 h light/8 h dark. Animals in control and treatment group were fed daily 0.5 mg carbon L^{-1} via a culture of *D. subspicatus* (Hammers-Wirtz and Ratte, 2003).

In treatments, once a week renewal of test medium and reapplication of ^{14}C-wMWCNT (100 µg L^{-1}) was performed (semi-batch approach). Therefore, test animals were sieved (mesh for brine shrimp, 180 µm), washed with 100 mL clean M4 medium and transferred (with 100 mL clean M4 medium, dilution was considered while preparation of ^{14}C-wMWCNT test dispersion) to beakers containing a newly prepared (100 µg ^{14}C-wMWCNT L^{-1}) nanomaterial dispersion. Just as in the treatments, the medium of the controls was renewed every week. Animals from controls were sieved (mesh for brine shrimp, 180, 300, 560 and 900 µm) and distributions of individuals per size were noted. Counted daphnids were washed into fresh M4 medium and incubated as described before.

In case of treatments four replicates were sampled after 7, 14, 21 and 28 d. The water body of every sample was sieved completely using a 4-part brine shrimp sieve set (see above). After that, 100 mL tap water were filled in test beaker and remaining daphnids were flushed out and sieved. The complete volume of water phase was collected in a 1 L bottle. Using tap water, size sorted animals were transferred in 4 single petri dishes and sieves were washed thoroughly. Subsequently, water was removed in order to immobilize test organisms and individuals per size distribution were acquired. After counting, the animals sorted by size were conveyed to smaller petri dishes and washed extensively using tap water to remove radioactive material from the animals' surface. The water used for rinsing was withdrawn and the animals were transferred to pre-weighted aluminum boats using distilled water. Boxed animals were dried for 24 h at 65 °C. If the number of individuals in a size class was < 10 and an exact weight determination therefore impossible, the animals were added to the aluminium boat of the next larger class. For a complete recovery, working utensils were wiped clean using methanol moistened tissues, which were submitted to LSC. The rinsing water was pooled with the collected water phase and the volume was dispersed for 10 min to obtain a homogeneous distribution of radioactivity. For quantification of radioactivity in water phase, two subsamples of 1 mL

per flask were mixed with 2 mL Ultima Gold™ XR scintillation cocktail (Perkin Elmer, Germany) and measured by means of LSC.

After determination of dry weight, animals were transferred to 20 mL LSC Vials using methanol. Vials were kept for 24 h under a fume hood (evaporation of methanol), subsequently 1 mL of solubilizer Soluene-350® (PerkinElmer) was added to the samples. Sample vials were closed and incubated at 60 °C. In the first hours, the liquid was swivelled every 30 min and incubation was finished after complete dissolving of biological matrix. After cooling the samples to room temperature, 19 mL LSC cocktail was added to each vial and the amount of radioactivity was determined.

3.3.10 Data evaluation and statistical analysis

Collected data was processed using Microsoft Excel® (Microsoft Office 365 ProPlus), GraphPad Prism (GraphPad Prism 5, USA), and SigmaPlot (SigmaPlot Version 12.0, USA). Outliers were identified by Dixon's Q test ($\alpha = 0.05$). To identify differences between treatments either a two-sample t-test by comparing the t-based 95% confidence intervals for mean values or a common t-test (p value to reject = 0.05) was performed. Raw data were tested for normal distribution with Shapiro-Wilk test (p value = 0.05) and variance homogeneity with Levene's test (p value = 0.05). If any of the above test criteria could not be met, a Mann-Whitney Rank Sum test was performed.

For data sets from the deposition experiment, in addition to evaluation of experimental data, the deposition kinetics were evaluated using Computer assisted kinetic evaluation (CAKE, Version 3.3 (Release), Tesella). A Hockey Stick (HS) model, i.e., an exponential decline function with a breaking point separating two kinetics (k_1 and k_2), was selected for the description of the data set.

Since the usual definition of bioaccumulation is inappropriate regarding nanomaterial uptake, an approximation of bioaccumulated wMWCNT in different aquatic organisms was performed based on a one-compartment model according to Connel (1998) (Eq. 3.1):

$$C_{b(t)} = C_w \frac{k_1}{k_2}(1 - e^{-k_2 t}) + C_{b(t0)} e^{-k_2 t} \qquad (3.1)$$

C_b and C_w are the wMWCNT concentration in biota (mg kg^{-1}) and water phase (mg L^{-1}), respectively, k_1 (L kg^{-1} h^{-1}) and k_2 (h^{-1}) represent the uptake and elimination rate constants and t indicates time (h). Assuming that C_w as well as k_1 and k_2 are constant over the test period, the bioaccumulation factor can be calculated as follows: $BAF = k_1/k_2 = C_b/C_w$. For green algae, a bioconcentration factor (BCF) was calculated using C_b/C_w (Bjorkland et al., 2017), where C_w was the applied wMWCNT concentration (0.1 mg L^{-1}). In case of *D. magna*, BCF in water exposure scenario was calculated using C_b/C_w and k_1/k_2, where C_w was the wMWCNT concentration in water measured at sampling date. Using k_1/k_2, uptake rate k_1 varied over time, so k_1 was calculated from time points where interaction of test organism and

wMWCNT were at maximum (pseudo-steady-state). According to Bjorkland et al. (2017), BAF was calculated using C_b/C_w, where C_w was the wMWCNT concentration in water and diet.

3.4 Results

3.4.1 Sedimentation of ^{14}C-wMWCNT

Concentration of ^{14}C-wMWCNT in top layer of static water phase (M4 medium) decreased over time (Fig. 3.2). After one day and three days the radioactivity level in the top layer of water dropped to a value of 87.7 ± 1.6% and 69.5 ± 0.9%, respectively. After 21 days only < 0.35% (0.2 ± 0.1%) of the initially applied radioactivity remained at the top layer of the water phase. An exponential regression fit to the decreasing concentrations resulted in a DT_{50} and DT_{90} of 3.91 d and 12.82 d, respectively. The application of a HS model to the data set produced very similar deposition times (DT_{50} = 4.38 d and DT_{90} = 10.50 d). Both, the exponential fit and the modelling (see SI, Fig. 3.9, Tab. 3.1) revealed a coefficient of determination of R^2 = 0.99 and showed a good description of the experimental data.

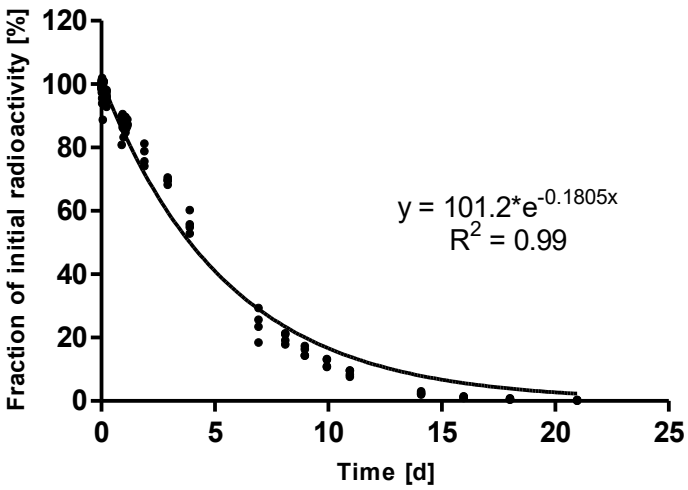

Figure 3.2: Deposition of ^{14}C-wMWCNT in a static water phase (M4 medium) over 21 days (d). The measured amount of radioactivity at t = 0 d was set to 100%. The proportion of decrease (%) of the initially applied radioactivity over the test period is shown. An exponential decay equation model was fitted to the experimental data. Data points represent single replicates (n = 4). (R^2 = coefficient of determination).

3.4.2 Nanomaterial characterization

Fig. 3.3 - B shows that the optimized method to disperse the used nanomaterials (wMWCNT concentration: 0.1 mg L^{-1}) resulted in small agglomerates (bundles) and single strand exfoliated CNT. Weathered MWCNT showed a length of 200 nm to 3 µm, visualized by means of TEM. The observed small agglomerates contained loosely associated individual CNT (Fig. 3.3 – B). The sickle-shaped structure in Fig. 3.3 - A shows a single cell of the green alga *R. subcapitata* to which long wMWCNT fibers are attached (Fig. 3.3 - A; also see Fig. 3.10 in the SI).

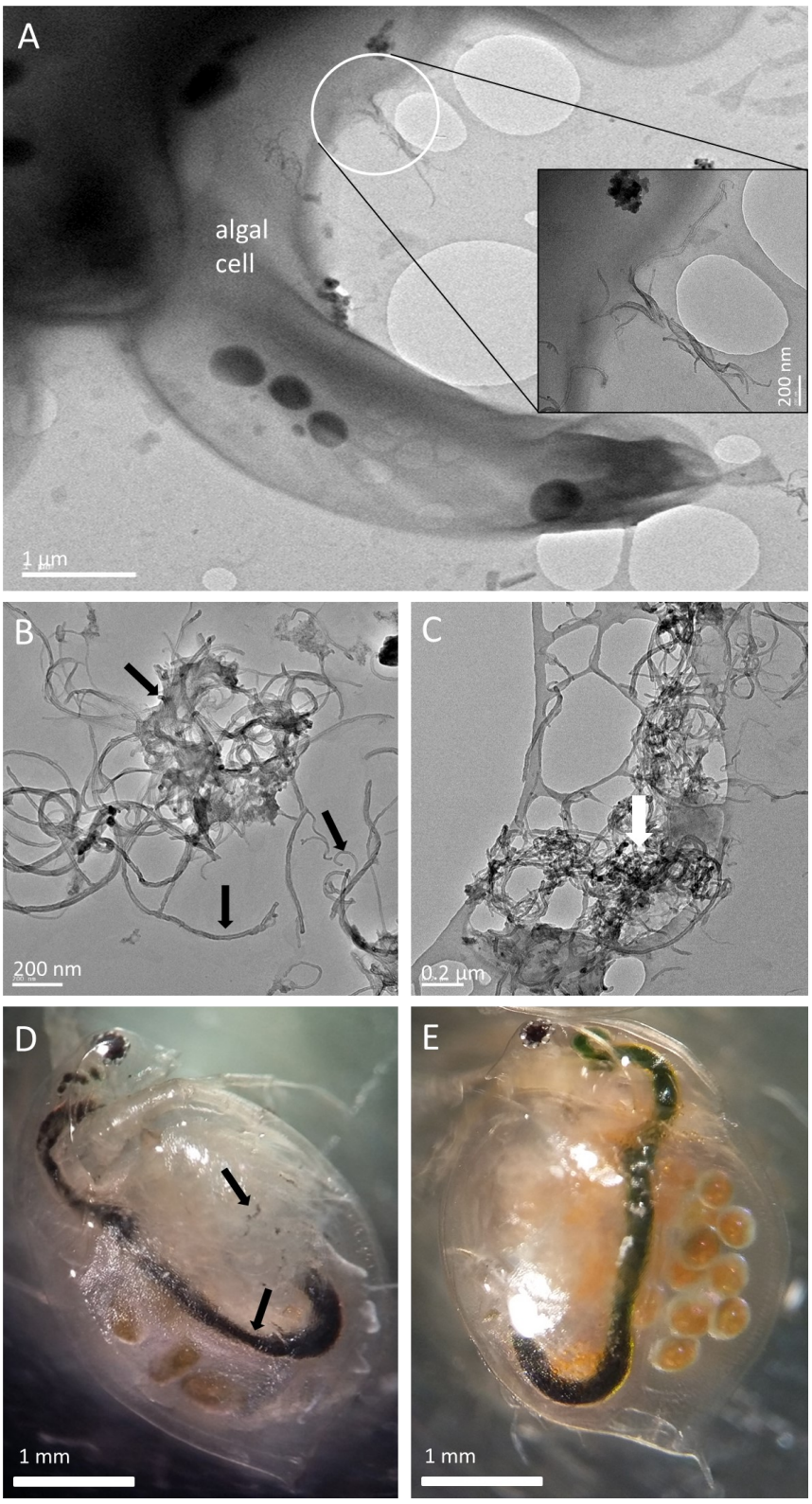

Figure 3.3 (A - E): Transmission electron microscopy (TEM) images of wMWCNT in association with green alga *R. subcapitata* (A), wMWCNT dispersion (0.1 mg L-1) (B) and excreted wMWCNT by *D. magna* after uptake period of 24 h (C). D and E show the light microscopy image of an adult *D. magna* exposed to 100 µg wMWCNT L^{-1} and without exposure over a period of 72 h, respectively.

We also identified wMWCNT excreted by *D. magna*. Excreted wMWCNT in faeces of *Daphnia* (Fig. 3.3 - C) occur in agglomerates, which appear much more condensed than, e.g., agglomerates in dispersion of 0.1 mg wMWCNT L^{-1} (Fig. 3.3 - B). Due to the compression of the nanomaterials, an exact estimation of wMWCNT length of the few recognizable single strands is difficult (about 0.8 to 1 µm). Fig. 3.3 - D shows an adult daphnid with internalized wMWCNT after an incubation period of 72 h. The black colored intestine, which appears green under normal conditions (Fig. 3.3 – E), is particularly well visible. Furthermore, associated small black particles can be seen on the filter apparatus (black arrow). The rest of the animal's body is free of foreign particles. Embryos are visible in the brood chamber. The animal appears pale and colourless.

3.4.3 ^{14}C-wMWCNT interaction with green algae

Recovery of radioactivity in tests with green algae was 95 to 112%. In a pretest, a wMWCNT concentration of 100 µg L^{-1} had no effect on the growth of green algae (see section 5.4.2 in chapter 5). For *C. reinhardtii*, interaction with ^{14}C-wMWCNT increased in the first 24 h (Fig. 3.4 - A), but between 24 h (maximum uptake: 1.6 ± 0.4 µg wMWCNT mg^{-1} dw^{-1}) and 96 h (0.9 ± 0.1 µg wMWCNT mg^{-1} dw^{-1}) a decrease in wMWCNT associated to the algae was recorded. Further, wMWCNT association with *R. subcapitata* was considerably lower and resulted in a maximum uptake after 48 h (0.7 ± 0.3 µg wMWCNT mg^{-1} dw^{-1}). Subsequently, the associated amount of wMWCNT decreased to 0.1 ± 0.03 µg wMWCNT mg^{-1} dw^{-1} (96 h) (Fig. 3.4 - A).

During the uptake experiments an exponential growth for both algal species was observed. Initial cell counts increased 5 times and 2.5 times within 96 hours in case of *C. reinhardtii* and *R. subcapitata*, respectively (Fig. 3.4 - B), indicating a significantly higher growth rate for *C. reinhardtii*. Considering the amounts of radioactivity associated with the algae a 24 h BCF (C_b/C_w) of 13,700 L kg^{-1} and a 48 h BCF (C_b/C_w) of 6,800 L kg^{-1} was calculated for *C. reinhardtii* and *R. subcapitata*, respectively.

In test systems with both algal species a total of 12 – 13 µg ^{14}C-wMWCNT was applied. The total associated amount of wMWCNT to green algae was calculated by extrapolation over time. After 48 h 14 ± 3 µg wMWCNT (per 9 ± 0.1 mg dry weight of algae) were already associated with *C. reinhardtii*, leaving no bioavailable fraction of wMWCNT. The total amount of wMWCNT associated to *R. subcapitata* fluctuated over the test period and after 48 h a maximum of 5 ± 2 µg wMWCNT (per 7 ± 0.2 mg dry weight of algae) was associated (see SI, Tab. 3.2).

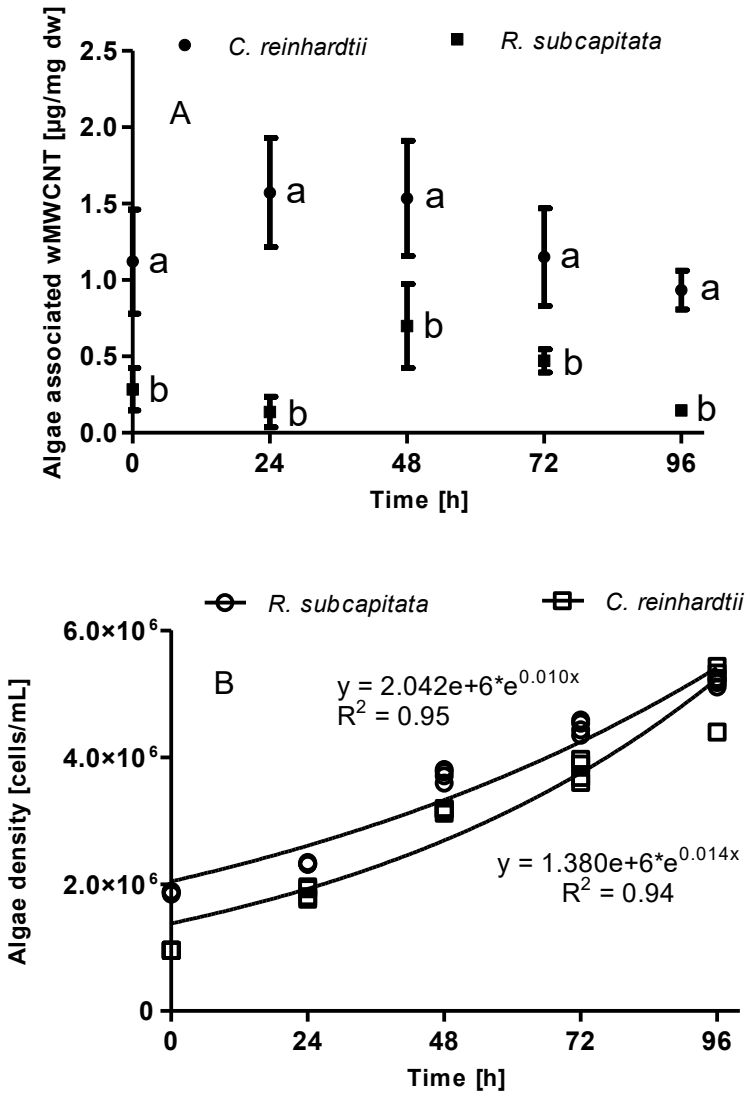

Figure 3.4: Weathered multi-walled carbon nanotube (wMWCNT) concentration linked to green algae over time. A ^{14}C-wMWCNT concentration of 100 µg L^{-1} was applied to suspensions of *R. subcapitata* (circles) and *C. reinhardtii* (squares) (A). The mean values and standard deviations are given (n = 4). For all timepoints, mean values for uptake of wMWCNT in *R. subcapitata* and *C. reinhardtii* proved to be significantly different (visualized using the letters a and b, t-test, α = 0.05). An exponential fit was plotted for the corresponding growth curves, algal density (cells mL^{-1}) was measured over time in uptake experiment (B). Growth rates for *C. reinhardtii* and *R. subcapitata* are µ = 0.014 h^{-1} and µ = 0.010 h^{-1}, respectively. A significant difference over time was identified (two-sample t-test). Data points represent single replicates (n = 4).

3.4.4 ^{14}C-wMWCNT uptake and elimination by *D. magna*

Daphnid mortality was below 10% in every test. In the uptake experiments the recovery of ^{14}C-wMWCNT was 83 ± 3 to 96 ± 6% and 87 ± 8 to 97 ± 8% for water exposure and trophic transfer, respectively. In the water exposure scenario, an increase in body burden was observed up to 18 hours (7.1 ± 1.5 µg wMWCNT mg^{-1} dw^{-1}). Subsequently, elimination process exceeded the ingestion resulting in decreasing internal wMWCNT concentrations (Fig. 3.5). For trophic transfer, the highest body burden was already observed after 2.5 h (0.07 ± 0.01 µg wMWCNT mg^{-1} dw^{-1}), which corresponds to

an uptake of two orders of magnitude smaller compared to water exposure. It has been shown that the addition of food significantly influences wMWCNT uptake in *D. magna*. Afterwards, elimination processes predominated ingestion. After 72 h only 0.014 ± 0.004 µg wMWCNT mg^{-1} dw^{-1} remained in test organisms. Without food addition, the elimination rate constant (k_2 = 0.015 h^{-1}, exponential fit, Fig. 3.5) was significantly lower than in presence of food (k_2 = 0.038 h^{-1}).

Even though the application of bioaccumulation factors to nanomaterials is not suitable, in the following accumulation factors to compare with the existing literature are given. For maximum uptake (18 h) in water exposure scenario a BCF (C_b/C_w) of 98,000 ± 30,000 L kg^{-1} was determined. Since no steady state was reached, the BCF changed over time and after 72 h the value was 40,000 ± 17,000 L kg^{-1}. Bioaccumulation changing over time was also observed in the trophic transfer scenario. After 2.5 h (maximum uptake) and 72 h the BAF's (C_b/C_w) amounted to 600 ± 70 L kg^{-1} and 120 ± 40 L kg^{-1}, respectively.

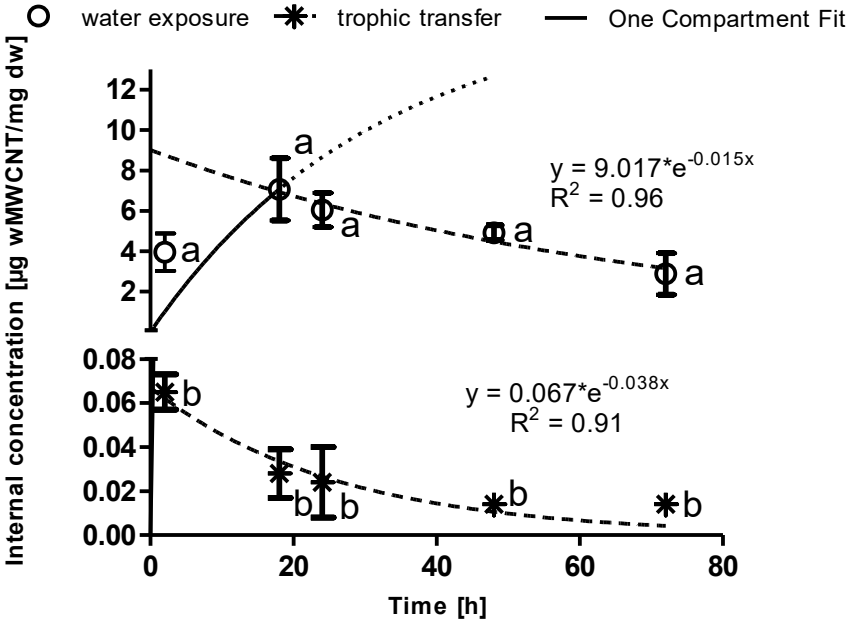

Figure 3.5: Uptake of ^{14}C-wMWCNT in *D. magna* after waterborne exposure (circles) and trophic transfer (asterisks). For trophic transfer green algae *R. subcapitata* was pre-loaded by radioactively labeled wMWCNT over 72 hours (h). A one compartment model (R^2 = 0.96) was fitted to experimental data of uptake via water exposure (solid line, 0 h – 18 h). Additionally, the further course of the modelling is shown (dotted line). An exponential fit was adapted to areas with uptake decline for water exposure (dashed line, 18 h – 72 h) and trophic transfer (dashed line) scenario. Error bars indicate standard deviation (n = 4). For all timepoints, mean values of uptake *via* water exposure and trophic transfer proved to be significantly different (visualized using the letters a and b, t-test, α = 0.05).

Elimination of ingested wMWCNT by *D. magna* was significantly faster in the setup with food supply, indicated by k_2 of 1.079 h^{-1} compared to that in absence of algae (0.032 h^{-1}; Fig. 3.6). In presence of algae a portion of 6, 1.6, 0.97, 0.71 and 0.84% of the initial body burden remained after 2.5, 5, 19, 24 and 48 h in the test organisms, i.e., after approximately 5 h the gut was almost completely cleared. At

the same time, elimination in clean M4 medium was slower, i.e., 52, 45, 42, 34 and 15% of the initial body burden remained in *Daphnia*. Thus, the presence of food has a significant influence on the uptake of wMWCNT as well as on its depuration.

With the use of a one compartment model, fitted to the data from 0 h to 18 h a kinetic BCF (k_1/k_2) for the water exposure scenario was determined. The uptake rate constant k_1 was calculated from the experimental data and k_2 was taken from the elimination experiment without food supply (k_2 = 0.032 h^{-1}, Fig. 3.6). Nevertheless, that only two time points could be applied, the coefficient of determination R^2 = 0.96 showed a good fit (Fig. 3.5). A kinetic BCF of 140,000 L kg^{-1} was calculated, three orders of magnitude greater compared to BAF's from trophic transfer. Due to the missing uptake data in trophic transfer scenario (0 h to 2.5 h), no k_1 could be calculated and therefore no kinetic BAF is given.

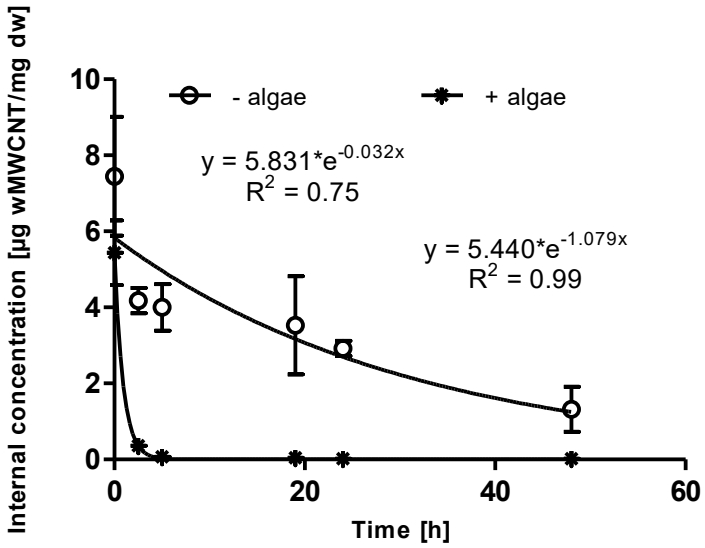

Figure 3.6: Internal ^{14}C-wMWCNT concentration in *D. magna* after depuration over a period of 48 hours (h). Start wMWCNT-concentration in -algae (circles) and +algae (asterisks) scenario was calculated from five and seven replicates, respectively. *Daphnia* were fed with green algae (0.1 mg carbon) after transfer to clean medium. Elimination rates (k_2) were determined (exponential fit) to 0.032 h^{-1} and 1.079 h^{-1} in scenario -algae and +algae, respectively. Elimination in presence and absence of algae was significantly different over time (two-sample t-test). Error bars indicate standard deviation (n = 4).

3.4.5 ^{14}C-wMWCNT uptake by D. magna population

No significant differences in population size between control and wMWCNT treatment groups were observed except for the last sampling date (Fig. 3.7). Within 14 days *D. magna* populations grew up rapidly from the start with 8 daphnids per sample to a maximum of approximately 200 individuals (control: 209 ± 40 individuals; wMWCNT treatment: 159 ± 85 individuals) and afterwards dropped to half of the population density. As shown in Fig. 3.8, body burden for ^{14}C-wMWCNT uptake in *D. magna* increased over time and a maximal value of 0.7 ± 0.2 µg wMWCNT mg^{-1} dw^{-1} was achieved after

28 days. A steady state was reached after weekly applications of 100 µg ^{14}C-wMWCNT L^{-1}. The 28 d BAF (C_b/C_w) was 6700 ± 2900 L kg^{-1}.

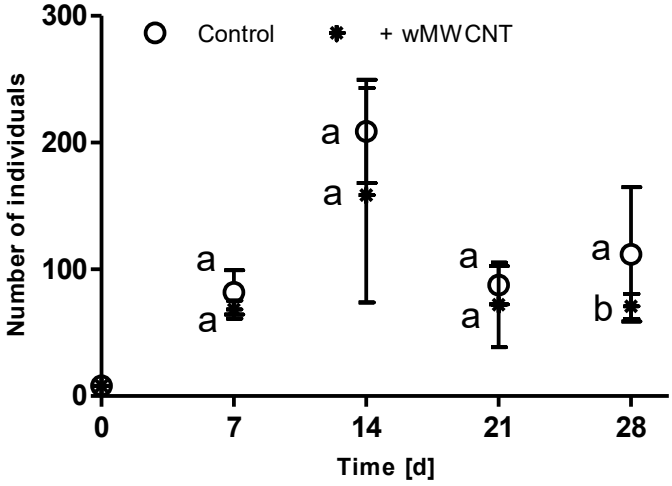

Figure 3.7: *D. magna* population dynamics. In 800 mL M4 medium, a population of *D. magna* developed from initially 5 neonate and 3 adult animals over 28 days. *D. magna* were fed daily 0.5 mg carbon (green algae). Two wMWCNT concentrations were tested: 0 mg L^{-1} (Control, circles) and 0.1 mg L^{-1} (asterisks). The total number of individuals over time is given. Error bars indicate the standard deviation on the mean of four replicates (n = 4). The combination of the letters a and b visualizes the identified significant difference (t-test, α = 0.05).

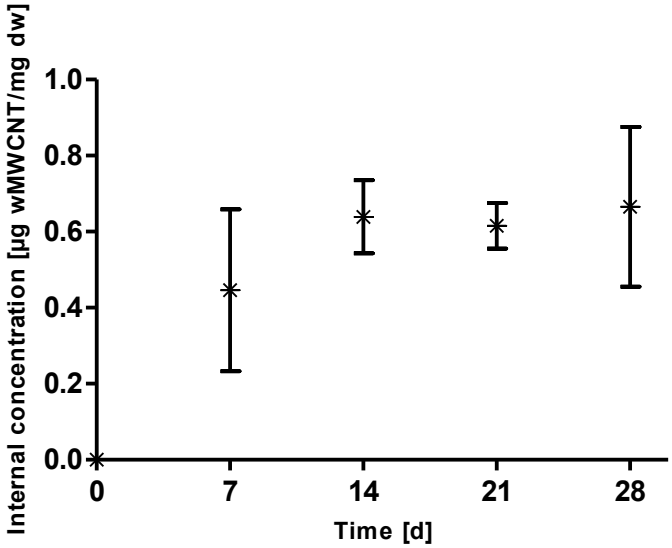

Figure 3.8: Uptake of ^{14}C-wMWCNT in a developing *D. magna* population over 28 days. Renewal of medium and simultaneous reapplication of ^{14}C-wMWCNT was performed once a week. Error bars indicate standard deviations for arithmetic average of four replicates (n = 4).

3.5 Discussion

3.5.1 Dispersion and settling of wMWCNT

Dispersion of 100 µg wMWCNT L^{-1} in the test media resulted in small agglomerates (Fig. 3.3 – B), formed by Van der Waals forces and electrostatic interactions (Kennedy et al., 2008; Zhou et al., 2015), and some single strands visualized by means of TEM. Similar behavior of CNT after a dispersion period of 4 h has been reported (Zhou et al., 2015), indicating that an increase of dispersion interval does not lead to a more homogeneous dispersion. The use of intensive sonication can further result in damage or shortening of CNT strands (Zhu et al., 2006; Saleh et al., 2008).

The M4 medium used contains among other ingredients divalent cations like Mg^{2+} and Ca^{2+} which will further influence the dispersion stability of CNT (Hyung et al., 2007; Chen et al., 2010; Schierz et al., 2014; Glomstad et al., 2018). Additionally, surface functionalization of CNT increases the stability of CNT dispersion in aqueous media (Jackson et al., 2013). Our weathering procedure of CNT using simulated sunlight irradiation was expected to lead to surface functionalization like hydroxyl groups (Klaine et al., 2008), however, we were not able to detect changes of the surface structure compared to the pristine material by using TGA and FTIR (see SI in chapter 2). A possible explanation is the autoxidation of the pristine MWCNT, which can occur due to the prolonged storage of this material. This is a change in surface functionalization, especially also as a function of surface occupancy. Other reasons could be that, e.g., COOH functionalities decarboxylate over time and thus the oxidative functionality cannot be detected, or that the sensitivity of the used method was not adequate to detect the surface modifications. Due to the use of radioactively labeled (^{14}C) wMWCNT, a homogeneous distribution in M4 medium was demonstrated by means of LSC.

In the present study a DT_{50} of 3.8 to 3.9 days was calculated for deposition of 100 µg wMWCNT L^{-1} under nonstirred (static) conditions. Kennedy et al. (2008) found a sedimentation half-life for MWCNT (100 mg L^{-1}) in reconstituted freshwater containing 100 mg L^{-1} natural organic matter (NOM) of 9 min. Schierz et al. (2014) calculated a half-life for single wall carbon nanotubes (SWCNT, 2.5 mg L^{-1}) of 7.4 hours in a mesocosm ecosystem. Since the addition of NOM increases the stability of CNT dispersions and thus reduces aggregation and deposition (Schierz et al., 2014; Glomstad et al., 2018), we conclude that the considerably higher DT_{50} values are caused by the lower initial concentration of introduced CNT. In addition, low CNT concentrations, as in our study, will reduce the probability that individual particles collide and interact. Thus, homo- and heteroaggregation, which is also influenced by the physical and chemical properties of the particles and the aqueous medium (Chen et al., 2010), in our experiment is rather low and consequently the sedimentation rate is reduced in comparison to other studies. We expect that sedimentation will be similarly slow or even slower at the much lower

environmental concentration in the ng L^{-1} range (Gottschalk et al., 2009; Gottschalk and Nowack, 2011).

3.5.2 Nanomaterial interaction with green algae

The association of algal cells and wMWCNT was visualized and quantified. TEM analysis showed the linkage of single wMWCNT fibers to cells of *R. subcapitata*. Penetration of the algal cell wall cannot be excluded (Fig. 3.3 - A, Fig. 3.10 in the SI), since this has already been observed (Wei et al., 2010; Long et al., 2012; Rhiem et al., 2015). Additionally, Rhiem et al. (2015) detected MWCNT single tubes in the cytosol of *D. subspicatus* cells but most were agglomerated at the surface of cells. An association of CNT with algal cells instead of the absorption into the cells was further suggested for MWCNT interaction with bacteria *P. aeruginosa* (Mortimer et al., 2016). Schwab et al. (2011) found strong binding of algal cells to CNT and suggested the formation of hydrogen bonds between the cell surface and oxidized gaps in the CNT structure, which could be an explanation for our findings.

During the test, the green algae *C. reinhardtii* and *R. subcapitata* initially showed an increase in the associated amount of wMWCNT which later decreased. Both algal species showed an exponential growth over the entire test period, indicating that the observed decrease in concentration is likely due to growth dilution. Furthermore, increased agglomeration with time may have reduced the bioavailability of the CNT (Klaine et al., 2008; Chen et al., 2010) and prevented further uptake of CNT. For the two algal species, a significant difference in the uptake of CNT was demonstrated: *C. reinhardtii* adsorbed 100% of applied CNT over time but *R. subcapitata* only ≤ 43%, indicating a different association behavior of CNT on the two algal species in the accumulation study.

It is known that algae produce extracellular polymeric saccharides (EPS), which interact with nanomaterials (Miao et al., 2009; Zhang et al., 2012; Adeleye and Keller, 2016; Zheng et al., 2019). Sijm et al. (1998) observed that sorption on algal exudates significantly reduced the bioavailability of hydrophobic organic chemicals as well. It is therefore likely that the two green algae produced exudates which differ in their composition (Xiao and Zheng, 2016), which might explain the higher uptake rate for *C. reinhardtii*. Additionally, in contrast to the samples with *C. reinhardtii*, in those with *R. subcapitata* CNT aggregates, covered by an unidentified material, were observed after 72 h (Fig. 3.12 in SI) leading to CNT precipitation and reducing CNT bioavailability. Zhang et al. (2013a) observed formations of similar agglomerates and suggested the presence of quantum dot-algal associates. We assume that these presented agglomerates are composed of algal cells, their exudates and CNT (Verdugo et al., 2004; Xiao and Zheng, 2016).

Sijm et al. (1998) observed a lower bioconcentration of hydrophobic organic chemicals in algae at higher algal densities and recognized that in addition to the physico-chemical properties of the test

substance, also the physiology (e.g., species, growth stage, structure) of the algae is of particular importance. Apart from the fact that the spherical *C. reinhardtii* is larger (diameter: 14 – 22 µm) than the sickle-shaped *R. subcapitata* (helical diameter: 5.6 - 11.7 µm; width: 1.9 - 3.6 µm), the two green algae differ in the composition of their cell wall. While the cell wall of the algal cells from the Selenastraceae family (*Raphidocelis subcapitata*) have one homogeneous layer surrounded by a remarkable mucilage, the cell wall of *C. reinhardtii* consists of five different layers, whereas the outer layer contains frayed areas depending on the cell status (Kiefer et al., 1997; Fawley et al., 2006; Baudelet et al., 2017). Therefore, we assume that CNT less likely interact with the mucilage adhering to the cell wall of *R. subcapitata*, but more intensely adsorb onto the inhomogeneous cell wall of *C. reinhardtii*.

A 24 h BCF (C_b/C_w) of 13,700 L kg^{-1} and a 48 h BCF (C_b/C_w) of 6,800 L kg^{-1} for wMWCNT accumulation was calculated for green algae *C. reinhardtii* and *R. subcapitata*, respectively. Rhiem et al. (2015) determined a bioconcentration factor of 5000 after 72 h exposure of *D. subspicatus* to MWCNT (1 mg L^{-1}). In calculating the BCF (C_b/C_w), the initial exposure concentration was used as C_w. Dispersion stability influences exposure concentration and sedimentation processes, i.e., organisms are exposed to test concentrations that change over time (Glomstad et al., 2018). In case of the test system with algae, agglomeration processes and the presence of exudates as well as the association of CNT to algae play a decisive role in the bioavailability of the nanomaterials in the water phase. Consequently, the concentration of the freely available CNT is reduced over time and C_w may have been overestimated. As a result, bioconcentration factors are underestimated and probably cannot accurately reflect the accumulation of CNT in algae. Therefore, and since the one-compartment model described has been simplified for application to the accumulation of wMWCNT in algae the given BCF's should be considered with reservation (Praetorius et al., 2014; Bjorkland et al., 2017). Regarding the uptake of wMWCNT, a differentiation between adsorption on and uptake in algal cells was not possible. Nevertheless, it has been shown that CNT associate to a large extent with green algae, which explains the observed food transfer of the nanomaterial to daphnids described below.

3.5.3 Nanomaterial uptake by *D. magna*

Maximum uptake of wMWCNT was observed after 18 h for waterborne exposure and after 2.5 h in trophic transfer scenario (Fig. 3.5). Maximum uptake within the first 24 h has been shown for MWCNT and fullerenes previously (Petersen et al., 2009; Tervonen et al., 2010; Petersen et al., 2011). In our test, maximum concentrations after water exposure and trophic transfer were 7.1 ± 1.5 µg wMWCNT mg^{-1} dw^{-1} and 0.07 ± 0.01 µg wMWCNT mg^{-1} dw^{-1}, respectively. Accumulated wMWCNT accounted for 0.71 wt% after water exposure and 0.007 wt% after trophic transfer of total *Daphnia* dry mass, similarly to a study with MWCNT by Petersen et al. (2011) and graphene by Guo et

al. (2013). In a previous study, Petersen et al. (2009) measured body burdens in the range of up to 70 µg mg^{-1} dw^{-1} in a study on the uptake of MWCNT (40, 100 and 400 µg L^{-1}) from the water phase in daphnids, i.e., considerably higher than the body burdens in our experiment. The author explained that the enormous difference in body burdens can be due to the smaller weight of the *Daphnia* used (5 – 7 days old). The weights of the 5 - 7 days old *Daphnia* (0.01 - 0.02 mg per individual) in the Petersen study of 2009 were equivalent to the weight of the neonate animals (≤ 24 h) in our study after 18 h exposure, which on average was 0.01 mg per individual (see SI, Tab. 3.3). In a more recent study (Petersen et al., 2011) and in the present study *Daphnia* were fed daily, which most likely resulted in fitter and healthier animals compared to the animals from the Petersen study of 2009.

As shown in Figure 3.5, body burden in water exposure increased over the first 18 h, followed by a decrease from 18 h to 72 h. Guo et al. (2013) revealed very similar results for graphene uptake in 1-day old daphnids (max. uptake of 250 µg L^{-1} after 24 h: 7.8 µg mg^{-1} dw^{-1}). Decrease in body burdens after 18 h probably resulted from agglomeration and settling of CNT, and thus lower concentrations in the water column. The deposition experiment (Fig. 3.2) showed that after 18, 24, 48 and 72 h a ^{14}C-wMWCNT portion of 88.4%, 87.7%, 77.5% and 69.5% remained in the water column, respectively. In addition to this fast sedimentation behavior in an abiotic test system, in the presence of animals, it was suggested that agglomeration of CNT is enhanced by passage through the gut tract and biomodification of the CNT surface (Roberts et al., 2007; Petersen et al., 2009; Guo et al., 2013).

As for trophic transfer, uptake of wMWCNT was two orders of magnitude lower compared to water exposure. A study of MWCNT uptake in *D. magna* showed that the presence of food during exposure revealed body burdens of up to 0.8 µg g^{-1} and 0.02 - 0.06 µg g^{-1} on dry mass basis for 5 to 15 days old daphnids after 24 h and 3 d, respectively (Cano et al., 2017; Cano et al., 2018). The fact that uptake in the presence of algae results in decreasing body burdens over time (Fig. 3.5) and k_2 is more than twice as large in the presence of food indicates that besides agglomeration and sedimentation processes, excretion determines the body burden, as described in the model of Connel (1998). Roberts et al. (2007) showed that solubilized lipid coated SWCNT were ingested by *D. magna* and egested as precipitated SWCNT without coating. Because survival of test organisms was dose-dependent, the authors suggested that *Daphnia* were able to accept lipid coating as food source. In our trophic transfer study, wMWCNT were loaded on algae, therefore algae from ingested algal-wMWCNT complexes might be absorbed in the digestive system leading to the significant increase in weight of the exposed daphnids compared to the animals from the water exposure study (see SI, Fig. 3.13). Animals after 72 h water phase exposure looked pale and their gut was filled with nanomaterial (Fig. 3.3 - D). Well-fed daphnids are more intensely colored than starving organisms and coloring corresponds to the food intake (Ebert, 2005). Nanomaterials were mainly observed in the gastrointestinal tract of the test

organisms and adhered to thoracopods. Previous studies already established that CNT are unlikely to be absorbed by the organism beyond the intestine (Petersen et al., 2009; Edgington et al., 2010; Parks et al., 2013; Edgington et al., 2014), which is one reason why they are not bioaccumulated in the classical sense like soluble chemicals (Praetorius et al., 2014; Bjorkland et al., 2017). Due to the lack of food, animals of waterborne exposure were obviously in poor physical constitution.

The calculated bioconcentration factors were 140,000 (kinetic BCF, L kg^{-1}) and 120 (BAF, L kg^{-1}) on dry mass basis for waterborne exposure and trophic transfer, respectively. For trophic transfer, bioconcentration factor was three orders of magnitude smaller than after water exposure. Mortimer et al. (2016) revealed similar differences in BCF values by two orders of magnitude of 35,000 L kg^{-1} and 800 L kg^{-1} when *T. thermophila* was exposed to MWCNT-amended medium and MWCNT encrusted bacteria, respectively. Petersen et al. (2009) described BCF values of 360,000 L kg^{-1}, 440,000 L kg^{-1} and 350,000 L kg^{-1} for exposure of *D. magna* to 40, 100 and 400 µg L^{-1} over 48 h. All abovementioned BCF values indicate high bioaccumulation of CNT which originate predominantly from accumulation of nanomaterial in the gut. CNT amounts attached to animals' outer surfaces can be considered negligible.

3.5.4 Nanomaterial excretion by *D. magna*

As shown in Fig. 3.6, daphnids were able to fully purge CNT from their intestine in presence of algae. Elimination of CNT in pure M4 medium was significantly slower and incomplete. The positive influence of food on elimination processes is also shown by the different weights of the animals in the experiment. The increasing weight of *Daphnia* in the scenario with algae from 0.127 to 0.267 mg per 10 neonates (see SI, Fig. 3.14 and Tab. 3.4) suggests that these animals were considerably fitter than their conspecifics (0.136 to 0.118 mg). Petersen et al. (2009) showed no excretion of MWCNT by *Daphnia* in clean or filtered lake water and after addition of algae during depuration, body burdens decreased only by 50 - 85% in the first hours. As already mentioned, *Daphnia* from this study were 5 – 7 days old and as heavy as the neonate daphnids in our study, which probably were not able to efficiently purge their guts due to health issues. The ability of daphnids to empty their intestines even without food source was also shown after gold nanoparticle intake (Lovern et al., 2008). It is known that daphnids can defecate by peristaltic movements, but still need the pressure of further ingested food (Ebert, 2005). Depuration of graphene and coated MWCNT in presence of algae revealed clearance of more than 90% and 89 - 99%, respectively (Petersen et al., 2011; Guo et al., 2013). The addition of algae as food source therefore facilitates excretion (Gillis et al., 2005; Kennedy et al., 2008; Petersen et al., 2011; Guo et al., 2013). Nevertheless, it was shown that depuration of CNT by neonate daphnids increased over time even without food intake since *Daphnia* take up water from their surroundings to stimulate their digestion (Fox, 1952).

3.5.5 Accumulation of wMWCNT by *D. magna* population

As shown in Fig. 3.7, population of *D. magna* grew rapidly in the first two weeks to a maximum of approximately 200 animals and then population density leveled off to an equilibrium size. Similar population dynamics were observed in laboratory (Hammers-Wirtz and Ratte, 2003) and model systems (Preuss et al., 2009). In our study, no significant differences on growth of population between control and treatment groups were observed except for the last sampling date. The significantly smaller population size after 28 d in the treatment group may be due to chance, but a long-term effect on the growth of a *D. magna* population caused by a wMWCNT concentration of 100 µg L^{-1} cannot be completely excluded, especially since the population size of the treatment over the whole period shows lower numbers than the controls. Biologically evaluated, the exposure to wMWCNT under normal feeding conditions for 28 days had no effect on population dynamics. Uptake of ^{14}C-wMWCNT increased from 0 d to 14 d before steady state was reached.

Maximal body burden was 0.7 ± 0.2 µg mg^{-1} dw^{-1} after 28 d. The value for the received body burden from population experiment (Fig. 3.8) is smaller than the maximum body burden from experiment without food apply (water exposure) and one order of magnitude higher than maximum body burden from trophic transfer scenario, where CNT were loaded to algae prior to exposition (Fig. 3.5). In population experiment steady state was reached unlike water exposure and trophic transfer scenario. The significant smaller body burden in population experiment compared to the water exposure group can be explained by the facilitated excretion due to feeding and because of *D. magna* in different growth stages - from neonates to adults - existed. The ratio of accumulated nanomaterial mass to total organism mass is smaller when larger organisms are applied (Petersen et al., 2011). As for the daily feeding in population experiment, *Daphnia* do not have a pronounced food preference and consumes particles ranging in size from 0.1 to 30 µm (Lynch, 1978), which is why algae and dispersed CNT were competing for uptake. The maximum body burden of wMWCNT in *D. magna* population experiment was, despite of weekly applications over 28 days, significantly smaller compared to exposure of neonates in the test medium without food. This can serve as further indication that CNT are not enriched and stored in tissues other than the intestine (Edgington et al., 2014).

The significant higher body burden in the population experiment can be explained by the fact that daphnids were fed daily with weekly ^{14}C-wMWCNT applications, compared to the trophic transfer study where a single application of CNT-loaded algae was performed. Additionally, the reduced settlement of CNT by aeration and turbulence of water phase led to a higher bioavailability of CNT. Furthermore, it has already been shown that increasing volumes of water at the same concentration leads to higher body burdens because of the larger amount of available CNT (Petersen et al., 2009). Our results suggest that the constant discharge of CNT into a water body under normal food conditions

causes the accumulation of these by *D. magna* until a steady state is reached. A further transport of CNT along the food chain is thus possible.

In the present study, a BAF of 6700 ± 2900 L kg^{-1} was calculated. Cano et al. (2017) investigated the uptake of MWCNT at a concentration of 0.1 mg L^{-1} in *D. magna* (60 individuals) at 600 mL water for 24 h and obtained body burdens up to 0.0008 µg MWCNT mg^{-1} dw^{-1} under the application of food. The body burden is two and three orders of magnitude smaller compared to our trophic transfer and population experiments, respectively, probably because of the short exposure duration of 24 h compared to 7 - 28 days of exposure in our study. Another reason for the lower accumulation in the study of Cano et al. (2017) may be the use of a surfactant (sodium dodecyl benzene sulfonate) that has been shown to have toxic effects on *D. magna* in high concentrations and therefore might have influenced the uptake of CNT by test animals. The influence of different food and starving conditions on uptake of CNT in an evolving *D. magna* population should be further investigated.

3.6 Conclusion and outlook

In the present study it was shown that weathered CNT at µg L^{-1} concentrations persist for several days in the water phase of a static aquatic system and interact with living organisms. Depending on the shape and metabolic activity of green algae, CNT associate to algal cells to a large extent and, as nanomaterial carriers, lead to food web transfer. In case of *D. magna*, trophic transfer resulted in orders of magnitude lower body burdens compared to waterborne exposure indicating no bioaccumulation. Daphnids excrete CNT in absence and presence of food.

To our knowledge we are the first to investigate uptake of CNT in a growing *D. magna* population. Multiple CNT (100 µg L^{-1}) applications lead to steady state body burdens in daphnids after 14 days but no toxic effects compared to control groups. Results indicate that uptake of nanomaterials by *D. magna* depends on CNT dispersion stability, food supply and therefore on the physiological constitution of test organisms. Finally, long residence times of CNT at low concentrations in the water phase increase the interaction and association probability with algae and subsequently lead to the food-chain transport of CNT to higher organisms.

Compared to other published investigations, our population experiment reflects natural conditions and resulted in a bioaccumulation factor of > 2000 for the weathered MWCNT which would be classified as a bioaccumulative chemical and therefore hazardous under the EU REACH regulation. However, it must be considered that bioaccumulation of nanomaterials differs from that of dissolved organic chemicals, because accumulation is located mainly in the intestine of organisms where they can be excreted again. Considering that the estimated environmental concentration of CNT (ng L^{-1}) is lower than our tested concentrations by five orders of magnitude we can assume, that currently no

risk is to be expected for aquatic organisms by exposure to CNT. But what happens when the release of CNT into the environment increases?

3.7 Supplementary information (SI)

3.7.1 Settling of ^{14}C-wMWCNT

Hockey Stick (HS) model created by CAKE (Computer assisted kinetic evaluation, Version 3.3 (Release)), a computer software developed by Tesella.

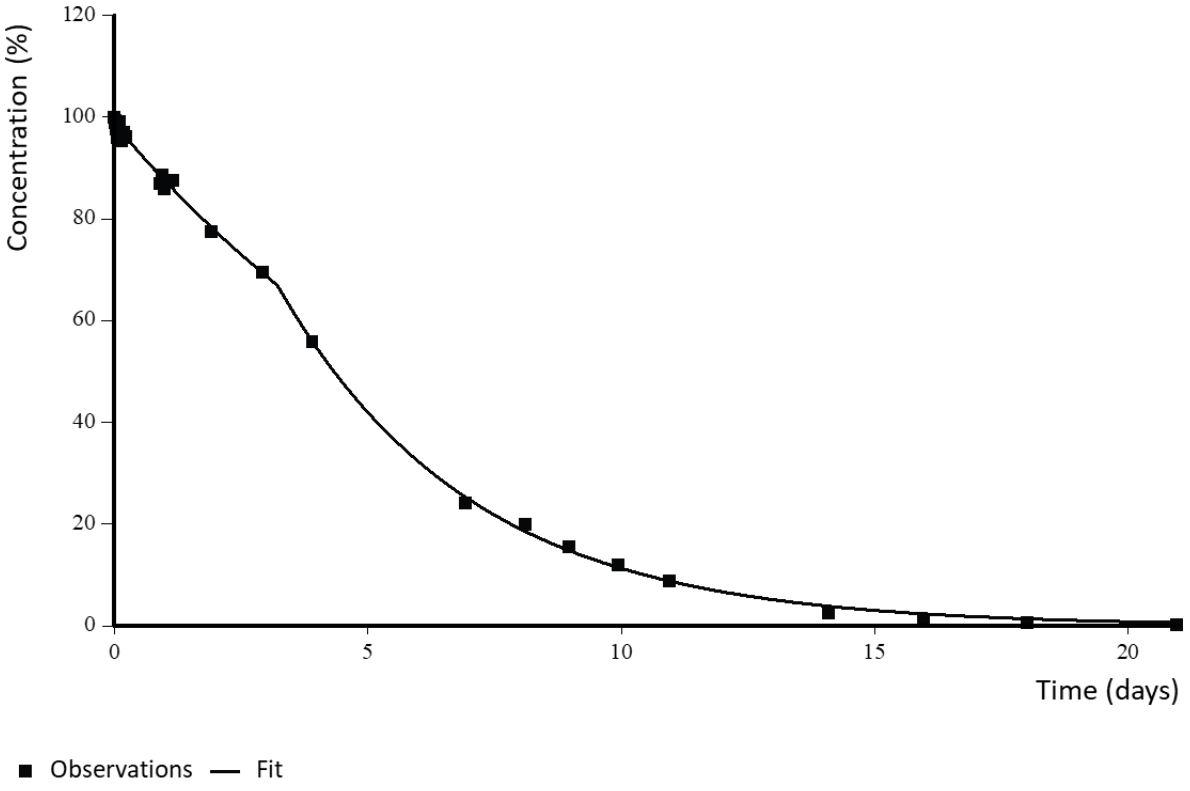

Figure 3.9: Graphical Summary (Hockey Stick model, CAKE).

Table 3.1: Statistical characteristics for all data (Hockey Stick model, CAKE).

Chi^2	
Error %	Degrees of Freedom
1.32	29
Coefficient of correlation r^2	
Observed vs. Predicted	Efficiency
0.9993	0.9993

3.7.2 Transmission electron microscopy (TEM)

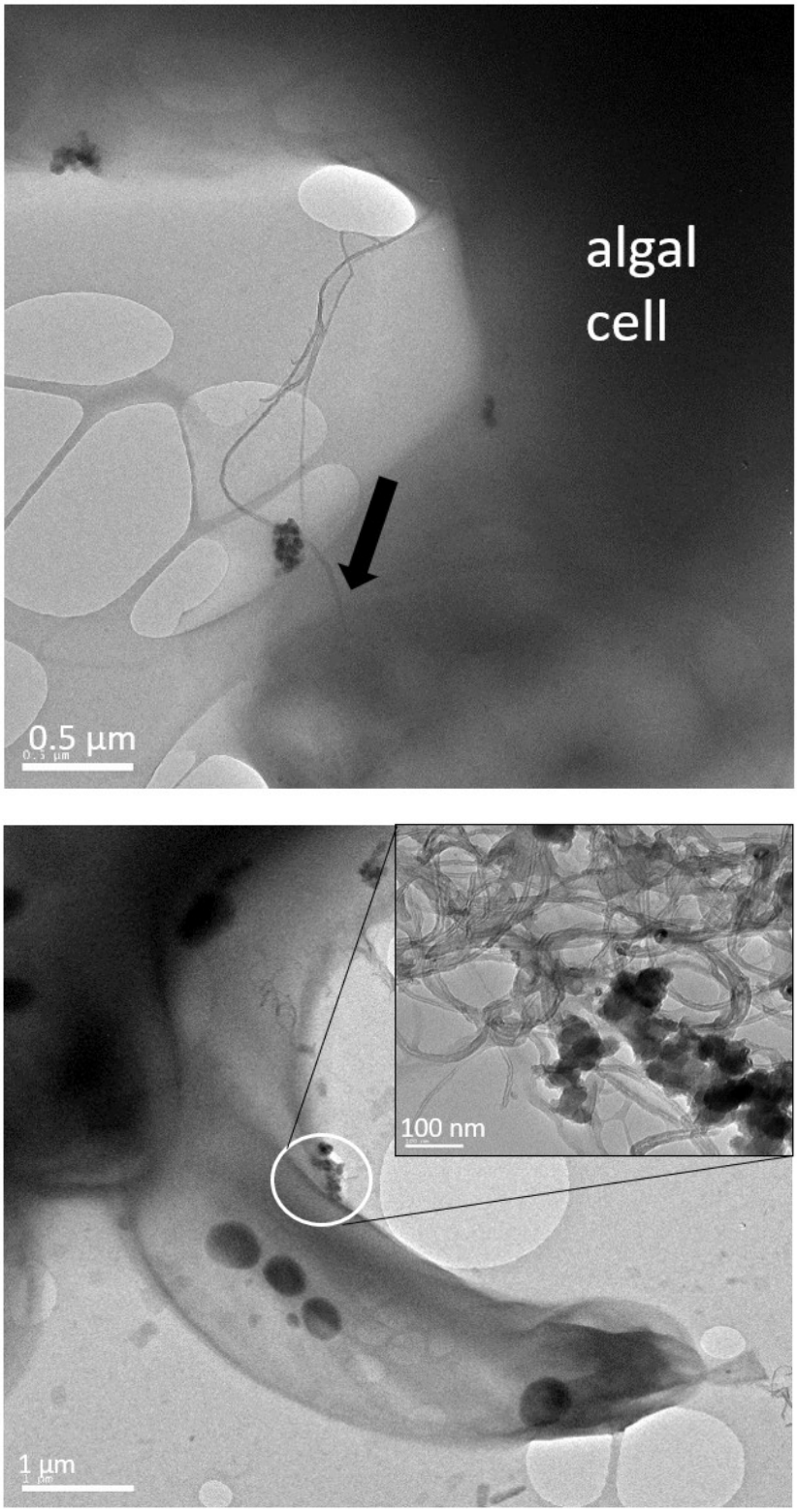

Figure 3.10: Transmission electron microscope (TEM) images from green alga *Raphidocelis subcapitata* associated with wMWCNT. Associated wMWCNT were highlighted by a black arrow or a white circle (contact site was enlarged). (Pictures were taken by Dr. Nina Siebers from Forschungszentrum Jülich GmbH).

3.7.3 Method for density gradient centrifugation

To determine the amount of algal-associated wMWCNT, free nanomaterials were separated from algal cells (*Chlamydomonas reinhardtii* and *Raphidocelis subcapitata*) by means of density gradient centrifugation. During reprocessing density gradient centrifugation was performed after identifying 100% value for radioactivity analysis and determination of algal density. In centrifugation vessels 40 g of colloidal silica suspension (Ludox® TM-40, 40% in distilled water, Sigma Aldrich, Germany) and 10 g distilled water were provided by layering distilled water carefully on top of Ludox using a Pasteur pipette. After pipetting, two layers should be visible. Subsequently, 20 g sample were added to centrifugation vessel as described before. Since algae and nanomaterials tend to settle down in static water bodies, samples must be rotated manually during drawing of all samples. After centrifugation (10 min and 943 × *g*) three different phases were visible in centrifugation vessel. From the bottom up Ludox, algae and water (distilled water and medium) were layered (Fig. 3.11).

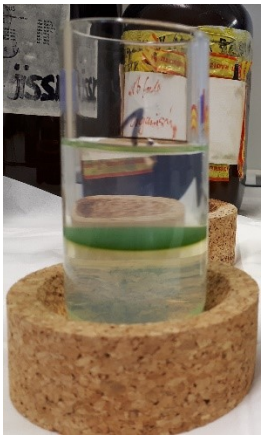

Figure 3.11: Three layers bottom up: Ludox, algae and water (distilled water and medium) after density gradient centrifugation.

First, Ludox phase was removed carefully by breaking through two top layers (water and algae) using a glas pipette and submitted completely (first experiment; 0 h) to LSC (liquid scintillation counter, Hidex SL 600, Hidex, Germany). Due to equal recovery in further reprocessings only aliquots of Ludox phase were measured by means of LSC. Beforehand Ludox phase was dispersed by means of ultrosonication (10 min, Sonopuls HD 2070, 70 W, pulse: 0.2 s, pause: 0.8 s) in order to distribute nanomaterials evenly. Water phase was pooled with Ludox phase to minimize LSC samples. Further, algal layer was removed from vessel using a Pasteur pipette and transferred to a second centrifugation vessel for further cleaning of algal cells. Therefore, 50 mL test medium were added to algae and centrifuged as described above. Supernatant was removed and measured using LSC as described above. Algal pellet was redissolved in 50 mL test medium and centrifuged a second time as described above. Supernatant was removed and quantification of radioactivity amount was performed using LSC (see above). In order to resolve the remaining algal pellet a volume of 1 mL test medium was added.

For determination of associated amount of wMWCNT see manuscript. Further, a total recovery was performed. Ludox phase as well as supernatant from both cleaning steps were dispersed as described above and aliquots of 3×10 g were submitted to LSC. The remaining algae, which were not needed for the determination of uptake after purification were submitted completely to LSC. It is important to make sure that the algae are sufficiently aliquoted, otherwise chemiluminescence and poor efficiency of the LSC measurement can occur. Using a methanol-soaked tissues, the used glassware was wiped clean and tissues were submitted to LSC.

3.7.4 Interaction of nanomaterials with green algae

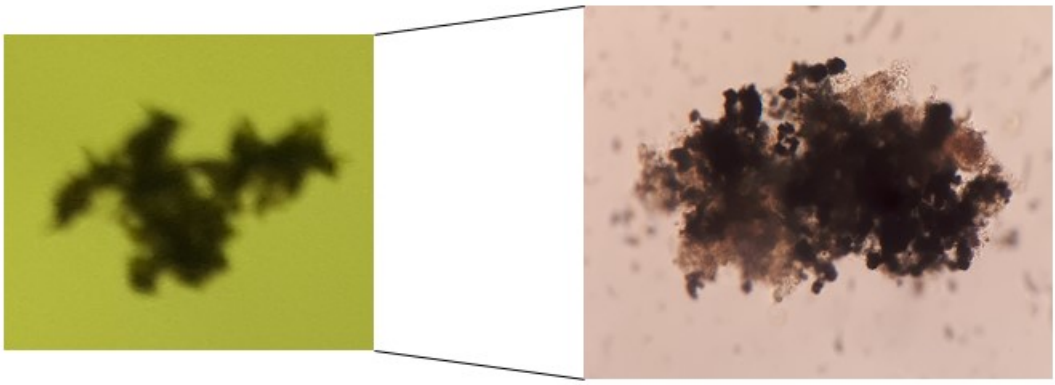

Figure 3.12: Presumptive agglomerates of wMWCNT in uptake experiment with *Raphidocelis subcapitata*, observed after 72 h of exposure.

Table 3.2: Total associated amount of wMWCNT (µg) to *C. reinhardtii* and *R. subcapitata* and the total dry weight of green algae in one sample (100 mL) from the experiment on interaction of wMWCNT with green algae. A total amount of 12 – 13 µg ^{14}C-wMWCNT was applied at test start. Values listed in the table were estimated by extrapolation of the subsamples taken during the experiment. The means and standard deviations on four replicates are given.

Chlamydomonas reinhardtii

time (h)	associated amount of wMWCNT (µg)		dry weight of algae (mg)	
	Mean	SD	Mean	SD
0	3.0	1.0	2.8	0.0
24	8.3	1.6	5.3	0.3
48	13.9	2.6	9.1	0.1
72	12.5	3.4	10.9	0.5
96	13.6	0.5	14.6	1.4

Raphidocelis subcapitata

time (h)	associated amount of wMWCNT (µg)		dry weight of algae (mg)	
	Mean	SD	Mean	SD
0	1.1	0.5	4.0	0.5
24	0.6	0.5	4.6	0.0
48	5.2	2.2	7.4	0.2
72	4.2	0.8	9.0	0.2
96	1.5	0.3	10.4	0.1

3.7.5 Weight of *Daphnia magna* in uptake and excretion experiment

Table 3.3: Dry weight (mg) of *Daphnia magna* neonates (10 individuals) in uptake experiment (water exposure and trophic transfer (dietary exposure)). SD = standard deviation.

	water exposure		dietary exposure	
time (h)	dry weight (mg)	SD	dry weight (mg)	SD
2	0.153	0.010	0.147	0.016
18	0.138	0.005	0.180	0.009
24	0.144	0.005	0.191	0.010
48	0.153	0.011	0.269	0.019
72	0.112	0.019	0.339	0.042

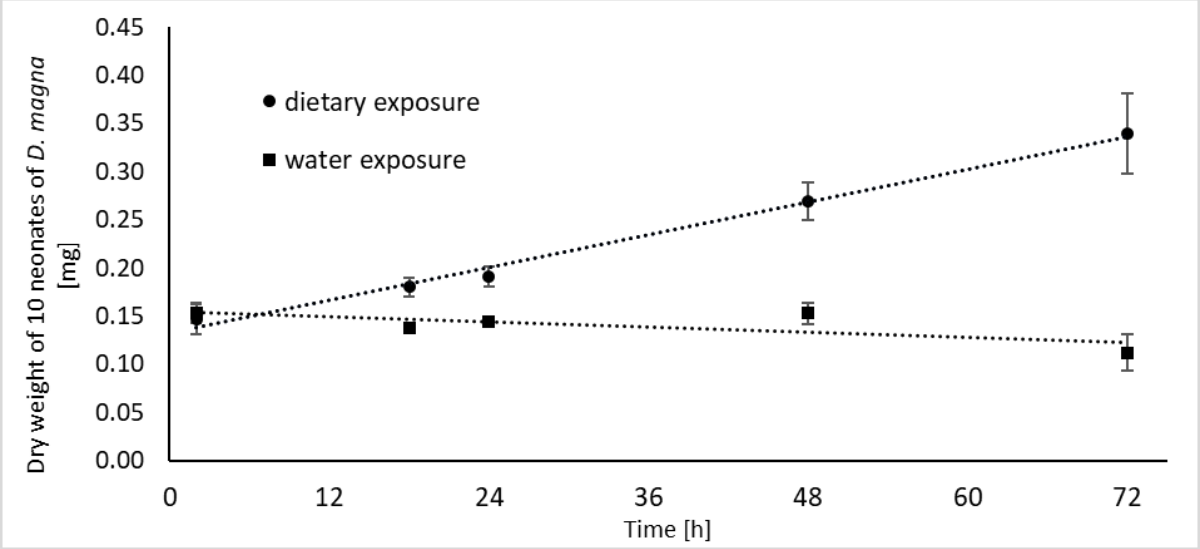

Figure 3.13: Dry weight of *Daphnia magna* neonates (10 individuals) after water exposure and trophic transfer (dietary exposure) to ^{14}C-wMWCNT over a period of 72 hours.

Table 3.4: Dry weight (mg) of *Daphnia magna* neonates (10 individuals) in excretion experiment (food conditions: -algae and + algae). SD = standard deviation.

	-algae		+algae	
time (h)	dry weight (mg)	SD	dry weight (mg)	SD
0	0.136	0.012	0.127	0.010
2.5	0.126	0.011	0.121	0.026
5	0.115	0.016	0.139	0.039
19	0.122	0.011	0.159	0.019
24	0.116	0.002	0.204	0.069
48	0.118	0.004	0.267	0.022

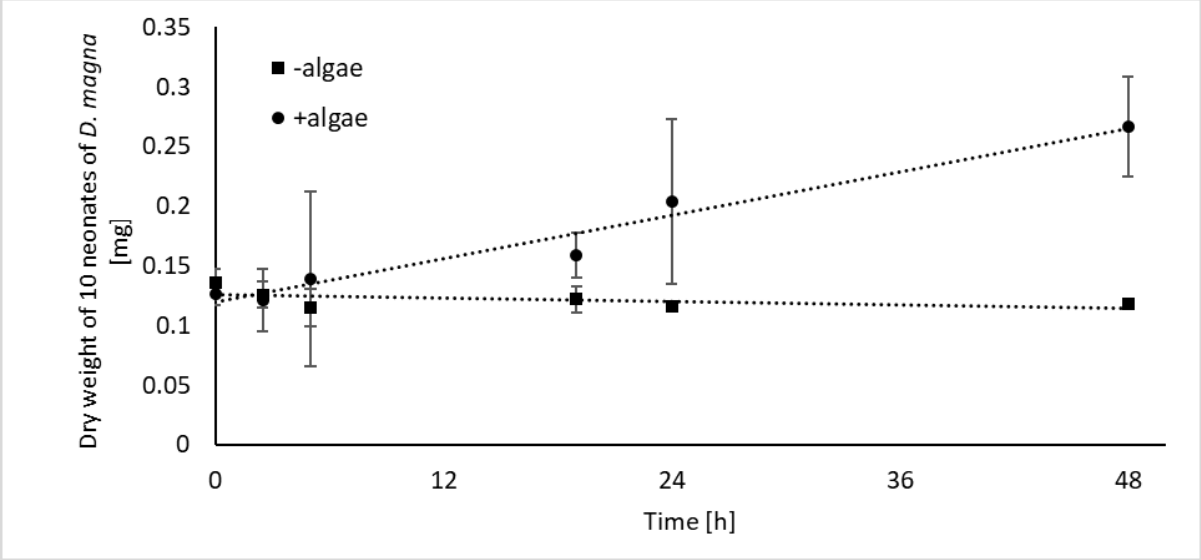

Figure 3.14: Dry weight of *Daphnia magna* neonates (10 individuals) after uptake of ^{14}C-wMWCNT for 24 h and an elimination period of 48 h in presence (+algae) and absence (-algae) of food.

3.7.6 Composition of test media

3.7.6.1 M4 medium

Table 3.5: Composition and preparation of M4 medium for tests with *D. magna*. Stock and test solutions were prepared using deionized water. The vitamin stock was stored frozen in small aliquots. Vitamins were added to the prepared media shortly before use. For more information see OECD No. 202.

Stock solution	Nutrient salt	Concentration in stock solution [L^{-1}]	Volume required for 1 L medium [mL]
$CaCl_2$ solution	$CaCl_2 \times 2\ H_2O$	117.6 g	2.5
$MgSO_4$ solution	$MgSO_4 \times 7\ H_2O$	49.3 g	2.5
KCl solution	KCl	2.2 g	2.64
$NaHCO_3$ solution	$NaHCO_3$	25.2 g	2.57
Cation solution	$MnCl_2 \times H_2O$	3605 mg	0.10
	LiCl	3060 mg	
	RbCl	710 mg	
	$SrCl_2 \times 6\ H_2O$	1520 mg	
	$CuCl_2 \times 2\ H_2O$	167.5 mg	
	$ZnCl_2$	130 mg	
	$CoCl_2 \times 6\ H_2O$	100 mg	
Anion solution	$NaNO_3$	548 mg	0.5
	H_3BO_3	5719 mg	
	NaBr	32 mg	
	$Na_2MoO_3 \times 2\ H_2O$	126 mg	
	K	6.5 mg	
	Na_2SeO_3	4.38 mg	
	NH_4VO_3	1.15 mg	
Silicate solution	Na_2SiO_3	21.475 mg	0.2
Ethylenediaminetetraacetic acid (EDTA)	$Na_2EDTA \times 2\ H_2O$	1000 mg	5
	$FeSO_4 \times 7\ H_2O$	398.2 mg	
Phosphate solution	KH_2PO_4	286 mg	0.5
	K_2HPO_4	368 mg	
Vitamin solution	Thiamine hydrochloride (B1)	750 mg	0.1
	Cyanocobalamin (B12)	10 mg	
	Biotin	75 mg	

3.7.6.2 Culture medium BG 11

Table 3.6: Composition and preparation of culture medium BG 11 for tests with *C. reinhardtii*. Stock and test solutions were prepared using deionized water. The medium was prepared according to BG 11 medium for Cyanobacteria provided by the Culture Collection of Algae (SAG, Göttingen University).

Stock solution	Nutrient salt	Concentration in stock solution [mL^{-1}]	Volume required for 1 L medium [mL]
1	$NaNO_3$	15 g	10
2	$K_2HPO_4 \times 3\ H_2O$	0.4 g	10
3	$MgSO_4 \times 7\ H_2O$	0.75 g	10
4	$CaCl_2 \times 2\ H_2O$	0.36 g	10
5	Citric acid	0.06 g	10
6	Ferric ammonium citrate	0.06 g	10
7	EDTA (dinatrium salt)	0.01 g	10
8	Na_2CO	0.2 g	10
Micronutrient solution	cf. culture medium according to Kuhl and Lorenzen (1964)		1

3.7.6.3 Culture medium according to Kuhl and Lorenzen (1964)

Table 3.7: Composition and preparation of culture medium according to Kuhl and Lorenzen (1964) for tests with *R. subcapitata*. Stock and test solutions were prepared using deionized water.

Stock solution	Nutrient salt	Concentration in stock solution [L^{-1}]	Volume required for 1 L medium [mL]
1	KNO_3	101.1 g	10
2	$NaH_2PO_4 \times H_2O$	62.0956 g	10
3	Na_2HPO_4	7.098 g	10
4	$MgSO_4 \times 7\ H_2O$	24.65 g	10
5	$CaCl_2 \times 2\ H_2O$	1.47 g	10
6	$FeSO_4 \times 7\ H_2O$ Fe-EDTA Complex	see below[1]	1
Micronutrient solution	H_3BO_3	61 mg	1
	$MnSO_4 \times H_2O$	169 mg	
	$ZnSO_4 \times 7\ H_2O$	287 mg	
	$CuSO_4 \times 5\ H_2O$	2.49 mg	
	$(NH_4)_6Mo_7O_{27} \times 4\ H_2O$	12.35 mg	

[1]Preparation of the Fe-EDTA complex: 0.69 g $FeSO_4 \times 7H_2O$ is dissolved with 0.93 g disodium salt of EDTA (Merck) in approximately 80 mL deionized water with brief boiling in a 100 mL volumetric flask. After cooling to room temperature, fill up to 100 mL.

3.8 References

Adeleye, A.S., Keller, A.A., 2016. Interactions between Algal Extracellular Polymeric Substances and Commercial TiO2 Nanoparticles in Aqueous Media. Environ Sci Technol 50, 12258-12265.

Barra, G., Guadagno, L., Vertuccio, L., Simonet, B., Santos, B., Zarrelli, M., Arena, M., Viscardi, M., 2019. Different Methods of Dispersing Carbon Nanotubes in Epoxy Resin and Initial Evaluation of the Obtained Nanocomposite as a Matrix of Carbon Fiber Reinforced Laminate in Terms of Vibroacoustic Performance and Flammability. Materials 12.

Baudelet, P.H., Ricochon, G., Linder, M., Muniglia, L., 2017. A new insight into cell walls of Chlorophyta. Algal Res 25, 333-371.

Bjorkland, R., Tobias, D., Petersen, E.J., 2017. Increasing evidence indicates low bioaccumulation of carbon nanotubes. Environ Sci Nano 4, 747-766.

Cano, A.M., Maul, J.D., Saed, M., Irin, F., Shah, S.A., Green, M.J., French, A.D., Klein, D.M., Crago, J., Canas-Carrell, J.E., 2018. Trophic Transfer and Accumulation of Multiwalled Carbon Nanotubes in the Presence of Copper Ions in Daphnia magna and Fathead Minnow (Pimephales promelas). Environ Sci Technol 52, 794-800.

Cano, A.M., Maul, J.D., Saed, M., Shah, S.A., Green, M.J., Canas-Carrell, J.E., 2017. Bioaccumulation, stress, and swimming impairment in Daphnia magna exposed to multiwalled carbon nanotubes, graphene, and graphene oxide. Environ Toxicol Chem.

Chen, K.L., Smith, B.A., Ball, W.P., Fairbrother, D.H., 2010. Assessing the colloidal properties of engineered nanoparticles in water: case studies from fullerene C-60 nanoparticles and carbon nanotubes. Environ Chem 7, 10-27.

Connel, D.W., 1998. Bioaccumulation of chemicals by aquatic organisms. in: Schüürmann, G., Markert, B. (Eds.). Ecotoxicology: ecological fundamentals, chemical exposure, and biological effects. John Wiley & Sons Inc., New York, USA, and Spektrum Akademischer Verlag, Heidelberg, Germany, pp. 439-450.

Ebert, D., 2005. Ecology, Epidemiology, and Evolution of Parasitism in Daphnia [Internet]. National Library of Medicine (US), National Center for Biotechnology Information, Bethesda (MD).

Edgington, A.J., Petersen, E.J., Herzing, A.A., Podila, R., Rao, A., Klaine, S.J., 2014. Microscopic investigation of single-wall carbon nanotube uptake by Daphnia magna. Nanotoxicology 8 Suppl 1, 2-10.

Edgington, A.J., Roberts, A.P., Taylor, L.M., Alloy, M.M., Reppert, J., Rao, A.M., Mao, J.D., Klaine, S.J., 2010. The Influence of Natural Organic Matter on the Toxicity of Multiwalled Carbon Nanotubes. Environmental Toxicology and Chemistry 29, 2511-2518.

Fawley, M.W., Dean, M.L., Dimmer, S.K., Fawley, K.P., 2006. Evaluating the morphospecies concept in the Selenastraceae (Chlorophyceae, Chlorophyta). J Phycol 42, 142-154.

Fox, H.M., 1952. Anal and Oral Intake of Water by Crustacea. J Exp Biol 29, 583-599.

Gerritsen, A., van der Hoeven, N., Pielaat, A., 1998. The acute toxicity of selected alkylphenols to young and adult Daphnia magna. Ecotoxicol Environ Saf 39, 227-232.

Gillis, P.L., Chow-Fraser, P., Ranville, J.F., Ross, P.E., Wood, C.M., 2005. Daphnia need to be gut-cleared too: the effect of exposure to and ingestion of metal-contaminated sediment on the gut-clearance patterns of D. magna. Aquat Toxicol 71, 143-154.

Glomstad, B., Zindler, F., Jenssen, B.M., Booth, A.M., 2018. Dispersibility and dispersion stability of carbon nanotubes in synthetic aquatic growth media and natural freshwater. Chemosphere 201, 269-277.

Gobas, F.A., de Wolf, W., Burkhard, L.P., Verbruggen, E., Plotzke, K., 2009. Revisiting bioaccumulation criteria for POPs and PBT assessments. Integr Environ Assess Manag 5, 624-637.

Gottschalk, F., Nowack, B., 2011. The release of engineered nanomaterials to the environment. J Environ Monitor 13, 1145-1155.

Gottschalk, F., Sonderer, T., Scholz, R.W., Nowack, B., 2009. Modeled environmental concentrations of engineered nanomaterials (TiO(2), ZnO, Ag, CNT, Fullerenes) for different regions. Environ Sci Technol 43, 9216-9222.

Guo, X., Dong, S., Petersen, E.J., Gao, S., Huang, Q., Mao, L., 2013. Biological uptake and depuration of radio-labeled graphene by Daphnia magna. Environ Sci Technol 47, 12524-12531.

Hammers-Wirtz, M., Ratte, H.T., 2003. Erstellung eines Gutachtens zur Entwicklung eines Verfahrensvorschlages für einen Daphnia Multi Generation Test. Federal Environmental Agency Germany.

Hennig, M.P., Maes, H.M., Ottermanns, R., Schaffer, A., Siebers, N., 2019. Release of radiolabeled multi-walled carbon nanotubes (C-14-MWCNT) from epoxy nanocomposites into quartz sand-water systems and their uptake by Lumbriculus variegatus. Nanoimpact 14.

Holden, P.A., Gardea-Torresdey, J.L., Klaessig, F., Turco, R.F., Mortimer, M., Hund-Rinke, K., Cohen Hubal, E.A., Avery, D., Barcelo, D., Behra, R., Cohen, Y., Deydier-Stephan, L., Ferguson, P.L., Fernandes, T.F., Herr Harthorn, B., Henderson, W.M., Hoke, R.A., Hristozov, D., Johnston, J.M., Kane, A.B., Kapustka, L., Keller, A.A., Lenihan, H.S., Lovell, W., Murphy, C.J., Nisbet, R.M., Petersen, E.J., Salinas, E.R., Scheringer, M., Sharma, M., Speed, D.E., Sultan, Y., Westerhoff, P., White, J.C., Wiesner, M.R., Wong, E.M., Xing, B., Steele Horan, M., Godwin, H.A., Nel, A.E., 2016. Considerations of Environmentally Relevant Test Conditions for Improved Evaluation of Ecological Hazards of Engineered Nanomaterials. Environ Sci Technol 50, 6124-6145.

Hou, W.C., Beigzadehmilani, S., Jafvert, C.T., Zepp, R.G., 2014. Photoreactivity of unfunctionalized single-wall carbon nanotubes involving hydroxyl radical: chiral dependency and surface coating effect. Environ Sci Technol 48, 3875-3882.

Hyung, H., Fortner, J.D., Hughes, J.B., Kim, J.H., 2007. Natural organic matter stabilizes carbon nanotubes in the aqueous phase. Environmental Science & Technology 41, 179-184.

Iijima, S., 1991. Helical Microtubules of Graphitic Carbon. Nature 354, 56-58.

Jackson, P., Jacobsen, N.R., Baun, A., Birkedal, R., Kuhnel, D., Jensen, K.A., Vogel, U., Wallin, H., 2013. Bioaccumulation and ecotoxicity of carbon nanotubes. Chem Cent J 7, 154.

Kennedy, A.J., Hull, M.S., Steevens, J.A., Dontsova, K.M., Chappell, M.A., Gunter, J.C., Weiss, C.A., Jr., 2008. Factors influencing the partitioning and toxicity of nanotubes in the aquatic environment. Environ Toxicol Chem 27, 1932-1941.

Kiefer, E., Sigg, L., Schosseler, P., 1997. Chemical and spectroscopic characterization of algae surfaces. Environmental Science & Technology 31, 759-764.

Klaine, S.J., Alvarez, P.J., Batley, G.E., Fernandes, T.F., Handy, R.D., Lyon, D.Y., Mahendra, S., McLaughlin, M.J., Lead, J.R., 2008. Nanomaterials in the environment: behavior, fate, bioavailability, and effects. Environ Toxicol Chem 27, 1825-1851.

Kuhl, A., Lorenzen, H., 1964. Handling and Culturing of Chlorella. in: Prescott, D.M. (Ed.). Methods in Cell Physiology. Academic Press; NEW YORK and London.

KunststoffWeb, 2020. Ocsial: Erweiterte Produktion von Kohlenstoff-Nanoröhrchen. Kunststoff Information, Bad Homburg. https://www.kunststoffweb.de/branchen-news/ocsial_erweiterte_produ

ktion_von_kohlenstoff-nanoroehrchen_t244537. Released: 02/28/2020; Retrieved: 09/17/2020, 10:05 am.

Long, Z., Ji, J., Yang, K., Lin, D., Wu, F., 2012. Systematic and quantitative investigation of the mechanism of carbon nanotubes' toxicity toward algae. Environ Sci Technol 46, 8458-8466.

Lovern, S.B., Owen, H.A., Klaper, R., 2008. Electron microscopy of gold nanoparticle intake in the gut of Daphnia magna. Nanotoxicology 2, 43-48.

Lynch, M., 1978. Complex Interactions between Natural Coexploiters Daphnia and Ceriodaphnia. Ecology 59, 552-564.

Maes, H.M., Stibany, F., Giefers, S., Daniels, B., Deutschmann, B., Baumgartner, W., Schaffer, A., 2014. Accumulation and distribution of multiwalled carbon nanotubes in zebrafish (Danio rerio). Environ Sci Technol 48, 12256-12264.

Mauter, M.S., Elimelech, M., 2008. Environmental applications of carbon-based nanomaterials. Environ Sci Technol 42, 5843-5859.

Miao, A.J., Schwehr, K.A., Xu, C., Zhang, S.J., Luo, Z., Quigg, A., Santschi, P.H., 2009. The algal toxicity of silver engineered nanoparticles and detoxification by exopolymeric substances. Environ Pollut 157, 3034-3041.

Mitrano, D.M., Motellier, S., Clavaguera, S., Nowack, B., 2015. Review of nanomaterial aging and transformations through the life cycle of nano-enhanced products. Environment International 77, 132-147.

Mortimer, M., Petersen, E.J., Buchholz, B.A., Orias, E., Holden, P.A., 2016. Bioaccumulation of Multiwall Carbon Nanotubes in Tetrahymena thermophila by Direct Feeding or Trophic Transfer. Environ Sci Technol 50, 8876-8885.

Naasz, S., Altenburger, R., Kuhnel, D., 2018. Environmental mixtures of nanomaterials and chemicals: The Trojan-horse phenomenon and its relevance for ecotoxicity. Sci Total Environ 635, 1170-1181.

Newland, B., Taplan, C., Pette, D., Friedrichs, J., Steinhart, M., Wang, W., Voit, B., Seib, F.P., Werner, C., 2018. Soft and flexible poly(ethylene glycol) nanotubes for local drug delivery. Nanoscale 10, 8413-8421.

OCSIAL, 2020. About us. OCSIAL, Leudelange, Luxembourg. https://ocsial.com/about/. Retrieved: 09/17/2020, 10:23 am.

OECD, 2004. Test No. 202: *Daphnia sp.*, Acute Immobilisation Test.

Parks, A.N., Portis, L.M., Schierz, P.A., Washburn, K.M., Perron, M.M., Burgess, R.M., Ho, K.T., Chandler, G.T., Ferguson, P.L., 2013. Bioaccumulation and toxicity of single-walled carbon nanotubes to benthic organisms at the base of the marine food chain. Environ Toxicol Chem 32, 1270-1277.

Petersen, E.J., Akkanen, J., Kukkonen, J.V., Weber, W.J., Jr., 2009. Biological uptake and depuration of carbon nanotubes by Daphnia magna. Environ Sci Technol 43, 2969-2975.

Petersen, E.J., Pinto, R.A., Mai, D.J., Landrum, P.F., Weber, W.J., Jr., 2011. Influence of polyethyleneimine graftings of multi-walled carbon nanotubes on their accumulation and elimination by and toxicity to Daphnia magna. Environ Sci Technol 45, 1133-1138.

Petersen, E.J., Lam, T., Gorham, J.M., Scott, K.C., Long, C.J., Stanley, D., Sharma, R., Liddle, J.A., Pellegrin, B., Nguyen, T., 2014. Methods to assess the impact of UV irradiation on the surface chemistry and structure of multiwall carbon nanotube epoxy nanocomposites. Carbon 69, 194-205.

Praetorius, A., Tufenkji, N., Goss, K.-U., Scheringer, M., von der Kammer, F., Elimelech, M., 2014. The road to nowhere: equilibrium partition coefficients for nanoparticles. Environmental Science: Nano 1, 317-323.

Preuss, T.G., Hammers-Wirtz, M., Hommen, U., Rubach, M.N., Ratte, H.T., 2009. Development and validatlion of an individual based Daphnia magna population model: The influence of crowding on population dynamics. Ecol Model 220, 310-329.

Preuss, T.G., Hammers-Wirtz, M., Ratte, H.T., 2010. The potential of individual based population models to extrapolate effects measured at standardized test conditions to relevant environmental conditions--an example for 3,4-dichloroaniline on Daphnia magna. J Environ Monit 12, 2070-2079.

Rhiem, S., Riding, M.J., Baumgartner, W., Martin, F.L., Semple, K.T., Jones, K.C., Schaffer, A., Maes, H.M., 2015. Interactions of multiwalled carbon nanotubes with algal cells: quantification of association, visualization of uptake, and measurement of alterations in the composition of cells. Environ Pollut 196, 431-439.

Roberts, A.P., Mount, A.S., Seda, B., Souther, J., Qiao, R., Lin, S., Ke, P.C., Rao, A.M., Klaine, S.J., 2007. In vivo biomodification of lipid-coated carbon nanotubes by Daphnia magna. Environ Sci Technol 41, 3025-3029.

Roco, M.C., 2011. The long view of nanotechnology development: the National Nanotechnology Initiative at 10 years (vol 13, pg 427, 2011). J Nanopart Res 13, 1335-1335.

SAG Göttingen University (Culture Collection of Algae), 2013. BG 11 Medium for Cyanobacteria. http://sagdb.uni-goettingen.de/culture_media/20%20BG11%20Medium.pdf. Retrieved 11/18/2020; 15:32 pm.

Saleh, N.B., Pfefferle, L.D., Elimelech, M., 2008. Aggregation kinetics of multiwalled carbon nanotubes in aquatic systems: measurements and environmental implications. Environ Sci Technol 42, 7963-7969.

Sarma, S.J., Bhattacharya, I., Brar, S.K., Tyagi, R.D., Surampalli, R.Y., 2015. Carbon Nanotube-Bioaccumulation and Recent Advances in Environmental Monitoring. Crit Rev Env Sci Tec 45, 905-938.

Schierz, A., Espinasse, B., Wiesner, M.R., Bisesi, J.H., Sabo-Attwood, T., Ferguson, P.L., 2014. Fate of single walled carbon nanotubes in wetland ecosystems. Environ-Sci Nano 1, 574-583.

Schlagenhauf, L., Buerki-Thurnherr, T., Kuo, Y.Y., Wichser, A., Nuesch, F., Wick, P., Wang, J., 2015. Carbon Nanotubes Released from an Epoxy-Based Nanocomposite: Quantification and Particle Toxicity. Environ Sci Technol 49, 10616-10623.

Schwab, F., Bucheli, T.D., Lukhele, L.P., Magrez, A., Nowack, B., Sigg, L., Knauer, K., 2011. Are carbon nanotube effects on green algae caused by shading and agglomeration? Environ Sci Technol 45, 6136-6144.

Sijm, D.T.H.M., Broersen, K.W., de Roode, D.F., Mayer, P., 1998. Bioconcentration kinetics of hydrophobic chemicals in different densities of Chlorella pyrenoidosa. Environmental Toxicology and Chemistry 17, 1695-1704.

Tervonen, K., Waissi, G., Petersen, E.J., Akkanen, J., Kukkonen, J.V., 2010. Analysis of fullerene-C60 and kinetic measurements for its accumulation and depuration in Daphnia magna. Environ Toxicol Chem 29, 1072-1078.

Thauer, E., Ottmann, A., Schneider, P., Moller, L., Deeg, L., Zeus, R., Wilhelmi, F., Schlestein, L., Neef, C., Ghunaim, R., Gellesch, M., Nowka, C., Scholz, M., Haft, M., Wurmehl, S., Wenelska, K., Mijowska, E., Kapoor, A., Bajpai, A., Hampel, S., Klingeler, R., 2020. Filled Carbon Nanotubes as Anode Materials for Lithium-Ion Batteries. Molecules 25.

Tsai, S.J., Hofmann, M., Hallock, M., Ada, E., Kong, J., Ellenbecker, M., 2009. Characterization and Evaluation of Nanoparticle Release during the Synthesis of Single-Walled and Multiwalled Carbon Nanotubes by Chemical Vapor Deposition. Environmental Science & Technology 43, 6017-6023.

Verdugo, P., Alldredge, A., Azam, F., Kirchman, D., Passow, U., Santschi, P., 2004. The oceanic gel phase: A bridge in the DOM-POM continuum. Mar Chem 92, 67-85.

Wei, L., Thakkar, M., Chen, Y., Ntim, S.A., Mitra, S., Zhang, X., 2010. Cytotoxicity effects of water dispersible oxidized multiwalled carbon nanotubes on marine alga, Dunaliella tertiolecta. Aquat Toxicol 100, 194-201.

Wohlleben, W., Meier, M.W., Vogel, S., Landsiedel, R., Cox, G., Hirth, S., Tomovic, Z., 2013. Elastic CNT-polyurethane nanocomposite: synthesis, performance and assessment of fragments released during use. Nanoscale 5, 369-380.

Xiao, R., Zheng, Y., 2016. Overview of microalgal extracellular polymeric substances (EPS) and their applications. Biotechnol Adv 34, 1225-1244.

Yeganeh, B., Kull, C.M., Hull, M.S., Marr, L.C., 2008. Characterization of airborne particles during production of carbonaceous nanomaterials. Environ Sci Technol 42, 4600-4606.

Zaib, Q., Aina, O.D., Ahmad, F., 2014. Using multi-walled carbon nanotubes (MWNTs) for oilfield produced water treatment with environmentally acceptable endpoints. Environ Sci Process Impacts 16, 2039-2047.

Zhang, L., Petersen, E.J., Habteselassie, M.Y., Mao, L., Huang, Q., 2013a. Degradation of multiwall carbon nanotubes by bacteria. Environ Pollut 181, 335-339.

Zhang, L., Petersen, E.J., Zhang, W., Chen, Y., Cabrera, M., Huang, Q., 2012. Interactions of 14C-labeled multi-walled carbon nanotubes with soil minerals in water. Environ Pollut 166, 75-81.

Zheng, S., Zhou, Q., Chen, C., Yang, F., Cai, Z., Li, D., Geng, Q., Feng, Y., Wang, H., 2019. Role of extracellular polymeric substances on the behavior and toxicity of silver nanoparticles and ions to green algae Chlorella vulgaris. Sci Total Environ 660, 1182-1190.

Zhou, L., Zhu, D., Zhang, S., Pan, B., 2015. A settling curve modeling method for quantitative description of the dispersion stability of carbon nanotubes in aquatic environments. J Environ Sci (China) 29, 1-10.

Zhu, B., Zhu, S., Li, J., Hui, X., Wang, G.X., 2018. The developmental toxicity, bioaccumulation and distribution of oxidized single walled carbon nanotubes in Artemia salina. Toxicol Res (Camb) 7, 897-906.

Zhu, Y., Zhao, Q.F., Li, Y.G., Cai, X.Q., Li, W., 2006. The interaction and toxicity of multi-walled carbon nanotubes with Stylonychia mytilus. J Nanosci Nanotechno 6, 1357-1364.

4 First quantitative study on accumulation of weathered multi-walled carbon nanotubes in zebrafish *Danio rerio* under simulated environmental conditions

4.1 Summary

Carbon nanotubes (CNT), due to their unique properties, have a wide range of applications in various fields, from their use as nanofillers in nanocomposites to the transmission of drugs in medicine. During production and disposal of nanomaterials, particles are released into the environment where they have an impact on the local fauna and flora. In an aquatic ecosystem, organisms from the first to the top trophic level can be affected. To address this concern, we investigated the accumulation of ^{14}C-labeled weathered multi-walled CNT (^{14}C-wMWCNT) in *Danio rerio* in microcosm experiments. The uptake of 0.1 mg ^{14}C-wMWCNT L^{-1} in *D. rerio* was determined over a period of two weeks via water phase exposure. The mean uptake over time in the whole fish was 91 µg wMWCNT g^{-1} dw^{-1}, with a major part (> 50%) of the CNT uptake being localized in the gastrointestinal tract. The calculated bioaccumulation factor (BAF) was 851 L kg^{-1}. Elimination of accumulated wMWCNT over time was observed as well. The animals were fed twice daily, which facilitated the excretion of the nanomaterials, leading to a body burden at the end of the elimination phase of 1.9 ± 1.3 µg wMWCNT g^{-1} dw^{-1}. A second experiment was performed by exposing *D. rerio* to a ^{14}C-wMWCNT loaded population from *Daphnia magna* and a single water phase exposure of 0.1 mg ^{14}C-wMWCNT L^{-1}. In the test period of 96 h a mean wMWCNT body burden for the zebrafish of 96 µg wMWCNT g^{-1} dw^{-1} was measured. Likewise, the wMWCNT accumulated mostly in the gastrointestinal tract (> 80%), which indicates that the uptake of the nanomaterials occurs mainly via the alimentary system.

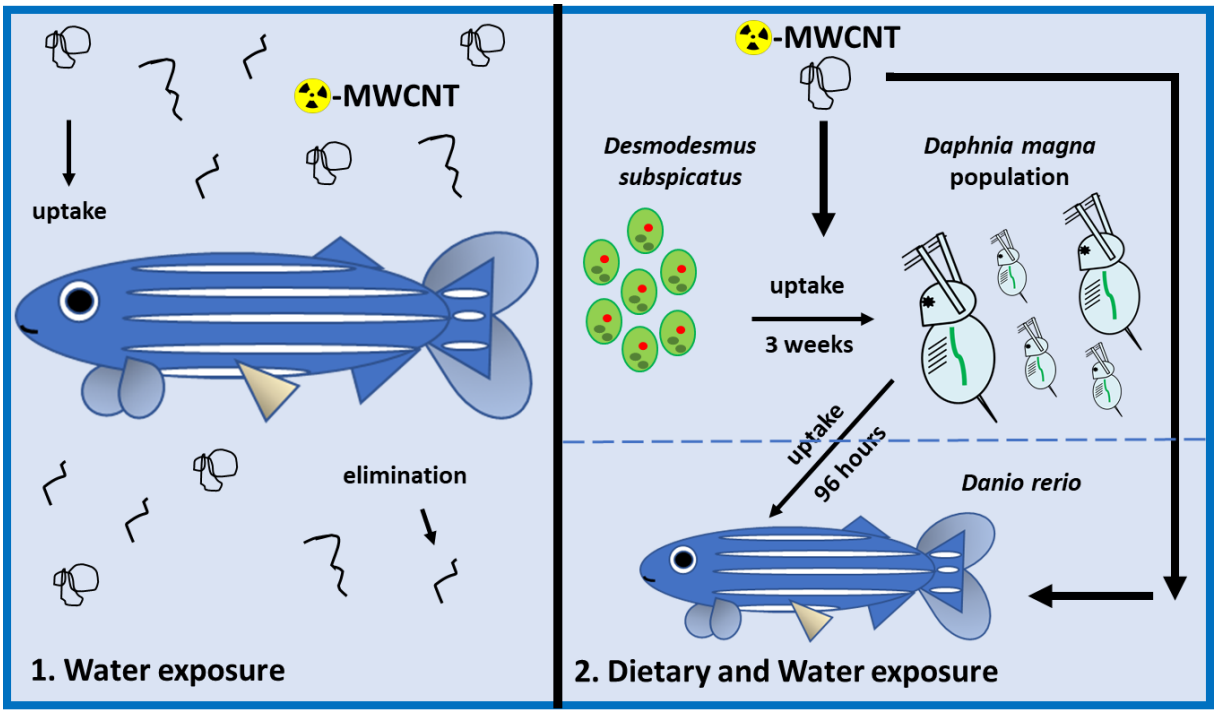

Figure 4.1: Graphical summary of chapter 4.

4.2 Introduction

Since their discovery in 1991 (Iijima, 1991), carbon nanotubes (CNT) have been the focus of research and industrial applications. The nanomaterials are known for their outstanding physicochemical properties, which is why CNT are used in various nanotechnology fields, such as nanocomposites, electronics, energy storage and others (Klaine et al., 2008; Jia and Wei, 2017; Campos et al., 2019). Due to their widespread application, an increased CNT production can be assumed. CNT are mostly supplied to the consumer market in fixed form in materials. Subsequently, modelling of the fate of engineered nanomaterials (ENM) has shown that in Europe the path of the product mainly leads via the waste incineration plant and landfill to elimination. As a result, the estimated concentration for CNT in surface waters is in the ng L^{-1} range and for sediments a yearly increase in the µg kg^{-1} range is predicted. The CNT concentration in water bodies might increase if further applications will be established, like the use of nanomaterials in pesticides (Kah et al., 2018). Additionally, the release of ENM into the atmosphere is classified as low, and rapid deposition from the air to soil and water bodies is suspected (Gottschalk et al., 2009; Sun et al., 2014). Here, we focus on the exposure of the aquatic environment to CNT and their accumulation in fish.

For the ecotoxicological evaluation of the risk of CNT, investigations are carried out about persistence, bioaccumulation and toxicity. The second area is very controversial regarding engineered nanomaterials, since the test methods used so far are adapted to the properties of soluble organic chemicals and not to nanomaterials such as CNT (Jackson et al., 2013; Bjorkland et al., 2017). Due to their material nature, the latter behave differently from classical chemicals, as a result, the conventional bioaccumulation model must be adapted.

Some studies on the uptake of carbon based nanomaterials (C-NM) in freshwater invertebrates and vertebrates have been carried out so far. Roberts et al. (2007) found out, that after the ingestion of lipid coated single walled CNT, *Daphnia magna* egested the precipitated nanotubes and was able to utilize the lipid coating as food source. In a study of Tervonen et al. (2010) large agglomerates of fullerenes were detected in the gut of *D. magna* after uptake. Further the bioaccumulation of MWCNT in *Lumbriculus variegatus* (Petersen et al., 2008) and *D. magna* (Petersen et al., 2009; Petersen et al., 2011) has been quantified. In fathead minnow, a low bioaccumulation of MWCNT (0.04 to 0.81 µg g^{-1}) after trophic transfer was observed (Cano et al., 2018). It seems that C-NM accumulation takes place almost entirely via the gastrointestinal tract, resulting in subsequent elimination, which is facilitated by the addition of food (Kennedy et al., 2008; Petersen et al., 2009; Bisesi et al., 2014; Maes et al., 2014; Shi et al., 2020). Zhang et al. (2015) showed the complete removal of iron oxide nanomaterial as well from zebrafish *Danio rerio*. In literature, no absorption of CNT across the gut epithelium after uptake was observed (Petersen et al., 2009; Jackson et al., 2013; Parks et al., 2013; Bjorkland et al.,

2017). Only very low levels of CNT distribution to organs across the gut lining were detected for the larvae of *Drosophila melanogaster* and the zebrafish (Leeuw et al., 2007; Maes et al., 2014). The uptake and distribution of CNT in different compartments of *D. rerio* has already been investigated and quantified as well (Maes et al., 2014). However, the previous investigations were carried out with individually kept animals. Additionally, trophic transfer of C-NM along the aquatic food chain remains the subject of current research. In a recent study the transfer of ^{13}C labeled fullerenols from *D. magna* to zebrafish was demonstrated (Shi et al., 2020). It therefore remains unclear how and to what extent CNT are adsorbed by fish in a near-natural microcosm.

In our study, we examined the uptake of ^{14}C labeled CNT in freshwater microcosm experiments with the zebrafish *D. rerio*. One test group included 30 individuals which were exposed equally to the nanomaterials. The uptake was investigated over a period of two weeks, a subsequent elimination was examined as well. In addition, *D. rerio* was exposed to CNT-loaded *D. magna* and water dispersed CNT at the same time. For this experiment, a *D. magna* population was cultivated for three weeks with a weekly application of 0.1 mg ^{14}C-wMWCNT L^{-1}. Working on a larger scale than in previously published studies, we aimed to obtain more environmentally relevant results.

4.3 Materials and methods

4.3.1 Synthesis and purification of ^{14}C-labeled MWCNT (^{14}C-MWCNT)

For a detailed description of synthesis of ^{14}C-MWCNT see section 2.3.1 in chapter 2.

4.3.2 Weathering of nanomaterials

For weathering and characterization of MWCNT see section 2.3.2 in chapter 2.

4.3.3 Test organisms

Green algae *Desmodesmus subspicatus* was obtained from SAG Göttingen (strain no. 86.81). Cultures of algae were kept in Kuhl and Lorenzen (1964) medium at 20 ± 2 °C with permanent aeration and constant illumination. Renewal of medium was performed every two weeks. To avoid the loss of liquid by evaporation, the round bottom flasks were covered with a stopper composed of cotton wool. Crustacean *Daphnia magna* (Straus) were cultured in M4 medium (OECD, 2004) (20 ± 2 °C, 16 h dark/8 h light photoperiod). Daphnids were fed three times a week from a culture of the green alga *Desmodesmus subspicatus*. In addition, *Daphnia* was fed yeast once a week during medium renewal. The zebrafish *Danio rerio* were acclimated for two months in an in-house keeping site before test start. Fish were fed with commercially available food flakes (Tetra Min®) in the morning and with rinsed brine shrimp nauplii (*Artemia salina*) in the evening. For more details see supplementary information (SI) at 4.7.1.

4.3.4 Experimental Setup

4.3.4.1 Microcosm study I: uptake and elimination of wMWCNT by zebrafish *D. rerio*

The required volume of fish water was prepared and aerated at least 24 hours before use. For the test start, two aquariums were filled with 45 L fish water each. Each aquarium was marked for the filling level, so that possible losses through evaporation could be filled up with distilled water. The fish water was composed as follows: 294 mg L^{-1} $CaCl_2 \times 2H_2O$, 123.3 mg L^{-1} $MgSO_4 \times 7H_2O$, 63 mg L^{-1} $NaHCO_3$, 5.5 mg L^{-1} KCl in distilled water. To obtain a concentration of 100 µg ^{14}C-wMWCNT L^{-1}, two times 4.5 mg ^{14}C-wMWCNT were weighted out on a microbalance (MYA 5.3Y, Radwag) and filled into a flask containing 250 mL fish water taken out of the respective aquarium. Subsequently, the flasks were put successively into an ice bath and nanomaterials were dispersed by means of ultrasonication with a micro tip for 20 min or until no more agglutinated CNT material was visible (Sonopuls HD 2070, 70 W, pulse: 0.2 s, pause: 0.8 s). Three subsamples of 0.5 mL were drawn, 2 mL of Ultima Gold™ XR scintillation cocktail (Perkin Elmer, Germany) was added, and samples were submitted to LSC (liquid scintillation counter, Hidex SL 600, Hidex, Germany) to verify a homogeneous dispersion of ^{14}C-wMWCNT, respectively. The used dispersion method has already been described before (Rhiem et al., 2015; Hennig et al., 2019). Afterwards, CNT dispersions were added to the respective aquarium (flasks were rinsed using fish water taken out of aquarium before application) and water phase was stirred thoroughly using the glass pipette introduced for aeration. Four aliquots of 1 mL were drawn from each aquarium to check the efficiency on homogenization using LSC. Afterwards 30 fish (male and female) were placed in each of the prepared aquariums (start of exposure). The animals were fed daily in the morning (food flakes, see above) and in the late afternoon (*D. magna*). During the weekends, fish was fed in the morning. The number of *Daphnia* fed corresponded to 1% of the wet weight of a fish. A water change with simultaneous afresh application of ^{14}C-wMWCNT (100 µg L^{-1}) as described above was carried out twice a week. During a water change the animals were transferred as gently as possible from the existing aquarium into the newly prepared aquarium with the aid of a scoop. During exposure, water temperature was kept at 26 ± 1 °C (by means of a heating rod) and light changed in a day to night rhythm of 16 to 8 hours. To prevent animals from jumping out of the tanks, they were covered with glass plates. Water quality monitoring was carried out regularly and the following parameters were checked: temperature, pH value, conductivity and the contents of nitrate, nitrite and ammonium. From one of the two aquariums, six fish each (five animals after 7 d) were sampled after 3 h, 1, 3, 7 and 14 d to examine the accumulation of wMWCNT. Amount of radioactivity was quantified in gills, gastrointestinal tract and the remaining fish carcass. For details on sampling, anesthesia and dissection of the fish see the SI at 4.7.2. The animals in the second aquarium were exposed to wMWCNT for 14 days and then rinsed and transferred to an aquarium with fish water not containing wMWCNT (Fig. 4.2). After 2, 6, 24, 48 and 96 h, six fish were removed and the elimination

of CNT by the fish was determined. Sampling, anesthesia and dissection of the fish was performed as described above.

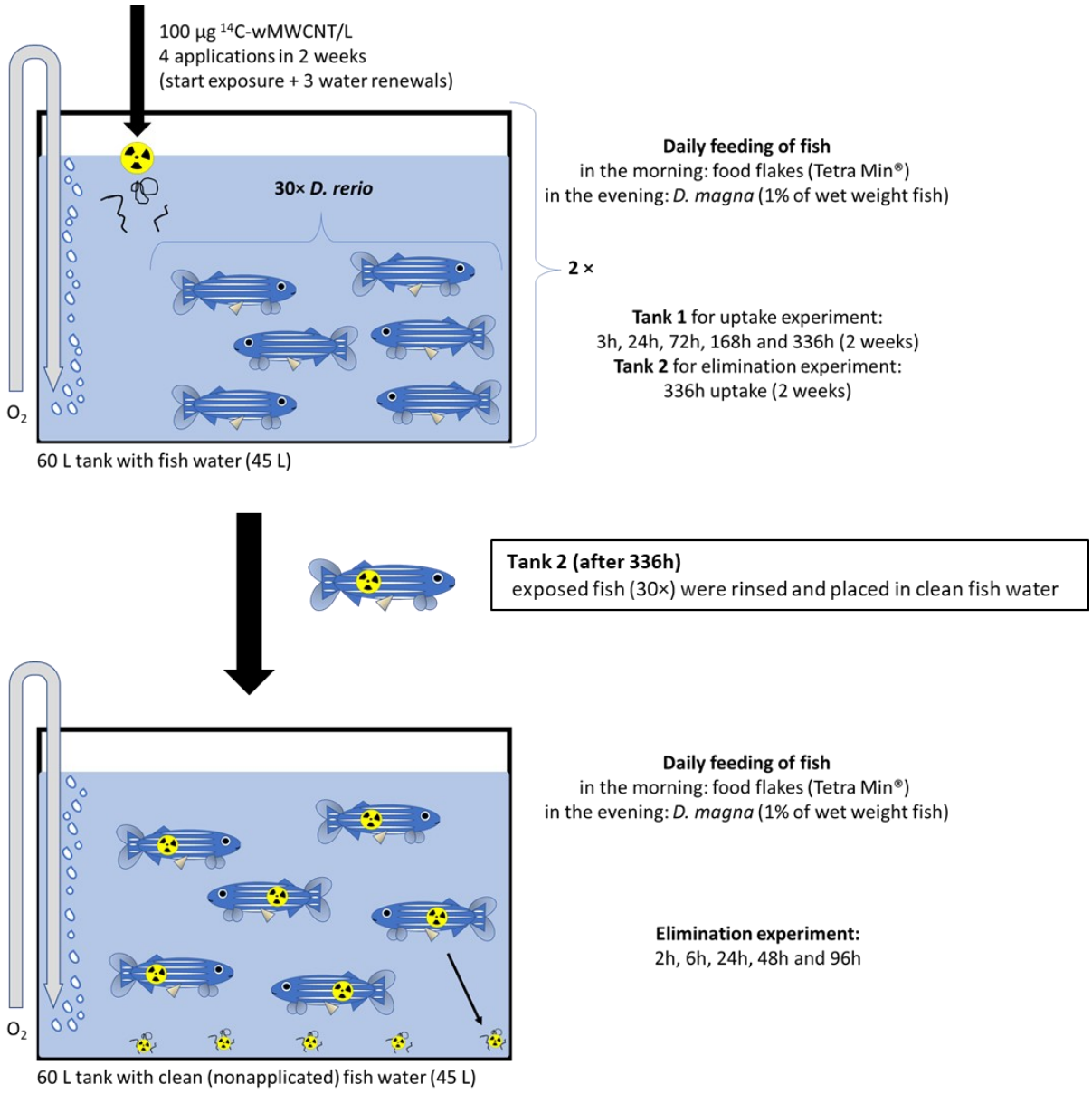

Figure 4.2: Experimental setup for uptake and elimination of wMWCNT by zebrafish *Danio rerio* (microcosm study I).

4.3.4.2 Microcosm study II: bioaccumulation of wMWCNT by *D. rerio* (trophic transfer)

A *D. magna* population of 250 neonates (≤ 24 h) and 150 adults (21 to 28 days old) (Agatz et al., 2012) was grown in an aquarium with 45 L M4 medium (OECD, 2004) for 21 days under exposure to ^{14}C-wMWCNT (100 µg L^{-1}). The application (0 h) was performed in M4 medium as described above. The water was changed once a week with renewed application (7 d and 14 d) of ^{14}C-wMWCNT. For water renewal the water phase was first withdrawn via a hose. The end which protruded into the water phase was closed with gauze so that no *Daphnia* was sucked in. After almost all water had been drained and the tank could be tilted, the remaining water phase was filtered through a brine shrimp sieve (mesh

size: 180 µm) to capture all daphnids. The animals were rinsed sufficiently with tap water and transferred to a 5 L cup with fresh M4 medium and stored at 20 °C until the water change was completed.

The daphnids were fed daily with 0.5 mg carbon L^{-1} in the form of the green alga *D. subspicatus*. Population of *D. magna* was kept at 19 ± 2 °C and a day/night light rhythm of 16 to 8 h. The water volume was aerated sufficiently by a glass pipette connected to an air pump. To avoid increased evaporation of liquid, the aquarium was closed with a glass plate. After 21 days the uptake of ^{14}C-wMWCNT in *D. magna* was quantified. For this purpose, five samples of daphnids were taken out of the aquarium, placed successively into a plain glass dish and washed two times extensively with M4 medium and distilled water. Washed animals were then transferred to pre-weighed aluminium boats and dried at 65 °C for 24 h. After determination of dry weight, daphnids were transferred to a micro glass mortar and homogenized using methanol. This way, radioactivity trapped in the animals was released and detected by LSC to avoid a defective quantification due to quenching processes by animal's carapace or compact agglomerated CNT. Afterwards, the crushed animal/methanol mass was transferred to an LSC vial. The micro mortar was cleaned carefully, and methanol used for rinsing was placed in the same scintillation vial. Quantification of accumulated radioactivity in *D. magna* was performed by means of LSC. A body burden of 1.5 ± 0.3 µg wMWCNT mg^{-1} dw^{-1} was found in *D. magna* after 3 weeks of exposure to 100 µg wMWCNT L^{-1} and daily feeding.

On day 21 another water change was performed with the application of 100 µg ^{14}C-wMWCNT L^{-1} (see above) in fish water. Subsequently, the previously sieved daphnids and 0.5 mg C (*D. subspicatus*) L^{-1} and 30 fish (male and female) were placed in the aquarium (start of exposure) (Fig. 4.3). By inserting a hot rod, the temperature for starting the exposure of the fish was set to 26 ± 1 °C, the light rhythm and aeration was performed as for *Daphnia* population. A mark was set for the fill level of 45 L to fill up any evaporation with distilled water. Fish was sampled after 2, 6, 24, 48 and 96 h. Sampling, anesthesia and dissection of the fish was performed as described above.

4.3.5 Quantification of radioactivity

After the dry weight of the individual fragments of each fish was determined, they were transferred individually into 20 mL LSC vials, covered with tissue solubilizer (Soluene-350®, PerkinElmer) and closed vials were incubated for 24 h at 60 °C. At the beginning of the incubation, the samples were swirled regularly (30 min) to achieve a good distribution of the solubilizer around the tissue. After complete dissolution of the biological matrix, the samples were cooled to room temperature and 0.1 mL 35% hydrogen peroxide solution was added for bleaching. Subsequently, 19 mL of scintillation cocktail (see above) was added to the samples with fish debris and 10 mL to the samples with gill, liver and intestine and the radioactivity was measured by LSC.

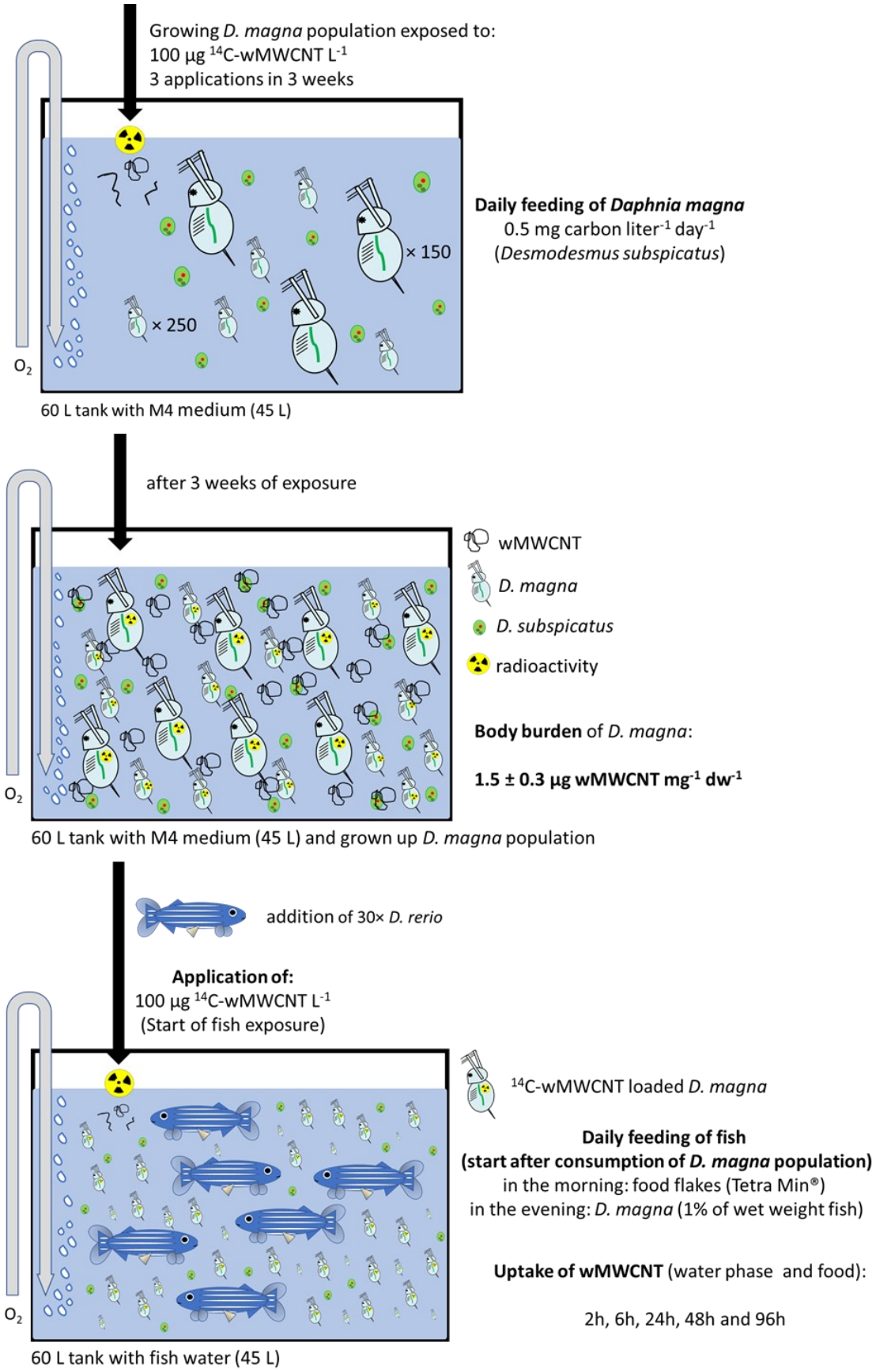

Figure 4.3: Experimental setup for bioaccumulation of wMWCNT by *Danio rerio* (trophic transfer, microcosm study II).

The samples with the fish debris showed a strong yellow coloration (despite bleaching), which predominantly led to a low efficiency (< 50%) and high values in chemiluminescence of the LSC measurement. For this reason and because enough radioactivity was present in the samples, the volume in samples were halved and filled again up to 20 mL with scintillation cocktail. The subsequent measurement of the radioactivity showed values with an efficiency of above 70%. The amount of radioactivity in the gut fraction partially exceeded the linear dynamic range in LSC measurement, so these samples also had to be diluted. It was also noticed that after treatment with the solubilizer as described above, smaller and bigger CNT agglomerates (adhesions of individual CNT strands in the gut of a fish) remained in some samples. Since it is known that the LSC measurement of agglutinations of radioactive material can lead to the extinction of the signals during LSC measurement, the recognizable CNT agglutinations were crushed with the aid of a small spatula. Afterwards, samples were measured another time by means of LSC. The use of an ultrasonic bath to crush the CNT agglomerates was also tested but did not result in the dispersion of the CNT agglomerates. The emptied aluminium boats and petri dishes were cleaned with a tissue soaked in methanol and radioactivity was measured by means of LSC. The burden of the whole fish or individual organs to ^{14}C-wMWCNT was related to the respective dry weight and expressed in the following as µg wMWCNT g^{-1} dw^{-1}.

4.3.6 Data evaluation

Collected data was processed using Microsoft Excel® (Microsoft Office 365 ProPlus) and GraphPad Prism (GraphPad Prism5, USA). Outliers were identified by Dixon's Q test ($\alpha = 0.05$).

4.4 Results

4.4.1 Microcosm study I: uptake of wMWCNT by zebrafish *D. rerio*

In the experiment on the uptake of wMWCNT in zebrafish, it was observed that nanomaterials were taken up or associated with the animal after a short time (Fig. 4.4 - A). However, the replicates showed a large standard deviation and the coefficient of variation (CV%) was between 47% and 180%. A steady state for the uptake of wMWCNT from the water phase was reached after 20 h after the application of a one compartment model. The maximum uptake of wMWCNT in the complete zebrafish was 121 ± 115 µg wMWCNT g^{-1} dw^{-1} fish after 168 h (1 week), i.e., 0.2% (10 µg) of the total amount of CNT present in the aquarium was associated with the fish. The mean wMWCNT content in complete fish was 91 µg wMWCNT g^{-1} dw^{-1} fish over a period from 24 h to 2 weeks (Fig. 4.4 - A, Y2). Since steady state was reached a bioconcentration factor (BCF = C_b/C_w) of 910 L kg^{-1} (91 mg kg^{-1}/0.1 mg L^{-1}) was calculated.

The gastrointestinal tract sampling and its separate measurement demonstrated that most of the absorbed amount of wMWCNT was localized in the intestine (Tab. 4.1 and Tab. 4.4 in the SI) and thus did not correspond to true bioaccumulation. The mean wMWCNT level in the intestine in the uptake

experiment was 1050 µg wMWCNT g^{-1} dw^{-1} and corresponded to > 80% of the total wMWCNT uptake from 72 h on. Large amounts of associated wMWCNT were also detected in the gills and the fish debris, i.e., the fish without gills and gastrointestinal tract (skin, eyes, fins and muscle tissue). As mentioned above, the liver was dissected during sampling and measured separately, but was included in the rest of the fish for reasons of uncertainty in subsequent calculations. The mean wMWCNT concentrations over 2 weeks uptake phase for the gill and fish debris compartments were 65 µg wMWCNT g^{-1} dw^{-1} and 21 µg wMWCNT g^{-1} dw^{-1}, respectively.

4.4.2 Microcosm study I: elimination of wMWCNT by zebrafish *D. rerio*

In the elimination experiment, a release of wMWCNT from the fish into the water phase was already observed after 2 h (Fig. 4.4 - C/D). In the complete fish, the body burden after the 2 week uptake phase amounted to 59 µg wMWCNT g^{-1} dw^{-1} fish and after the tested elimination periods of 2, 6, 24, 48 and 96 h amounted to 5, 6, 9, 5 and 2 µg wMWCNT g^{-1} dw^{1} fish, respectively (see SI, Tab. 4.5). The data set for elimination also showed high standard deviations (with coefficients of variation of 56% to 215%) and a strong variation over time, which is why the model used overestimates the speed of dissociation of the material from the fish. For the complete fish, an elimination rate constant (k_2) of 1.223 h^{-1} (Fig. 4.4 - D), and an uptake rate constant (k_1) of 1042 L kg^{-1} h^{-1} was calculated. The BCF calculated by means of k_1 and k_2 is 852 L kg^{-1}, thus confirming the abovementioned BCF value (C_b/C_w) of 910 L kg^{-1}.

As in the uptake experiment, the accumulated nanomaterials in the elimination experiment were predominantly located in the gastrointestinal tract (Tab. 4.2). Since the animals were fed twice daily in the elimination experiment, excretion was facilitated and the initial wMWCNT load in the gut of 668 µg wMWCNT g^{-1} dw^{-1} fish was reduced by 97% (23 µg wMWCNT g^{-1} dw^{-1} fish) within 96 h. A complete evacuation of the intestine was not observed. The amount of wMWCNT taken up in the gills and fish debris was reduced by > 99% and > 98%, respectively, which shows that the association of wMWCNT in gills and fish debris is reversible. It is assumed that the associated amount of wMWCNT in the fish debris compartment is mainly influenced by the outer surface of the fish.

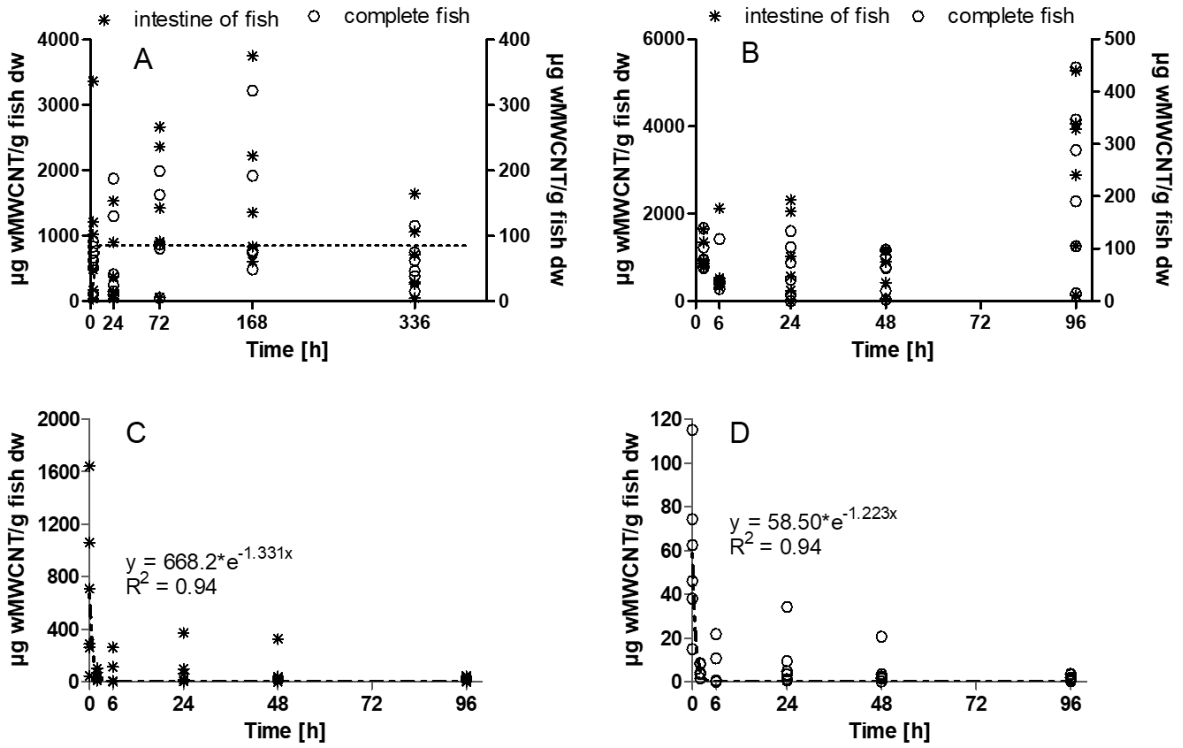

Figure 4.4: Concentration of weathered multi-walled carbon nanotubes (wMWCNT) in zebrafish *Danio rerio* for uptake and elimination scenarios in function of time. (A) Uptake of wMWCNT in digestive tract of zebrafish (asterisks, left Y-axis, Y1) and complete fish (unfilled circles, right Y-axis, Y2) after exposure to 100 µg wMWCNT L^{-1} via water phase. A one compartment model (blue dotted line) is fitted to the data. (B) Uptake of wMWCNT in digestive tract of zebrafish (asterisks, left Y-axis, Y1) and complete fish (unfilled circles, right Y-axis, Y2) after exposure to 100 µg wMWCNT L^{-1} via water phase and to a wMWCNT pre-contaminated population of *Daphnia magna*. (C) Elimination of wMWCNT from digestive tract of zebrafish and (D) from complete fish in clean fish water, after uptake of 100 µg wMWCNT L^{-1} via water phase over two weeks. An exponential model is fitted to data sets from elimination experiment (R^2: coefficient of determination).

4.4.3 Microcosm study II: bioaccumulation of wMWCNT by *D. rerio* (trophic transfer)

As in the uptake study, wMWCNT quickly associated with the zebrafish over time, with the highest levels of wMWCNT being detected in the whole fish and in the gastrointestinal tract of the fish of 232 ± 159 µg wMWCNT g^{-1} dw^{-1} and 2926 ± 1920 µg wMWCNT g^{-1} dw^{-1}, respectively, after 96 h. Again, concentrations varied strongly with coefficients of variation of 33% to 186% (Fig. 4.4 - B). As described above, the largest amounts of wMWCNT accumulated in the gastrointestinal tract, corresponding to more than 82% of the overall uptake after 2 h (Tab. 4.3). In gills and fish debris, the mean wMWCNT level over time was 22 µg wMWCNT g^{-1} dw^{-1} and 9 µg wMWCNT g^{-1} dw^{-1}, respectively (see SI, Tab. 4.6).

Table 4.1: Partitioning of wMWCNT in different compartments of zebrafish (microcosm study I, uptake experiment). *D. rerio* was exposed to 100 µg ^{14}C-wMWCNT L^{-1} in fish water (water phase exposure) over 14 days (336 h). The percentage of the total amount of recovered radioactivity (%) in different compartments of zebrafish is presented. The sum depicts the total amount of wMWCNT associated (ingested or attached) to one single fish and is expressed as wMWCNT in µg. The mean value (Mean) and standard deviation (SD) on six replicates (five replicates after 168 h) is shown.

time (h)	gills (%)	gut (%)	fish debris (%)	sum (µg)
3	5.28	15.47	79.26	3.70
	11.01	49.01	39.99	3.09
	3.71	66.43	29.85	2.96
	15.46	54.74	29.80	4.99
	0.55	96.27	3.18	6.84
	12.40	17.99	69.61	0.29
Mean	8.07	49.99	41.95	3.65
SD	5.75	30.50	28.14	2.19
24	2.30	57.44	40.26	10.02
	3.77	17.61	78.62	0.67
	9.49	32.53	57.98	1.33
	9.52	66.51	23.97	1.12
	0.21	76.49	23.30	4.81
	0.57	48.94	50.50	5.50
Mean	4.31	49.92	45.77	3.91
SD	4.22	21.84	21.26	3.62
72	5.05	74.00	20.95	4.34
	0.25	61.71	38.04	0.42
	0.30	83.80	15.90	5.13
	2.54	79.21	18.25	4.35
	0.64	88.16	11.20	8.14
	0.01	95.26	4.73	15.34
Mean	1.46	80.36	18.18	6.29
SD	1.98	11.70	11.29	5.07
168	0.01	98.79	1.20	4.73
	4.62	80.83	14.56	5.36
	0.69	96.73	2.58	3.30
	2.70	62.68	34.62	10.56
	0.01	96.83	3.16	24.26
Mean	1.61	87.17	11.22	9.64
SD	2.01	15.49	14.13	8.62
336	13.87	73.51	12.62	0.57
	0.04	95.15	4.80	9.12
	0.94	90.38	8.68	5.87
	6.60	78.76	14.64	7.11
	2.45	89.64	7.91	1.25
	18.38	70.21	11.41	2.13
Mean	7.05	82.94	10.01	4.34
SD	7.52	10.18	3.56	3.51

Table 4.2: Partitioning of wMWCNT in different compartments of zebrafish (microcosm study I, elimination experiment). *D. rerio* was exposed to 100 µg ^{14}C-wMWCNT L^{-1} in fish water (water phase exposure) over 14 days, followed by a 96 h depuration period. The percentage of the total amount of recovered radioactivity (%) in different compartments of zebrafish is presented. The sum depicts the total amount of wMWCNT associated to one single fish and is expressed as wMWCNT in µg. The mean value (Mean) and standard deviation (SD) on six replicates is shown.

time (h)	gills (%)	gut (%)	fish debris (%)	sum (µg)
2	0.005	87.26	12.73	0.21
	17.18	50.91	31.90	0.17
	0.07	59.19	40.74	0.23
	0.11	85.57	14.29	0.08
	0.13	98.70	1.17	0.53
	0.52	60.10	39.38	0.45
Mean	3.00	73.62	23.37	0.28
SD	6.95	19.31	16.24	0.17
6	1.49	80.40	18.11	0.004
	0.31	71.06	28.64	0.03
	1.54	92.90	5.56	0.45
	0.85	71.37	27.78	0.05
	0.08	73.95	25.97	1.21
	0.35	12.58	87.07	0.04
Mean	0.77	67.04	32.19	0.30
SD	0.63	27.91	28.25	0.48
24	0.02	85.14	14.83	0.23
	0.01	95.57	4.42	3.10
	1.08	21.40	77.52	0.04
	0.18	6.13	93.69	0.15
	2.08	81.45	16.47	0.08
	0.13	86.97	12.90	0.56
Mean	0.58	62.78	36.64	0.69
SD	0.84	38.55	38.50	1.19
48	2.45	88.40	9.15	0.01
	2.55	96.31	1.14	0.13
	0.02	99.95	0.04	1.71
	0.21	83.67	16.12	0.13
	0.01	99.76	0.23	0.15
Mean	1.03	94.55	4.42	0.30
SD	1.04	93.77	5.18	0.41
96	0.03	99.61	0.36	0.13
	0.26	27.03	72.71	0.03
	0.00	55.97	44.03	0.26
	0.00	80.19	19.81	0.05
	0.65	95.08	4.27	0.12
	0.01	99.30	0.69	0.27
Mean	0.16	76.20	23.65	0.14
SD	0.26	29.26	29.26	0.10

Table 4.3: Partitioning of wMWCNT in different compartments of zebrafish (microcosm study II). *D. rerio* was exposed to 100 µg ^{14}C-wMWCNT L^{-1} in fish water (water phase exposure) over 96 h, whereby the test system additionally contained ^{14}C-wMWCNT pre-exposed *D. magna* of all sizes. The percentage of the total amount of recovered radioactivity (%) in different compartments of zebrafish is presented. The sum depicts the total amount of wMWCNT associated to one single fish and is expressed as wMWCNT in µg. The mean value (Mean) and standard deviation (SD) on six replicates is shown.

time (h)	gills (%)	gut (%)	fish debris (%)	sum (µg)
2	0.20	85.55	14.25	6.82
	0.06	76.58	23.37	6.36
	0.25	98.00	1.75	5.89
	0.25	87.59	12.16	11.38
	0.19	88.23	11.58	4.76
	0.24	84.51	15.26	3.94
Mean	0.20	86.74	13.06	6.53
SD	0.07	6.92	6.98	2.60
6	0.43	94.05	5.52	0.79
	0.29	77.75	21.96	1.66
	0.18	97.85	1.96	1.79
	0.43	67.91	31.66	3.31
	1.15	62.30	36.56	1.80
	0.04	91.41	8.55	7.76
Mean	0.42	81.88	17.70	2.85
SD	0.39	14.76	14.48	2.54
24	1.59	75.10	23.31	2.65
	5.33	45.04	49.63	0.03
	0.23	83.59	16.18	0.53
	0.11	98.89	1.00	3.33
	0.96	96.05	2.99	4.85
	0.02	99.77	0.20	7.77
Mean	1.37	83.07	15.55	3.19
SD	2.03	21.01	19.12	2.87
48	0.90	93.47	5.63	3.79
	4.71	83.92	11.37	0.33
	2.37	93.42	4.21	1.43
	0.58	97.91	1.51	4.16
	0.02	98.79	1.20	5.81
Mean	11.78	85.75	2.47	3.65
SD	3.39	92.21	4.40	3.19
96	0.57	91.94	7.50	30.59
	0.33	94.55	5.12	31.73
	1.46	89.14	9.40	24.82
	0.17	96.63	3.20	12.31
	7.32	53.12	39.55	0.77
	1.43	79.34	19.24	4.70
Mean	1.88	84.12	14.00	17.49
SD	2.72	16.34	13.71	13.40

4.5 Discussion

The complete data set showed large scatter between the individual replicates (cf., Fig. 4.4), since after application, the hydrophobic properties of wMWCNT lead to their agglomeration and consequently to the sedimentation of nanomaterials (Glomstad et al., 2018). This process results in wMWCNT agglomerates of different sizes, which are then taken up by fish of one treatment to varying degrees. We also suspect that the uptake of wMWCNT in an individual fish depends on various parameters, such as size and appetite. Also, other researchers reported large scattering of nanomaterial uptake in fish (Maes et al., 2014; Cano et al., 2018).

A homogeneous distribution of wMWCNT in aqueous solution was confirmed directly after using ultrasonication. Nevertheless, CNT agglomeration in the water phase, turbulence by aeration bubbling and fish movement led to an inhomogeneous distribution of the nanomaterials in the test system (see SI, Fig. 4.5), which further leads to a changed exposure for individual organisms. Also, adding small amounts of CNT homogeneously to large water volumes (here 45 L) is a challenge. However, working with fish, experimental conditions must meet the requirements of the Animal Welfare Act, which asks for a minimum volume per fish.

wMWCNT were mainly absorbed through the gastrointestinal tract, i.e., by swallowing during food intake and drinking as was previously described for MWCNT (Maes et al., 2014). It is known that freshwater fish swallow small amounts of water. Smith et al. (2007) observed the intake of water containing SWCNT and suspected that it was stress-induced drinking. Besides the accumulation in the gastrointestinal tract, wMWCNT accumulated in the gills and fish debris (fish without intestine and gills). Maes et al. (2014) showed that MWCNT accumulate only to a very small extent in muscle tissue. Therefore, we assume that the detected amount of wMWCNT represents mainly skin-associated nanomaterials, already observed at the first sampling times, and with no increase over time.

Because the main mass of wMWCNT is localized in the intestine, excretion depends on the amount of ingested food, which in turn probably depends on the size and appetite of the individual fish. The addition of food facilitates the excretion of nanomaterials enriched in the gut of *D. magna* (Kennedy et al., 2008; Petersen et al., 2009), and a physical clearance process is also suspected in fish (Zhang et al., 2015). In our study, fish were fed twice daily, but no complete excretion of the nanomaterials was observed during the 96 hour elimination phase. Still a percentage of 39% of body burden of fish after uptake phase has been detected in the intestine after elimination unlike in the gills and the fish debris, where the percentage amounted to 0.12% and 0.66% at the end of the elimination phase, respectively. Consequently, the transfer of the fish into fresh uncontaminated water was adequate for the adhering CNT to be rinsed off by the natural water movement. Also, renewing of the mucus layer over time,

which is increased in fish upon stress, may also contribute to the release of the adsorbed nanomaterials (Vatsos et al., 2010; Fernandez-Alacid et al., 2018).

We calculated a bioaccumulation factor (BAF) of 851 L kg^{-1} on dry weight basis for zebrafish in the uptake experiment. This value was calculated as BCF by dividing k_1 and k_2, but since the fish were fed twice a day and consumed the food in contaminated water, bioaccumulation is a more valid term, although the food associated CNT amounts could not be determined. It was also observed that the fish picked up food from the bottom of the aquarium, whereby sedimented wMWCNT agglomerates could have been additionally ingested. This behavior has already been observed before (Myer et al., 2017). Since the data set showed a large variability and the concentration of wMWCNT in the aqueous phase was not constant over time, and since the simplified model is under debate (Bjorkland et al., 2017), the BAF value obtained must be used with caution. The BAF calculated in our study is one order of magnitude higher than the BAF of 73 L kg^{-1} obtained for the uptake of MWCNT in *D. rerio* (Maes et al., 2014), in which the nanomaterial concentration for exposure was 1 mg L^{-1} instead of 0.1 mg L^{-1}. Additionally, the fish were exposed individually in only 500 mL medium compared to our studies with *D. rerio* populations in almost ten times larger volumes of medium (45 L). As one reason for the higher BAF in our study, we assume that the nanomaterial exposure concentrations in the water phase were constant and bioavailable for a longer period. At low concentrations, the probability of interaction of the nanotubes is smaller than at higher concentrations and thus agglomeration and sedimentation rates are reduced. On the other hand, it is conceivable that the fish in our study swallowed more water and therefore ingested more nanomaterials, because they were exposed to stress (due to intraspecific competition and catching events) in addition to the CNT load. The keeping of fish in groups has caused the removal of six fish at a sampling time and the transfer during a water change led to stress for the animals during capture events. Apart from the stressful moments described above, the fish showed a normal swimming behavior.

The body burden of *D. rerio* after the exposure to wMWCNT in the microcosm study II was in the same range as the body burden in the uptake experiment (96 µg wMWCNT g^{-1} dw^{-1}) with no further increase over time. An interesting speculation is that the size of CNT may influence the uptake and body burden of fish. The uptake in feat head minnow via food exposure resulted in body burdens of 0.81 ± 0.19 µg MWCNT g^{-1} and 0.04 ± 0.11 µg MWCNT g^{-1} for MWCNT with a length of 10 to 50 µm (outer diameter: 8 – 15 nm) and 10 to 30 µm (outer diameter: 20 – 30 nm) respectively (Cano et al., 2018). In our study, the fish were exposed simultaneously via food and water phase, with the applied wMWCNT being considerably shorter (≥ 1 µm, outer diameter: 5 – 20 nm). This should be considered in further studies. In the present study, to our knowledge, the uptake of radioactive CNT in *D. rerio*

population was determined for the first time in a microcosm experiment. We showed that various factors have a considerable influence on the test result and require further research.

It is known and already the subject of current research that chemicals adsorb on nanomaterials, hence, can be taken up together with them by aquatic organisms, which can change the effects and the potential for bioaccumulation of the chemicals. It was found, that after uptake, adsorbed fluoranthene to MWCNT was not bioavailable for *P. promelas* and that only the freely dissolved fluoranthene represented the bioavailable fraction (Linard et al., 2015). Another study showed, that bioconcentration factors for diphenhydramine uptake in presence of MWCNT in *P. promelas* increased and indicated that adsorbed diphenhydramine to MWCNT was accumulated by fish (Myer et al., 2017). In the study from Yan et al. (2017) a quick release of roxithromycin from MWCNT in bile salt of crucian carp was observed and therefore an increased bioaccumulation potential was suggested. Based on our results, and the results of Maes et al. (2014), it is likely that the complexes of nanomaterials and chemicals are mainly accumulated in the gastrointestinal tract of the animal, but the chemicals might be as well transferred to other organs as described above.

4.6 Conclusion and outlook

Weathered MWCNT loaded *D. magna* are consumed by *D. rerio* leading to nanomaterial transfer along the food chain. Food chain transfer does not occur in the classical sense, since the nanomaterials, regardless of the species (primary or secondary consumer), are mainly absorbed via the gastrointestinal tract from which the absorbed CNT are subsequently excreted. CNT adhering to filter organs, gills or the skin of fish and daphnids are only a minor burden. It must also be mentioned that the tested CNT concentrations, although lower than in previous studies, are still five orders of magnitude above the expected environmental concentration in the ng L^{-1} range and environmental risk is considered low. It remains to be investigated whether and to what extent the ingested CNT cause long-term damage to the exposed animals.

4.7 Supplementary information (SI)

4.7.1 Test organism

Zebrafish (*Danio rerio*) was purchased on 29th April 2019 from Zoo & Aquarium Bünten GmbH (Rotter Bruch 6, 52068 Aachen) and kept in the keeping site of the Institute for Environmental Research (BioV, Worringer Weg 1, 52074 Aachen). The age of the animals was given with 9 to 12 months. To ensure healthy animals, prior to tests, fish were first treated with a remedy for ornamental fish (eSHa 2000). Fish were held in 2 × 140 L tanks filled with water from an osmosis facility enriched by sodium free sea salt and sodium carbonate. In keeping site, over a week, one-third of water volume is exchanged automatically. Temperature of water phase was set to 26 ± 1 °C and a day to night rhythm of 14 to 10 h was adjusted. All experiments with fish were conducted in accordance with article 8 (1) of the German Animal Welfare Act (TVA no. 30167, reference no. 81-02.04.2018.A391) and with permission of the federal authorities (Ministry for Environment, Agriculture, Conservation and Consumer Protection of the State of North Rhine-Westphalia, Germany, registration number: 81-02.04.2018.A391 2010/63/EU 2010; TvT e.V. 2010).

4.7.2 Sampling, anesthesia and dissection of fish

At each sampling time, six fish were carefully taken one after the other (by random) with a scoop from the respective aquarium. The animal was exposed to as little stress as possible during the procedure. After the successful removal of a fish, it was placed directly into a prepared bath with an overdose of the narcotic benzocaine. To prepare the narcotic working solution, 300 mg of benzocaine (ethyl 4-aminobenzoate, Sigma-Aldrich, product no. 112909, CAS no. 94-09-7) was dissolved in 1 L of fish water and then, while stirring, enough substance was added until precipitation was visible. After numbness, the animals were put to death by decapitation. Immediately prior to decapitation, the test organisms were briefly swabbed (to avoid the falsification of determination of wet weight of fish by remaining water drops on fish skin) with a tissue and the length and weight were noted.

For a complete dissection of the fish, the head was first separated from the rest of the body using a dissection scissor (decapitation). In the next step, the right and left operculum (gill covers) were removed under a microscope and the gills were dissected and placed in a pre-weighed aluminium boat to determine the dry weight at 60 °C. Furthermore, the internal organs were exposed through a superficial incision on the ventral side (from anus to cranial side) of the fish using another clean dissection scissor. Gastrointestinal tract and liver were separated from the remaining tissue and placed in pre-weighed aluminium boats for dry weight determination at 60 °C as well. Care was taken not to damage the organs. The fish used were very small, so the liver could not always be identified and separated from the rest. Because of this uncertainty, the liver was counted as part of the rest of the body in further calculations. The dry weight of the remaining tissue of the fish (fish debris) after

dissection was also determined, therefore fish debris was placed in a pre-weighed small petri dish and dried at 60 °C. In addition, it should be mentioned that the necessary incision from anus to cranial side does not exclude the possibility that small amounts of intestinal contents have reached other compartments and thus increased the amount of recovered radioactivity in these very compartments.

4.7.3 Quantification of ^{14}C-wMWCNT in the water phase in microcosm tanks

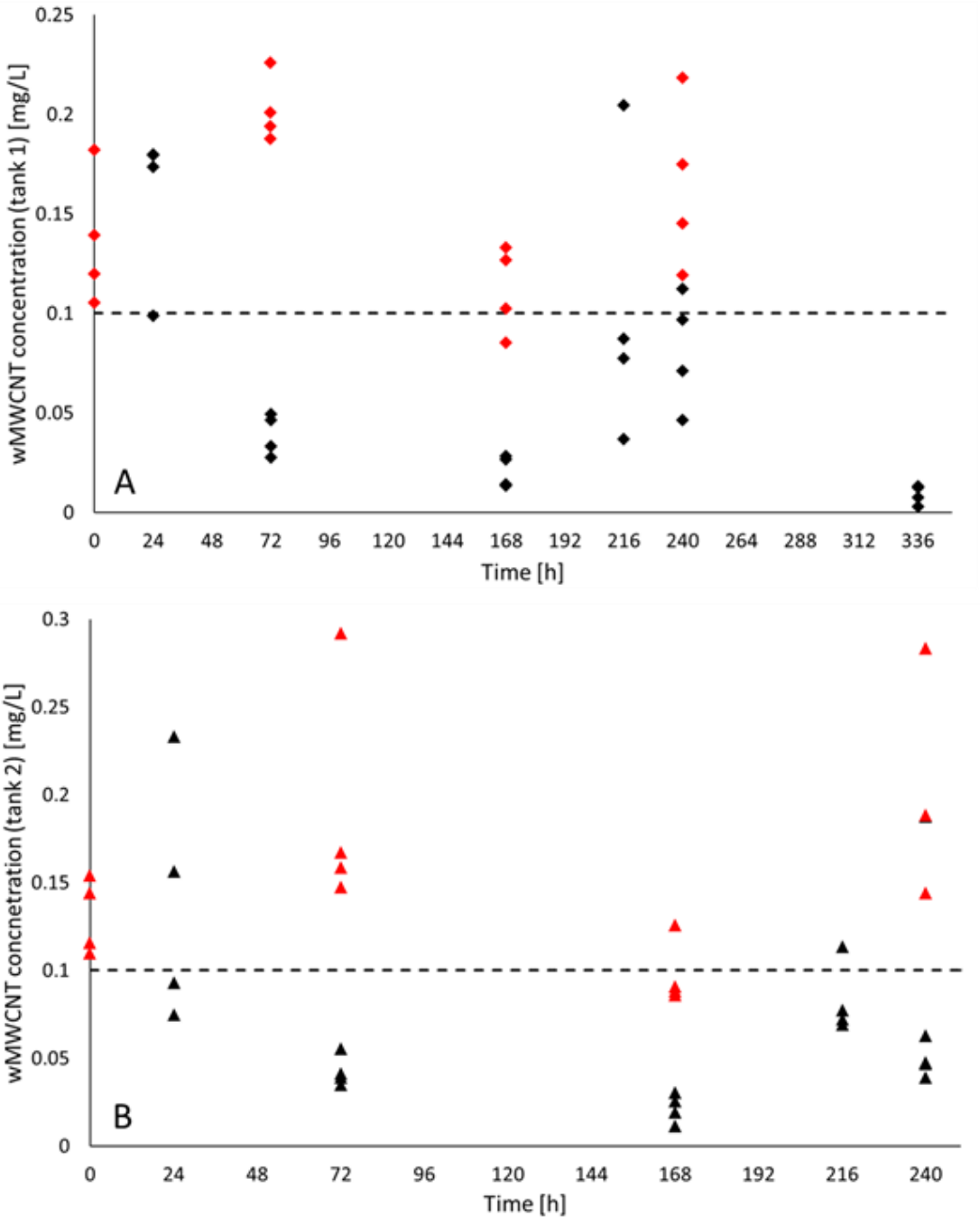

Figure 4.5: Distribution of ^{14}C-wMWCNT in fish water (45 L) after application (0 h) and during test period in the uptake (tank 1 (A)) and elimination experiment (uptake phase, tank 2 (B)). Water renewals and the simultaneous application of 0.1 mg wMWCNT L^{-1} (black dashed line) were performed after 72, 168 and 240 h. On days of the water change the radioactivity in the water phase was measured twice, once before (black triangles) and once after the water change (red triangles). Four replicates were drawn out of one tank.

Table 4.4: Partitioning of wMWCNT in different compartments of zebrafish (microcosm study I, uptake experiment). *D. rerio* (wet weight: 306 ± 79 mg) was exposed to 100 µg ^{14}C-wMWCNT L^{-1} in fish water (waterborne exposure) over 14 days (336 h). The uptake of wMWCNT in different compartments of zebrafish and per complete fish is presented (µg g^{-1} dw^{-1}). The respective dry weight of every single fish is represented (mg). The mean value (Mean) and standard deviation (SD) on six replicates (five replicates after 168 h) is shown.

time (h)	gills (µg g^{-1} dw^{-1})	gut (µg g^{-1} dw^{-1})	fish debris (µg g^{-1} dw^{-1})	complete fish (µg g^{-1} dw^{-1})	dry weight (mg)
3	101.16	171.58	43.94	51.39	72.05
	145.62	481.08	28.12	62.52	49.43
	55.22	3364.74	23.55	73.83	40.06
	252.13	1210.39	27.36	83.65	59.71
	20.93	1019.92	3.27	91.61	74.72
	38.54	34.88	8.20	10.72	27.40
Mean	102.27	1047.10	22.41	62.29	53.89
SD	86.29	1225.59	14.77	29.08	18.50
24	119.04	1532.70	84.49	187.52	53.43
	10.66	35.75	8.07	9.44	71.48
	66.23	98.60	15.91	24.28	54.68
	45.10	149.41	4.08	15.30	73.00
	5.55	374.40	10.66	41.19	116.67
	22.52	898.68	73.23	130.00	42.30
Mean	44.85	514.92	32.74	67.95	68.59
SD	42.83	589.82	36.11	73.44	26.28
72	229.60	2360.91	37.33	162.74	26.64
	0.44	59.86	2.02	4.90	85.81
	6.32	883.49	14.53	80.85	63.49
	50.67	1424.98	16.03	80.35	54.16
	12.18	913.47	11.14	86.65	93.96
	0.43	2665.44	10.58	199.08	77.08
Mean	49.94	1384.69	15.27	102.43	66.86
SD	90.01	982.18	11.85	68.83	24.45
168	0.15	835.55	1.07	77.04	61.34
	68.11	1353.81	11.91	74.11	72.31
	13.12	609.77	1.39	48.37	68.26
	107.79	2221.41	73.96	191.80	55.07
	0.74	3751.08	11.52	322.00	75.33
Mean	37.98	1403.53	27.04	121.34	56.19
SD	48.00	1276.69	30.64	114.54	8.25
336	43.09	44.09	45.09	46.09	72.84
	2.17	1061.17	6.33	115.15	79.24
	15.52	1642.69	7.06	74.35	78.98
	178.57	709.59	10.09	62.55	113.62
	10.88	263.04	1.29	14.91	83.97
	271.56	288.80	4.92	38.02	55.96
Mean	86.97	668.23	12.46	58.51	80.77
SD	111.78	600.56	16.24	34.50	18.83

Table 4.5: Partitioning of wMWCNT in different compartments of zebrafish (microcosm study I, elimination experiment). *D. rerio* (wet weight: 331 ± 60 mg) was exposed to 100 µg ^{14}C-wMWCNT L^{-1} in fish water (waterborne exposure) over 14 days, followed by a 96 h depuration period. The uptake of wMWCNT in different compartments of zebrafish and in complete fish is presented (µg g^{-1} dw^{-1}). The respective dry weight of every single fish is represented (mg). The mean value (Mean) and standard deviation (SD) on six replicates is shown.

time (h)	gills (µg g^{-1} dw^{-1})	gut (µg g^{-1} dw^{-1})	fish debris (µg g^{-1} dw^{-1})	complete fish (µg g^{-1} dw^{-1})	dry weight (mg)
2	0.01	32.68	0.51	3.54	59.07
	16.49	21.20	1.29	3.55	46.71
	0.11	36.10	1.94	4.29	54.63
	0.06	11.61	0.27	1.61	51.37
	0.40	102.56	0.11	8.53	61.61
	1.33	70.04	3.55	8.11	55.96
Mean	3.06	45.70	1.28	4.94	54.89
SD	6.60	34.20	1.31	2.77	5.35
6	0.03	0.91	0.01	0.06	63.44
	0.04	4.23	0.13	0.40	65.28
	4.62	114.66	0.68	10.76	41.92
	0.23	7.40	0.18	0.59	82.89
	0.61	261.95	6.25	21.90	55.29
	0.05	1.01	0.63	0.63	63.66
Mean	0.93	65.03	1.31	5.72	62.08
SD	1.82	106.27	2.43	8.94	13.42
24	0.04	60.63	0.80	4.84	48.53
	0.12	372.37	1.70	34.21	90.60
	0.23	2.19	0.53	0.63	57.63
	0.16	3.42	3.50	3.37	44.92
	0.77	18.33	0.22	1.21	65.16
	0.32	97.75	1.39	9.43	59.02
Mean	0.27	92.45	1.36	8.95	60.98
SD	0.26	142.10	1.18	12.77	16.27
48	0.09	1.28	0.01	0.11	58.09
	1.43	25.86	0.03	2.46	52.50
	0.09	327.22	0.01	20.69	82.90
	0.12	19.76	0.28	1.57	83.48
	0.00	17.33	0.01	1.92	78.64
	1.45	38.56	0.18	3.60	84.23
Mean	0.53	71.67	0.09	5.06	73.31
SD	0.71	125.78	0.12	7.74	14.20
96	0.02	22.07	0.01	1.27	100.04
	0.03	1.49	0.31	0.38	70.66
	0.00	33.94	1.76	3.65	70.91
	0.00	9.13	0.17	0.78	59.69
	0.35	24.97	0.09	1.92	62.90
	0.01	44.68	0.03	3.26	83.43
Mean	0.07	22.71	0.39	1.88	74.60
SD	0.14	15.80	0.68	1.33	14.92

Table 4.6: Partitioning of wMWCNT in different compartments of zebrafish (microcosm study II). *D. rerio* (wet weight: 310 ± 89 mg) was exposed to 100 µg ^{14}C-wMWCNT L^{-1} in fish water (water phase exposure) over 96 h, whereby the test system additionally contained ^{14}C-wMWCNT loaded *D. magna* of all sizes. The uptake of wMWCNT in different compartments of zebrafish and in complete fish is presented (µg g^{-1} dw^{-1}). The respective dry weight of every single fish is represented (mg). The mean value (Mean) and standard deviation (SD) on six replicates is shown.

time (h)	gills (µg g^{-1} dw^{-1})	gut (µg g^{-1} dw^{-1})	fish debris (µg g^{-1} dw^{-1})	complete fish (µg g^{-1} dw^{-1})	dry weight (mg)
2	6.70	915.05	12.54	79.40	85.95
	1.28	770.58	20.57	78.07	81.50
	5.06	862.06	1.26	64.31	91.60
	13.34	1640.05	18.83	139.23	81.77
	3.63	807.91	8.12	63.00	75.60
	6.17	1350.70	17.41	102.31	38.51
Mean	6.03	1057.73	13.12	87.72	75.82
SD	4.08	354.52	7.38	28.94	19.03
6	2.52	444.26	1.41	23.29	33.91
	2.20	509.22	8.54	35.01	47.39
	1.67	527.14	0.75	34.32	52.25
	5.45	427.19	13.38	38.40	86.32
	11.81	321.58	13.13	32.51	55.44
	1.37	2129.93	11.04	118.44	65.49
Mean	4.17	726.55	8.04	47.00	56.80
SD	4.02	691.34	5.67	35.37	17.79
24	19.14	561.34	10.39	40.66	65.24
	0.65	2.64	0.20	0.36	75.62
	0.56	239.25	2.12	11.90	44.19
	2.22	1019.61	0.82	73.46	45.34
	25.95	2310.63	3.35	102.87	47.15
	1.04	2052.95	0.30	134.05	57.99
Mean	8.26	1031.07	2.86	60.55	55.92
SD	11.29	957.80	3.88	52.43	12.69
48	18.35	1139.75	6.30	97.59	38.85
	3.89	45.41	0.33	2.68	123.93
	13.62	422.51	0.88	19.23	74.24
	20.45	1141.46	1.42	84.60	49.11
	0.36	1180.78	0.85	64.82	89.64
	222.45	890.02	1.72	62.95	57.94
Mean	46.52	803.32	1.92	55.31	72.29
SD	86.55	468.39	2.20	37.06	31.09
96	51.62	4065.73	23.90	288.03	106.22
	37.13	3941.21	26.76	445.96	71.16
	94.45	5272.33	36.67	346.50	71.64
	9.49	2886.49	6.76	190.49	64.64
	34.75	127.57	6.54	14.99	51.39
	35.32	1263.15	22.58	104.68	44.92
Mean	43.79	2926.08	20.54	231.77	68.33
SD	28.29	1920.04	11.83	159.41	21.46

4.8 References

Agatz, A., Hammers-Wirtz, M., Gabsi, F., Ratte, H.T., Brown, C.D., Preuss, T.G., 2012. Promoting effects on reproduction increase population vulnerability of Daphnia magna. Environmental Toxicology and Chemistry 31, 1604-1610.

Bisesi, J.H., Jr., Merten, J., Liu, K., Parks, A.N., Afrooz, A.R., Glenn, J.B., Klaine, S.J., Kane, A.S., Saleh, N.B., Ferguson, P.L., Sabo-Attwood, T., 2014. Tracking and quantification of single-walled carbon nanotubes in fish using near infrared fluorescence. Environ Sci Technol 48, 1973-1983.

Bjorkland, R., Tobias, D., Petersen, E.J., 2017. Increasing evidence indicates low bioaccumulation of carbon nanotubes. Environ Sci Nano 4, 747-766.

Campos, R.B.V., da Rocha, T.D.D., Camargo, S.A.D., 2019. Production and Applications of Carbon Nanotube Buckypapers. J Aerosp Technol Man 11, 45-49.

Cano, A.M., Maul, J.D., Saed, M., Irin, F., Shah, S.A., Green, M.J., French, A.D., Klein, D.M., Crago, J., Canas-Carrell, J.E., 2018. Trophic Transfer and Accumulation of Multiwalled Carbon Nanotubes in the Presence of Copper Ions in Daphnia magna and Fathead Minnow (Pimephales promelas). Environ Sci Technol 52, 794-800.

Fernandez-Alacid, L., Sanahuja, I., Ordonez-Grande, B., Sanchez-Nuno, S., Viscor, G., Gisbert, E., Herrera, M., Ibarz, A., 2018. Skin mucus metabolites in response to physiological challenges: A valuable non-invasive method to study teleost marine species. Sci Total Environ 644, 1323-1335.

Glomstad, B., Zindler, F., Jenssen, B.M., Booth, A.M., 2018. Dispersibility and dispersion stability of carbon nanotubes in synthetic aquatic growth media and natural freshwater. Chemosphere 201, 269-277.

Gottschalk, F., Sonderer, T., Scholz, R.W., Nowack, B., 2009. Modeled environmental concentrations of engineered nanomaterials (TiO(2), ZnO, Ag, CNT, Fullerenes) for different regions. Environ Sci Technol 43, 9216-9222.

Hennig, M.P., Maes, H.M., Ottermanns, R., Schaffer, A., Siebers, N., 2019. Release of radiolabeled multi-walled carbon nanotubes (C-14-MWCNT) from epoxy nanocomposites into quartz sand-water systems and their uptake by Lumbriculus variegatus. Nanoimpact 14.

Iijima, S., 1991. Helical Microtubules of Graphitic Carbon. Nature 354, 56-58.

Jackson, P., Jacobsen, N.R., Baun, A., Birkedal, R., Kuhnel, D., Jensen, K.A., Vogel, U., Wallin, H., 2013. Bioaccumulation and ecotoxicity of carbon nanotubes. Chem Cent J 7, 154.

Jia, X.L., Wei, F., 2017. Advances in Production and Applications of Carbon Nanotubes. Topics Curr Chem 375.

Kah, M., Kookana, R.S., Gogos, A., Bucheli, T.D., 2018. A critical evaluation of nanopesticides and nanofertilizers against their conventional analogues. Nat Nanotechnol 13, 677-684.

Kennedy, A.J., Hull, M.S., Steevens, J.A., Dontsova, K.M., Chappell, M.A., Gunter, J.C., Weiss, C.A., Jr., 2008. Factors influencing the partitioning and toxicity of nanotubes in the aquatic environment. Environ Toxicol Chem 27, 1932-1941.

Klaine, S.J., Alvarez, P.J., Batley, G.E., Fernandes, T.F., Handy, R.D., Lyon, D.Y., Mahendra, S., McLaughlin, M.J., Lead, J.R., 2008. Nanomaterials in the environment: behavior, fate, bioavailability, and effects. Environ Toxicol Chem 27, 1825-1851.

Kuhl, A., Lorenzen, H., 1964. Handling and Culturing of Chlorella. in: Prescott, D.M. (Ed.). Methods in Cell Physiology. Academic Press; NEW YORK and London.

Leeuw, T.K., Reith, R.M., Simonette, R.A., Harden, M.E., Cherukuri, P., Tsyboulski, D.A., Beckingham, K.M., Weisman, R.B., 2007. Single-walled carbon nanotubes in the intact organism: near-IR imaging and biocompatibility studies in Drosophila. Nano Lett 7, 2650-2654.

Linard, E.N., van den Hurk, P., Karanfil, T., Apul, O.G., Klaine, S.J., 2015. Influence of carbon nanotubes on the bioavailability of fluoranthene. Environ Toxicol Chem 34, 658-666.

Maes, H.M., Stibany, F., Giefers, S., Daniels, B., Deutschmann, B., Baumgartner, W., Schaffer, A., 2014. Accumulation and distribution of multiwalled carbon nanotubes in zebrafish (Danio rerio). Environ Sci Technol 48, 12256-12264.

Myer, M.H., Henderson, W.M., Black, M.C., 2017. Effects of multiwalled carbon nanotubes on the bioavailability and toxicity of diphenhydramine to Pimephales promelas in sediment exposures. Environ Toxicol Chem 36, 320-328.

OECD, 2004. Test No. 202: *Daphnia sp.*, Acute Immobilisation Test.

Parks, A.N., Portis, L.M., Schierz, P.A., Washburn, K.M., Perron, M.M., Burgess, R.M., Ho, K.T., Chandler, G.T., Ferguson, P.L., 2013. Bioaccumulation and toxicity of single-walled carbon nanotubes to benthic organisms at the base of the marine food chain. Environ Toxicol Chem 32, 1270-1277.

Petersen, E.J., Akkanen, J., Kukkonen, J.V., Weber, W.J., Jr., 2009. Biological uptake and depuration of carbon nanotubes by Daphnia magna. Environ Sci Technol 43, 2969-2975.

Petersen, E.J., Huang, Q., Weber, W.J., 2008. Ecological uptake and depuration of carbon nanotubes by Lumbriculus variegatus. Environ Health Perspect 116, 496-500.

Petersen, E.J., Pinto, R.A., Mai, D.J., Landrum, P.F., Weber, W.J., Jr., 2011. Influence of polyethyleneimine graftings of multi-walled carbon nanotubes on their accumulation and elimination by and toxicity to Daphnia magna. Environ Sci Technol 45, 1133-1138.

Rhiem, S., Riding, M.J., Baumgartner, W., Martin, F.L., Semple, K.T., Jones, K.C., Schaffer, A., Maes, H.M., 2015. Interactions of multiwalled carbon nanotubes with algal cells: quantification of association, visualization of uptake, and measurement of alterations in the composition of cells. Environ Pollut 196, 431-439.

Roberts, A.P., Mount, A.S., Seda, B., Souther, J., Qiao, R., Lin, S., Ke, P.C., Rao, A.M., Klaine, S.J., 2007. In vivo biomodification of lipid-coated carbon nanotubes by Daphnia magna. Environ Sci Technol 41, 3025-3029.

Shi, Q.Y., Zhang, H., Wang, C.L., Ren, H.Y., Yan, C.Z., Zhang, X., Chang, X.L., 2020. Bioaccumulation, biodistribution , and depuration of C-13-labelled fullerenols in zebrafish through dietary exposure. Ecotox Environ Safe 191.

Smith, C.J., Shaw, B.J., Handy, R.D., 2007. Toxicity of single walled carbon nanotubes to rainbow trout, (Oncorhynchus mykiss): respiratory toxicity, organ pathologies, and other physiological effects. Aquat Toxicol 82, 94-109.

Sun, T.Y., Gottschalk, F., Hungerbuhler, K., Nowack, B., 2014. Comprehensive probabilistic modelling of environmental emissions of engineered nanomaterials. Environ Pollut 185, 69-76.

Tervonen, K., Waissi, G., Petersen, E.J., Akkanen, J., Kukkonen, J.V., 2010. Analysis of fullerene-C60 and kinetic measurements for its accumulation and depuration in Daphnia magna. Environ Toxicol Chem 29, 1072-1078.

Vatsos, I.N., Kotzamanis, Y., Henry, M., Angelidis, P., Alexis, M.N., 2010. Monitoring stress in fish by applying image analysis to their skin mucous cells. Eur J Histochem 54, 107-111.

Yan, Z., Lu, G., Sun, H., Ma, B., 2017. Influence of multi-walled carbon nanotubes on the effects of roxithromycin in crucian carp (Carassius auratus) in the presence of natural organic matter. Chemosphere 178, 165-172.

Zhang, Y., Zhu, L., Zhou, Y., Chen, J.M., 2015. Accumulation and elimination of iron oxide nanomaterials in zebrafish (Danio rerio) upon chronic aqueous exposure. J Environ Sci-China 30, 223-230.

5 A study to investigate the 'Trojan-horse' effect of the biocide triclocarban and weathered multi-walled carbon nanotubes to green algae and freshwater crustacean

5.1 Summary

In recent years, the production of carbon nanotubes (CNT) has been optimized to an industrial scale extent and therefore, an increased release of the nanomaterials into the aquatic environment can be expected. CNT are known to adsorb organic compounds and thus implications of aquatic contaminants might be changed. We investigated the interaction of weathered multi-walled CNT (wMWCNT) and the biocide triclocarban (TCC) as well as mixture toxicities of both on growth of *Chlamydomonas reinhardtii* and *Raphidocelis subcapitata* and immobilization of *Daphnia magna*. At first, the adsorption of TCC onto different wMWCNT concentrations (100, 400 and 1000 µg L^{-1}) was determined using radiolabeled TCC (^{14}C-TCC). The obtained log K_{wMWCNT} value of 7.36 ± 0.44 L kg^{-1} described a strong adsorption capacity of wMWCNT towards TCC. Regarding ecotoxicity, exposure of wMWCNT alone showed that first effects occur in the mg L^{-1} range for green algae and crustacean. TCC alone caused 50% effect (EC_{50}) at 20.6 µg L^{-1}, 22.1 µg L^{-1} and 36.5 µg L^{-1} in *D. magna*, *C. reinhardtii* and *R. subcapitata*, respectively. The inhibitory effect of TCC on green algae was reduced when wMWCNT concentrations above 100 µg L^{-1} (up to 2 mg L^{-1}) were added to the test medium until no difference to the control was detected above 1 mg wMWCNT L^{-1}. Regarding *D. magna*, there was no impact of 100 µg wMWCNT L^{-1} on TCC toxicity in immobilization test. But considering the lowered freely dissolved TCC concentration in presence of CNT, an increase in toxicity was observed. Because of our results and the fact that algae do not absorb CNT to a large extent, we conclude no 'Trojan-horse' effect for the tested green algae. However, the high uptake of CNT and co-adsorbed TCC in *D. magna* suggest a true 'Trojan-horse' effect.

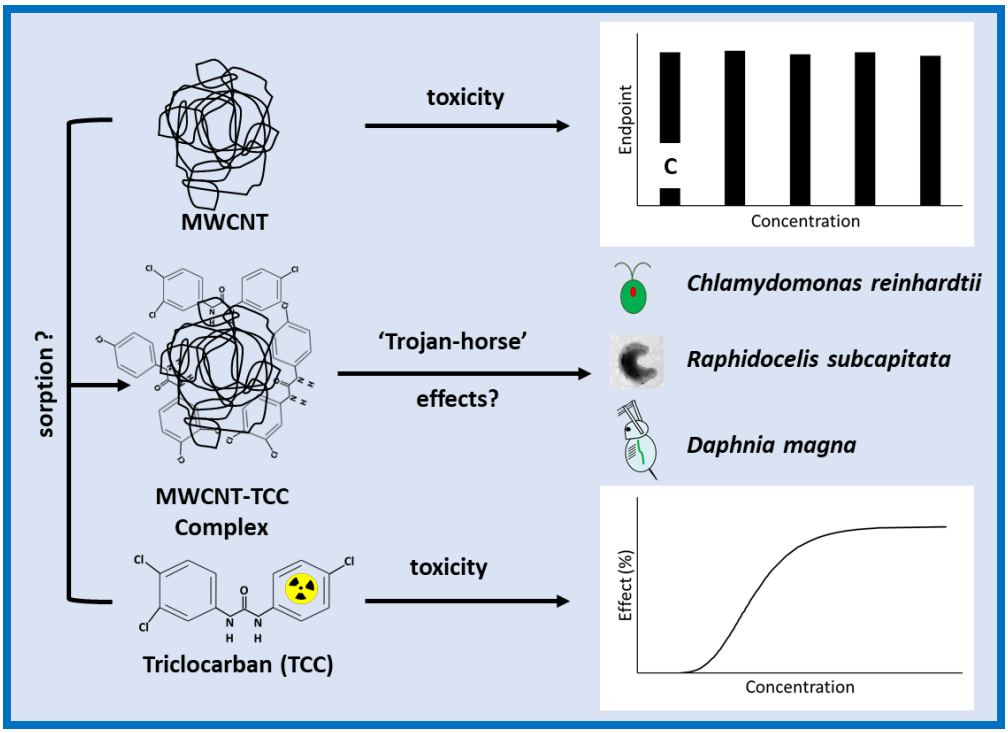

Figure 5.1: Graphical summary of chapter 5.

5.2 Introduction

The antimicrobial agent triclocarban (TCC) is classified as persistent (Snyder and O'Connor, 2013), bioaccumulative (Coogan et al., 2007; Schebb et al., 2011) and toxic (Simon et al., 2015). Due to its disinfectant properties, TCC is used in pharmaceutical and personal care products, i.e., soaps, cosmetics, detergents and cleaning agents (Heidler et al., 2006; Sapkota et al., 2007). After the introduction of TCC in 1957, the biocide was mass produced and distributed with a total tonnage reported in 1998 by the United States Environmental Protection Agency greater than 500,000 to 1,000,000 pounds per year (TCC Consortium, 2002; Halden, 2014). As a component of everyday care products, TCC ends up in wastewater and finally in our environment. A concentration of 5.6 µg TCC L^{-1} and 6.8 µg TCC L^{-1} has been detected in U.S. surface water and wastewater, respectively (Halden and Paull, 2004). A half-life of 60 days, 108 to 120 days and 540 days is assumed for the biodegradation of TCC in water, soil and sediments (Halden and Paull, 2005; Ying et al., 2007). In September 2016, the U.S. Food and Drug Administration banned TCC in over-the-counter products, with a couple of exceptions (Halden et al., 2017). In the EU, TCC is currently under evaluation in the framework of the Community rolling action plan (European Chemical Agency) for concerns about reprotoxicity and its role as an endocrine disruptor (French Agency for food; environmental and occupational health and safety (anses), 2018). In the aquatic trias, consisting of green algae, water flea and fish, acute toxicity tests showed EC_{50} values between 10 and 85 µg TCC L^{-1} (Tamura et al., 2013) and therefore reached the measured environmental concentration range. Due to the persistence of TCC and its intensive use over several decades, an environmental risk can still be assumed.

The pollution of our environment is an omnipresent topic. In addition to organic chemicals, various solids can be found in the water, from plastic bottles to nanomaterials. A nanomaterial is a material with at least one dimension below 100 nm (Klaine et al., 2008) and carbon nanotubes (CNT) are among the most produced carbonaceous nanomaterials with an annual production volume of ~100 tons (OCSIAL About). There are two known forms of CNT: single-walled (SWCNT) and multi-walled CNT (MWCNT) (Ajayan, 1999). Owing to their unique properties, such as mechanical strength, low density and thermal stability, CNT find many different applications in nanocomposites, energy storage and water treatment etc. (Iijima, 2002; Zaib et al., 2014; Barra et al., 2019; Thauer et al., 2020). In their most common application, CNT are firmly embedded in a polymer matrix, which is why the main release of nanomaterials occurs at production sites and therefore the emission of CNT into the environment is limited. Consequently, the predicted environmental concentrations for surface waters are in the pg L^{-1} to ng L^{-1} and for sediments in the µg kg^{-1} range (Sun et al., 2014; Gottschalk et al., 2015). The investigation of the acute toxicity of CNT to aquatic organisms has already been the subject of various research studies. Effects were mainly detected at nanomaterial concentrations in the mg L^{-1} range, and it was found that SWCNT lead to effects at lower concentrations than MWCNT (Zhu et al.,

2009; Kowk et al., 2010; Lukhele et al., 2015; Simon et al., 2015; Cano et al., 2017; Bacchetta et al., 2018) but overall, the toxicity is considered low.

In addition, the following characteristics make CNT auspicious adsorbents: a remarkable hydrophobicity, a high specific surface area as well as hollow and layered structures (Upadhyayula et al., 2009; Zhang et al., 2011). Over the last two decades, researchers investigated CNT adsorption of polycyclic aromatic hydrocarbons (Yang et al., 2006; Yang and Xing, 2007), pharmaceuticals (Oleszczuk et al., 2009; Yu et al., 2014), polychlorinated biphenyls (Beless et al., 2014; Velzeboer et al., 2014) and others. Nevertheless, the adsorption of hydrophobic organic chemicals to carbon nanotubes and the subsequent influence on fate, bioavailability, and toxicity of the contaminant in aquatic systems shows large knowledge gaps. Therefore, we investigated adsorption of TCC on MWCNT and so called 'Trojan-horse' effects by the adsorbent-adsorbate complex onto freshwater green algae and crustacean.

The mixture toxicity of nanomaterials and organic compounds has been investigated in the past two decades. The impact of nanomaterials on accumulation of chemicals in aquatic organisms has also been in the focus of research. The outcome seems to depend mainly on the adsorption-desorption interaction between the chemical compound and nanomaterial as well as on the tested species. For example, Baun et al. (2008) showed that phenanthrene adsorbed on C_{60} fullerenes (6 – 10 mg L^{-1}) causes an increase in toxicity in the green alga *Pseudokirchneriella subcapitata* and the crustacean *Daphnia magna*. However, atrazine, methyl parathion and pentachlorophenol cause reduced or unaltered toxicity in the presence of C_{60} fullerenes. In the same study, an increased phenanthrene uptake in *D. magna* was observed in co-exposure to nanomaterials. Likewise, SWCNT (15 mg L^{-1}) increased phenanthrene accumulation in the digestive tract, liver and brain tissue of Japanese medaka *Oryzias latipes* (Su et al., 2013). Schwab et al. (2013) examined the effect of diuron on the photosynthetic activity of *Chlorella vulgaris* with and without MWCNT (10 mg L^{-1}) and found a reduction of the adverse effect in the presence of MWCNT. Only when the free dissolved diuron concentration was considered, an increase in toxicity was observed, and it was suggested that the adsorbed diuron fraction was bioavailable. A reduced bioavailability of polycyclic aromatic hydrocarbons (PAH's) in the presence of MWCNT (1.5 mg L^{-1}) for *Pimphales promelas* was confirmed by gallbladder analysis (Linard et al., 2017). Myer et al. (2017) revealed that sediment-embedded MWCNT (318 µg g^{-1}) did not affect the diphenhydramine induced growth inhibition of *P. promelas* and neither a change in body burden was observed in the presence of MWCNT. In contrast, a study by Yan et al. (2017) reported an increased accumulation of the antibiotic roxithromycin (ROX) and an enhanced oxidative stress measured in the liver in the presence of MWCNT (100 µg L^{-1}) in the crucian carp *Carassius auratus*. Desorption of ROX from the nanomaterial in the digestive tract was also

suspected. Since the behavior of neither, chemical nor nanomaterial, can be evaluated with certainty, it is difficult to assign a mechanism of action to the observed results.

With the help of the classification system described in Naasz et al. (2018) we aimed to allocate the observations from our study to a 'Trojan-horse' effect or no 'Trojan-horse' effect mechanism. Therefore, we investigated adsorption of the biocide TCC onto MWCNT and tested the mixture toxicity of both towards green algae *Chlamydomonas reinhardtii* and *Raphidocelis subcapitata* and water flea *Daphnia magna*. In addition, we first investigated the toxic effects of each individual substance to arrange our next steps.

5.3 Materials and methods

5.3.1 Synthesis and purification of ^{14}C-labeled MWCNT (^{14}C-MWCNT)

For a detailed description of synthesis of ^{14}C-MWCNT see section 2.3.1 in chapter 2.

5.3.2 Weathering of nanomaterials

For weathering and characterization of MWCNT see section 2.3.2 in chapter 2.

5.3.3 Adsorption of ^{14}C-triclocarban on weathered MWCNT in freshwater medium

In all approaches, an algal growth medium (see SI, Tab. 5.5) mixed with the biocide sodium azide (NaN_3, 200 mg L^{-1}, Sigma Aldrich, Germany) was used as aqueous phase. All tests were performed at 18 ± 1 °C. The method used is based on a three-phase test system, which was first presented by Jonker and Koelmans (2001) to investigate sorption of hydrophobic organic chemicals to soot. The concept of this methodology foresees a third phase, in addition to sorbent and water. The third phase is a homopolymer (Polyoxymethylene (POM), film, 300 mm × 300 mm, thickness: 0.5 mm, density: 1.41 g cm^{-2}, Goodfellow GmbH, Germany), which has been shown to adsorb the substance of interest (Hennig, 2019). The passive sampling principle supports a more precise description of the sorption in contrast to conventional methods, such as filtration and centrifugation, since the CNT does not have to be separated from the water phase (small particles of the CNT remain in the water phase after the application of conventional methods). The mass balance for TCC in this three-phase test system is described by the following Eq. 5.1:

$$Q_{tot} = C_{wMWCNT} M_{wMWCNT} + C_W V_W + C_{POM} M_{POM} \quad (5.1)$$

Q_{tot} describes the total amount of a chemical in the test system (µg). C_{MWCNT}, C_{POM} and C_W represent TCC concentrations in wMWCNT and POM (µg kg^{-1}) as in water phase (µg L^{-1}), respectively. Accordingly, M_{MWCNT}, M_{POM} und V_W are the masses of wMWCNT and POM (kg) and the volume of the water phase (L). For the determination of the distribution coefficient of TCC between water phase and wMWCNT (K_{wMWCNT}) and the distribution coefficient of TCC between water phase and POM (K_{POM}), substitutions ($\mathbf{K_{wMWCNT}} = C_{wMWCNT}/C_W$; $\mathbf{K_{POM}} = C_{POM}/C_W$) need to be performed and rewriting of equation 5.1 gives:

$$K_{wMWCNT} = \frac{1}{M_{wMWCNT}} \left(\frac{K_{POM} Q_{tot}}{C_{POM}} - M_{POM} K_{POM} - V_W \right) \quad (5.2)$$

The determination of the distribution coefficient K_{wMWCNT} requires three experiments to be performed. At first the equilibration time (t_{eq}) for the adsorption of TCC to the POM material needs to be obtained and subsequently K_{POM} and K_{wMWCNT} can be calculated from two different test approaches. Based on the equilibrium time t_{eq} of 11 days for the sorption of ^{14}C-TCC to POM (Hennig, 2019), a test duration of 21 days was considered appropriate for the following two experiments.

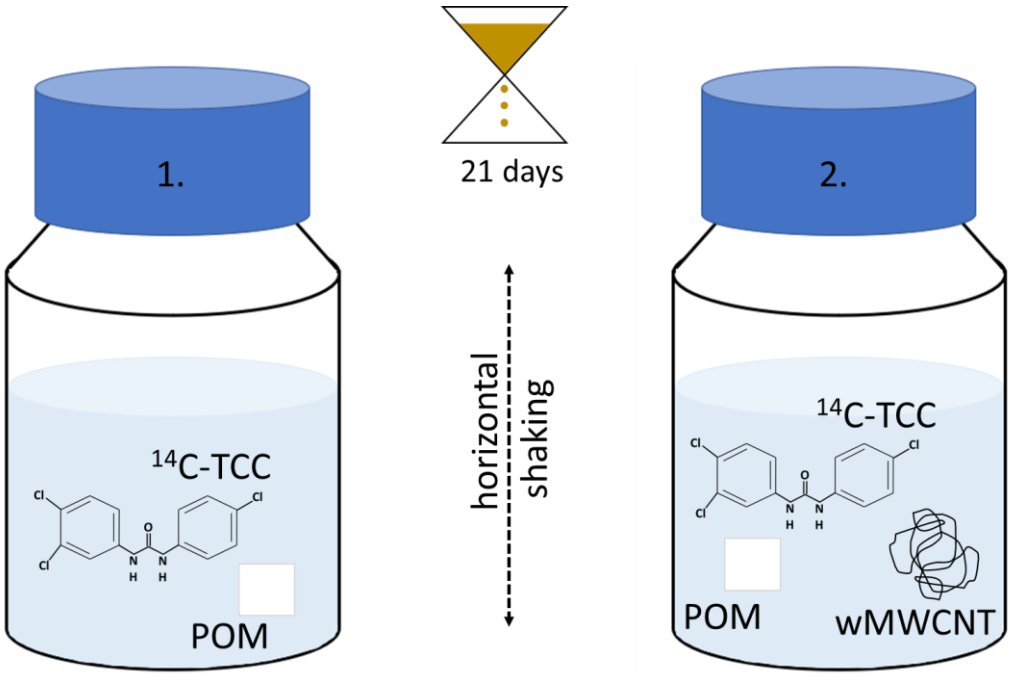

Figure 5.2: Experimental design in adsorption study to determine the distribution of ^{14}C-triclocarban (^{14}C-TCC) between water phase and weathered multiwalled carbon nanotubes (wMWCNT). (1.) Two-phase and (2.) three-phase test system with polyoxymethylene (POM) for the determination of distribution coefficients K_{POM} and K_{wMWCNT}, respectively. In both approaches, six different ^{14}C-TCC concentrations were tested. The distribution of ^{14}C-TCC between water phase and nanomaterial was investigated for three different wMWCNT concentrations: 100, 400 and 1000 µg L^{-1}. Incubation for all samples was at 18 ± 1 °C for 21 days horizontal on a laboratory shaker (120 rpm, dark).

The POM sheet was first cut into squares with the dimension of 1 × 1 cm and as described in the literature cold-extracted with hexane (30 min) and methanol (3 × 30 min), air-dried and weighted before test start (Jonker and Koelmans, 2001).

Determination of K_{POM}. Six different ^{14}C-TCC (chlorophenyl ring-14C(U), specific activity: 30.0 mCi mmol^{-1}, purity: 96.2%, Moravek Inc., California, US) concentrations were investigated: 10, 20, 30, 40, 50 and 60 µg L^{-1}. ^{14}C-TCC was applied per concentration to 240 mL of prepared medium, resulting in four replicates with 50 mL water phase each. A POM piece was then added to each replicate and the samples were incubated on a laboratory shaker (120 rpm, dark) for 21 days. In

addition, four controls with the highest ^{14}C-TCC concentration were added to verify that the test substance remained stable during the experiment.

Determination of K_{wMWCNT}. The procedure was the same as in the experiment to determine K_{POM}. Additionally, in this experiment the corresponding amounts of wMWCNT (test concentrations: 100, 400 and 1000 µg L^{-1}) were dispersed (Sonopuls HD 2070, 70 W, pulse: 0.2 s, pause: 0.8 s, 2 × 10 min) in the prepared test medium before application of the ^{14}C-TCC. For conditions on incubation see determination of K_{POM}.

After termination of the two experiments, the POM squares were removed from the water phase using tweezers, wiped with a wet tissue and extracted using a Soxhlet apparatus and methanol as extraction agent for 3 h. The extracts were then concentrated to dryness on a rotary evaporator, redissolved in methanol and afterwards in ethyl acetate and measured by means of LSC (liquid scintillation counter, Hidex 600/300 SL, Finland). The extracted POM squares were also added to LSC vials, mixed with Ultima Gold™ XR scintillation cocktail (Perkin Elmer, Germany) and submitted to LSC. For a complete recovery of radioactivity in the experiment on K_{POM} determination, additionally, the radioactivity in the water phase was determined. For this purpose, two aliquots of 1 mL were drawn from each replicate, scintillation cocktail was added, and the amount of radioactivity was measured by means of LSC. The amount of radioactivity determined in the POM extract and in the POM piece itself could be used to calculate K_{POM} and K_{wMWCNT} (see Eq. 5.1 and 5.2).

5.3.4 Test organisms

Green algae *Chlamydomonas reinhardtii* (strain no. 23.90) and *Raphidocelis subcapitata* (strain no. 61.81) were obtained from SAG Göttingen and cultured in BG 11 medium (SAG, 2013) and medium according to Kuhl and Lorenzen (1964), respectively. Cultures of algae were kept at 20 ± 2 °C, permanent aeration and constant illumination. Renewal of medium was performed every two weeks. *Daphnia magna* (Straus) were cultured in M4 medium (OECD, 2004) (20 ± 2 °C, 16 h dark/8 h light photoperiod). Daphnids were fed daily, except on weekends from a culture of the green alga *Desmodesmus subspicatus*. In addition, *Daphnia* was fed with yeast once a week during medium renewal. The green alga *Desmodesmus subspicatus* (strain no. 86.81) is in house cultured at the Institute for Environmental Research (RWTH Aachen, Worringerweg 1, 52074 Aachen) as food supply for water flea keeping and is treated as described above for *Raphidocelis subcapitata*.

5.3.5 Algal growth inhibition test

The algal growth inhibition test was carried out in accordance with OECD Guideline 201. The test medium used was that described in the SI (Tab. 5.5). The test was incubated in 250 mL Erlenmeyer flasks. The green algae examined were *Raphidocelis subcapitata* and *Chlamydomonas reinhardtii*.

Incubation was carried out for 72 h in an incubator at 120 rpm, a temperature of 22 ± 2 °C and a light intensity of 4300 to 7500 lx. Each treatment and control group consisted of three technical replicates and are displayed in the following.

To determine the **toxicity of TCC** to green algae, the following concentration series (nominal concentrations) were applied: *R subcapitata*: 16, 22, 31, 43, 52 and 60 µg TCC L^{-1}; *C. reinhardtii*: 10, 15, 23, 34 and 51 µg TCC L^{-1}. Acetone was used as solvent. In addition to the test concentrations, the test included a blank (control of the medium and background for the measurement of the algal cell count), a solvent control and a growth control (control of algal growth in test medium).

To determine the **toxicity of wMWCNT** to the green algae under investigation, the nanomaterials were dispersed (see above) in the prepared test medium before the test was started. Two concentration series were selected because no toxicity effects were observed in the lower concentration range. The following test series were used for both green algae: (1) 100, 220, 484, 700, 1064 and 2342 µg wMWCNT L^{-1}; (2) 1, 2, 4, 8 and 16 mg wMWCNT L^{-1}. No solvent was used in experiments with wMWCNT only. In addition to growth control and medium control (blank), two additional blanks (medium with the corresponding concentration of wMWCNT) were added to each wMWCNT concentration and incubated. Since wMWCNT can influence the fluorescence measurement, an adequate blank for further calculations was created.

To investigate **'Trojan-horse' effects** of TCC and wMWCNT to green algae, both substances of interest were added simultaneously to the growth inhibition test. Two different test approaches were performed for both green algae: TCC variable (see above; toxicity of TCC) + wMWCNT (100 µg L^{-1}); wMWCNT variable (toxicity of wMWCNT, test series (1); see above) + TCC (highest test concentration of toxicity test). Prior to exposure, the TCC was loaded to wMWCNT during a 2 h **loading process**. Therefore, wMWCNT were dispersed in the test medium as described above and filled into 500 mL graduated flasks. Afterwards the required amount of TCC was added and flasks were incubated in the dark on a laboratory shaker at 120 rpm for 2 hours. Subsequently, green algae were added, and the test was prepared and incubated as described above.

The measurement of algal cell count was performed after 0, 24, 48 and 72 h. For this purpose, 2 mL were taken from each sample vessel and transferred to a 24 well plate (TPP®, Trasadingen, Switzerland). The flasks were swivelled extensively by hand before sampling to ensure an even distribution of the algal cells and to avoid settling. Cell density was determined using a fluorescence reader (Tecan M200, Männedorf, Switzerland, software: Magellan). The measured values for extinction were adjusted by the blank and the cell density was determined using a calibration curve (one for each green algal species, see SI, Fig. 5.11).

5.3.6 *Daphnia magna* acute immobilisation test

The acute immobilization test with *Daphnia magna* was performed according to OECD Guideline 202. The M4 test medium used is also described in the guideline (OECD, 2004). The test organisms applied had an age of ≤ 24 h. Small, round 10 mL glasses were used as test vessels. Acetone was used as solvent when TCC was tested. To check the validity criteria, a control group (clean M4 medium) was added to the treatments in each test. Each treatment and control group consisted of four technical replicates.
To determine the **toxicity of TCC**, the following concentration series (nominal concentrations) was chosen: 7.5, 11, 17, 25 and 38 µg TCC L^{-1}.

The **toxicity of wMWCNT** to filter feeding daphnids was investigated in the presence and absence of food (green algae). Hence, the immobilization test was performed twice as described above, where seven different wMWCNT concentrations were tested: 0.1, 1, 2, 4, 8, 16 and 32 mg L^{-1}. Nanomaterials were dispersed as described in the algal growth inhibition test. After test preparation, the animals in one approach were fed with the green algae *Desmodesmus subspicatus*.

To investigate **'Trojan-horse' effects**, the abovementioned TCC test series was loaded to 100 µg wMWCNT L^{-1} (see loading process) and exposition of *D. magna* was monitored for 48 h.

5.3.7 High performance liquid chromatography (HPLC)

In order to examine the stability of TCC during the sorption study the four controls were checked by HPLC analysis (Agilent Infinity II 1260, Agilent, USA). For this purpose, the water phases of the control preparations were completely transferred into 100 mL pointed flasks and reduced to dryness using a rotary evaporator. Subsequently, the TCC was re-dissolved in 1 mL acetonitrile and added to an HPLC vial (Chromatography Service, Germany). LSC analysis was used to check whether radioactivity was completely transferred. To prepare the radioactive TCC standard, 2 µL were taken from the ^{14}C-TCC stock solution and diluted in 1 mL acetonitrile (8333.33 Bq mL^{-1}). For the analysis of samples and standard a 15 cm Eclipse XDB C18 column (5 µm ZORBAX, size: 4.6 × 150 mm, Agilent, USA) was used. The program was set to 15 min at a solvent flow rate of 0.8 mL min^{-1}. The solvent mixture consisted of millipore water (eluent A) and acetonitrile (eluent B). The use of a mobile phase, consisting of acetonitrile and water, has already been successfully tested regarding the biocide TCC (Halden and Paull, 2005; Coogan et al., 2007). HPLC analysis was performed at room temperature. The mobile phase gradient program is listed in Tab. 5.1. The injection volume for both, samples and standard was 50 µL (^{14}C-TCC standard: 416.67 Bq mL^{-1}).

Table 5.1: Gradient program of the used HPLC method.

time (min)	eluent A (water)	eluent B (acetonitrile)	duration (min)
0	90	10	1
1	30	70	9
10	10	90	5
15	90	10	1

Absorption spectrum (Fig. 5.3) and radioactive signals were detected by a diode array detector DAD (Agilent G7115A, Agilent, USA) and a Raytest Ramona liquid cell detector (Elysia, Belgium), respectively. The HPLC chromatograms were evaluated by means of the software Elysia Raytest GINA X™ (Version 10.1, Servicepack 2).

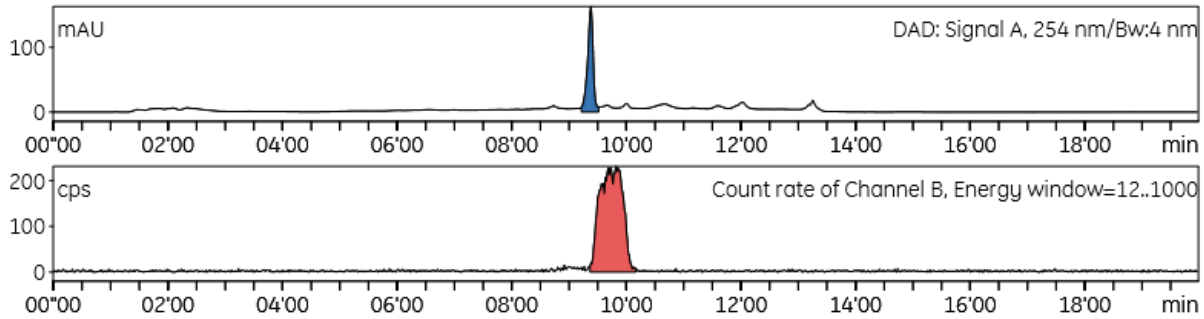

Figure 5.3: Example chromatogram of a control sample generated in the sorption study. The signal strength (mAU/cps (counts per second)) is plotted against time. The retention time for the ^{14}C-TCC standard was 9.52 min for radioactive channel and 9.22 min for DAD detector. Peak area was integrated using software Elysia Raytest GINA X™ (Version 10.1, Servicepack 2).

5.3.8 Data evaluation

Collected data was processed using Microsoft Excel® (Microsoft Office 365 ProPlus), GraphPad Prism (GraphPad Prism 5, USA), ToxRat® (ToxRat Professional, Version 3.2.1) and SigmaPlot (SigmaPlot Version 12.0, USA). Outliers were identified by Dixon's Q test ($\alpha = 0.05$). R^2 significance was checked by testing the Pearson correlation coefficient against 0 ($\rho = 0$) depending on the degree of freedom (FG = n - 2). Differences between control and treatments were identified using a t-test (p value to reject = 0.05). Raw data were checked for normal distribution with Shapiro-Wilk test (p value = 0.05) and variance homogeneity with Levene's test (p value = 0.05). If any of the above test criteria could not be met, a Mann-Whitney Rank Sum test was performed.

A detailed explanation of the applied calculations to the data from the sorption study can be found in Jonker and Koelmans (2001) and Hennig (2019). The distribution coefficients were calculated as described in 5.3.3 (see Eq. 5.2). As CNT are considered carbon adsorbents, the Dubinin-Astakhov model (DAM) is the most suitable fit (Dubinin and Astakhov, 1971; Yang et al., 2006). The DAM is part of the Polanyi theory, which has already been used to calculate the sorption of polycyclic aromatic hydrocarbons to CNT. The DAM is described by the following equation 5.3:

$$\log C_{wMWCNT} = logQ^0 - (\frac{\varepsilon_{SW}}{E})^b \quad (5.3)$$

where C_{wMWCNT} is the equilibrium adsorbed concentration of TCC (µg kg^{-1}) and Q^0 represents the maximum adsorption capacity (µg kg^{-1}); E (kJ mol^{-1}) is the 'correlating divisor' and b is the fitting parameter. The correlating divisor E describes the overall adsorption energy consisting of the interaction energies predominant in the sorption test system (Crittenden et al., 1999). The effective adsorption potential is described by ε_{SW} (kJ mol^{-1}) and calculated by the following equation 5.4:

$$\varepsilon_{SW} = RTln(\frac{C_{SW}}{C_W}) \quad (5.4)$$

R is the universal gas constant (8.314 × 10^{-3} kJ mol^{-1} K^{-1}), T (K) is the absolute temperature and C_{SW} represents the water solubility of TCC. A water solubility of 0.045 mg L^{-1} was used and was derived from Snyder et al. (2010). C_W is the equilibrium aqueous concentration of TCC (µg L^{-1}). The estimation of the model parameter values (Q^0, E and b) and standard errors was performed by a common software program (GraphPad Prism 5, USA). Weighted sum of squares was 1/Y^2.

The statistical analysis of the data from toxicity tests with green algae and daphnids was performed with ToxRat®. In tests with green algae the collected data set was first tested for normal distribution using Shapiro-Wilk's test (p = 0.01). Further, a two-sample comparison of the two controls using a Student-t test for Variance homogeneity (α = 0.05) was applied. In the following calculations (percentage growth inhibition, NOEC/LOEC) the solvent control was considered as a reference. The concentration-related results were further evaluated by means of Probit analysis using linear max. likelihood regression (p = 0.05). This function allowed calculating the TCC concentrations, which caused 10, 20 and 50% inhibition of growth of algae ($EC_{10/20/50}$) at different time points. For the determination of threshold concentrations (LOEC/NOEC) the statistical characteristics of the sample were tested for normal distribution and variance homogeneity with Shapiro-Wilk's test and Levene's test, respectively (for both tests p = 0.01). Statistical effect-thresholds were calculated using the Williams multiple sequential t-test, the multiple sequentially-rejective Welsh-t-test after Bonferroni-Holm or the multiple sequentially-rejective median (2 × 2-table) test after Bonferroni-Holm (for all tests α = 0.05). The described procedure was performed for effects on growth rate and yield (biomass(t) – biomass(t_{0h})).

For the statistical analysis of the data sets from tests on immobilization of *D. magna*, the control and solvent control were first tested for significant differences using a Fisher's exact binomial test (α = 0.05). Subsequently, the solvent control served as reference in further calculations. The applied Probit analysis using linear maximum likelihood regression (p = 0.05) revealed dose response relationships and effect concentrations ($EC_{10/20/50}$) were determined. For the identification of threshold concentrations, a step-down Cochran-Armitage test procedure (α = 0.05) was applied to the data.

Based on the assumption that the adsorption of TCC to wMWCNT affects the free dissolved fraction of TCC ($TCC_{fDissolved}$) in the test medium, $TCC_{fDissolved}$ should be calculated in the toxicity tests with green algae and daphnids. Assuming that the distribution of TCC between water phase and CNT in the presence of test organisms occurs in the same way as in the sorption study without test organisms and considering that TCC absorption and degradation by the test organisms and other interactions are disregarded, $TCC_{fDissolved}$ can be calculated using equation (5.5):

$$TCC_{fDissolved} = TCC_{nom} - TCC_{fsorbed} \quad (5.5)$$

where $TCC_{fDissolved}$ represents the free dissolved fraction of TCC (µg L^{-1}) and TCC_{nom} (µg L^{-1}) is the nominal TCC concentration applied to the test system. $TCC_{fsorbed}$ describes the adsorbed fraction of TCC on wMWCNT derived from the obtained max. adsorption capacity Q^0 (7.5 µg kg^{-1}). Since sorption of TCC on wMWCNT reached saturation in every test approach this calculation method was the appropriate one.

5.4 Results

5.4.1 Adsorption of TCC on wMWCNT

Adsorption isotherm (Fig. 5.4 - A) and distribution coefficient K_{POM} for the sorption of ^{14}C-TCC to POM in algal growth medium was determined. The recovery of radioactivity was 92.5 ± 3.8% for samples and 92.0 ± 0.5% for controls. The results thus showed that the method (see 5.3.3) used to extract ^{14}C-TCC from POM was successful. To obtain the sorption isotherm, log C_{POM} was plotted against log C_W and a linear regression model was fitted to the data (coefficient of determination > 0.99). The calculated logarithmic distribution coefficient K_{POM} was 3.51 ± 0.03. HPLC analysis revealed, that in control samples only TCC was detected and therefore stability of test substance during the study was proved.

Subsequently, using the distribution coefficient K_{POM}, the logarithmic distribution coefficients K_{wMWCNT} of 6.75, 6.96 and 7.36 (Tab. 5.2) were determined for the following wMWCNT concentrations: 100, 400 and 1000 µg L^{-1} (CNT100, CNT400, CNT1000), respectively. Further, with the transformation of Eq. 5.1 the freely dissolved ^{14}C-TCC concentration in water phase (C_W, µg L^{-1}) and the adsorbed ^{14}C-TCC concentration on wMWCNT (C_{wMWCNT}, µg kg^{-1}) was calculated. Values were plotted, following by an examination using the Dubinin-Astakhov model (see 5.3.8). Considering the standard deviations, no difference was found for the maximum adsorption capacity Q^0: 7.55 ± 0.19, 8.15 ± 1.14 and 7.47 ± 0.02 µg kg^{-1} for CNT100, CNT400 and CNT1000, respectively. The values for the fitting parameters E and b varied among wMWCNT concentrations (Tab. 5.2). Standard deviations were considerably higher compared to the distribution coefficient K_{POM}. Additionally, it was observed that the coefficient of determination increased with increasing amounts of wMWCNT, therefore we used

only the Q^0 value derived from the highest wMWCNT concentration (CNT1000) in further calculations (see Tab. 5.2). The poor fit of the DAM to the data of the CNT100 (R^2 = 0.33) and CNT400 (R^2 = 0.68) scenarios is also shown in Fig. 5.4 - B. The values for C_{CNT} of the individual replicates of the two scenarios show a large scattering, whereas the CNT1000 scenario shows only a very small variation (R^2 = 0.94).

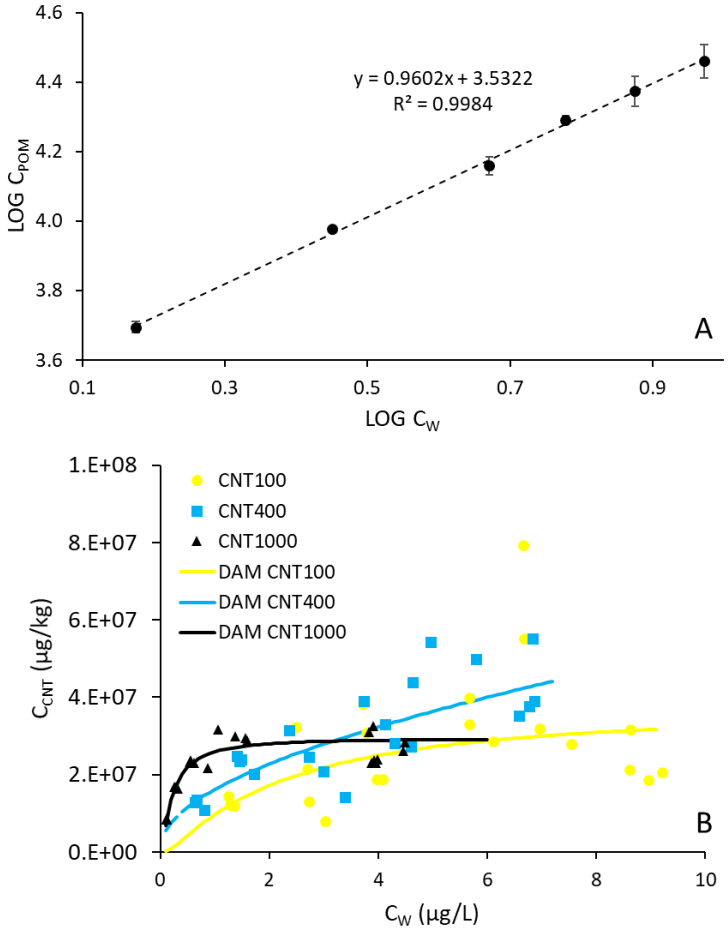

Figure 5.4: Logarithmic isotherm for the sorption of ^{14}C-TCC on POM (A) and sorption isotherms for the adsorption of ^{14}C-TCC on wMWCNT in three different nanomaterial concentrations (100, 400 and 1000 µg L^{-1}) (B). C_W is the TCC concentration in aqueous phase (µg L^{-1}), C_{POM} represents the absorbed TCC concentration to POM (µg kg^{-1}) and C_{CNT} demonstrates the TCC concentration adsorbed to wMWCNT (µg kg^{-1}). In A, data points represent the mean on four replicates ± standard deviation, the dashed trend line was fitted using Microsoft Excel®. In B, single replicates are shown (n = 4), the coloured lines were fitted using the parameters received from the Dubinin-Astakhov model (DAM) (Microsoft Excel®, GraphPad Prism 5). (R^2 = coefficient of determination).

Table 5.2: Distribution coefficients (log K_{wMWCNT}) ± standard deviation and fitting parameters ± standard error of the sorption isotherms (Dubinin-Astakhov model, DAM) describing the distribution of ^{14}C-triclocarban between aqueous solution and dispersed wMWCNT in three different concentrations (100, 400 and 1000 µg L^{-1}). DAM was applied using GraphPad Prism 5 (USA). (R^2: coefficient of determination).

wMWCNT conc. [µg L^{-1}]	distribution coefficient	fitting parameters from DAM			
	log K_{wMWCNT}	log Q^0 [µg kg^{-1}]	E [J mol^{-1}]	b	R^2
100	6.75 ± 0.24	7.55 ± 0.19	11.31 ± 2.46	2.95 ± 3.16	0.33
400	6.96 ± 0.21	8.15 ± 1.14	10.01 ± 13.09	0.86 ± 1.33	0.68
1000	7.36 ± 0.44	7.47 ± 0.02	16.24 ± 0.27	5.29 ± 0.75	0.94

5.4.2 Effects of wMWCNT

The wMWCNT toxicity tests met all the validity criteria prescribed by the OECD Guideline 201. Regarding the green alga *C. reinhardtii*, no effects were observed for both endpoints (yield, growth rate) in the tested concentration range of 0.1 to 16 mg wMWCNT L^{-1} and the slope of the concentration-response relationship was not significantly different from zero (Fig. 5.5 – A/B). In the case of *R. subcapitata*, no effects could be detected up to a wMWCNT concentration of 2 mg L^{-1}. Only a nanomaterial concentration above 4 mg L^{-1} (LOEC, yield, Tab. 5.3) showed a significantly different yield of algal cells compared to the control. On the other hand, the growth rate was significantly influenced above a wMWCNT concentration of 8 mg L^{-1}. The slope of the dose response relationship for the lower wMWCNT concentrations (Fig. 5.5 - C) was not significantly different to zero. However, at higher nanomaterial concentrations (Fig. 5.5 - D) cell counts decreased above 4 mg L^{-1} and the slope of relationship was significant different to zero. Therefore, an EC_{50} of 6.9 mg L^{-1} and 21.1 mg L^{-1} could be reliably determined for the endpoints yield and growth rate of algae, respectively.

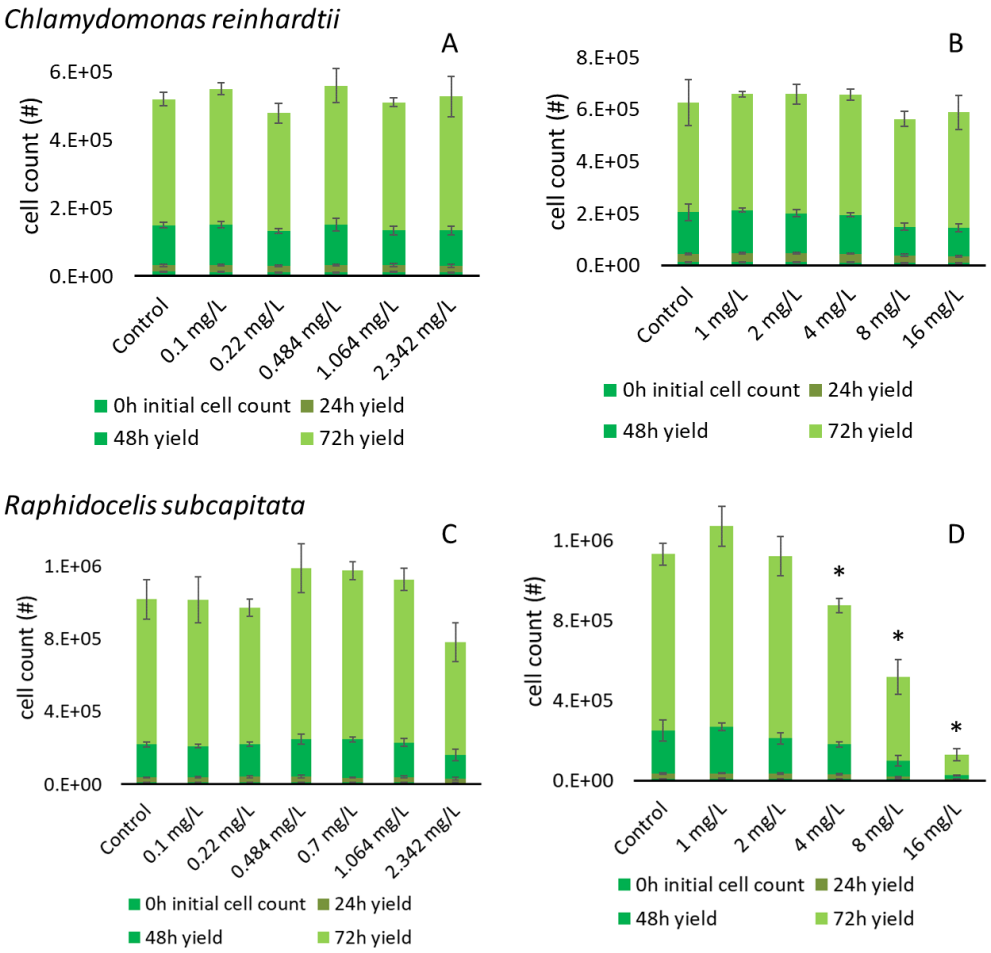

Figure 5.5: Toxicity of wMWCNT to green algae *Raphidocelis subcapitata* (A, B) and *Chlamydomonas reinhardtii* (C, D) at low (left panels A and C) and high (B and D) wMWCNT concentrations. A wMWCNT concentration range from 0.1 to 16 mg L^{-1} was tested. Algal cell count (yield per time point, mean of n = 3 and standard deviations) is plotted against nanomaterial concentration. Investigated time units were 0, 24, 48 and 72 hours. Data sets were evaluated using ToxRat® and asterisk show significant differences to control samples for yield end point.

In the *Daphnia* acute test, all required validity criteria were met. No acute toxicity of wMWCNT to *D. magna* in the presence of food was determined, since after 48 h no acute effects were detected within the tested concentration range (0.1 to 32 mg L^{-1}). The slope of the relationship from concentration to response showed no significant difference to zero. In the test with absence of food, the following 48 h lethal concentration ($LC_{10/20/50}$) values were obtained: 6.3 mg L^{-1} (2.8 - 9.8 mg L^{-1}), 11.4 mg L^{-1} (6.9 - 18.0 mg L^{-1}) and 35.4 mg L^{-1} (21.6 - 104.7 mg L^{-1}). Values in parentheses reveal 95% confidence intervals. The threshold values after 48 h were 8 mg L^{-1} and 16 mg L^{-1} for NOEC and LOEC, respectively. The slope of the relationship in the test approach without food was significantly different to zero but 95% confidence intervals showed a large range, since an effect of only 50% was achieved in the highest tested wMWCNT concentration of 32 mg L^{-1} (Fig. 5.6).

Table 5.3: Effect concentrations (72 h) for the exposure of green algae *Chlamydomonas reinhardtii* and *Raphidocelis subcapitata* to various wMWCNT concentrations (mg L^{-1}). Yield and growth rate were investigated for endpoints. $EC_{10/20/50}$: effective concentration for 10/20/50% reduction; NOEC: no observed effect concentration; LOEC: lowest observed effect concentration. (LCL-UCL): lower 95% confidence limit to upper 95% confidence limit.

C. reinhardtii	EC_{10} [mg L^{-1}] (LCL-UCL)	EC_{20} [mg L^{-1}] (LCL-UCL)	EC_{50} [mg L^{-1}] (LCL-UCL)	NOEC [mg L^{-1}]	LOEC [mg L^{-1}]
Yield	0.0 n.d.	0.0 n.d.	0.0 n.d.	0.0	0.0
Growth rate	n.d. n.d.	n.d. n.d.	n.d. n.d.	≥ 16.0	> 16.0
R. subcapitata	EC_{10} [mg L^{-1}] (LCL-UCL)	EC_{20} [mg L^{-1}] (LCL-UCL)	EC_{50} [mg L^{-1}] (LCL-UCL)	NOEC [mg L^{-1}]	LOEC [mg L^{-1}]
Yield	2.7 (1.8-4.0)	3.7 (2.5-5.4)	6.9 (4.3-10.8)	2.0	4.0
Growth rate	6.4 (5.1-8.2)	9.7 (7.6-12.3)	21.1 (14.7-29.8)	4.0	8.0
D. magna	EC_{10} [mg L^{-1}] (LCL-UCL)	EC_{20} [mg L^{-1}] (LCL-UCL)	EC_{50} [mg L^{-1}] (LCL-UCL)	NOEC [mg L^{-1}]	LOEC [mg L^{-1}]
+ food	11.4 n.d.	75.0 n.d.	n.d n.d.	≥ 32.0	> 32.0
- food	6.3 (2.8-9.8)	11.4 (6.9-18.0)	35.4 (21.6-104.7)	8.0	16.0

n.d.: not determined due to mathematical reasons or inappropriate data

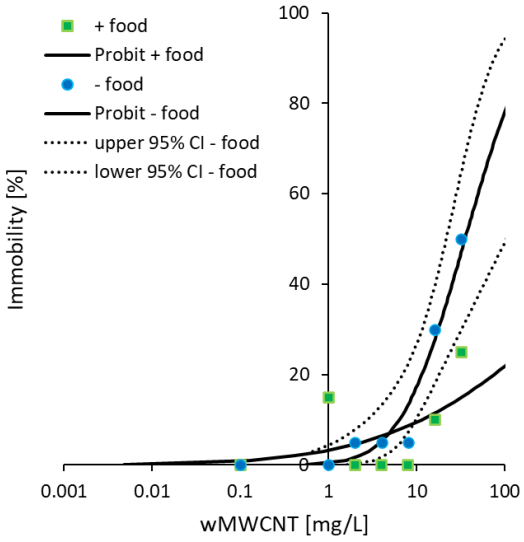

Figure 5.6: Dose response curves (DRC) after a test on acute immobilization (%) of *D. magna* at different wMWCNT concentrations in the presence (green squares) and absence of food (blue circles) over 48 hours. Data points show the mean of four replicates. Solid lines demonstrate the Probit fit of DRC. Dotted lines show the lower and upper 95% confidence intervals for the – food scenario. For the + food scenario no 95% confidence intervals could be determined by using ToxRat®.

5.4.3 'Trojan-horse' effects

5.4.3.1 Green algae

The testing of TCC_{nom} alone revealed a dose response relationship for both investigated green algae (Fig. 5.7). For *C. reinhardtii*, the 72 h EC_{50} was 22.1 µg TCC L^{-1} and NOEC and LOEC values were 10.0 µg TCC L^{-1} and 15.0 µg TCC L^{-1}, respectively. In the TCC_{nom} + wMWCNT scenario, EC_{50}, NOEC and LOEC values were slightly shifted to 29.1 µg TCC L^{-1}, 10 µg TCC L^{-1} and 15 µg TCC L^{-1}, respectively (Fig. 5.7 - A and Tab. 5.4). Considering the maximum adsorption capacity Q^0, we calculated the freely dissolved TCC concentrations ($TCC_{fDissolved}$, Eq. 5.5). The corresponding dose-response curve (Fig. 5.7 - B) revealed a slightly higher TCC toxicity (72 h EC_{50}: 26.9 µg TCC L^{-1}, NOEC: 7.0 µg TCC L^{-1}, LOEC: 12.0 µg TCC L^{-1}) compared to the TCC_{nom} + wMWCNT scenario, but a lower TCC toxicity compared to TCC_{nom} in absence of the nanotubes (Fig. 5.7 - B). No interference was observed for confidence intervals of effect concentrations (Tab. 5.4), indicating that there is a statistically significant difference between the three tested scenarios. Thus, regarding *C. reinhardtii* the addition of 100 µg wMWCNT L^{-1} reduced the toxicity of TCC.

In case of *R. subcapitata* a 72 h EC_{50} of 36.5 µg TCC L^{-1} and a NOEC and LOEC of 15.0 µg TCC L^{-1} and 22.0 µg TCC L^{-1}, respectively, were achieved for the scenario with TCC_{nom} alone. In presence of wMWCNT the toxicity of TCC was unchanged (72 h EC_{50}: 35.4 µg TCC L^{-1}, Tab. 5.4), but with respect to the freely dissolved concentration ($TCC_{fDissolved}$, Fig. 5.7 - D) toxicity increased significantly (72 h EC_{50}, NOEC and LOEC: 32.4, 13.0 and 19.0 µg TCC L^{-1}, respectively).

All required validity criteria were met. No significant differences between solvent control and growth control were detected. The regressions revealed significant results, i.e., the slopes of the dose-response relationships were significantly different from zero.

Figure 5.8 shows the results from the algal growth inhibition test with different wMWCNT concentrations and a fixed TCC concentration of 51 µg L^{-1} and 60 µg L^{-1} for the green algae *Chlamydomonas reinhardtii* and *Raphidocelis subcapitata*, respectively. TCC alone inhibited algal growth (cf. Fig. 5.8, PC TCC) but the effect decreased with increasing wMWCNT concentrations. The respective mean growth rate achieved within the test period was 1.5 d^{-1} and 1.4 d^{-1} for *C. reinhardtii* and *R. subcapitata*. All validity criteria were achieved.

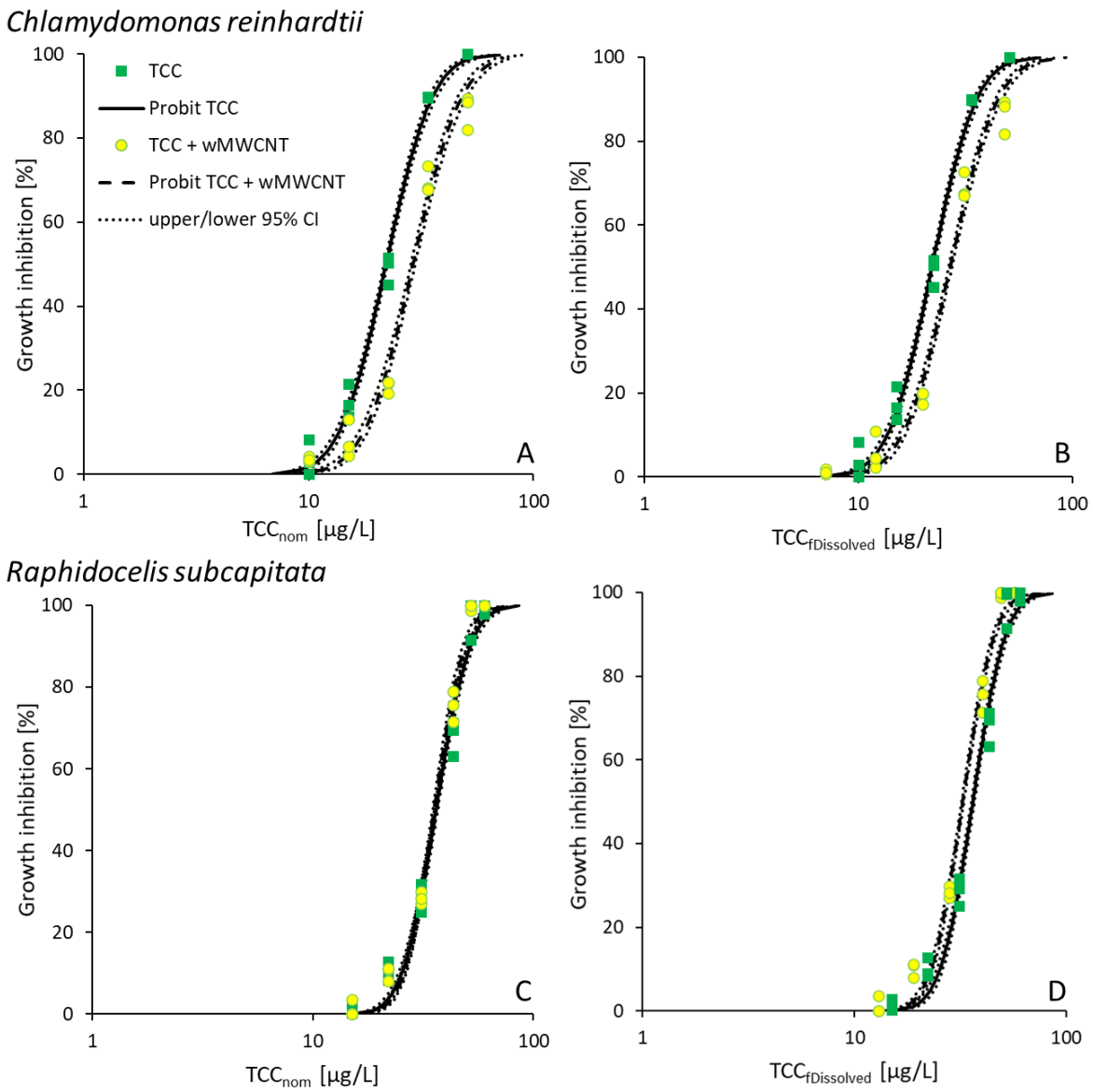

Figure 5.7: Dose response curves (DRC) after investigating growth inhibition (%) of different triclocarban (TCC) concentrations in the presence (yellow circles) and absence of 100 µg wMWCNT L^{-1} (green squares) to the green algae *Chlamydomonas reinhardtii* (A, B) and *Raphidocelis subcapitata* (C, D) over 72 hours. Growth inhibition was plotted against nominal TCC concentration (A, C) and against the freely dissolved TCC concentration (B, D). Data points show single values of three replicates. Solid and dashed lines illustrate the Probit fit of DRC. Dotted lines show the lower and upper 95% confidence intervals calculated by ToxRat®.

Compared to the negative control, the green algae *C. reinhardtii* showed a significantly inhibited cell yield after 24, 48 and 72 h exposure with TCC in presence of 0.1 to 0.7 mg wMWCNT L^{-1}. For higher wMWCNT concentrations (1.064 mg L^{-1} and 2.342 mg L^{-1}) this effect disappeared. In contrast to *C. reinhardtii*, the cell yield for *R. subcapitata* did not show a significant difference between control and treatment after 24 h along the applied nanomaterial concentrations. But after 48 and 72 h, the cell yield in treatments in the presence of 0.1 to 0.7 wMWCNT L^{-1} was decreased significantly compared to the controls. In the presence of 1.064 mg wMWCNT L^{-1} no significant differences in yield

compared to the control were observed at no time. The highest wMWCNT concentration revealed a significant difference compared to the control after 48 h, but this difference disappeared after 72 h. In addition, a stronger growth rate (0.25, 0.34, 1.12 and 1.28 d^{-1}) was observed for *P. subcapitata* in the wMWCNT concentrations of 0.1 to 0.7 mg L^{-1}, compared to *C. reinhardtii* (0.04, 0.17, 0.51 and 0.82 d^{-1}). No differences in growth rate (1.4 d^{-1}) at wMWCNT concentrations of 1.064 and 2.342 mg L^{-1} were monitored for both investigated green algae. In summary, the toxicity of TCC to green algae was significantly reduced by the addition of dispersed wMWCNT in concentrations ≥ 1.064 mg L^{-1}.

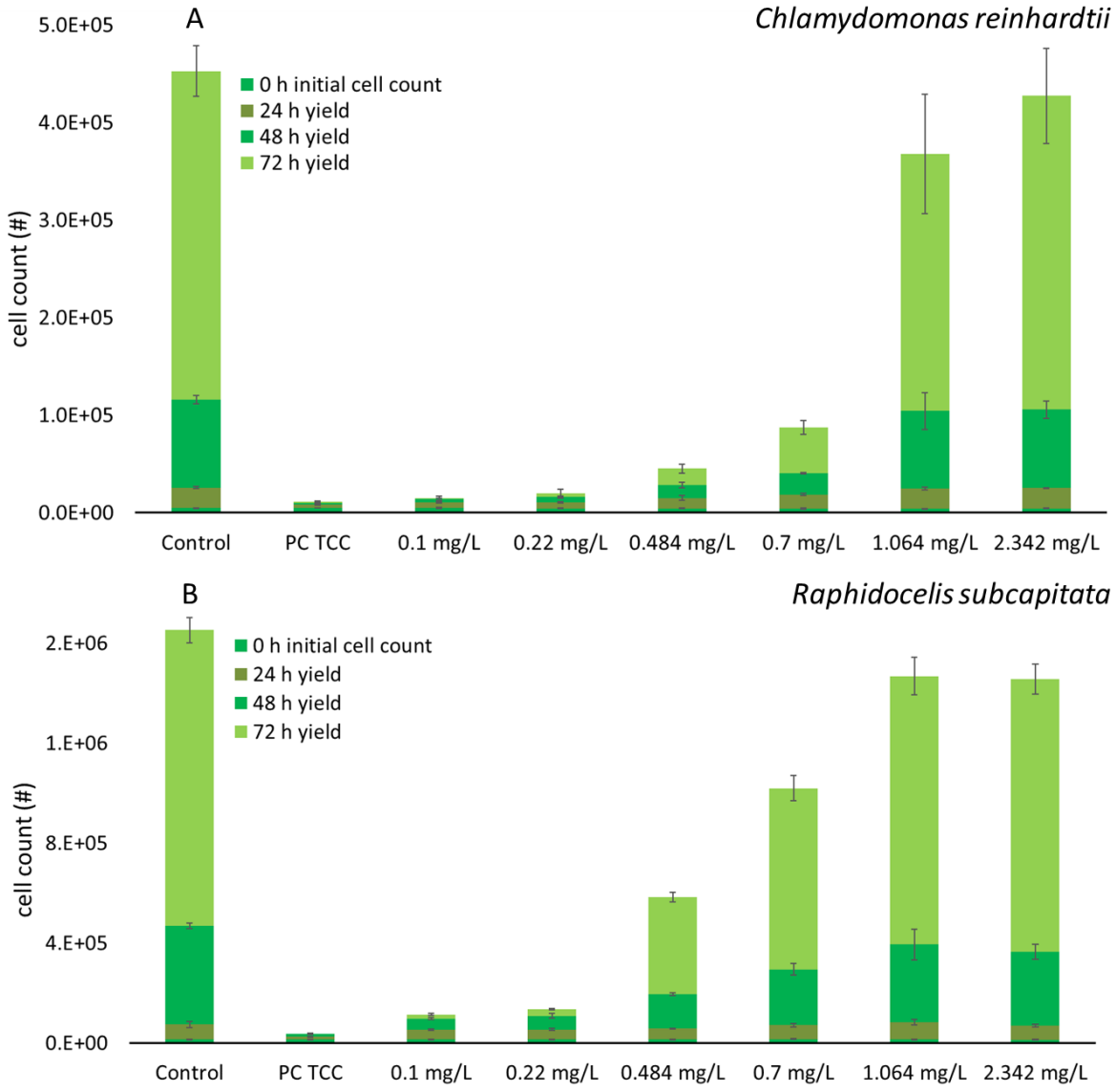

Figure 5.8: Algal growth inhibition test - investigating the effect of various wMWCNT concentrations (mg L^{-1}) on the toxicity of triclocarban (TCC) to green algae *Chlamydomonas reinhardtii* (A) and *Raphidocelis subcapitata* (B). Nominal TCC concentration was 51 µg L^{-1} for *C. reinhardtii* and 60 µg L^{-1} for *R. subcapitata*. The obtained yield of algal cells after 0, 24, 48 and 72 hours is given. PC TCC: positive control of TCC without the application of wMWCNT. Whiskers indicate standard deviation on the mean of three replicates.

5.4.3.2 Daphnids

The test on immobilization using *D. magna* revealed a dose-dependent toxicity for TCC_{nom} alone with a 48 h EC_{50} of 20.6 µg TCC L^{-1} and threshold values of 11.0 µg TCC L^{-1} and 17.0 µg TCC L^{-1} for NOEC and LOEC, respectively (Tab. 5.4). The addition of 100 µg wMWCNT L^{-1} led to a leftward shift of the dose-response curve (Fig.5. 9 - A) and therefore indicated a higher toxicity of TCC_{nom} toward *D. magna* in presence of the investigated nanomaterials, resulting in a 48 h EC_{50} of 16.9 µg TCC L^{-1} in this scenario (TCC_{nom} + wMWCNT) and with respect to the freely dissolved TCC concentration in 13.5 µg TCC L^{-1}. Due to the large ranges of 95% confidence intervals obtained for the scenarios (TCC_{nom} and TCC_{nom} + wMWCNT), no significant difference was identified. However, the 48 h EC_{50} of $TCC_{fDissolved}$ scenario was significantly lower compared to that value obtained in the TCC_{nom} alone scenario. The validity criteria required by OECD Guideline 202 were achieved in all scenarios. No significant differences in immobilization between control and solvent control were determined. In each scenario, a statistically significant concentration-effect relationship could be established, i.e., the slope of the DRC was significantly different from zero.

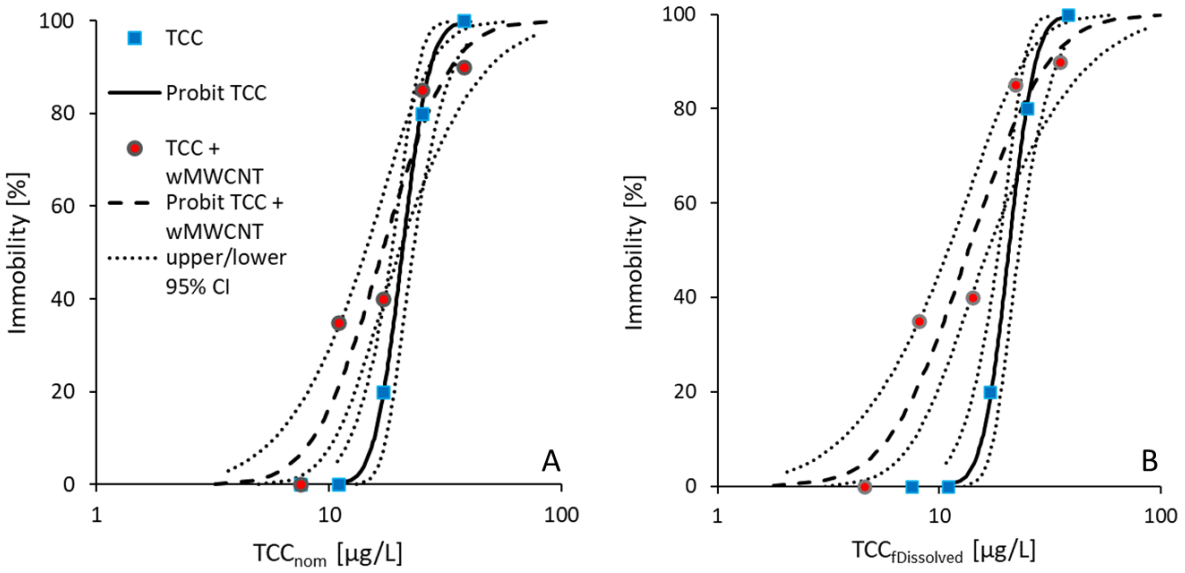

Figure 5.9: Dose response curves (DRC) after investigating acute immobilization (%) of *D. magna* at different triclocarban (TCC) concentrations (nominal, µg L^{-1}) in the presence (red circles) and absence (blue squares) of 100 µg wMWCNT L^{-1} over 48 hours. Immobilization (%) was plotted against nominal TCC concentration (A) and against the freely dissolved TCC concentration (B). Data points show the mean of four replicates. Solid and dashed line reveal the Probit fit of DRC. Dotted lines represent the 95% confidence intervals calculated using ToxRat®.

Table 5.4: Summary of toxicological endpoints for green algae *C. reinhardtii* and *R. subcapitata* and crustacean *D. magna* in triclocarban (TCC, µg L^{-1}) effect studies in presence (+ wMWCNT) and absence of wMWCNT. TCC_{nom} represents the nominal applied TCC concentration to the tests, whereas $TCC_{fDissolved}$ stands for the calculated fraction of freely dissolved TCC in the test system with wMWCNT. The listed $EC_{10/20/50}$ (EC = effect concentration) gives the TCC concentration at which 10, 20 and 50% effect occurs. NOEC: no observed effect concentration; LOEC: lowest observed effect concentration. For green algae, the inhibition of growth rate after 72 h was investigated as endpoint. In case of *D. magna*, immobility after 48 h was recorded. L/UCL: lower and upper confidence limit.

C. reinhardtii	EC_{10} [µg L^{-1}] (LCL-UCL)	EC_{20} [µg L^{-1}] (LCL-UCL)	EC_{50} [µg L^{-1}] (LCL-UCL)	NOEC [µg L^{-1}]	LOEC [µg L^{-1}]
TCC	13.7 (13.1 – 14.1)	16.1 (15.6 – 16.5)	22.1 (21.7 – 22.5)	10.0	15.0
TCC_{nom} + wMWCNT	17.5 (16.7 – 18.3)	20.9 (20.1 – 21.5)	29.1 (28.5 – 29.7)	10.0	15.0
$TCC_{fDissolved}$ + wMWCNT	16.0 (15.4 – 16.6)	19.1 (18.6 – 19.7)	26.9 (26.4 – 27.3)	7.0	12.0
R. subcapitata	EC_{10} [µg L^{-1}] (LCL-UCL)	EC_{20} [µg L^{-1}] (LCL-UCL)	EC_{50} [µg L^{-1}] (LCL-UCL)	NOEC [µg L^{-1}]	LOEC [µg L^{-1}]
TCC	26.1 (25.8 – 26.4)	29.3 (29.0 – 29.6)	36.5 (36.1 – 37.0)	15.0	22.0
TCC_{nom} + wMWCNT	25.7 (24.9 – 26.4)	28.7 (28.0 – 29.3)	35.4 (34.9 – 35.9)	15.0	22.0
$TCC_{fDissolved}$ + wMWCNT	22.9 (22.3 – 23.4)	25.8 (25.3 – 26.2)	32.4 (32.0 – 32.8)	13.0	19.0
D. magna	EC_{10} [µg L^{-1}] (LCL-UCL)	EC_{20} [µg L^{-1}] (LCL-UCL)	EC_{50} [µg L^{-1}] (LCL-UCL)	NOEC [µg L^{-1}]	LOEC [µg L^{-1}]
TCC	15.6 (12.3 – 17.5)	17.2 (14.3 – 19.0)	20.6 18.5 – 22.9)	11.0	17.0
TCC_{nom} + wMWCNT	8.5 (5.8 – 10.6)	10.8 (8.1 – 12.9)	16.9 (14.3 – 20.0)	7.5	11.0
$TCC_{fDissolved}$ + wMWCNT	5.9 (3.6 – 7.7)	7.8 (5.4 – 9.8)	13.5 (11.0 – 16.6)	4.6	8.1

5.5 Discussion

5.5.1 Adsorption of TCC on wMWCNT

The linear adsorption coefficients for the distribution of TCC between aqueous phase and wMWCNT (log K_{wMWCNT}) are listed in Tab. 5.2. In this study, log K_{wMWCNT} values of 6.75, 6.96 and 7.36 at wMWCNT concentrations of 100, 400 and 1000 µg wMWCNT L^{-1}, respectively, were shown to be very similar due to the overlap of the respective standard deviations (Tab. 5.2). Since nanomaterials were introduced into the test system for the determination of K_{wMWCNT}, the standard deviations were higher than those for K_{POM} (test system without wMWCNT, see Tab. 5.2). Dispersed, nonfunctionalized CNT tend to agglomerate in aqueous medium, which leads to an uneven distribution of these and thus to a more inhomogeneous test system than without nanomaterials (Glomstad et al., 2018).

The distribution coefficients obtained in this study are comparable to K_d values found in the literature for the adsorption of organic chemicals on carbon nanotubes, soot and activated carbon (Jonker and Koelmans, 2001; Chen et al., 2011; Georgi et al., 2015). Hennig (2019) already investigated adsorption of TCC on pristine MWCNT (1 mg L^{-1}) in different aqueous phases (log K_{MWCNT} range: 7.48 to 7.70) and revealed a log K_{MWCNT} value of 7.60 in OECD test medium used for algal growth inhibition test. Since the K_d values from our study are slightly lower than the values of Hennig (2019) for pristine MWCNT, we assume that weathering of our nanomaterials and the associated changes in surface structure has an influence on the strength of sorption. However, an investigation of weathered and nonweathered MWCNT using TGA and FTIR could not confirm any differences between the material surfaces (see chapter 2).

The abovementioned log K_d values for adsorption of TCC on wMWCNT indicate an even stronger sorption behavior compared to adsorption of some polycyclic aromatic hydrocarbons and some pharmaceuticals on MWCNT with log K_d values below 5 (Yang et al., 2006; Oleszczuk et al., 2009). It can be assumed that TCC adsorption on MWCNT is due to the fact that the high-energy method used to disperse the nanomaterials led to MWCNT being present mainly in single strands or loose small agglomerates, which consequently increased the specific surface area of the MWCNT and thus the number of available sorption sites (Chen et al., 2011). Likewise, a strong sorption affinity for TCC has already been shown on sewage sludge and soil (Wu et al., 2009; Wick et al., 2011).

Since the adsorption of hydrophobic organic chemicals (HOC's) to CNT is not considered a linear process, a nonlinear model (DAM) was further adapted to the data set of the sorption study. Nonlinear adsorption models have been used before to describe the sorption of HOC's to carbonaceous nanomaterials (CNM) (Oleszczuk et al., 2009; Zhang et al., 2012; Huffer et al., 2013). Besides the applied model, the Langmuir model and the Freundlich model were used to describe sorption processes (Velzeboer et al., 2014). The chosen model has already been proven to describe the adsorption of HOC's to MWCNT under different environmental conditions (Zhang et al., 2012; Hennig, 2019). The DAM fitted well to the data set of the high wMWCNT concentration of 1000 µg L^{-1}, but the fit accuracy decreased with decreasing CNT concentrations (Tab. 5.2). This may be due to experimental reasons because the calculated values for C_{CNT} showed more scattering at lower wMWCNT concentrations (Fig. 5.4). The calculation of C_{CNT} depends on C_{POM} since this value is variable and included twice in the calculation (Huffer et al., 2013). C_{POM} represents the concentration of TCC adsorbed to the POM piece, which is determined after TCC distributed equally between the aqueous phase, CNT and POM piece during the study. Sorption processes and upcoming agglomeration of nanomaterials may lead to a nonequal distribution of TCC and/or wMWCNT. This heterogeneity might have occurred after production of the TCC-wMWCNT solution for application prior to the setup of

single replicates, resulting in a greater effect on C_{POM} at the lower wMWCNT concentrations within the individual test system and consequently on TCC adsorption on wMWCNT (C_{CNT}). Regardless that the low quantities of wMWCNT used are tainted with a high degree of uncertainty the fit parameters for the DAM did not show any differences due to the partially very large standard errors (Tab. 5.2).

The logarithmic maximum adsorption capacity (log Q^0, Tab. 5.2) was in the range of 7.47 to 8.15 µg kg^{-1}. Since the same wMWCNT material was examined in the three tested concentration scenarios, which was dispersed in the same way in aqueous medium, concentration-independent sorption characteristics were to be expected. Due to the remarkable high standard errors of the parameters in CNT100 and CNT400 scenario, only the values obtained from the CNT1000 scenario were considered in further calculations. Like log K_{wMWCNT}, values obtained for log Q^0 are consistent with previously published literature and research. Hennig (2019) revealed logarithmic maximum adsorption capacities between 7.7 µg kg^{-1} and 8.0 µg kg^{-1} for the adsorption of TCC on pristine MWCNT. Since the values for Q^0 and K_{CNT} obtained in the study on the sorption of TCC on pristine MWCNT were the same as those obtained using wMWCNT, it can be assumed that the weathering process did not lead to any significant changes in the surface structure, as could already be shown using TGA and FTIR (see chapter 2). Studies investigating the sorption of PAH's (phenanthrene, pyrene) on functionalized and nonfunctionalized MWCNT obtained log Q^0 values between 7.7 µg kg^{-1} and 8.4 µg kg^{-1} (Zhang et al., 2012; Zindler et al., 2016).

5.5.2 Effects of wMWCNT

In the algal growth inhibition test, no effects on the green algae *C. reinhardtii*, in a wMWCNT concentration range of 0.1 to 16 mg L^{-1} were observed. *R. subcapitata* showed growth inhibition starting at a wMWCNT concentration of 4 mg L^{-1}, with the endpoint yield being more sensitive compared to the endpoint growth rate. The OECD guideline recommends a range for the test concentration, where the achieved growth inhibition is between 5% and 75%. Although the tested concentration range in our study showed a maximum growth inhibition of 38% after 72 h for the green algae *R. subcapitata*, higher wMWCNT concentrations were not used in the test. On one hand, the predicted environmental CNT concentration in surface water is in the ng L^{-1} range and therefore 5 orders of magnitude below the lowest tested wMWCNT concentration tested in this study (Gottschalk et al., 2009). And on the other hand, higher wMWCNT concentrations lead to a higher probability of agglomeration and sedimentation, which consequently does change the exposure concentration in a noncomprehensible way (Glomstad et al., 2018).

The different response of the two green algae to the exposure to wMWCNT may be related to the physical properties (structure, movement, exudates) of the individual algae. *Chlamydomonas reinhardtii*, which showed no change in growth under wMWCNT exposure, is larger than

Raphidocelis subcapitata and has two long flagella for locomotion and an eye spot for light-controlled cell movement to optimize cell nutrition at low or high light intensities (Kühnle, 1990; Kiefer et al., 1997; Fawley et al., 2006). Due to this, presumably *C. reinhardtii* was able to evade wMWCNT exposure to a certain extent by directed swimming movements, or its size offered the advantage of a larger surface area for light uptake and as a result was able to reproduce unaffected even at higher wMWCNT concentrations.

Based on the observed agglutination of algae and wMWCNT in a study which investigated wMWCNT uptake in *R. subcapitata* (see section 3.7.4 in chapter 3), it is also likely that in this study such agglutinations occurred in the nonvisible range, which could have led to an impaired ability of reproduction at higher wMWCNT concentrations for *R. subcapitata*. The inhibition of algal growth due to a shading effect by well dispersed CNT was already demonstrated and quantified by Schwab et al. (2011). In the same study, it was assumed that increased algal concentrations in CNT agglomerates could lead to changed growth conditions. Furthermore, the controls showed a lower growth rate for *C. reinhardtii* of 1.2 d^{-1} compared to the growth rate of 1.5 d^{-1} for *R. subcapitata* at similar initial cell counts of 13,500 cells mL^{-1} and 11,500 cells mL^{-1}, respectively, i.e., more aged cells were found in the approach with *R. subcapitata* over the test duration of 72 h. Since a lower integrity is expected in senescent cells (Yoo et al., 2012), it is possible that the nanomaterials interacted more with the fragile parts of the cells, which might have led to a larger effect compared to the slower-growing algae *C. reinhardtii*.

As shown in Fig. 5.5, the exposure of green alga *R. subcapitata* to weathered MWCNT at a concentration of 21.1 mg L^{-1} (14.7 – 29.8 mg wMWCNT L^{-1}) caused 50% of growth inhibition and the threshold value for the lowest observed effect was 8.0 mg L^{-1}. In a study of Schwab et al. (2011), *Chlorella vulgaris* and *Raphidocelis subcapitata* were exposed to pristine MWCNT in algal test medium, well dispersed by using an ultrasonication bath. After an exposure of 96 h, the growth of *C. vulgaris* and *R. subcapitata* was inhibited at LOEC of 0.53 mg L^{-1} and 5.5 mg L^{-1} with 50% effect concentrations (EC_{50}) of 1.8 and 20.0 mg L^{-1}, respectively (Schwab et al., 2011).

The nanomaterials used in our study are most comparable to pristine MWCNT, as neither TGA nor FTIR analysis could identify differences in surface structure between nonweathered and weathered MWCNT. Therefore, our results are consistent with those from the literature. Furthermore, Lukhele et al. (2015) observed similar values for *R. subcapitata* exposed to DWCNT (72 h EC_{50}: 17.95 mg L^{-1}). As well as *C. vulgaris*, the marine green alga *Dunaliella tertiolecta* showed a more sensitive reaction towards CNT exposure with a 96 h EC_{50} value of 0.82 mg L^{-1} (Wei et al., 2010). In contrast, our investigations revealed that *Chlamydomonas reinhardtii* responds much less sensitively to wMWCNT exposure as lowest effects are anticipated at concentrations above 16 mg L^{-1}. Since all

abovementioned effect concentrations are at least five orders of magnitude larger than the predicted environmental CNT concentration in surface waters (Gottschalk et al., 2009), very likely no risk on growth of green algae is to be expected.

In the presence of food, *D. magna* were not immobilized at a wMWCNT concentration range of 0.1 to 32 mg L^{-1}. Although the OECD Guideline 202 recommends a test series with 100% effect at the highest concentration, no higher wMWCNT concentrations were tested, due to the abovementioned reasons. An extraordinary amount of nanomaterial in the test system is comparable to the addition of several tons of sand to a lake. The subsiding sand particles will cover all organisms they encounter on their way. If these organisms are not able to escape from the sand particles, they will bury them among themselves. Such an image could be partially observed in the acute *D. magna* immobilization test investigating with high wMWCNT concentrations. In the test with food, more immobilized animals were monitored after 24 h compared to 48 h. Since the added green algae also sediment in a static system, in this approach the animals were stressed by both, wMWCNT and sinking algal particles. However, the immobilized daphnids were able to regenerate and regain their ability within 24 h to swim, most likely they were able to free themselves from the nanomaterials with the help of their swimming extremities (antennae), whereby the presence of food provided energy for the strenuous act of disentanglement. Furthermore, juvenile *Daphnia* moult every few days (1 – 2 days), which most likely led to the carapace being cleaned of adherent particles (Ebert, 2005; Smirnov, 2016). Additionally, it was shown that the presence of algae as food source facilitates excretion of nanomaterials from the gut and therefore reduces the body burden (Gillis et al., 2005; Kennedy et al., 2008; Petersen et al., 2011). Similar to our observations, Zhang et al. (2013) found algal-nanoparticle (quantum dot) aggregates, so consequently the coating of CNT with algae in our study might have reduced the friction between the test organism and the nanomaterial, resulting in reduced CNT toxicity in presence of green algae.

In contrast, the absence of food led to a significant immobilization of 5%, 30% and 50% at wMWCNT concentrations of 2 to 8 mg L^{-1}, 16 mg L^{-1} and 32 mg L^{-1}, respectively. As the control approaches show, a 48 h hunger phase has no effect on the mobility of the *Daphnia*, but without food, effects caused by CNT exposure were observed that were absent in the presence of food. The fact that a significantly higher immobilization was recorded in the absence of green algae could also be due to the starvation of the animals in this test approach. It is known that daphnids ingest CNT and that CNT main accumulation site is in the gastrointestinal tract (Petersen et al., 2009; Petersen et al., 2011; Fan et al., 2016; Bacchetta et al., 2018). Daphnids are suspension (filter) feeders and gather their food by means of a filter apparatus. Subsequently, absorbed food is passed through the gut by peristaltic contractions (Ebert, 2005). The process on utilization of putative food consumes energy that cannot be recovered

from the ingested nanomaterials. It is also possible that the pure wMWCNT (without the algal coat) could become entangled in the gastrointestinal tract, which would result in further energy-sapping intestinal movements. Additionally, *Daphnia* use one pair of antennae for locomotion, but if they become stuck by the wMWCNT and lose their function, this may also lead to increased immobilization. It is known that epithelial cells do not phagocytose particles (Ebert, 2005), but physical disruption of epithelial cells by nanoparticles was observed in the mg L^{-1} range (Leroueil et al., 2007; Nel et al., 2009; Bacchetta et al., 2018), therefore the increased immobilization might be caused by direct and indirect effects as described above.

Toxicity of pristine MWCNT was considered in previous research and ecotoxicological values on immobilization and mortality of *Daphnia magna* were reported. Zhu et al. (2009) found 48 h EC_{50} and LC_{50} of 8.7 mg L^{-1} and 22.8 mg L^{-1}, respectively. In a study of Edgington et al. (2010) 96 h LC_{50} between 1.9 mg L^{-1} and 2.8 mg L^{-1} in the presence of 2 to 19 mg DOC L^{-1} was observed, both studies indicated effects at lower MWCNT concentrations than found in our study (EC_{50}: 35.4 mg L^{-1}, Tab. 5.3). And Wang et al. (2016) found an 24 h LC_{50} of 42.5 mg L^{-1} for pristine MWCNT. In contrast, a study from 2018 revealed no effects up to a MWCNT (pristine) concentration of 50 mg L^{-1} (Bacchetta et al., 2018). However, the exposure volume here was 100 mL, which is 10 times larger than the volume of the water phase in our study. Petersen et al. (2009) found out that uptake of CNT by *Daphnia magna* depends on the volume of the water phase used for exposure, therefore it could be assumed that the medium volume used has an influence on CNT toxicity as well. The larger volume offers more space to escape the sinking or already deposited nanomaterials. Ultimately, the effect concentrations determined in this study are in line with the data already published. Since the abovementioned values are in the mg L^{-1} range, but the environmental concentration for surface waters is estimated to be six orders of magnitude lower, no acute effects of MWCNT on *Daphnia magna* are expected.

5.5.3 'Trojan-horse' effects

5.5.3.1 Green algae

Triclocarban inhibited growth of *C. reinhardtii* and *R. subcapitata* with 72 h EC_{50} values of 22.1 µg TCC L^{-1} and 36.5 µg TCC L^{-1}, respectively (Tab. 5.4). Thus, the calculated effect concentrations of TCC in this study are in the same order of magnitude, as it was already reported for green algae. Research by Yang et al. (2008) revealed a 72 h IC_{50} of 17 µg TCC L^{-1} and Tamura et al. (2013) showed a 72 h EC_{50} of 29 µg TCC L^{-1} (95% CI: 25 – 35 µg TCC L^{-1}) for *R. subcapitata*. The IC_{50} is the mean inhibition concentration and can be compared directly with the EC_{50} from algal growth inhibition test. In previous studies, we have also investigated the toxicity of TCC to *Desmodesmus subspicatus* and obtained a 72 h EC_{50} value of 21 µg TCC L^{-1} (Hennig, 2019). Since the compared species belong to the group of green algae, a similar reaction towards TCC exposure was expected.

Because wMWCNT concentrations lower than 2 mg L^{-1} have no effect on growth of green algae and since we showed that the addition of 1 mg MWCNT L^{-1} to a TCC test series in an algal growth inhibition test completely eliminated TCC toxicity (Hennig, 2019), we assumed that the addition of 100 µg wMWCNT L^{-1} might also positively influence the growth of green algae in the presence of toxic TCC concentrations. In case of *C. reinhardtii* our assumption was confirmed. In the presence of wMWCNT, the determined EC_{50} values (Tab. 5.4) showed that the adverse effect of TCC was significantly reduced by 24% at the highest TCC test concentration compared to the TCC_{nom} alone scenario (Fig. 5.7 - A). But for *R. subcapitata*, a significantly stronger inhibition of algal growth at the highest TCC test concentration in presence of wMWCNT (7%) was observed (Fig. 5.7 - C). Even more, when based on the freely dissolved fraction of TCC, the dose-response curve is shifted to the left, indicating higher toxicity in the presence of nanomaterials (Fig. 5.7 - D). However, independent of the test approach, the effect concentrations shown (Tab. 5.4) are all within a range assumed for the toxicity of TCC on green algae as described above.

In contrast to *R. subcapitata*, *C. reinhardtii* reacted more sensitively to the exposure with TCC alone (Tab. 5.4) while tolerating higher wMWCNT concentrations (Fig. 5.5 - B/D). It can be assumed that adsorption of TCC to the added wMWCNT had a positive effect on the growth of *C. reinhardtii*, although, the results of the adsorption study (see section 5.4.1) showed that at a nanomaterial concentration of 100 µg L^{-1} the applied TCC is not efficiently adsorbed on the nanotubes (0.029 µg TCC adsorbs onto 1 µg wMWCNT). Therefore, between 68% and 94% of the nominal TCC concentration was freely dissolved and thus bioavailable in the test with *C. reinhardtii*. In addition, the wMWCNT adsorbed TCC fraction might have followed different mechanisms. Either the wMWCNT-TCC complexes were not absorbed by *C. reinhardtii* in the first place (Fig. 5.10, path 2), or algal associated (either absorbed in or adhered onto the cell) wMWCNT-TCC sorbates retained the TCC (Fig. 5.10, path 1b or 2b). Another possibility is that desorbed TCC was rapidly absorbed and degraded to nontoxic metabolites by the green algae, which is in line with the finding that 15 - 20% desorption of diuron from CNT occurred in the presence of algae (Schwab et al., 2014). However, the toxicity decrease in case of *C. reinhardtii* was small (cf., Tab. 5.4).

The increase in toxicity in the presence of wMWCNT (100 µg L^{-1}) for *R. subcapitata* may be because the investigated nanomaterial has a generally higher influence on this green alga as shown above (Fig. 5.5 - B/D). Additionally, the freely dissolved TCC concentration in the test with *R. subcapitata* was between 80% and 95% of the nominal test concentration, which indicates a higher TCC exposure concentration compared to *C. reinhardtii*. On the other hand, desorption (inside or outside the cell) of TCC in the ternary test system with *R. subcapitata* might be increased compared to *C. reinhardtii* (Fig. 5.10, path 1a or 2a). In a study of Suzuki et al. (2018), it was revealed that *R. subcapitata* has more

lipid biosynthesis related genes than *C. reinhardtii*, therefore a higher fat content in *R. subcapitata* might have promoted the desorption of TCC from wMWCNT. Furthermore, it is known that green algae from the *Selenastraceae* family form a conspicuous mucilage layer containing proteins that have been shown to interact with nanoparticles. Possibly, these might have led to additional sorption sites and thus increased TCC concentration in the immediate vicinity of the algae (Leppard, 1995; Bellingeri et al., 2019). Although in our study the wMWCNT were initially loaded with TCC, desorption from the wMWCNT is likely, as various studies have already shown that the adsorption of organic chemicals on CNT is reversible (Pan and Xing, 2008; Yan et al., 2008; Oleszczuk et al., 2009). An enhanced toxicity of diuron in the presence of a MWCNT concentration of 10 mg L^{-1} towards *Chlorella vulgaris* was reported by Schwab et al. (2013). The lower adsorption capacity of diuron with a Freundlich coefficient K_f of maximum $10^{6.28}$ µg/kg (µg/L)$^{-n}$ compared to TCC with a K_f value of $10^{10.49}$ µg/kg (µg/L)$^{-n}$ (Hennig, 2019) presumably led to the desorption and bioavailability of diuron at such high MWCNT concentrations. Nevertheless, the dose-response relationships of TCC_{nom} alone and TCC_{nom} + wMWCNT as well as $TCC_{fDissolved}$ + wMWCNT for *R. subcapitata*, despite significantly different effect concentrations, showed a high degree of similarity to each other (Tab. 5.4).

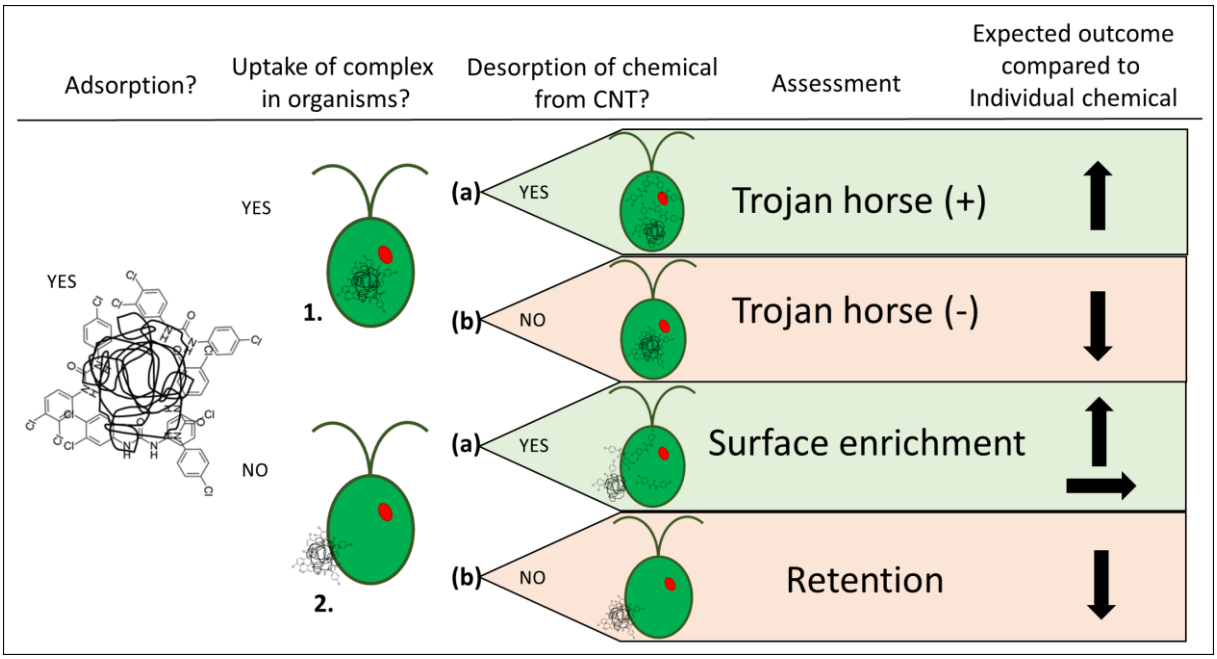

Figure 5.10: Considerations about possible mechanisms after the mixed exposure of weathered multi-walled carbon nanotubes (wMWCNT) and the biocide triclocarban towards green algae. The extent of sorption depends on the ratio of wMWCNT to TCC in aqueous phase: low concentrations of nanomaterial lead to incomplete sorption of TCC, i.e., freely dissolved TCC is still bioavailable. Arrows represent: ↑ enhanced toxicity expected, ↓ decreased toxicity expected and → unaltered toxicity expected. Self-made illustration based on Naasz et al. (2018).

Therefore, and since *R. subcapitata* showed no significant difference in growth rate compared to control samples, when wMWCNT concentrations above 1 mg L^{-1} were added to the highest TCC test

concentration (Fig. 5.8 - B) (i.e., in case of association of CNT-TCC sorbates and the desorption of TCC in the immediate vicinity of algae, toxicity would be increased especially at higher CNT concentrations), it should be considered that the influence of the presence of 100 µg wMWCNT L^{-1} on TCC toxicity was very low to nonexistent.

Regarding the internalization of CNT into algal cells, previous studies reported penetration of cells and a strong binding of CNT to algal cells as well as single strands were detected and visualized in the cell's cytosol (Wei et al., 2010; Schwab et al., 2011; Long et al., 2012; Rhiem et al., 2015). In these studies, the investigated green algae were the freshwater species *D. subspicatus*, *Chlorella sp*., *R. subcapitata* and the marine species *Dunaliella tertiolecta*. In chapter 3 we quantified the association of wMWCNT with green algae and showed that *C. reinhardtii* significantly accumulates more nanomaterial compared to *R. subcapitata*. Therefore, a locally enhanced exposure concentration (Schwab et al., 2013) of TCC due to wMWCNT-TCC complexes attached onto the surface of *C. reinhardtii* leading to an increased toxicity, instead of the observed toxicity enhancement for *R. subcapitata*, would be plausible. However, since the cell walls of *C. reinhardtii* and *R. subcapitata* exerted a different barrier function due to different surface structures (Kiefer et al., 1997; Fawley et al., 2006; Baudelet et al., 2017), it can be assumed, that these physical differences, among others, accounted for the observed contrary effects.

Furthermore, it should be noted that the freely dissolved TCC concentration was calculated under the assumption that the presence of green algae has no influence on the adsorption of TCC onto wMWCNT. Only adsorption sites provided by the nanomaterials were considered in the abovementioned calculations. If an additional third phase, e.g., in the form of green algae is added to this two-phase test system, more complex interactions may occur which cannot be predicted or calculated. This leads to the fact that the calculation of freely dissolved TCC concentrations bear some uncertainty (Schwarzenbach et al., 2003). Since the absorption and metabolism of TCC by green algae within a few hours has already been shown (Hennig, 2019), it can be assumed that in a ternary test system not only the nanomaterial acts as a sorbent for TCC, but also the compartments of the green algae cell (Schwab et al., 2014). Predicting the sorption dynamics for such a ternary test system is therefore very difficult and should be used with caution. Another possibility is the measurement of the freely dissolved TCC concentration in the test system, which presents a different challenge (Schwab et al., 2013).

Following, the addition of different amounts of wMWCNT to the highest TCC test concentration from the algal growth inhibition test showed that at increasing nanomaterial concentrations the inhibition of green algal growth decreases (Fig. 5.8). Presumably, increasing wMWCNT concentrations led to an increased TCC adsorption and therefore to a lower bioavailability of TCC to green algae. Based on the maximum adsorption capacity (Tab. 5.2), the freely dissolved TCC concentration at a wMWCNT

concentration of 1.064 mg L^{-1} was 20 µg TCC L^{-1} and 29 µg TCC L^{-1} for *C. reinhardtii* and *R. subcapitata*, respectively. These calculated values are in the range of the LOEC. However, considering the uncertainty of extrapolations it may be also possible, that the freely dissolved concentrations were in the NOEC range, as was shown by the experimental data (Fig. 5.8). Following calculations, at the highest wMWCNT concentration, TCC was completely adsorbed onto the nanomaterials.

For the above reasons, scenario 2b in Fig. 5.10 is the most likely toxicity path for green algae. We assume that the CNT-TCC complex has not been absorbed by the algal cells and that there has been no or only minimal desorption of TCC from the nanomaterial. Due to an incomplete adsorption of TCC at a low wMWCNT concentration of 100 µg L^{-1} we assume that the presence of nanomaterials in these experiments (Fig. 5.7) had no effect on the toxicity of TCC to green algae (Fig. 5.10, path 2a). Desorption of TCC from associated or incorporated wMWCNT must therefore be low, otherwise toxicity at high CNT concentrations would have been observed (Fig. 5.8). It could also be assumed that the two-hour loading process of wMWCNT with TCC stabilized the adsorption and thereby weakened the desorption. The work of Hennig (2019) revealed that *D. subspicatus* accumulates 23% and 58% of the applied radioactivity as ^{14}C-TCC after 72 h in presence and absence of 1 mg MWCNT L^{-1}, respectively, which indicates, that TCC is less bioavailable in the presence of CNT. But since it has already been reported that organic substances desorb from CNT in the presence of algae and CNT have been detected in the cytosol of green algae, a mixture of mechanisms (Fig. 5.10) of action can most likely be assumed (Schwab et al., 2014; Rhiem et al., 2015; Naasz et al., 2018).

5.5.3.2 Daphnids

Considering toxicity of TCC in acute immobilization test on *D. magna*, the determined 48 h LC_{50} of 21 µg TCC L^{-1} is slightly higher than previously described in published research. Tamura et al. (2013) revealed a lower 48 h EC_{50} of 10 µg TCC L^{-1} (95% CI: 7 – 12 µg TCC L-1). In a study of Simon et al. (2015) different age groups of *D. magna* were investigated and 96 h EC_{50} values ranged between 13 µg TCC L^{-1} and 33 µg TCC L^{-1}, with the neonate daphnids – as used in our study - as the most sensitive ones. However, Hennig (2019) showed a 48 h EC_{50} of 21 µg TCC L^{-1} which corresponds to the herein determined effect concentration.

Further, the addition of 100 µg wMWCNT L^{-1} to variable TCC test concentrations in immobilization test revealed no significant difference compared to the test without nanomaterials, except when considering the freely dissolved TCC concentrations (Tab. 5.4). *Daphnia* have been shown to accumulate CNT on several occasions (Petersen et al., 2009; Petersen et al., 2011; Edgington et al., 2014; Cano et al., 2018), therefore it is very likely that CNT-TCC sorbates are also absorbed. The observed significant toxicity increase would only have occurred if the TCC desorbed within the

daphnids and thus reached the target site faster or in larger quantities due to the 'Trojan-horse' effect than in absence of wMWCNT (Fig. 5.10, path 1a).

The main uptake route of the molecule TCC in *Daphnia* is *via* passive diffusion, besides swallowing, of the contaminant from the water phase, into the fatty tissue of the target organism. Co-exposure to CNT leads to an increased oral uptake and ingestion of CNT-TCC complexes. Yan et al. (2017) observed a high and fast release of the antibiotic roxithromycin from MWCNT in the bile salt of crucian carp, suggesting that digestive and solubilizing juices in the intestine of *Daphnia* may also have had a desorbing effect on TCC. Meanwhile, it has also been reported that after the uptake of lipid-coated SWCNT, lipid-free SWCNT were excreted after passage through the intestine of *D. magna* and it was suspected that the *Daphnia* might have used the lipid as food source (Roberts 2007). Therefore, desorption of TCC from wMWCNT after ingestion by *Daphnia* might be possible.

Based on our results, it can be assumed that an interplay between path 1a and 1b (Fig. 5.10), dependent on the nanomaterial concentration, is most likely for the mixed toxicity of TCC and wMWCNT in *D. magna* (Naasz et al., 2018). In our study, the addition of 100 µg wMWCNT L^{-1} to a TCC test series had only a minor effect on the immobilization of *D. magna*. However, Hennig (2019) presented an acute toxic effect of 40% on immobilization in the presence of 1 mg MWCNT L^{-1} at the highest TCC test concentration of 38 µg TCC L^{-1}. Therefore, the incomplete adsorption of TCC onto wMWCNT at 100 µg L^{-1} and the desorption of TCC after ingestion of TCC-wMWCNT complexes is most likely responsible for the minimal increase in toxicity in presence of wMWCNT in our study. If the enhanced toxicity in presence of wMWCNT is derived only from the higher internalized TCC concentrations resulting from ingested wMWCNT-TCC sorbates, then at higher CNT concentrations an increased toxicity would have been expected, which was not the case in the study of Hennig (2019). Unless at higher CNT concentrations, TCC is trapped in CNT agglomerates during intestinal passage, preventing it from being bioavailable even after desorption leading to a reduced toxicity despite internalization of CNT-TCC sorbates (Fig. 5.10, path 1b). Linard et al. (2017) suggested that the reduction of bioavailability of CNM-bound PAH's is due to desorption hysteresis occurring during ingestion of CNM-PAH's complexes which may be changed by the agglomeration of the CNM's in the intestine of *Pimphales promelas*. Additionally, the co-exposure of MWCNT and diphenhydramine to *Ceriodaphnia dubia* revealed a toxicity reduction as well (Myer and Black, 2017). Further, Fang et al. (2011) observed an enhanced uptake of tri- (TBT) and dibutyltin (DBT) in *D. magna* in the presence of nano-charcoal, which was attributed to the accumulation of nano-charcoal-bound TBT and DBT. But despite an increased uptake, they found a decrease for the toxicity of TBT in the presence of nano-charcoal and an unaltered toxicity for DBT. Therefore, a 'Trojan-horse' effect is very likely in the case

of *Daphnia magna*, where the amount of nanomaterial determines the bioavailability of the desorbed TCC fraction.

5.6 Conclusion and outlook

Acute effects of MWCNT on green algae and crustacean are expected in the mg L^{-1} range, concluding no risk with the current magnitudes lower predicted environmental concentration. In this study, we have shown that weathered MWCNT adsorb the biocide TCC almost as strongly as pristine MWCNT. MWCNT concentrations above 1 mg L^{-1} significantly reduce the freely dissolved TCC concentration by adsorption, and thus decrease TCC toxicity for green algae. The underlying mechanisms of action are different for green algae and daphnids, as each has a different type of interaction with the nanomaterials and the CNT-TCC sorbates. A true 'Trojan-horse' effect was suspected for *Daphnia*, since CNT-TCC associates are absorbed orally by them. Whether TCC desorbs from the CNT after uptake or remains strongly adsorbed was not investigated and therefore cannot be distinguished. In contrast to daphnids, sorption of the CNT-TCC complex to the algal surface is the dominant mechanism instead of incorporation. Based on our results, no significant desorption of TCC from the CNT-TCC associates occurred in the presence of green algae.

The adsorption of TCC to wMWCNT does not follow a black and white pattern and is strongly dependent on the concentration of nanomaterial and other competing phases in the test system. Therefore, in most cases both CNT-bound TCC and freely dissolved TCC are present in the system, which poses special challenges and should be the concern of further research (Linard et al., 2017; Naasz et al., 2018). Generally, calculated freely dissolved contaminant concentrations should always be handled with caution especially when assessing the toxicity in presence of carbon based nanomaterials. Many factors, such as sorption, agglomeration and sedimentation, inclusion of contaminants in agglomerates, uptake and degradation of contaminant and/or nanomaterial etc., play a decisive role in the research of mixed toxicities of organic chemicals and nanomaterials, which is why this topic requires further attention. Although no concerning increase in TCC toxicity in presence of CNT has been observed, the accumulation of organic chemicals as 'Trojan-horse' riders along the food chain cannot be excluded.

5.7 Supplementary information (SI)

5.7.1 Test media composition

Table 5.5: Composition of the aqueous phase in the test for the adsorption of triclocarban on weathered MWCNT. The medium is a deviation of the OECD algal growth medium from OECD Guideline No. 201 (OECD, 2006). For sterilisation, the stock solutions were either filtered using a membrane filtration (pore diameter: 0.2 µm) or by autoclaving (120 °C, 15 min) and stored at 4 °C in the dark.

Nutrient	Concentration in stock solution
Stock solution 1: macro nutrients	
NH_4Cl	1,50 g/L
$MgCl_2*6H_2O$	1,20 g/L
$CaCl_2*2H_2O$	1,80 g/L
$MgSO_4*7H_2O$	1,50 g/L
KH_2PO_4	0,16 g/L
Stock solution 2: iron	
$FeCl_3*6H_2O$	64 mg/L
$Na_2EDTA*2H_2O$	100 mg/L
Stock solution 3: trace elements	
H_3BO_3	185 mg/L
$MnCl_2*4H_2O$	415 mg/L
$ZnCl_2$	3 mg/L
$CoCl_2*6H_2O$	1,5 mg/L
$CuCl_2*2H_2O$	0,01 mg/L
$Na_2MoO_4*2H_2O$	7 mg/L
Stock solution 4: bicarbonate	
$NaHCO_3$	50 g/L
Stock solution 5: buffer	
KH_2PO_4	18.15 g/L
K_2HPO_4	11.67 g/L

Instructions for the preparation of 1 L medium: Put 500 mL of deionized water into a volumetric flask and add 10 mL of stock solution 1 and 5. Subsequently pipette 1 mL each of stock solution 2, 3 and 4 in and made up to 1 L with deionized water. The medium was aerated using an air pump at least for some hours before use.

5.7.2 Calibration curves to determine algal density

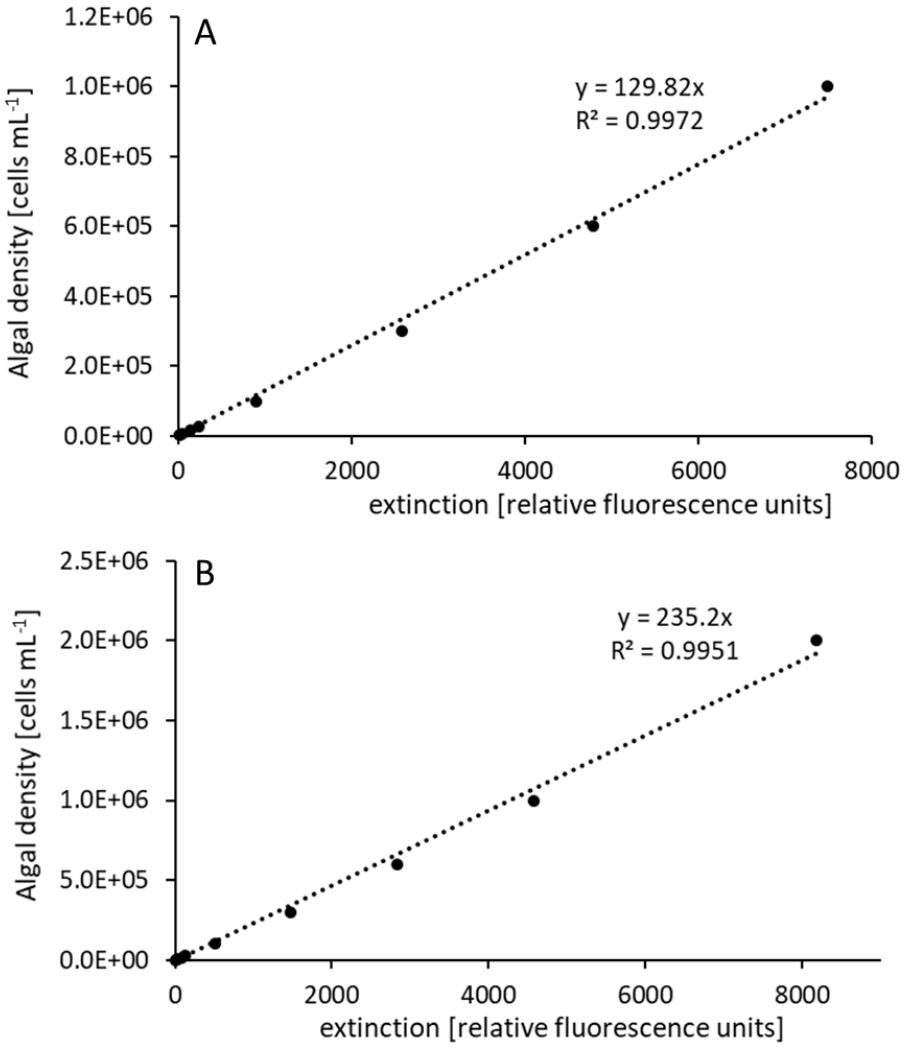

Figure 5.11: Calibration curves for the conversion of measured extinction (excitation wavelength: 485 nm, emission wavelength: 685 nm) to algal density (cells mL^{-1}) for the green algae *Chlamydomonas reinhardtii* (A) and *Raphidocelis subcapitata* (B). Enumeration of algal cells was performed in the test medium described in Tab. 5.5. (R^2 = coefficient of determination).

5.8 References

Ajayan, P.M., 1999. Nanotubes from Carbon. Chem Rev 99, 1787-1800.

Bacchetta, R., Santo, N., Valenti, I., Maggioni, D., Longhi, M., Tremolada, P., 2018. Comparative toxicity of three differently shaped carbon nanomaterials on Daphnia magna: does a shape effect exist? Nanotoxicology 12, 201-223.

Barra, G., Guadagno, L., Vertuccio, L., Simonet, B., Santos, B., Zarrelli, M., Arena, M., Viscardi, M., 2019. Different Methods of Dispersing Carbon Nanotubes in Epoxy Resin and Initial Evaluation of the Obtained Nanocomposite as a Matrix of Carbon Fiber Reinforced Laminate in Terms of Vibroacoustic Performance and Flammability. Materials 12.

Baudelet, P.H., Ricochon, G., Linder, M., Muniglia, L., 2017. A new insight into cell walls of Chlorophyta. Algal Res 25, 333-371.

Baun, A., Sorensen, S.N., Rasmussen, R.F., Hartmann, N.B., Koch, C.B., 2008. Toxicity and bioaccumulation of xenobiotic organic compounds in the presence of aqueous suspensions of aggregates of nano-C-60. Aquatic Toxicology 86, 379-387.

Beless, B., Rifai, H.S., Rodrigues, D.F., 2014. Efficacy of carbonaceous materials for sorbing polychlorinated biphenyls from aqueous solution. Environ Sci Technol 48, 10372-10379.

Bellingeri, A., Bergami, E., Grassi, G., Faleri, C., Redondo-Hasselerharm, P., Koelmans, A.A., Corsi, I., 2019. Combined effects of nanoplastics and copper on the freshwater alga Raphidocelis subcapitata. Aquat Toxicol 210, 179-187.

Cano, A.M., Maul, J.D., Saed, M., Irin, F., Shah, S.A., Green, M.J., French, A.D., Klein, D.M., Crago, J., Canas-Carrell, J.E., 2018. Trophic Transfer and Accumulation of Multiwalled Carbon Nanotubes in the Presence of Copper Ions in Daphnia magna and Fathead Minnow (Pimephales promelas)

Environ Sci Technol 52, 794-800.

Cano, A.M., Maul, J.D., Saed, M., Shah, S.A., Green, M.J., Canas-Carrell, J.E., 2017. Bioaccumulation, stress, and swimming impairment in Daphnia magna exposed to multiwalled carbon nanotubes, graphene, and graphene oxide. Environ Toxicol Chem.

Chen, X., Xia, X., Wang, X., Qiao, J., Chen, H., 2011. A comparative study on sorption of perfluorooctane sulfonate (PFOS) by chars, ash and carbon nanotubes. Chemosphere 83, 1313-1319.

Coogan, M.A., Edziyie, R.E., La Point, T.W., Venables, B.J., 2007. Algal bioaccumulation of triclocarban, triclosan, and methyl-triclosan in a North Texas wastewater treatment plant receiving stream. Chemosphere 67, 1911-1918.

Crittenden, J.C., Sanongraj, S., Bulloch, J.L., Hand, D.W., Rogers, T.N., Speth, T.F., Ulmer, M., 1999. Correlation of Aqueous-Phase Adsorption Isotherms. Environmental Science & Technology 33, 2926-2933.

Dubinin, M.M., Astakhov, V.A., 1971. Development of Ideas of Volume Filling of Micropores during Adsorption of Gases and Vapours by Microporous Adsorbents .1. Carbonaceous Adsorbents. B Acad Sci Ussr Ch+, 5-+.

Ebert, D., 2005. Ecology, Epidemiology, and Evolution of Parasitism in Daphnia [Internet]. National Library of Medicine (US), National Center for Biotechnology Information, Bethesda (MD).

Edgington, A.J., Petersen, E.J., Herzing, A.A., Podila, R., Rao, A., Klaine, S.J., 2014. Microscopic investigation of single-wall carbon nanotube uptake by Daphnia magna. Nanotoxicology 8 Suppl 1, 2-10.

Edgington, A.J., Roberts, A.P., Taylor, L.M., Alloy, M.M., Reppert, J., Rao, A.M., Mao, J.D., Klaine, S.J., 2010. The Influence of Natural Organic Matter on the Toxicity of Multiwalled Carbon Nanotubes. Environmental Toxicology and Chemistry 29, 2511-2518.

Fan, W.H., Liu, Y.Y., Xu, Z.Z., Wang, X.R., Li, X.M., Luo, S.L., 2016. The mechanism of chronic toxicity to Daphnia magna induced by graphene suspended in a water column. Environ-Sci Nano 3, 1405-1415.

Fang, L., Borggaard, O.K., Holm, P.E., Hansen, H.C., Cedergreen, N., 2011. Toxicity and uptake of TRI- and dibutyltin in Daphnia magna in the absence and presence of nano-charcoal. Environ Toxicol Chem 30, 2553-2561.

Fawley, M.W., Dean, M.L., Dimmer, S.K., Fawley, K.P., 2006. Evaluating the morphospecies concept in the Selenastraceae (Chlorophyceae, Chlorophyta). J Phycol 42, 142-154.

French Agency for food; environmental and occupational health and safety (anses) (2018). "Justification Document for the Selection of a CoRAP Substance- Triclocarban." Justification Document for the Selection of a CoRAP Substance. URL:https://echa.europa.eu/documents/10162/9801478/corap_update_2018-2020_en.pdf/85e5f709-da61-8b06-855c-79302dc17c70. 03/08/2021; 3:16 pm.

Georgi, A., Schierz, A., Mackenzie, K., Kopinke, F.D., 2015. Colloidal activated carbon for in-situ groundwater remediation--Transport characteristics and adsorption of organic compounds in water-saturated sediment columns. J Contam Hydrol 179, 76-88.

Gillis, P.L., Chow-Fraser, P., Ranville, J.F., Ross, P.E., Wood, C.M., 2005. Daphnia need to be gut-cleared too: the effect of exposure to and ingestion of metal-contaminated sediment on the gut-clearance patterns of D. magna. Aquat Toxicol 71, 143-154.

Glomstad, B., Zindler, F., Jenssen, B.M., Booth, A.M., 2018. Dispersibility and dispersion stability of carbon nanotubes in synthetic aquatic growth media and natural freshwater. Chemosphere 201, 269-277.

Gottschalk, F., Lassen, C., Kjoelholt, J., Christensen, F., Nowack, B., 2015. Modeling Flows and Concentrations of Nine Engineered Nanomaterials in the Danish Environment. Int J Env Res Pub He 12, 5581-5602.

Gottschalk, F., Sonderer, T., Scholz, R.W., Nowack, B., 2009. Modeled environmental concentrations of engineered nanomaterials (TiO(2), ZnO, Ag, CNT, Fullerenes) for different regions. Environ Sci Technol 43, 9216-9222.

Halden, R.U., 2014. On the need and speed of regulating triclosan and triclocarban in the United States. Environ Sci Technol 48, 3603-3611.

Halden, R.U., Lindeman, A.E., Aiello, A.E., Andrews, D., Arnold, W.A., Fair, P., Fuoco, R.E., Geer, L.A., Johnson, P.I., Lohmann, R., McNeill, K., Sacks, V.P., Schettler, T., Weber, R., Zoeller, R.T., Blum, A., 2017. The Florence Statement on Triclosan and Triclocarban. Environ Health Perspect 125, 064501.

Halden, R.U., Paull, D.H., 2004. Analysis of triclocarban in aquatic samples by liquid chromatography electrospray ionization mass spectrometry. Environ Sci Technol 38, 4849-4855.

Halden, R.U., Paull, D.H., 2005. Co-occurrence of triclocarban and triclosan in U.S. water resources. Environ Sci Technol 39, 1420-1426.

Heidler, J., Sapkota, A., Halden, R.U., 2006. Partitioning, persistence, and accumulation in digested sludge of the topical antiseptic triclocarban during wastewater treatment. Environ Sci Technol 40, 3634-3639.

Hennig, M.P., 2019. Presence of multi-walled carbon nanotubes (MWCNT) in the environment: release from polymer/MWCNT composites and their interaction with the biocide triclocarban (TCC). Dissertation. URL: http://publications.rwth-aachen.de/record/774407/files/774407.pdf

Huffer, T., Kah, M., Hofmann, T., Schmidt, T.C., 2013. How redox conditions and irradiation affect sorption of PAHs by dispersed fullerenes (nC60). Environ Sci Technol 47, 6935-6942.

Iijima, S., 2002. Carbon nanotubes: past, present, and future. Physica B 323, 1-5.

Jonker, M.T., Koelmans, A.A., 2001. Polyoxymethylene solid phase extraction as a partitioning method for hydrophobic organic chemicals in sediment and soot. Environ Sci Technol 35, 3742-3748.

Kennedy, A.J., Hull, M.S., Steevens, J.A., Dontsova, K.M., Chappell, M.A., Gunter, J.C., Weiss, C.A., Jr., 2008. Factors influencing the partitioning and toxicity of nanotubes in the aquatic environment. Environ Toxicol Chem 27, 1932-1941.

Kiefer, E., Sigg, L., Schosseler, P., 1997. Chemical and spectroscopic characterization of algae surfaces. Environmental Science & Technology 31, 759-764.

Klaine, S.J., Alvarez, P.J., Batley, G.E., Fernandes, T.F., Handy, R.D., Lyon, D.Y., Mahendra, S., McLaughlin, M.J., Lead, J.R., 2008. Nanomaterials in the environment: behavior, fate, bioavailability, and effects. Environ Toxicol Chem 27, 1825-1851.

Kowk, K.W.H., Leung, K.M.Y., Flahaut, E., Cheng, J.P., Cheng, S.H., 2010. Chronic toxicity of double-walled carbon nanotubes to three marine organisms: influence of different dispersion methods. Nanomedicine-Uk 5, 951-961.

Kuhl, A., Lorenzen, H., 1964. Handling and Culturing of Chlorella. in: Prescott, D.M. (Ed.). Methods in Cell Physiology. Academic Press; NEW YORK and London.

Kühnle, E., 1990. Studium ionaler Prozesse bei der Phototransduktion der einzelligen Alge Chlamydomonas reinhardtii. Wissenschaftliche Forschungsbeiträge Biologie/Biochemie/Chemie Bd. 47. Intemann Verlag.

Leppard, G.G., 1995. The Characterization of Algal and Microbial Mucilages and Their Aggregates in Aquatic Ecosystems. Science of the Total Environment 165, 103-131.

Leroueil, P.R., Hong, S., Mecke, A., Baker, J.R., Jr., Orr, B.G., Banaszak Holl, M.M., 2007. Nanoparticle interaction with biological membranes: does nanotechnology present a Janus face? Acc Chem Res 40, 335-342.

Linard, E.N., Apul, O.G., Karanfil, T., van den Hurk, P., Klaine, S.J., 2017. Bioavailability of Carbon Nanomaterial-Adsorbed Polycyclic Aromatic Hydrocarbons to Pimphales promelas: Influence of Adsorbate Molecular Size and Configuration. Environ Sci Technol 51, 9288-9296.

Long, Z., Ji, J., Yang, K., Lin, D., Wu, F., 2012. Systematic and quantitative investigation of the mechanism of carbon nanotubes' toxicity toward algae. Environ Sci Technol 46, 8458-8466.

Lukhele, L.P., Mamba, B.B., Musee, N., Wepener, V., 2015. Acute Toxicity of Double-Walled Carbon Nanotubes to Three Aquatic Organisms. J Nanomater 2015.

Maes, H.M., Stibany, F., Giefers, S., Daniels, B., Deutschmann, B., Baumgartner, W., Schaffer, A., 2014. Accumulation and distribution of multiwalled carbon nanotubes in zebrafish (Danio rerio). Environ Sci Technol 48, 12256-12264.

Myer, M.H., Black, M.C., 2017. Multi-walled Carbon Nanotubes Reduce Toxicity of Diphenhydramine to Ceriodaphnia dubia in Water and Sediment Exposures. Bull Environ Contam Toxicol 99, 321-327.

Myer, M.H., Henderson, W.M., Black, M.C., 2017. Effects of multiwalled carbon nanotubes on the bioavailability and toxicity of diphenhydramine to Pimephales promelas in sediment exposures. Environ Toxicol Chem 36, 320-328.

Naasz, S., Altenburger, R., Kuhnel, D., 2018. Environmental mixtures of nanomaterials and chemicals: The Trojan-horse phenomenon and its relevance for ecotoxicity. Sci Total Environ 635, 1170-1181.

Nel, A.E., Madler, L., Velegol, D., Xia, T., Hoek, E.M., Somasundaran, P., Klaessig, F., Castranova, V., Thompson, M., 2009. Understanding biophysicochemical interactions at the nano-bio interface. Nat Mater 8, 543-557.

OCSIAL About. URL: https://ocsial.com/about/. Retrieved 09/17/2020; 10:47 am.

OECD, 2004. Test No. 202: *Daphnia sp*., Acute Immobilisation Test.

OECD, 2006. Test No. 201: Freshwater Alga and Cyanobacteria, Growth Inhibition Test.

Oleszczuk, P., Pan, B., Xing, B.S., 2009. Adsorption and Desorption of Oxytetracycline and Carbamazepine by Multiwalled Carbon Nanotubes. Environmental Science & Technology 43, 9167-9173.

Pan, B., Xing, B., 2008. Adsorption mechanisms of organic chemicals on carbon nanotubes. Environ Sci Technol 42, 9005-9013.

Petersen, E.J., Akkanen, J., Kukkonen, J.V., Weber, W.J., Jr., 2009. Biological uptake and depuration of carbon nanotubes by Daphnia magna. Environ Sci Technol 43, 2969-2975.

Petersen, E.J., Pinto, R.A., Mai, D.J., Landrum, P.F., Weber, W.J., Jr., 2011. Influence of polyethyleneimine graftings of multi-walled carbon nanotubes on their accumulation and elimination by and toxicity to Daphnia magna. Environ Sci Technol 45, 1133-1138.

Rhiem, S., Riding, M.J., Baumgartner, W., Martin, F.L., Semple, K.T., Jones, K.C., Schaffer, A., Maes, H.M., 2015. Interactions of multiwalled carbon nanotubes with algal cells: quantification of association, visualization of uptake, and measurement of alterations in the composition of cells. Environ Pollut 196, 431-439.

SAG, 2013. (Culture Collection of Algae), BG 11 Medium for Cyanobacteria. URL: http://sagdb.uni-goettingen.de/culture_media/20%20BG11%20Medium.pdf. Göttingen University. Retrieved 03/08/2021; 3:43 pm.

Sapkota, A., Heidler, J., Halden, R.U., 2007. Detection of triclocarban and two co-contaminating chlorocarbanilides in US aquatic environments using isotope dilution liquid chromatography tandem mass spectrometry. Environ Res 103, 21-29.

Schebb, N.H., Flores, I., Kurobe, T., Franze, B., Ranganathan, A., Hammock, B.D., Teh, S.J., 2011. Bioconcentration, metabolism and excretion of triclocarban in larval Qurt medaka (Oryzias latipes). Aquat Toxicol 105, 448-454.

Schwab, F., Bucheli, T.D., Camenzuli, L., Magrez, A., Knauer, K., Sigg, L., Nowack, B., 2013. Diuron sorbed to carbon nanotubes exhibits enhanced toxicity to Chlorella vulgaris. Environ Sci Technol 47, 7012-7019.

Schwab, F., Bucheli, T.D., Lukhele, L.P., Magrez, A., Nowack, B., Sigg, L., Knauer, K., 2011. Are carbon nanotube effects on green algae caused by shading and agglomeration? Environ Sci Technol 45, 6136-6144.

Schwab, F., Camenzuli, L., Knauer, K., Nowack, B., Magrez, A., Sigg, L., Bucheli, T.D., 2014. Sorption kinetics and equilibrium of the herbicide diuron to carbon nanotubes or soot in absence and presence of algae. Environ Pollut 192, 147-153.

Schwarzenbach, R.P., Gschwend, P.M., Imboden, D.M., 2003. Environmental organic chemistry. John Wiley & Sons, Inc., Hoboken, New Jersey. , p. 287.

Simon, A., Preuss, T.G., Schaffer, A., Hollert, H., Maes, H.M., 2015. Population level effects of multiwalled carbon nanotubes in Daphnia magna exposed to pulses of triclocarban. Ecotoxicology 24, 1199-1212.

Smirnov, N.N., 2016. The Recent State and Prospects of Studying the Cladocera (Crustacea) Physiology. Zool Zh 95, 788-804.

Snyder, E.H., O'Connor, G.A., 2013. Risk assessment of land-applied biosolids-borne triclocarban (TCC). Sci Total Environ 442, 437-444.

Snyder, E.H., O'Connor, G.A., McAvoy, D.C., 2010. Measured physicochemical characteristics and biosolids-borne concentrations of the antimicrobial Triclocarban (TCC). Sci Total Environ 408, 2667-2673.

Su, Y., Yan, X., Pu, Y., Xiao, F., Wang, D., Yang, M., 2013. Risks of single-walled carbon nanotubes acting as contaminants-carriers: potential release of phenanthrene in Japanese medaka (Oryzias latipes). Environ Sci Technol 47, 4704-4710.

Sun, T.Y., Gottschalk, F., Hungerbuhler, K., Nowack, B., 2014. Comprehensive probabilistic modelling of environmental emissions of engineered nanomaterials. Environ Pollut 185, 69-76.

Suzuki, S., Yamaguchi, H., Nakajima, N., Kawachi, M., 2018. Raphidocelis subcapitata (=Pseudokirchneriella subcapitata) provides an insight into genome evolution and environmental adaptations in the Sphaeropleales. Sci Rep 8, 8058.

Tamura, I., Kagota, K., Yasuda, Y., Yoneda, S., Morita, J., Nakada, N., Kameda, Y., Kimura, K., Tatarazako, N., Yamamoto, H., 2013. Ecotoxicity and screening level ecotoxicological risk assessment of five antimicrobial agents: triclosan, triclocarban, resorcinol, phenoxyethanol and p-thymol. J Appl Toxicol 33, 1222-1229.

TCC Consortium. High Production Volume (HPV) Chemical Challenge Program Data Availability and Screening Level Assessment for Triclocarban, CAS#: 101-20-2, 2002. In Exposure and Risk Screening Methods for Consumer Product Ingredients. The Soap and Detergent Association. Washington DC, USA (April, 2005). URL: https://www.aciscience.org/docs/Exposure_and_Risk_Screening_Methods.pdf. Retrieved 03/08/2021; 3:16 pm.

Thauer, E., Ottmann, A., Schneider, P., Moller, L., Deeg, L., Zeus, R., Wilhelmi, F., Schlestein, L., Neef, C., Ghunaim, R., Gellesch, M., Nowka, C., Scholz, M., Haft, M., Wurmehl, S., Wenelska, K., Mijowska, E., Kapoor, A., Bajpai, A., Hampel, S., Klingeler, R., 2020. Filled Carbon Nanotubes as Anode Materials for Lithium-Ion Batteries. Molecules 25.

Upadhyayula, V.K., Deng, S., Mitchell, M.C., Smith, G.B., 2009. Application of carbon nanotube technology for removal of contaminants in drinking water: a review. Sci Total Environ 408, 1-13.

Velzeboer, I., Kwadijk, C.J., Koelmans, A.A., 2014. Strong sorption of PCBs to nanoplastics, microplastics, carbon nanotubes, and fullerenes. Environ Sci Technol 48, 4869-4876.

Wang, X., Qu, R., Liu, J., Wei, Z., Wang, L., Yang, S., Huang, Q., Wang, Z., 2016. Effect of different carbon nanotubes on cadmium toxicity to Daphnia magna: The role of catalyst impurities and adsorption capacity. Environ Pollut 208, 732-738.

Wei, L., Thakkar, M., Chen, Y., Ntim, S.A., Mitra, S., Zhang, X., 2010. Cytotoxicity effects of water dispersible oxidized multiwalled carbon nanotubes on marine alga, Dunaliella tertiolecta. Aquat Toxicol 100, 194-201.

Wick, A., Marincas, O., Moldovan, Z., Ternes, T.A., 2011. Sorption of biocides, triazine and phenylurea herbicides, and UV-filters onto secondary sludge. Water Res 45, 3638-3652.

Wu, C., Spongberg, A.L., Witter, J.D., 2009. Adsorption and degradation of triclosan and triclocarban in soils and biosolids-amended soils. J Agric Food Chem 57, 4900-4905.

Yan, X.M., Shi, B.Y., Lu, J.J., Feng, C.H., Wang, D.S., Tang, H.X., 2008. Adsorption and desorption of atrazine on carbon nanotubes. J Colloid Interface Sci 321, 30-38.

Yan, Z., Lu, G., Sun, H., Ma, B., 2017. Influence of multi-walled carbon nanotubes on the effects of roxithromycin in crucian carp (Carassius auratus) in the presence of natural organic matter. Chemosphere 178, 165-172.

Yang, K., Wang, X.L., Zhu, L.Z., Xing, B.S., 2006. Competitive sorption of pyrene, phenanthrene, and naphthalene on multiwalled carbon nanotubes. Environmental Science & Technology 40, 5804-5810.

Yang, K., Xing, B., 2007. Desorption of polycyclic aromatic hydrocarbons from carbon nanomaterials in water. Environ Pollut 145, 529-537.

Yang, L.H., Ying, G.G., Su, H.C., Stauber, J.L., Adams, M.S., Binet, M.T., 2008. Growth-inhibiting effects of 12 antibacterial agents and their mixtures on the freshwater microalga Pseudokirchneriella subcapitata. Environ Toxicol Chem 27, 1201-1208.

Ying, G.G., Yu, X.Y., Kookana, R.S., 2007. Biological degradation of triclocarban and triclosan in a soil under aerobic and anaerobic conditions and comparison with environmental fate modelling. Environ Pollut 150, 300-305.

Yoo, G., Park, W.K., Kim, C.W., Choi, Y.E., Yang, J.W., 2012. Direct lipid extraction from wet Chlamydomonas reinhardtii biomass using osmotic shock. Bioresource Technol 123, 717-722.

Yu, F., Ma, J., Han, S., 2014. Adsorption of tetracycline from aqueous solutions onto multi-walled carbon nanotubes with different oxygen contents. Sci Rep 4, 5326.

Zaib, Q., Aina, O.D., Ahmad, F., 2014. Using multi-walled carbon nanotubes (MWNTs) for oilfield produced water treatment with environmentally acceptable endpoints. Environ Sci Process Impacts 16, 2039-2047.

Zhang, S., Jiang, Y., Chen, C.S., Creeley, D., Schwehr, K.A., Quigg, A., Chin, W.C., Santschi, P.H., 2013. Ameliorating effects of extracellular polymeric substances excreted by Thalassiosira pseudonana on algal toxicity of CdSe quantum dots. Aquat Toxicol 126, 214-223.

Zhang, S., Shao, T., Karanfil, T., 2011. The effects of dissolved natural organic matter on the adsorption of synthetic organic chemicals by activated carbons and carbon nanotubes. Water Res 45, 1378-1386.

Zhang, X., Kah, M., Jonker, M.T., Hofmann, T., 2012. Dispersion state and humic acids concentration-dependent sorption of pyrene to carbon nanotubes. Environ Sci Technol 46, 7166-7173.

Zhu, X.S., Zhu, L., Chen, Y.S., Tian, S.Y., 2009. Acute toxicities of six manufactured nanomaterial suspensions to Daphnia magna. J Nanopart Res 11, 67-75.

Zindler, F., Glomstad, B., Altin, D., Liu, J., Jenssen, B.M., Booth, A.M., 2016. Phenanthrene Bioavailability and Toxicity to Daphnia magna in the Presence of Carbon Nanotubes with Different Physicochemical Properties. Environ Sci Technol 50, 12446-12454.

6 Final discussion and statement

Due to the predominant application of CNT in nanocomposites and the high stability of these materials, the predicted environmental concentration is very low. Since an increased CNT production during the last years was performed and their application in products of daily use is considered, an increased exposure of the environment is expected as well.

Therefore, in this work we examined the environmental fate of weathered MWCNT in an aquatic sediment system, the uptake of such nanomaterials within the freshwater food web, and the toxicity of the biocide triclocarban to green algae and daphnids in the presence and absence of weathered MWCNT to identify possible 'Trojan-horse' effects.

We showed that the dissipation of wMWCNT from water at a concentration of about 5 orders of magnitude above the PEC (100 µg L^{-1}) takes several days to weeks before their complete deposition into the sediment. However, much slower sedimentation kinetics are expected at the current low PEC for CNT because the potential for CNT to form aggregates is lower than at higher nanomaterial concentrations. Due to the marginal complete degradation of wMWCNT in these compartments of an aquatic ecosystem, both, pelagic and benthic organisms might be at risk.

The uptake of CNT by aquatic consumers occurs usually *via* ingestion or their adsorption to the outer compartments of the animals (gills, skin, filter apparatus). In addition, it is known that CNT strongly accumulate in orally feeding organisms (gastrointestinal tract as uptake site) but can be excreted easily if a suitable food source is available, resulting in a low bioaccumulation potential of CNT under environmental conditions. Our studies showed a high accumulation of wMWCNT (10 mL, 100 µg L^{-1}) in the water flea *D. magna* over a period of 72 h when no food (green algae) was supplied. The uptake of wMWCNT (10 mL, 100 µg L^{-1}) after exposure of *D. magna* to wMWCNT-loaded green algae for 72 h showed a 100-fold lower body burden. Additionally, after an uptake phase of 24 h, a complete elimination of wMWCNT by *Daphnia* in presence of food was observed. However, exposure of a growing *D. magna* population for 28 days and four weekly applications of wMWCNT (800 mL, 100 µg L^{-1}) resulted in a body burden with daily feeding that was only 10 times lower than the body burden without feeding for 72 h. In a further experiment (45 L, 100 µg L^{-1}, 21 days, daily food), a body burden was measured only four times lower compared to the uptake in the experiment without food over 72 h. The results show that an increased water volume at constant nanomaterial concentrations, despite an adequate amount of food, leads to an increased accumulation of wMWCNT in *D. magna* (cf., Tab. 6.1). Due to this, it remains to be examined whether the duration of exposure has an influence on the ability of the *Daphnia* to excrete CNT and if CNT cause damage during long-term exposure, e.g., in the form of penetration of the gut lumen, thus creating anchor points for further assimilation of nanomaterials. Considering that aquatic ecosystems contain large amounts of water, and that *Daphnia*

acts as filter feeders and are prey to species of the higher trophic levels in the aquatic ecosystems, food chain transfer is very likely.

Table 6.1: Summary of maximum body burdens and accumulation factors for uptake of wMWCNT (0.1 mg L^{-1}) by different freshwater organisms at various test conditions.

Test organism	wMWCNT treatment	Exposure volume (L)	Count of exposed organisms	Maximum body burden (µg mg^{-1} dw^{-1})	Accumulation factor (L kg^{-1})
Chlamydomonas reinhardtii	Water exposure (96 h)	0.1	1×10^6 cells mL^{-1}	1.6 ± 0.4	24 h BCF 13,700
Raphidocelis subcapitata	Water exposure (96 h)	0.1	2×10^6 cells mL^{-1}	0.7 ± 0.3	48 h BCF 6,800
Daphnia magna	Water exposure (72 h)	0.03	10 neonates	7.1 ± 1.5	18 h BCF 140,000
	Trophic transfer (72 h)	0.03	10 neonates	0.07 ± 0.01	2.5 h BAF 600
	Population experiment (4 weeks)	0.8	Initial: 3 adults 5 neonates	0.7 ± 0.2	28 d BAF 6,700
	Population experiment (3 weeks)	45	Initial: 150 adults 250 neonates	1.5 ± 0.3	-*
Danio rerio	Water exposure (2 weeks)	45	30	0.121 ± 0.115	BAF 852
	Water and dietary exposure (96 h)	45	30	0.232 ± 0.159	-*

*wMWCNT concentration in water and diet could not be determined and therefore no accumulation factor was calculated

The influence of the water volume on the uptake of CNT was further observed when conducting microcosm studies with zebrafish *D. rerio* (45 L, 100 µg L^{-1}, food supply: twice daily). As reported for daphnids, in this species the nanomaterials accumulate mainly in the gastrointestinal tract. In our study, a ten times higher bioaccumulation factor was determined compared to a bioaccumulation factor described in the literature where single *D. rerio* was exposed to 1 mg MWCNT L^{-1} in 500 mL water phase. This phenomenon is explained either by the larger total amount of CNT, or by a more stable dispersion state of the nanomaterials and therefore a higher bioavailability in the microcosm test system. Both options increase the risk of CNT accumulation along the food chain in aquatic ecosystems. In general, more long-term studies with low concentrations should be conducted on a

large scale, even if these are more complex and more expensive. The information content is very valuable for the protection of our ecosystems.

Since CNT are taken up by aquatic organisms and pollutants, like hydrophobic organic chemicals adsorb onto nanomaterials, so-called 'Trojan-horse' effects might occur. After absorption of the CNT-chemical complex by an organism, the result is either an increased or decreased reaction in comparison to a reaction in absence of the nanomaterial. We have investigated the adsorption of the biocide TCC on weathered MWCNT and found a strong adsorption capacity as already determined for pristine MWCNT. In algal growth inhibition tests with the green algae *C. reinhardtii* and *R. subcapitata*, the addition of 100 µg wMWCNT L^{-1} had little or no influence on the effect of TCC, but at higher wMWCNT concentrations (above 1 mg L^{-1}) the effect of TCC was completely vanished. Based on the sorption study, only a slight adsorption of TCC onto the low wMWCNT concentration and an almost complete adsorption in the case of the high wMWCNT concentration could be calculated. Since green algae only incorporate CNT to a limited extent, no 'Trojan-horse' effect was assumed. Meanwhile, a 'Trojan-horse' effect was assumed for *D. magna*, since CNT are ingested in large quantities. The present study investigated the addition of 100 µg wMWCNT L^{-1} to the TCC test series in the immobilization test with *D. magna* leading to no enhanced adverse effects. However, previous studies in our working group showed that the addition of higher MWCNT amounts (1 mg MWCNT L^{-1}) to the same TCC test series reduced the TCC toxicity for *D. magna*. Whether the TCC strongly adsorbs to the CNT or the CNT agglomerates encapsulate the TCC and thus reduce bioavailability remains to be investigated. The results show that a large amount of nanomaterial is required for intensive adsorption of chemicals on CNT and to alter the fate of an aquatic pollutant, which is why no increased 'Trojan-horse' effects are to be expected with the current PEC for CNT in surface waters (ng L^{-1}). However, as is already being examined, CNT can play an important role in the remediation of polluted water due to their excellent adsorption capacity for organic pollutants.

The performed weathering of MWCNT should lead to the testing of more environmentally relevant scenarios compared to pristine MWCNT. However, an investigation using TGA and FTIR could not identify differences between weathered and pristine MWCNT. Weathering of CNT in this study was performed by filling MWCNT agglomerates in dry state into Petri dishes, which were closed with a quartz glass lid and consequently exposed to UV light using a weathering testing apparatus. Even though the samples were shaken daily, the impact of irradiation might have occurred only on the surface of the MWCNT agglomerates, resulting in no changes inside the agglomerates. Perhaps an amount of 0.8 g MWCNT agglomerates was simply too large for the size of the Petri dishes used and it would have been better to use a smaller amount of MWCNT per sample. In other research, the nanomaterials were placed into aqueous phase before the exposure to light, thus increasing the

surface area. A stronger exposure energy could also have been needed. Finally, based on the results of the characterization of the exposed MWCNT, it can be assumed that the weathered MWCNT differed little to not from the pristine MWCNT.

In conclusion, at the current production volume and application of CNT no acute impacts on aquatic ecosystems are anticipated for our environment. Even on long-term exposures it is very unlikely that effects will occur, despite a higher accumulation of CNT in *D. magna* and *D. rerio* at larger water volumes as reported in our study. Furthermore, CNT are not among ubiquitous pollutants, as they are only released into the environment at production sites or after their usage for several years. Nevertheless, an appropriate waste disposal needs to be ensured as well as an enhanced release of CNT into the environment should be avoided. If CNT production keeps on rising and environmental exposure is expected to increase, due to changing application areas, nanomaterial research should continue with chronic exposures. Until then, probably no danger from the small-scale carbonaceous nanotubes is expected in the aquatic environment.

7 Appendix

(A) Contributions in publications and chapters

Abbreviation of names:

IP	M. Sc. Irina Politowski
MH	Dr. Michael Patrick Hennig
PR	B. Sc. Philipp Regnery
HS	Prof. Dr. Heinz Sturm
UB	Dr. Ulrike Braun
FW	M. Sc. Fabian Wittmers
NS	Dr. Nina Siebers
RO	Dr. Richard Ottermanns
HH	Prof. Dr. Henner Hollert
SS	Dr. Sabrina Schiwy
BG	Birgitta Goffart
KV	M. Sc. Katrin Voigt
AS	Prof. Dr. Andreas Schäffer

Chapters

Summary/Zusammenfassung: IP designed the concept and wrote both parts.

Chapter 1: Overall introduction and objectives of the thesis
IP designed the concept for this chapter. IP wrote this chapter.

Chapter 2: Distribution of weathered multi-walled carbon nanotubes in an aquatic sediment system (This chapter has been published in a modified version in Chemosphere)

Summary	IP designed the concept for this section. IP wrote this section.
Introduction	IP designed the concept for this section. IP wrote this section.
Material and methods	IP (80%) and PR (20%) designed the concept for this section. IP wrote this section.
Results	IP (50%) and MH (50%) designed the study. IP (30%) and PR (70%) performed the experiments. NS performed transmission electron microscopy. RO assisted statistical analysis of data sets. IP (90%) and PR (10%) evaluated the data and IP wrote this section. HS and UB performed TGA and FTIR analyses to characterize the weathered nanomaterial.

Data collected by PR was used by the latter to obtain the bachelor's degree (see (D) Supervision).

Discussion	IP designed the concept for this section. IP wrote this section.
Conclusion and outlook	IP designed the concept for this section. IP wrote this section.

Chapter 3: Uptake of green algae associated multi-walled carbon nanotubes in water flea *Daphnia magna* – a trophic transfer investigation (This chapter has been published in a modified version in NanoImpact)

Summary	IP designed the concept for this section. IP wrote this section.
Introduction	IP designed the concept for this section. IP wrote this section.
Material and methods	IP (80%) and FW (20%) designed the concept for this section. IP wrote this section.

Results	IP (60%) and MH (40%) designed the study. IP (50%) and FW (50%) performed the experiments with radioactive nanomaterials. NS performed transmission electron microscopy. RO assisted statistical analysis of data sets. BG supervised the housing of test organisms. IP (80%) and FW (20%) evaluated the data and IP wrote this section.

Data collected by FW was used by the latter to obtain the bachelor's degree (see (D) Supervision).

Discussion	IP designed the concept for this section. IP wrote this section.
Conclusion and outlook	IP designed the concept for this section. IP wrote this section.

Chapter 4: First quantitative study on accumulation of weathered multi-walled carbon nanotubes in zebrafish *Danio rerio* under simulated environmental conditions

Summary	IP designed the concept for this section. IP wrote this section.
Introduction	IP designed the concept for this section. IP wrote this section.
Material and methods	IP (60%), MH (20%), HH (10%) and SS (10%) designed the concept for this section. HH and SS have played a major role in writing the animal experiment application and in communicating with the local authorities. IP wrote this section.
Results	IP (65%), MH (25%), HH (5%) and SS (5%) designed the study. IP (90%), HH (5%) and SS (5%) performed the experiments. BG assisted in the processing of the samples. IP evaluated the complete data and IP wrote this section.
Discussion	IP designed the concept for this section. IP wrote this section.
Conclusion and outlook	IP designed the concept for this section. IP wrote this section.

Chapter 5: A study to investigate the 'Trojan-horse' effect of the biocide triclocarban and weathered multi-walled carbon nanotubes to green algae (*Raphidocelis subcapitata, Chlamydomonas reinhardtii*) and freshwater crustacean (*Daphnia magna*)

Summary	IP designed the concept for this section. IP wrote this section.
Introduction	IP designed the concept for this section. IP wrote this section.
Material and methods	IP designed the concept for this section. IP wrote this section.
Results	IP (80%) and MH (20%) designed the study. IP (85%) and KV (15%) performed the experiments. IP evaluated the complete data and IP wrote this section.

Data collected by KV was used by the latter to obtain the master's degree (see (D) Supervision).

Discussion	IP designed the concept for this section. IP wrote this section.
Conclusion and outlook	IP designed the concept for this section. IP wrote this section.

Chapter 6: Final discussion and statement
IP designed the concept for this chapter. IP wrote this chapter.

AS supervised and proofread this work.

(B) Peer-reviewed publications

Published

- Politowski, I., Wittmers, F., Hennig, M. P., Siebers, N., Goffart, B., Roß-Nickoll, M., Ottermanns, R. and Schäffer, A. (2021). A trophic transfer study: accumulation of multi-walled carbon nanotubes associated to green algae in water flea *Daphnia magna*. NanoImpact 22: 100303.

- Politowski, I., Regnery, P., Hennig, M. P., Siebers, N., Ottermanns, R. and Schäffer, A. (2021). Fate of weathered multi-walled carbon nanotubes in an aquatic sediment system. Chemosphere 277: 130319.

Submitted

- Weise, K., Kurth, T., Politowski, I., Winkelmann, C., Schäffer, A., Kretschmar, S., Berendonk, T. U. and Jungmann, D. (2021). A workflow to investigate the impacts of weathered multi-walled carbon nanotubes to the mudsnail *Lymnaea stagnalis*. Environmental Science and Pollution Research.

(C) Conference contributions

Platform presentations

- Benner, L., Politowski, I., Hennig, M. P., Schäffer, A. (2019): Influence of weathered multi-walled carbon nanotubes on the distribution of the biocide triclocarban in a sediment-water system. SETAC Europe 28th Annual Meeting (May 2019, Helsinki, Finland).

- Politowski, I., Hennig, M. P., Wittmers, F., Hollert, H., Schäffer, A. (2017): Influence of weathered multiwalled carbon nanotubes in the environment: chronic and mixture effects with the biocide triclocarban as co-contaminant on freshwater algae. Young Water Researchers Symposium at RWTH Aachen University on November 24, 2017 in Aachen, Germany.

- Hennig, M. P., Politowski, I., Schäffer, A. (2017): Influence of weathered multiwalled carbon nanotubes in the environment: chronic and mixture effects with the biocide triclocarban as co-contaminant on freshwater algae. NANO-Transfer International Conference & Winter School on October 19 and 20, 2017 in Aachen, Germany.

- Politowski, I., Hennig, M. P., Maes, H. M., Schäffer, A. (2016): Metabolism of the biocide triclocarban in the freshwater algae Desmodesmus subspicatus and the impact of multi-walled carbon nanotubes on its toxicity and bioaccumulation. 13th Annual Meeting International Symposium on Persistent and Toxic Substances on Oktober 11 to 14, 2016 in Leipzig, Germany.

- Politowski, I., Hennig, M. P., Maes, H. M., Schäffer, A. (2016): Metabolism of the biocide triclocarban in the freshwater algae Desmodesmus subspicatus and the impact of multi-walled carbon nanotubes on its toxicity and bioaccumulation. SETAC GLB (Society of Environmental Toxicology and Chemistry – Europe German Language Branch e.V.) on September 5 to 8, 2016 in Tübingen, Germany.

Poster presentations

- Politowski, I., Hennig, M. P., Wittmers, F., Hollert, H., Schäffer, A. (2019): Bioaccumulation of radiolabelled weathered multiwalled carbon nanotubes in various aquatic organisms: water and dietary exposure. SETAC Europe 29th Annual Meeting (May 2019, Helsinki, Finland).

- Politowski, I., Hennig, M. P., Hollert, H., Schäffer, A. (2018): Influence of weathered multiwalled carbon nanotubes in the environment: chronic and mixture effects with the biocide triclocarban as co-contaminant on freshwater algae. SETAC Europe 28th Annual Meeting (May 2018, Rome, Italy)

- Politowski, I., Hennig, M. P., Regnery, P., Voigt, K., Schäffer, A. (2018): CNT exposure to freshwater green algae *Pseudokirchneriella subcapitata* and *Chlamydomonas reinhardtii*: uptake and chronic effects. NanoTox 2018 - 9th International Conference on Nanotoxicology (September 2018, Neuss, Germany).

- Politowski, I., Hennig, M. P., Schäffer, A., Maes, H. M. (2017): The impact of multiwalled carbon nanotubes on toxicity and bioaccumulation of triclocarban in the freshwater algae *Desmodesmus subspicatus*. NanoImpact Conference on March 12 to 17, 2017 in Ascona, Switzerland.

- Politowski, I., Hennig, M. P., Schäffer, A. (2017): NANO-Transfer: Das Verhalten gealterter Kohlenstoffnanoröhren in der aquatischen Umwelt. NanoCare-Clustertreffen 2017 am 04. und 05. Mai in Karlsruhe, Deutschland.

- Politowski, I., Hennig, M. P., Schäffer, A., Maes, H. M. (2017): The impact of multiwalled carbon nanotubes on toxicity and bioaccumulation of triclocarban in the freshwater algae *Desmodesmus subspicatus.* Scientific Stakeholder Meeting on Nanomaterials in the Environment. 10th and 11th October 2017, German Environment Agency (UBA), Dessau-Rosslau, Germany. **Best Poster Award**.

(D) Supervision

Bachelor theses

Philipp Regnery (2018). Verbleib von radioaktiv markierten belichteten mehrwandigen Kohlenstoffnanoröhren (^{14}C-wMWCNT) in einem natürlichen Wasser/Sediment-System: Verteilung, Sedimentation und Mineralisation. FH Aachen, University of Applied Sciences

Fabian Wittmers (2018). Bioakkumulation von radioaktiv markierten, belichteten, mehrwandigen Kohlenstoffnanoröhren in *Daphnia magna*: Vergleich von Wasser- und Nahrungsexposition. RWTH Aachen University

Master theses

Lena Benner (2019). Influence of weathered multi-walled carbon nanotubes on the distribution and mineralisation of the biocide triclocarban in a natural water-sediment system. RWTH Aachen University

Katrin Voigt (2019). Acute and chronic effects of weathered multiwalled carbon nanotubes in combination with the biocide triclocarban to the freshwater crustacean *Daphnia magna* and the green algae *Chlamydomonas reinhardtii*. RWTH Aachen University

Joe Reiser (2019). Weathered multi-walled carbon nanotubes acting as possible "Trojan-horses" for the biocide triclocarban in sediment toxicity tests. RWTH Aachen University

Martin Siedt (2018). Einfluss von verwitterten mehrwandigen Kohlenstoffnanoröhren auf Verteilung, Mineralisation und Bildung nicht-extrahierbarer Rückstände von ^{14}C-Bisphenol A in einem natürlichen Wasser-Sediment System. RWTH Aachen University

Others

Philipp Regnery (2018). Das Verhalten von Nanomaterialien in der Umwelt: Chronische Effekte des Biozids Triclocarban auf die Grünalgen *Pseudokirchneriella subcapitata* und *Chlamydomonas reinhardtii* in An- und Abwesenheit von belichteten mehrwandigen Kohlenstoffnanoröhren. **Praxissemester**.

Michael Gundlach (2018). Analyse der Metabolisierungsprodukte von radioaktiv markiertem Triclocarban unter Verwendung unterschiedlicher Algenkulturmedien der Alge *Desmodesmus subspicatus*. **Forschungspraktikum**.